AD-A131 091 MICROWAVE INTERACTION WITH THIN MULTIPLE CONDUCTIVE 1/3
COATINGS(U) ROME AIR DEVELOPMENT CENTER GRIFFISS AFB NY
V M MARTIN MAR 83 RADC-TR-83-62
UNCLASSIFIED F/G 11/3 NL

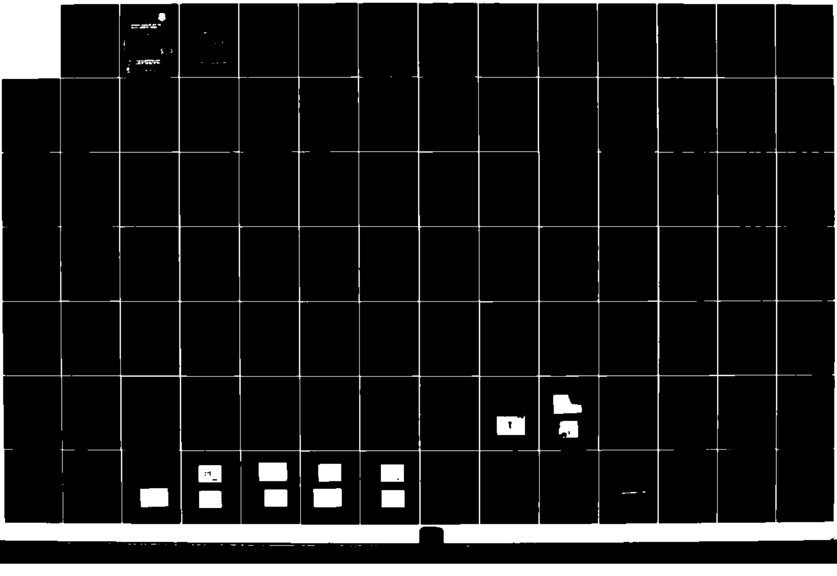

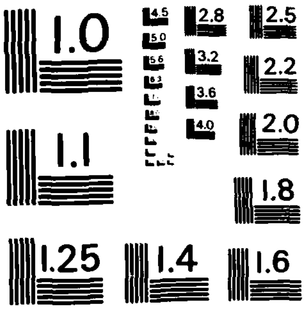
1.0
4.5
5.0
5.6
6.3
2.8
3.2
3.6
4.0
2.5
2.2
2.0
1.1
1.8
1.25
1.4
1.6

MICROCOPY RESOLUTION TEST CHART
NATIONAL BUREAU OF STANDARDS-1963-A

ADA131091

[illegible]

MICROWAVE INTERACTION WITH THIN [illegible]NGS

UNCLASSIFIED
SECURITY CLASSIFICATION OF THIS PAGE (When Data Entered)

REPORT DOCUMENTATION PAGE		READ INSTRUCTIONS BEFORE COMPLETING FORM
1. REPORT NUMBER RADC-TR-83-62	2. GOVT ACCESSION NO. AD-A131091	3. RECIPIENT'S CATALOG NUMBER
4. TITLE (and Subtitle) MICROWAVE INTERACTION WITH THIN MULTIPLE CONDUCTIVE COATINGS		5. TYPE OF REPORT & PERIOD COVERED Final Technical Report Nov 81 - Nov 82
		6. PERFORMING ORG. REPORT NUMBER N/A
7. AUTHOR(s) Victor M. Martin		8. CONTRACT OR GRANT NUMBER(s) N/A
9. PERFORMING ORGANIZATION NAME AND ADDRESS United States Air Force Academy Colorado Springs CO 80840		10. PROGRAM ELEMENT, PROJECT, TASK AREA & WORK UNIT NUMBERS 62702F 23380403
11. CONTROLLING OFFICE NAME AND ADDRESS Rome Air Development Center (RBC) Griffiss AFB NY 13441		12. REPORT DATE March 1983
		13. NUMBER OF PAGES 232
14. MONITORING AGENCY NAME & ADDRESS(if different from Controlling Office) Same		15. SECURITY CLASS. (of this report) UNCLASSIFIED
		15a. DECLASSIFICATION/DOWNGRADING SCHEDULE N/A

16. DISTRIBUTION STATEMENT (of this Report)

Approved for public release; distribution unlimited.

17. DISTRIBUTION STATEMENT (of the abstract entered in Block 20, if different from Report)

Same

18. SUPPLEMENTARY NOTES

RADC Project Engineer: Jacob Scherer (RBC)

19. KEY WORDS (Continue on reverse side if necessary and identify by block number)

Measurement Techniques
Electromagnetic Radiation
Electromagnetic Compatibility
Thermography
Surface Currents
Surface Temperature
Infrared
Conductive Coatings

20. ABSTRACT (Continue on reverse side if necessary and identify by block number)

This report presents the analytic solution for the surface temperatures of the first layer of a system of N layers being exposed to microwave radiation. This provides for a correlation between surface temperatures and surface currents present in the system. The surface temperature is to be measured via infrared thermography.

Thermography has been available for some time as an aid in determining temperature differentials. Burton, et al, have demonstrated that thermographic techniques can be used qualitatively to detect temperature differentials associated with Joule (I^2R) heating from surface currents induced by incident electromagnetic waves on particular shapes. These surface currents result from the interaction of the conducting object with the incident electric field. The tangential component of the electric field with the object surface causes charge to migrate along the surface until electrical equilibrium is established. Thus, the rate of charge migration determines the surface current. Therefore, if the object has some finite resistivity, joule heating will be observed. The heating on the object surface causes surface temperature variations which may be detected with an infrared camera (thermography).

Observing surface heating directly on a highly conductive metallic surface such as aluminum is exceedingly difficult because of the small amount of energy deposited and the large thermal conductivity of the metal. Therefore, an alternative approach is to place a thin resistive coating over the metallic surface. We then observe the heating in the coating which is correlated to surface currents in the metal. We will analyze this situation so that we can design an optimum coating for a given situation and, secondly, so that we can understand the quantitative relationship between surface currents and observed surface temperatures. We will then have an accurate method of measuring surface current amplitudes thermographically.

Thus, the procedure will be to solve the electromagnetic problem for a system of N layers so that we can calculate the absorbed energy in the resistive layer. The thermodynamics is then addressed for the system which yields the coating surface temperature. Experimental verification confirms the validity of the analytic results. Recommendations are then made for various coating schemes.

DTIC COPY INSPECTED 2

CONTENTS

CHAPTER

I. INTRODUCTION 1

II. ELECTROMAGNETICS IN GENERAL 8

III. SINGLE BOUNDARY ANALYSIS 12

IV. ELECTROMAGNETIC N-LAYER ANALYSIS 29

V. THERMAL ANALYSIS 38

VI. EXPERIMENTAL VERIFICATION 51

VII. APPLICATION OF MODEL TO TWO-DIMENSIONAL TARGETS 64

VIII. RECOMMENDATIONS AND CONCLUSIONS 106

BIBLIOGRAPHY 140

APPENDIX

A. ELECTRICAL CONDUCTIVITY MEASUREMENT 144

B. ELECTRICAL PERMITTIVITY 154

C. COMPUTER PROGRAM (One-B) 165

D. COMPUTER PROGRAM (Basic) 175

E. COMPUTER PROGRAM (Signif) 186

F. COMPUTER PROGRAM (Uo-3D) 190

G. COMPUTER PROGRAM (Uthick) 204

H. COMPUTER PROGRAM (Contor) 216

I. COMPUTER PROGRAM (Epslon) 224

TABLES

Table

1. Relative Permittivity for Various Dielectrics.................................. 154

2. Measured Relative Permittivity at 10 GHz.... 164

FIGURES

Figure

1. Plane Wave Interaction with a Single Interface.................................... 10

2. Plane Wave Interface on a Single Boundary..... 12

3. Reflectance from a Single Plane Interface ($\sigma=0$)............................... 21

4. Directional Spectral Emissivity at 3 Microns ($\sigma=0$)............................ 22

5. Reflectance from a Single Plane Interface ($\sigma=3.00$ mhos/m)..................... 23

6. Directional Spectral Emissivity at 3 Microns ($\sigma=3.00$ mhos/m)................. 24

7. Reflectance from a Single Plane Interface ($\sigma=500$ mhos/m)..................... 25

8. Directional Spectral Emissivity at 3 Microns ($\sigma=500$ mhos/m).................. 26

9. Reflectance from a Single Plane Interface (Copper)........................... 27

10. Directional Spectral Emissivity at 3 Microns (Copper)........................ 28

11. N-Layer Electromagnetic Interaction........... 29

12. Auxiliary Matrix for Parallel Polarization ($k_n=\beta_n \text{Cos}\theta_n$)................................ 34

13. Auxiliary Matrix for Perpendicular Polarization ($k_n=\beta_n \text{Cos}\theta_n$).................... 35

14. Three Layer Electromagnetic Response.......... 36

15. Three Layer Thermal Transient Response........ 38

16. Infrared Versus Convection Comparison......... 42

17. Infrared Versus Convection Comparison......... 43

18. Infrared Versus Convection Comparison......... 44

19. Two Layer Electromagnetic Heating Profiles.... 47

20. Two Layer Electromagnetic Heating Profiles.... 48

21. Two Layer Electromagnetic Heating Profiles.... 49

22. Two Layer Electromagnetic Heating Profiles.... 50

23. Schematic of Convective Exponent Experiment... 53

24. Results of Convective Exponent Measurements... 55

25. Schematic of N-Layer Verification............ 57

26. One Layer Electromagnetic Heating............ 59

27. One Layer Electromagnetic Heating............ 60

28. One Layer Electromagnetic Heating............ 61

29. Two Layer Electromagnetic Heating............ 62

30. Three Layer Electromagnetic Heating.......... 63

31. Photograph of Monopole and Parabolic Reflector.................................. 65

32. Actual Quarter Wave Monopole................. 66

33. Anechoic Chamber With Electrically Small Target and Infrared Camera in Foreground...... 66

34. A Uniform Current Sheet Radiator............. 68

35. 1.0λ Square Plate Current Distribution........ 71

36. .15λ Square Plate Current Distribution........ 72

37. Photograph of 1.0λ Square Plate.............. 73

38. Infrared Photograph of a 1.0λ Square Plate.... 74

39. Thermal Profile Across the Center of a 1.0λ Square Plate................................. 74

40. Actual Photograph of a 0.5λ Square Plate...... 75

41. Infrared Photograph of a 0.5λ Square Plate.... 75

42. Thermal Profile Across the Center of a 0.5λ Square Plate.................................... 76

43. Actual Photograph of a 0.25λ Square Plate..... 76

44. Infrared Photograph of a 0.25λ Square Plate... 77

45. Thermal Profile Across the Center of a 0.25λ Square Plate.................................... 77

46. Current Uniformity on a .15λ Plate............ 78

47. Current at the Center of a Disc as a Function of c................................... 79

48. Cross Section of a Conductive Coating Displaced Away From Conductor Surface......... 81

49. Parallel Waveguide Sheets..................... 82

50. Photograph of Electrically Large Plate in Place in the Anechoic Chamber................. 85

51. Photograph of the Single 1.5 cm Hole in the Aluminum Plate............................... 85

52. Photograph of the Double Hole Configuration... 86

53. Infrared Photograph of Artificially Heated Double Hole Configuration for Size Comparison with Microwave Results....................... 86

54. Infrared Photograph of Single Hole Heating Pattern Resulting from Microwave Radiation (1° C Scale)................................... 87

55. Horizontal Thermal Profile of Single Hole Heating Pattern (1° C Scale).................. 87

56. Same as Figure 54 Except 2° C Scale........... 88

57. Same as Figure 55 Except 2° C Scale........... 88

58. Infrared Results of Double Hole Microwave Heating Pattern (1° C Scale).................. 89

59. Horizontal Thermal Profile of Double Hole Heating (1° C Scale)........................ 89

60. Same as Figure 58 Except 2° C Scale........... 90

61. Same as Figure 59 Except 2° C Scale........... 90

62. Irradiated, Finite Size, Conducting Substrate with Hypothetical Surface Current Distribution.................................. 92

63. Thermovision Photograph of 1.5 cm Square Sample (No Substrate)........................ 98

64. Thermal Profile (Horizontal) through the Center of the 1.5 cm Square Sample (2.45 GHz at 25 mw/cm^2)...................... 98

65. Thermovision Photograph of 1.0λ Square Plate (Horizontal white line indicates area where thermal profile was taken.).................. 99

66. Thermal Profile from 1.0λ Square Plate with ΔT_{∞} Plotted................................. 99

67. Thermovision Photograph of 0.5λ Square Plate (Horizontal white line indicates area where thermal profile was taken.).................. 100

68. Thermal Profile from 0.5λ Square Plate with ΔT_{∞} Plotted................................. 100

69. Thermovision Photograph of 1.5 cm Square Sample (Copper Substrate).................... 101

70. Thermal Profile (Horizontal) through the Center of the 1.5 cm Square Sample (2.45 GHz at 25 mw/cm^2)...................... 101

71. Thermovision Photograph of 1.0λ Square Plate with a Copper Substrate...................... 102

72. Thermal Profile Corresponding to White Line in Figure 71................................... 102

73. Thermovision Photograph of a 0.5λ Square Plate with a Copper Substrate................. 103

74. Thermal Profile Corresponding to White Line in Figure 73................................. 103

75. Carbon/Paraffin/Styrofoam Thermal Contours.... 111

76. Carbon/Paraffin/Styrofoam Thermal Contours.... 112

77. Carbon/Paraffin/Styrofoam/Copper Difference Contours.................................... 113

78. Carbon/Paraffin/Styrofoam Thermal Contours.... 114

79. Carbon/Paraffin/Styrofoam/Copper Thermal Contours.................................... 115

80. Carbon/Paraffin/Styrofoam/Copper Difference Contours.................................... 116

81. Carbon/Paraffin/Styrofoam Thermal Contours.... 117

82. Carbon/Paraffin/Styrofoam/Copper Thermal Contours.................................... 118

83. Carbon/Paraffin/Styrofoam/Copper Difference Contours.................................... 119

84. Carbon/Paraffin/Neoprene Thermal Contours..... 120

85. Carbon/Paraffin/Neoprene/Copper Thermal Profiles.................................... 121

86. Carbon/Paraffin/Neoprene/Copper Difference Contours.................................... 122

87. Carbon/Paraffin/Neoprene Thermal Contours..... 123

88. Carbon/Paraffin/Neoprene/Copper Thermal Contours.................................... 124

89. Carbon/Paraffin/Neoprene/Copper Difference Contours.................................... 125

90. Carbon/Paraffin/Neoprene Thermal Contours..... 126

91. Carbon/Paraffin/Neoprene/Copper Thermal Contours.................................... 127

92. Carbon/Paraffin/Neoprene/Copper Difference Contours.................................... 128

93. Aquadaq/Plexiglas Thermal Contours........... 129

94. Aquadaq/Plexiglas/Copper Thermal Contours..... 130

95. Aquadaq/Plexiglas/Copper Difference Contours.. 131

96. Coating Sample Cross Section.................. 145

97. Drawing of a Typical Disc Sample............. 146

98. Square Sample Electrical Connections.......... 147

99. Disc Sample with Clamps Attached.............. 148

100. Schematic of Conductivity Measurements........ 148

101. Electrical Conductivity Versus Absolute Temperature (Aquadaq Coating)................. 150

102. Electrical Conductivity Versus Carbon/Paraffin Mixing Ratios.................................. 152

103. Electrical Conductivity Versus Carbon/Paraffin Mixing Ratios with Empirical Model............ 153

104. Schematic Arrangement of Permittivity Measurements.................................. 104

105. Permittivity Plot for Styrofoam at 10 GHz..... 157

106. Permittivity Plot for Window Glass at 10 GHz.. 158

107. Permittivity Plot for Paraffin at 10 GHz...... 159

108. Permittivity Plot for Styrene at 10 GHz....... 160

109. Permittivity Plot for Phenolic at 10 GHz...... 161

110. Permittivity Plot for Plexiglas at 10 GHz..... 162

111. Permittivity Plot for Neoprene at 10 GHz...... 163

CHAPTER I

INTRODUCTION

This paper deals with the microwave induced heating in thin multiple conductive coatings. An understanding of this phenomenon is needed so an optimum coating may be designed for the thermographic detection of surface currents. This process uses a thermographic camera to detect temperature variations on an object's surface. These temperature variations are caused by joule heating (I^2R) due to surface currents. Thus, it is possible to relate surface currents to surface temperature variations. Once this is done the thermographic system can measure surface currents on an entire object very quickly and relatively easily. However, there is still a significant limitation to this type of measurement system. The limitation is that we measure a single scalar quantity (temperature) at each point on the surface; hence, we only obtain the magnitude of the total surface current at that point and have no phase or direction information.

Nonetheless, current amplitude information alone is a valuable piece of information. For example, in the study of Electromagnetic Pulse (EMP) phenomena we might want to know where the greatest current density amplitudes are located on an aircraft to aid in the proper placement of cable bundles. Or possibly in radar cross section studies, we might want to know where the greatest current densities exist before a design or numerical solution is attempted. And lastly, measured surface current amplitude information would be extremely valuable in the verification of numerous numerical techniques designed to provide amplitude, phase, and direction information. This thesis which relates coating temperature to incident microwave power levels is organized in the following manner.

The second chapter begins with a discussion of electromagnetics in general. It considers the phasor form of Maxwell's equations in a conductive medium and then reviews their simultaneous solution. The result yields the type form the wave must take as it propagates in the medium and discusses some of its characteristics. Particular areas of discussion include attenuation in a medium and the complex form of Snell's law.

The third chapter deals exclusively with the solution of a single boundary electromagnetic problem. The boundary is a semi-infinite plane located at the z=0 interface between air and a conductive medium. The solution is completed for various incident angles and for polarizations both parallel and perpendicular to the plane of incidence. The single boundary problem provides two useful insights to our overall problem. First, it is done in a general manner so the same overall approach is used in the solution to the N-layer system later in chapter four. Second, the results may be used to provide information concerning the theoretical infrared emissivity of the coatings that are to be placed on the various object surfaces. The rate and direction of infrared emission are both directly proportional to this emissivity factor. Therefore, our detection effectiveness is very dependent on surface emissivity. Various plots are presented which illustrate the reflectivity and emissivity for materials with conductivities of 0 to 5×10^7 mhos/m.

Chapter four presents a detailed solution for the N-layer electromagnetic interaction problem. The problem considers both parallel and perpendicular polarizations at a particular incident angle. Each layer is considered to have a particular electrical conductivity. The solution is developed in terms of an expanded matrix in a manner similar to that used in chapter three. A computer program is included in appendix D that will do the solution for up to a 10 layer system and display the results with a Hewlett-Packard 9845B mini-computer. Included is an example of the plot obtained for a three layer system with the layers having conductivities of .5, 1.0, and 1.5 mhos/m respectively. Of note in this development is that there are no approximations used other than assuming semi-infinite slab dimensions.

In the next chapter we tie the electromagnetic interaction to the thermodynamics of the problem. Thus, for a given layer configuration we relate surface temperature to a given microwave input power. Initially in the development, a simplified model is presented that allows us to estimate the transient response of the system. Then somewhat later the steady state thermal characteristics of the system are analyzed. In this analysis we assume there are no heat losses from other than the $z=0$ interface; that is, we assume one of the layers below the conductive coating to be a perfect insulator. At the $z=0$ interface we consider both infrared and convective heat losses. The steady state solution to the heat equation yields a transcendental equation that must be solved numerically. A computer program is written that does this solution and plots surface temperature versus electrical conductivity and coating thickness on a three dimensional plot. Plots are illustrated for typical two and three layer systems.

As in any theoretical development, we must have experimental verification before the results may be used with any confidence. Chapter six provides experimental verification of the computer results for various layer configurations. The three primary sources of error in the experiments resulted from the lack of semi-infinite planes to irradiate with microwaves; thus, samples much smaller than a wavelength were used to avoid resonance problems. Also, the problem of assuming zero heat conduction losses from the $z=z_n$ interface was partially solved by placing the samples on a styrofoam substrate. Finally, the third major source of error resulted from the convective heat transfer coefficient used which itself was an empirical value. See for example Holman's book, Heat Transfer. Nonetheless, predicted surface temperatures were very close to the measured values.

Chapter seven is a mostly qualitative discussion of the relationship of our one-dimensional model to the more complicated two or even three-dimensional "real world" experiments. In particular, the two areas discussed involve the validity of using a small finite shape in the experimental verification of Chapter VI and the question of "nearest neighbor" significance in the actual measurement of surface currents on electrically large targets. Theoretical as well as experimental results are presented that help establish the validity and usefulness of our one-dimensional model as applied toward the "real world" situation.

In Chapter VIII recommendations and conclusions are made in regards to what to use as an optimum coating in the thermographic detection of microwave induced surface currents. Basically, there are two situations that must be considered. The first considers geometry only. If we are interested only in the geometrical aspects of a problem such as studying the currents on an entire aircraft, the simpler approach is to build a model of foam and then coat it with a thick (two skin depths) layer of material with a conductivity of from 300 to 750 mhos/m. Hence, the currents we measure are the currents in the coating itself; we simulate a highly conductive object with one of lesser conductivity. The other, and more difficult, situation is one in which the material an object is made matters and cannot be approximated. This situation would occur if several different materials were used in the construction of a particular shape (For example, there might be ferromagnetic materials, copper, aluminum, and composites all located on the underside of an aircraft of spacecraft.). Here we would like to determine how these different materials behave together. Therefore, we place our coating directly on the object itself. By appropriate design of the coating, we can detect the current distribution under our coating.

Various coating options are described in the final chapter as well as their advantages and disadvantages. The various appendices contain the experimental arrangements for measuring such material characteristics as electrical conductivity and permittivity. Also included are all the major computer programs used in any of the numerical analysis with the 9845B computer. This computer uses a Hewlett-Packard enhanced BASIC language that would be easily modified for use on a computer using either Fortran or Pascal.

Overall then, this paper begins by presenting the development of a one-dimensional model for the electromagnetic interaction with a system of N layers with differing electrical characteristics. We then use this model in a thermodynamic analysis to arrive at the steady state surface temperature of the system of layers. Thus, we arrive at a model which predicts the equilibrium surface temperature of a system of N discrete layers in the presence of electromagnetic radiation. This model is verified experimentally and its applicability to two-dimensional targets is discussed. Finally, recommendations are made in regards to particular coating design.

CHAPTER II

GENERAL ELECTROMAGNETIC ANALYSIS

In electromagnetic analysis we will study the simple one boundary problem and then progress to multiple boundaries. Throughout this analysis we will assume a time dependence for E and H of the form $e^{-j\omega t}$. We will first calculate the form the field must take by looking at the solution of Maxwell's equations in a conductive medium.

In a charge free conductor and with the assumed time dependence, Maxwell's equations may be written as follows:

$$\vec{\nabla} \times \vec{E} = j\omega\mu \vec{H} \qquad (1)$$

$$\vec{\nabla} \times \vec{H} = (\sigma - j\omega\varepsilon) \vec{E} \qquad (2)$$

$$\vec{\nabla} \cdot \vec{E} = 0 \qquad (3)$$

$$\vec{\nabla} \cdot \vec{H} = 0 \qquad (4)$$

Solving equations (1) through (4) simultaneously[10] we can arrive at the vector wave equation

$$\nabla^2 \vec{E} + \beta^2 \vec{E} = 0 \qquad (5)$$

where

β^2 is defined by

$$\beta^2 \equiv \omega^2\mu\varepsilon + j\,\omega\mu\sigma \qquad (6)$$

A wave equation may also be developed for $\vec{H}$; however, its value is readily available through equation (1). Solving, we have

$$\vec{H} = -\frac{j}{\omega\mu}\vec{\nabla} \times \vec{E} \tag{7}$$

The solution of (5) is well known[11] and may be written as

$$\vec{E} = \vec{E}_o\, e^{j(\vec{\beta}\cdot\vec{r} - \omega t)} \tag{8}$$

where $\vec{\beta}$ is the wave vector. Thus,

$$\vec{\beta} = \sqrt{\omega^2\mu\varepsilon + j\omega\mu\sigma}\;\hat{n} \tag{9}$$

with $\hat{n}$ being in the direction of wave propagation. Since β is complex, its real and imaginary components may be found by letting $\beta = \alpha + j\gamma$ where α and γ are defined to be real. Making the above substitution and equating real and imaginary parts, we arrive at two simultaneous equations given by

$$\alpha^2 - \gamma^2 = \omega^2\mu\varepsilon \tag{10}$$

$$2\alpha\gamma = \omega\mu\sigma \tag{11}$$

Solving (10) and (11) by substitution we find expressions for α and γ given by

$$\alpha = \omega\sqrt{\frac{\mu\varepsilon}{2}}\sqrt{1 + \sqrt{1 + \left(\frac{\sigma}{\omega\varepsilon}\right)^2}} \tag{12}$$

$$\gamma = \omega\sqrt{\frac{\mu\varepsilon}{2}}\sqrt{-1 + \sqrt{1 + \left(\frac{\sigma}{\omega\varepsilon}\right)^2}} \tag{13}$$

For the case of good conductors $\left(\frac{\sigma}{\omega\varepsilon}\right) \gg 1$; thus, we have $\alpha = \gamma = \frac{1}{\delta}$ where δ is the characteristic skin depth of the medium in question. It is given by

$$\delta \equiv \sqrt{\frac{2}{\omega\mu\sigma}} \tag{14}$$

From this point on we will omit the $e^{-j\omega t}$ time dependence, since it will occur in all of our terms, and proceed with the more familiar phasor notation. Thus we will write for the electric field

$$\vec{E} = \vec{E}_o \, e^{j\vec{\beta}\cdot\vec{r}} \qquad (15)$$

This is a shorthand notation and it is to be understood that the $e^{-j\omega t}$ is always present even though it is not written.

Lastly, it is advantageous to develop the complex Snell's law. Consider the single interface below separating two conductive materials.

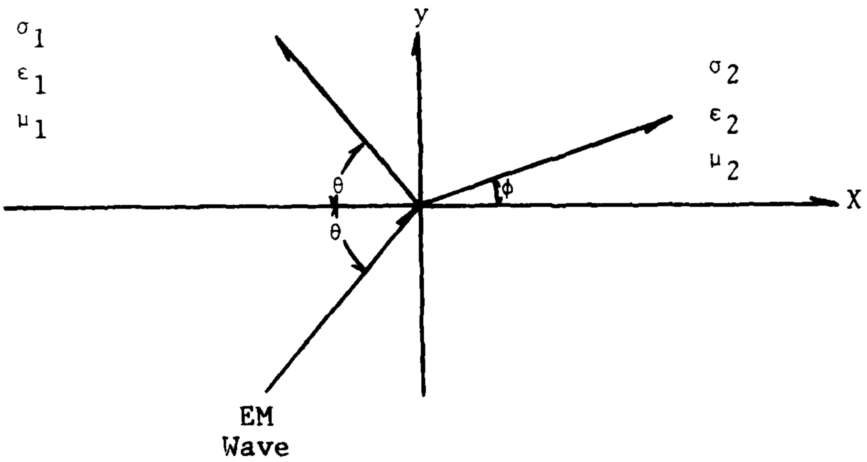

Figure 1: Plane Wave Interaction with a Single Interface

We know the wave phase must be the same on each side of the boundary at any given point on the boundary; otherwise, the wave would "tear" and dispersion would occur. This phase requirement may be satisfied by having[12]

$$\vec{\beta}_1 \cdot \vec{r} \equiv \vec{\beta}_2 \cdot \vec{r} \qquad (16)$$

Again referring to the drawing, we have

$$\beta_2(\cos\theta\ \hat{x} + \sin\theta\ \hat{y})\cdot\vec{r} \equiv \beta_2(\cos\phi\ \hat{x} + \sin\phi\ \hat{y})\cdot\vec{r} \qquad (17)$$

Since $\vec{r} = y\ \hat{y}$ defines the interface, the result is

$$\beta_1\ \sin\theta = \beta_2\ \sin\phi \qquad (18)$$

Thus, $\sin\phi$ is in general complex and is given by

$$\sin\phi = \frac{\beta_1}{\beta_2}\sin\theta = \frac{\alpha_1 + j\gamma_1}{\alpha_2 + j\gamma_2}\sin\theta \qquad (19)$$

We may also write the expression for $\cos\phi$ by recognizing that for any complex z, $\sin^2 z + \cos^2 z = 1$ [13]; thus,

$$\cos\phi = \sqrt{1 - \frac{\alpha_1^2 - \gamma_1^2 + j\ 2\alpha_1\ \gamma_1}{\alpha_1^2 - \gamma_2^2 + j\ 2\alpha_2\ \gamma_2}\sin^2\theta} \qquad (20)$$

We can look at Snell's Law in the case of an air/good conductor interface. If the medium on the left is air, β_1 reduces to $\frac{2\pi}{\lambda}$, where λ is the free space wavelength. In the good conductor we have $\alpha \simeq \gamma \simeq \frac{1}{\delta}$; then we have $\sin\phi = (\frac{2\pi}{\lambda})(\frac{1}{\alpha_2 + j\gamma_2})\sin\theta$ (21)

With algebraic manipulation this reduces to

$$\sin\phi = \frac{1}{2c}\sqrt{\frac{2\omega}{\mu_2\sigma_2}}\ (1 - j)\ \sin\theta \qquad (22)$$

In the good conductor limit we have therefore,

$$\sin\phi \simeq 0 \qquad (23)$$

which implies $\phi \simeq 0$

Hence, regardless of the incident angle θ, the wave will propagate approximately normal to the surface after entering medium 2.

CHAPTER III

SINGLE BOUNDARY ANALYSIS

With the basic equations developed, we can now do the actual field calculation. We will begin with the single boundary which will provide two important pieces of information. First, it will provide needed insight for the solution of the more complex multi-layer problem, and second, it will provide a method of calculating theoretical infrared spectral emissivities. This information will be very valuable in the thermodynamic analysis of the multi-layer problem later in the development.

We begin by considering the diagram below in which we have an incident electromagnetic wave from the left. Parallel incidence is illustrated.

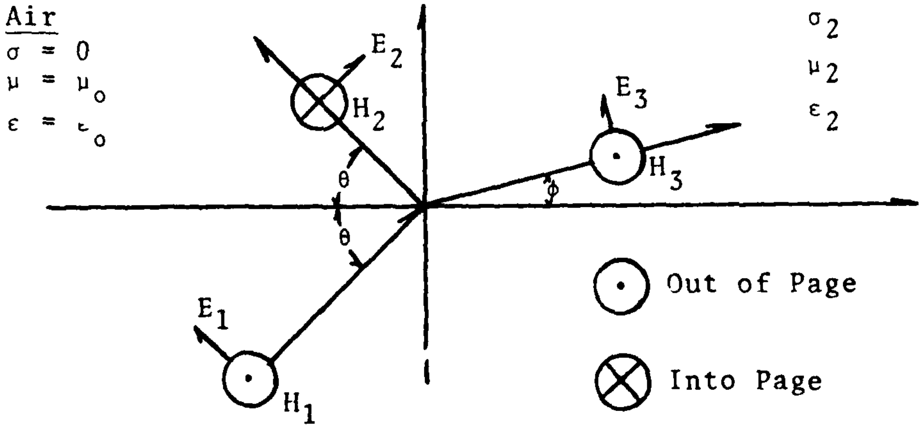

Figure 2: Plane Wave Interface on a Single Boundary

From the previous development we know that

$$\alpha = \omega\sqrt{\frac{\mu_2\varepsilon_2}{2}}\sqrt{1+\sqrt{1+\left(\frac{\sigma_2}{\omega\varepsilon_2}\right)^2}} \qquad (24)$$

$$\gamma = \omega\sqrt{\frac{\mu_2\varepsilon_2}{2}}\sqrt{-1+\sqrt{1+\left(\frac{\sigma_2}{\omega\varepsilon_2}\right)^2}} \qquad (25)$$

$$\beta_2 = \alpha + j\,\gamma \qquad \beta_o \equiv \frac{2\pi}{\lambda} \qquad (26)$$

$$\sin\phi = \beta_o\left(\frac{\alpha - j\gamma}{\alpha^2+\gamma^2}\right)\sin\theta \qquad (27)$$

$$\cos\theta = \sqrt{1-\beta_o^2\,\frac{\sin^2\theta\,(\alpha^2-\gamma^2-j\,2\alpha\gamma)}{(\alpha^2+\gamma^2)^2}} \qquad (28)$$

We will need the real and imaginary parts of $\cos\phi$ later so it is advantageous to calculate them now. We begin by letting $\cos\phi = x + j\,y$ where x and y are defined to be real. Thus,

$$\cos^2\phi = x^2 - y^2 + j\,2xy \qquad (29)$$

Equating real and imaginary parts, we obtain two simultaneous equations:

$$x^2 - y^2 = 1 - \beta_o^2\,\frac{\sin^2\theta\,(\alpha^2-\gamma^2)}{(\alpha^2+\gamma^2)^2} \qquad (30)$$

$$xy = \beta_o^2\,\frac{\sin^2\theta\,\alpha\gamma}{(\alpha^2+\gamma^2)^2} \qquad (31)$$

Solving (30) and (31) by substitution, yields the following

$$x = \sqrt{P + \sqrt{P^2 + Q^2}} \qquad (32)$$

$$y = \sqrt{-P + \sqrt{P^2 + Q^2}} \qquad (33)$$

where

$$P \equiv \frac{1}{2} - \beta_o^2 \frac{\sin^2\theta(\alpha^2-\gamma^2)}{2(\alpha^2+\gamma^2)^2} \tag{34}$$

$$Q \equiv \beta_o^2 \frac{\sin^2\theta \ \alpha \ \gamma}{(\alpha^2+\gamma^2)^2} \tag{35}$$

In the good conductor limit where $(\frac{\sigma}{\omega\epsilon}) >> 1$ these reduce to

$$x = \sqrt{\frac{1}{2} + \frac{1}{2}\sqrt{1 + \frac{1}{4}(\beta_o \ \delta \ \sin\theta)^4}} \tag{36}$$

$$y = \sqrt{-\frac{1}{2} + \frac{1}{2}\sqrt{1 + \frac{1}{4}(\beta_o \ \delta \ \sin\theta)^4}} \tag{37}$$

For example if the incident frequency is 2.5 GHz and σ = 10 mhos/m we have $\cos\phi \simeq 1.00002 + j(.007)$ which indicates that ϕ may be considered to be approximately zero for values of $\sigma > 10$. In some numerical calculations this could vastly shorten the computer time.

By considering the geometry of the problem, we may write the wave vectors as follows:

$$\vec{\beta}_1 = \beta_o (\sin\theta \ \hat{x} + \cos\theta \ \hat{z}) \tag{38}$$

$$\vec{\beta}_2 = \beta_o (\sin\theta \ \hat{x} - \cos\theta \ \hat{z}) \tag{39}$$

$$\vec{\beta}_3 = \beta_2 (\sin\phi \ \hat{x} + \cos\phi \ \hat{z}) \tag{40}$$

Since we are considering an infinite plane, we are interested only in the z dependence of the fields; thus we may take $\vec{r} = z \ \hat{z}$. We have

$$\vec{\beta}_1 \cdot \vec{r} = \beta_o \ z \cos\theta \tag{41}$$

$$\vec{\beta}_2 \cdot \vec{r} = -\beta_o \ z \cos\theta \tag{42}$$

$$\vec{\beta}_3 \cdot \vec{r} = (\alpha + j\gamma)\ z \cos\phi \qquad (43)$$

At this point we divide the problem into two parts since we must consider parallel and perpendicular polarization of the E vector separately.

E Parallel

If $\vec{E}$ is parallel to the plane of incidence we may write the vector fields with reference to the diagram. We have

$$\vec{E}_1 = E_1\, e^{j\,\beta_o z \cos\theta}\ (\cos\theta\ \hat{x} - \sin\theta\ \hat{z}) \qquad (44)$$

$$\vec{H}_1 = \frac{\beta_o}{\omega\mu}\, E_1\, e^{j\,\beta_o\, z \cos\theta}\ \hat{y} \qquad (45)$$

$$\vec{E}_2 = E_2\, e^{-j\,\beta_o\, z \cos\theta}\ (\cos\theta\ \hat{x} + \sin\theta\ \hat{z}) \qquad (46)$$

$$\vec{H}_2 = -\frac{\beta_o}{\omega\mu}\, E_2\, e^{-j\,\beta_o\, z \cos\theta}\ \hat{y} \qquad (47)$$

$$\vec{E}_3 = E_3\, e^{j\,\beta_2\, z \cos\theta}\ (\cos\phi\ \hat{x} - \sin\phi\ \hat{z}) \qquad (48)$$

$$\vec{H}_3 = \frac{\beta_2}{\omega\mu_2}\, E_3\, e^{j\,\beta_2\, z \cos\phi}\ \hat{y} \qquad (49)$$

To satisfy the boundary conditions at z = 0, we equate the tangential field components of E and H there; thus, we have

$$E_1 \cos\theta + E_2 \cos\theta = E_3 \cos\phi \qquad (50)$$

$$\frac{\beta_o}{\omega\mu} E_1 - \frac{\beta_o}{\omega\mu} E_2 = \frac{\beta_2}{\omega\mu_2} E_3 \qquad (51)$$

Since we know the value of E_1, (50) and (51) may be rearranged and written in matrix form as follows [14]

$$\begin{bmatrix} \cos\theta & -\cos\phi \\ \frac{\beta_o}{\mu} & \frac{\beta_2}{\mu_2} \end{bmatrix} \times \begin{bmatrix} E_2 \\ E_3 \end{bmatrix} = \begin{bmatrix} -E_1 \cos\theta \\ \frac{\beta_o}{\mu} E_1 \end{bmatrix} \tag{52}$$

Equation (52) may now be solved to yield values of E_2 and E_3. Before solving (52) we will derive the solution for perpendicular incidence and then develop a common method of solution.

E Perpendicular

We may proceed directly to the field equations; they are given by

$$\vec{E}_1 = E_1 e^{j \beta_o z \cos\theta} \hat{y} \tag{53}$$

$$\vec{H}_1 = \frac{\beta_o}{\omega\mu} E_1 e^{j \beta_o z \cos\theta} (-\cos\theta \hat{x} + \sin\theta \hat{z}) \tag{54}$$

$$\vec{E}_2 = E_2 e^{-j \beta_o z \cos\theta} \hat{y} \tag{55}$$

$$\vec{H}_2 = \frac{\beta_o}{\omega\mu} E_2 e^{-j \beta_o z \cos\theta} (\cos\theta \hat{x} + \sin\theta \hat{z}) \tag{56}$$

$$\vec{E}_3 = E_3 e^{j \beta_2 z \cos\theta} \hat{y} \tag{57}$$

$$\vec{H}_3 = \frac{\beta_2}{\omega\mu_2} E_3 e^{j\beta_2 z \cos\phi} (-\cos\phi \hat{x} + \sin\phi \hat{z}) \tag{58}$$

As before, we apply the boundary conditions at the $z = 0$ interface which yields

$$E_1 + E_2 = E_3 \tag{59}$$

$$-\frac{\beta_o \cos\theta}{\omega\mu} E_1 + \frac{\beta_o \cos\theta}{\omega\mu} E_2 = -\frac{\beta_2 \cos\phi}{\omega\mu_2} E_3 \tag{60}$$

Again these equations simplify and may be put into matrix form.

$$\begin{bmatrix} 1 & -1 \\ \frac{\beta_o}{\mu} \cos\theta & \frac{\beta_2}{\mu_2} \cos\phi \end{bmatrix} \text{x} \begin{bmatrix} E_2 \\ E_3 \end{bmatrix} = \begin{bmatrix} -E_1 \\ \frac{\beta_o}{\mu} \cos\theta \end{bmatrix} \tag{61}$$

Analytic Solution

Equations (52) and (61) may be solved directly with little difficulty; however, since we are developing a general technique for a multi-layer system, it is worthwhile to do the solution numerically. The technique is relatively straight forward in that the coefficient matrices are loaded into a computer along with the constant vector. For example, if we have the matrix equation $Ax = B$, we would load the auxiliary matrix

$$\left[\begin{array}{ccc:c} a_{11} & --- & a_{1n} & b_1 \\ \vdots & a_{22} \ddots & \vdots & \vdots \\ a_{n1} & --- & a_{nn} & b_n \end{array}\right] \tag{62}$$

into the computer. It would be an $N \times N + 1$ dimensional matrix. We then do a Gauss-Jordan row reduction to put the A portion into identity format. The B column will now correspond to the solution vector of x. This is relatively easy to program unless A happens to be complex. In this case the complex equation Ax = B may be expanded into its real and imaginary parts to yield a matrix equation of only real terms which may be handled in a straight forward manner. For example if the set of equations,

$$a_{11} x_1 + a_{12} x_2 = b_1 \tag{63}$$

$$a_{21} x_1 + a_{22} x_2 = b_2 \tag{64}$$

is complex, we may in complex notation write a complex matrix equation as

$$\begin{bmatrix} a_{11} & a_{12} \\ a_{21} & a_{22} \end{bmatrix} \times \begin{bmatrix} x_1 \\ x_2 \end{bmatrix} = \begin{bmatrix} b_1 \\ b_2 \end{bmatrix} \tag{65}$$

Likewise we may write (63) and (64) in an expanded format in terms of its real and imaginary parts. If we let R and I designate Real and Imaginary respectively, we have

$$(Ra_{11}+jIa_{11})(Rx_1+jIx_1) + (Ra_{12}+jIa_{12})(Rx_2+jIx_2) = Rb_1 + jIb_1 \tag{66}$$

$$(Ra_{21}+jIa_{21})(Rx_1+jIx_1) + (Ra_{22}+jIa_{22})(Rx_2+jIx_2) = Rb_2 + jIb_2 \qquad (67)$$

Equating real and imaginary parts in (66) and (67) we have

$$Ra_{11}\ Rx_1 - Ia_{11}\ Ix_1 + Ra_{12}\ Rx_2 - Ia_{12}\ Ix_2 = Rb_1 \qquad (68)$$

$$Ia_{11}\ Rx_1 + Ra_{11}\ Ix_1 + Ia_{12}\ Rx_2 + Ra_{12}\ Ix_2 = Ib_1 \qquad (69)$$

$$Ra_{21}\ Rx_1 - Ia_{21}\ Ix_1 + Ra_{22}\ Rx_2 - Ia_{22}\ Ix_2 = Rb_2 \qquad (70)$$

$$Ia_{21}\ Rx_1 + Ra_{21}\ Ix_1 + Ia_{22}\ Rx_2 + Ra_{22}\ Ix_2 = Ib_2 \qquad (71)$$

or in matrix format we have a matrix of real terms only written as follows[15]:

$$\left[\begin{array}{cc|cc} Ra_{11} & -Ia_{11} & Ra_{12} & -Ia_{12} \\ Ia_{11} & Ra_{11} & Ia_{12} & Ra_{12} \\ \hline Ra_{21} & -Ia_{21} & Ra_{22} & -Ia_{22} \\ Ia_{21} & Ra_{21} & Ia_{22} & Ra_{22} \end{array}\right] \times \begin{bmatrix} Rx_1 \\ Ix_1 \\ Rx_2 \\ Ix_2 \end{bmatrix} = \begin{bmatrix} Rb_1 \\ Ib_1 \\ Rb_2 \\ Ib_2 \end{bmatrix} \qquad (72)$$

Thus, to numerically solve a 2 x 2 complex matrix a computer must reduce a 4 x 4 matrix, and in general to solve an N x N complex matrix we must generate a 2N x 2N real matrix.

There are some advantages to this approach in that after the reduction is complete we have all our variables written in real and imaginary format. Also, the expanded matrix is easy to generate if one partitions the original complex matrix and then notes that each complex element goes into a 2 x 2 matrix that is nearly semetric except for one sign.

Numeric Solution

The numeric solution takes the material characteristics (σ_2,μ_2, ϵ_2) and then constructs the expanded auxiliary matrix, Para (I,J) and Perp (I,J) corresponding to the Parallel or Perpendicular solutions respectively. The program then does a Gauss-Jordan elimination for each of these as it iterates through 1° increments from 0 to 90°. For each iteration a reflectivity coefficient is calculated and stored. After the routine is complete the reflectivity coefficients are plotted as a function of θ for both parallel and perpendicular polarizations on the same plot. Additionally a plot of spectral emissivity (absorbance) is calculated. For the emissivity, λ is set equal to 3 μm and is calculated as ϵ = (1 - Reflectivity). The result is then plotted as ϵ versus θ. The program written for a Hewlett-Packard 9845B computer is listed in appendix C. Figures 3 through 10 are the microwave reflectance and emissivity plots for a dielectric and a conductor with conductivities of 0, 3, 500, and $5\text{x}10^7$ mhos/meter respectively.

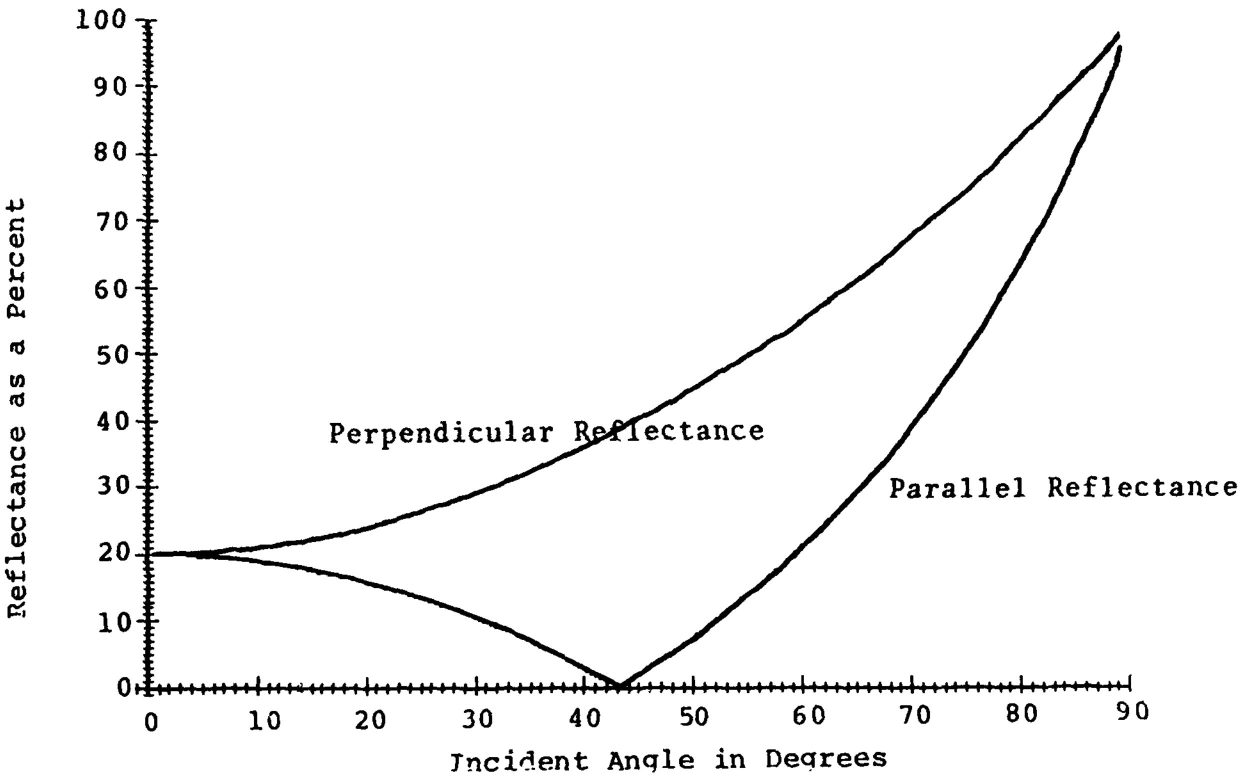

Figure 3: Reflectance from a Single Plane Interface (σ=0)

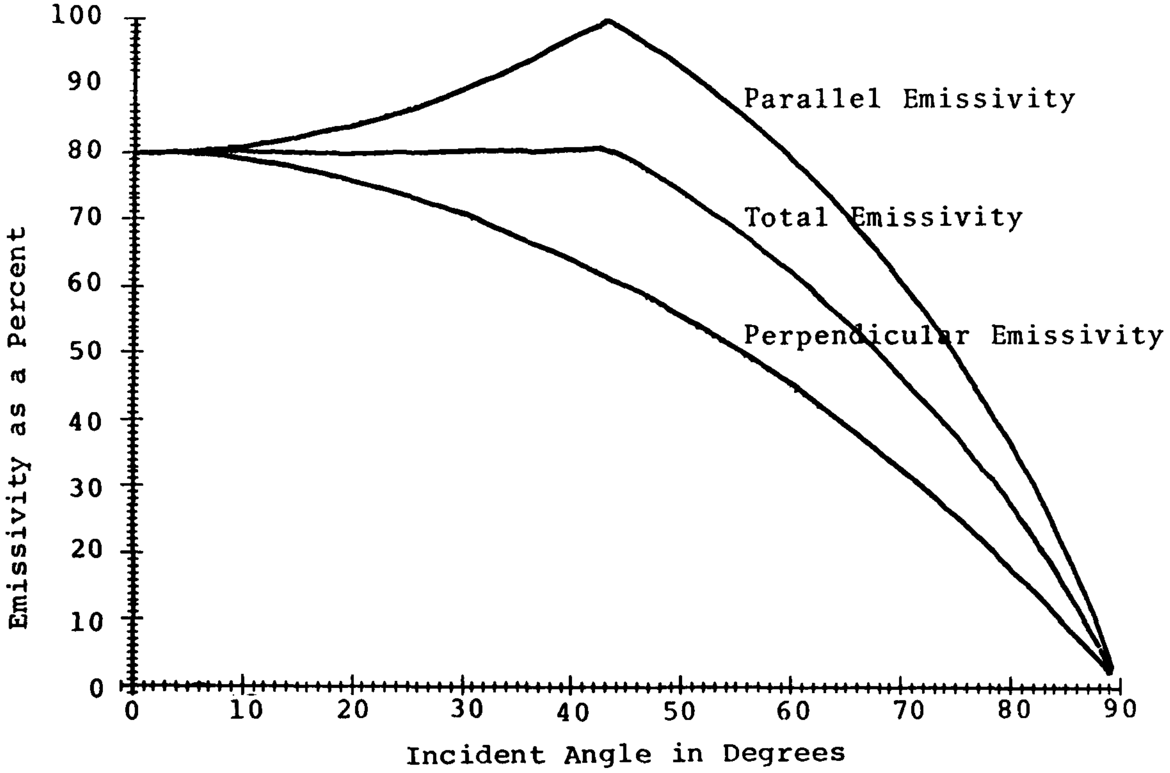

Figure 4: Directional Spectral Emissivity at 3 Microns ($\sigma=0$)

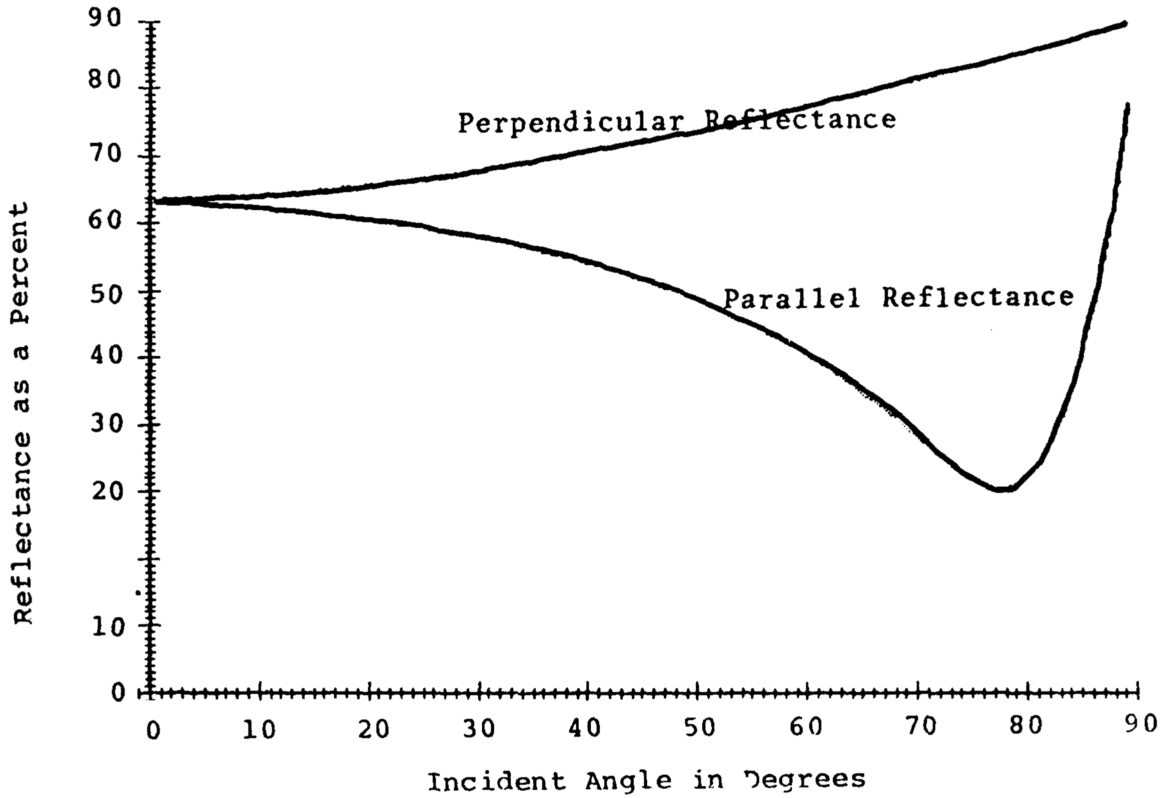

Figure 5: Reflectance from a Single Plane Interface (σ=3.00 mhos/m)

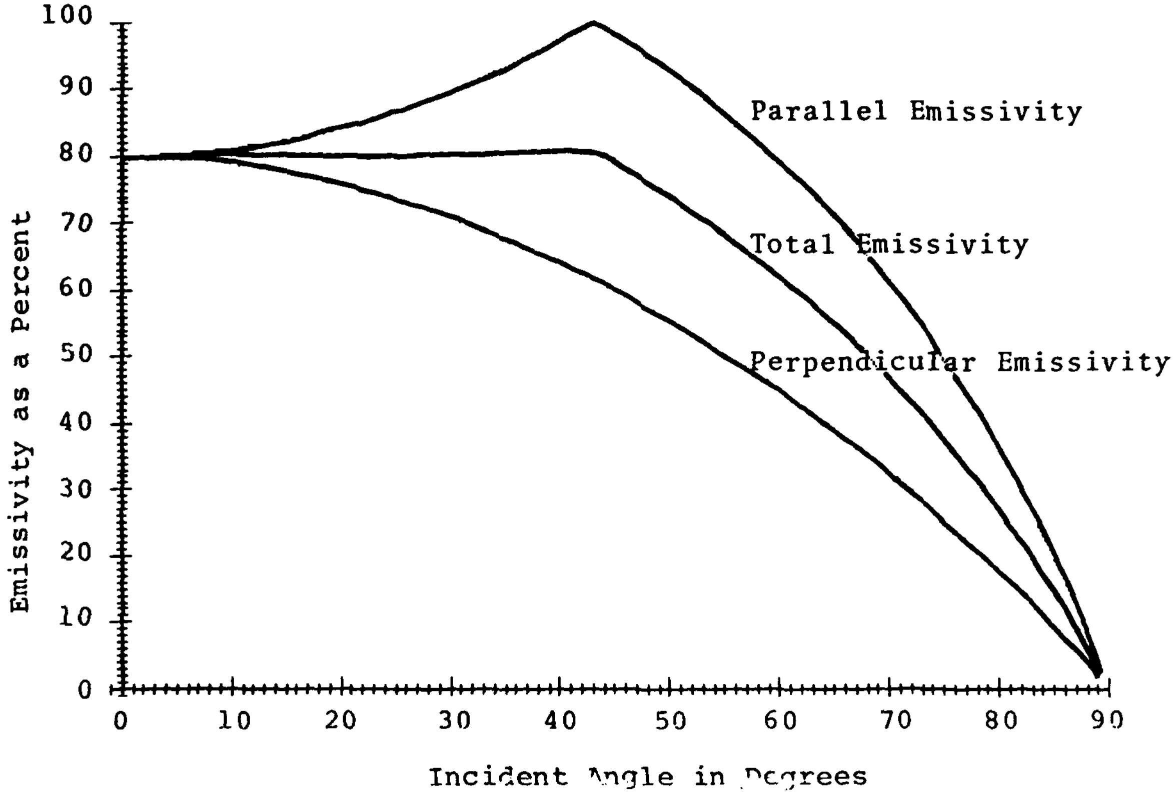

Figure 6: Directional Spectral Emissivity at 3 Microns (σ=3 mhos/m)

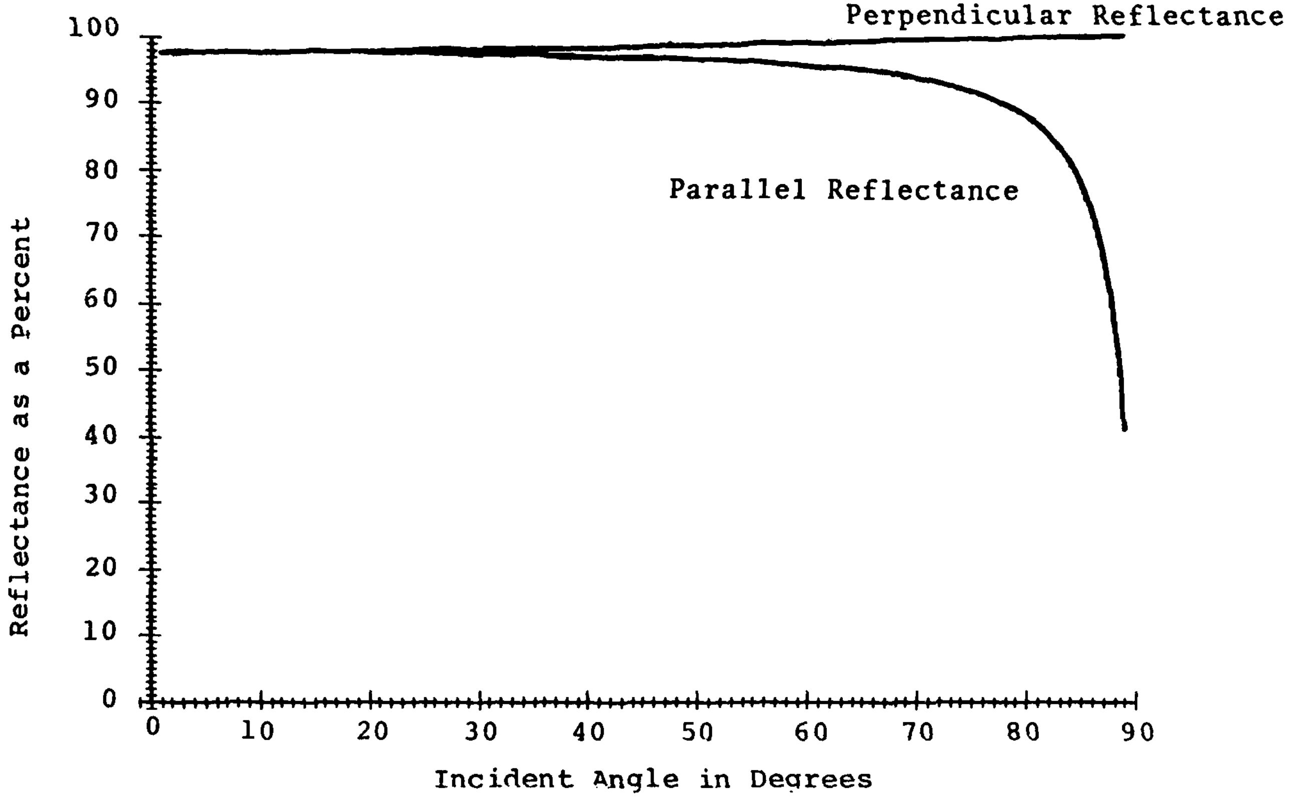

Figure 7: Reflectance from a Single Plane Interface (σ=500 mhos/m)

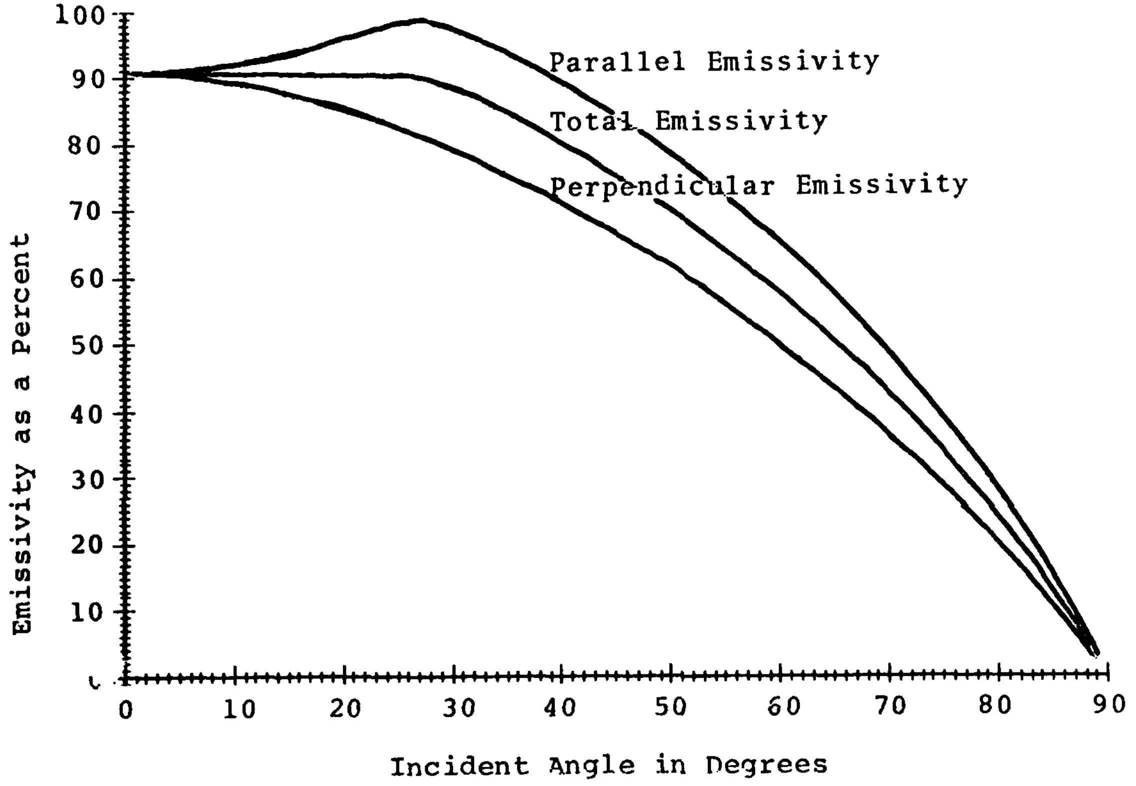

Figure 8: Directional Spectral Emissivity at 3 Microns (σ=500 mhos/m)

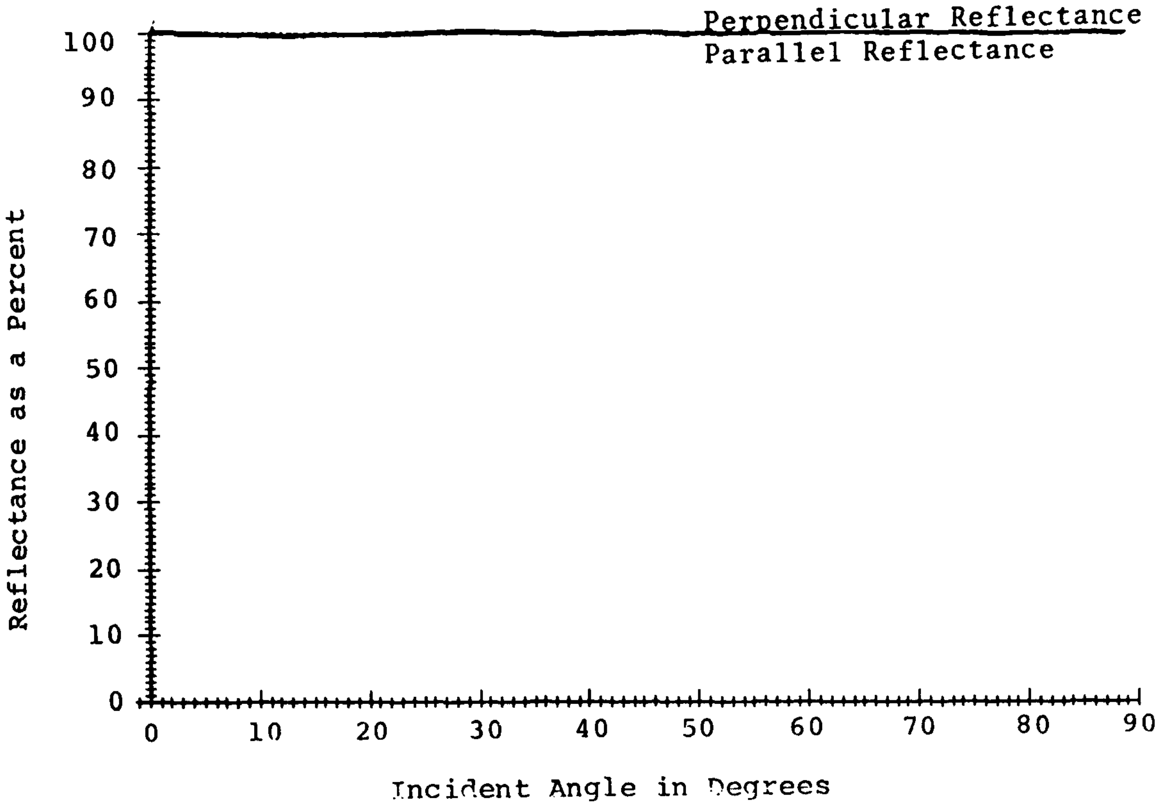

Figure 9: Reflectance from a Single Plane Interface (Copper)

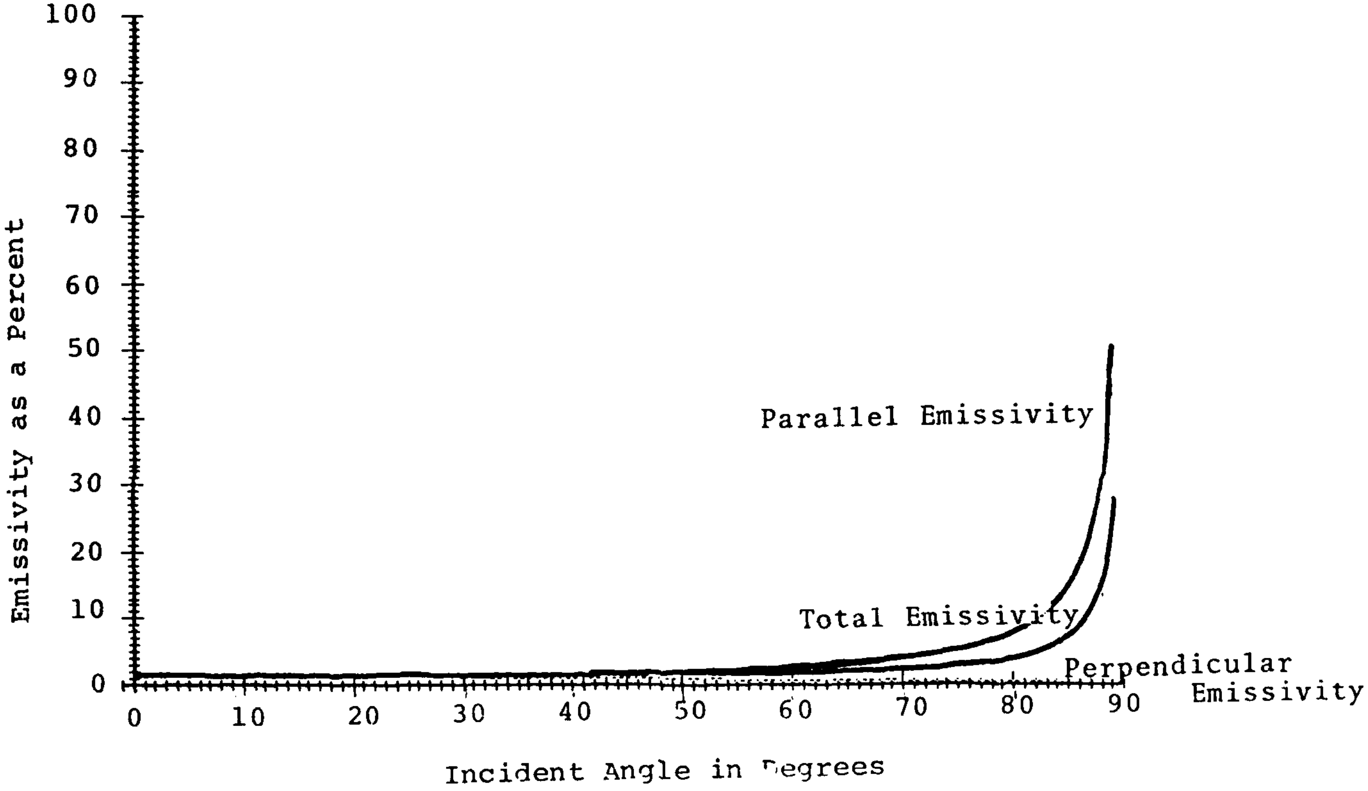

Figure 10: Directional Spectral Emissivity at 3 Microns (Copper)

CHAPTER IV

ELECTROMAGNETIC N-LAYER ANALYSIS

We now consider the problem of N-layers with air on each side. See the diagram below.

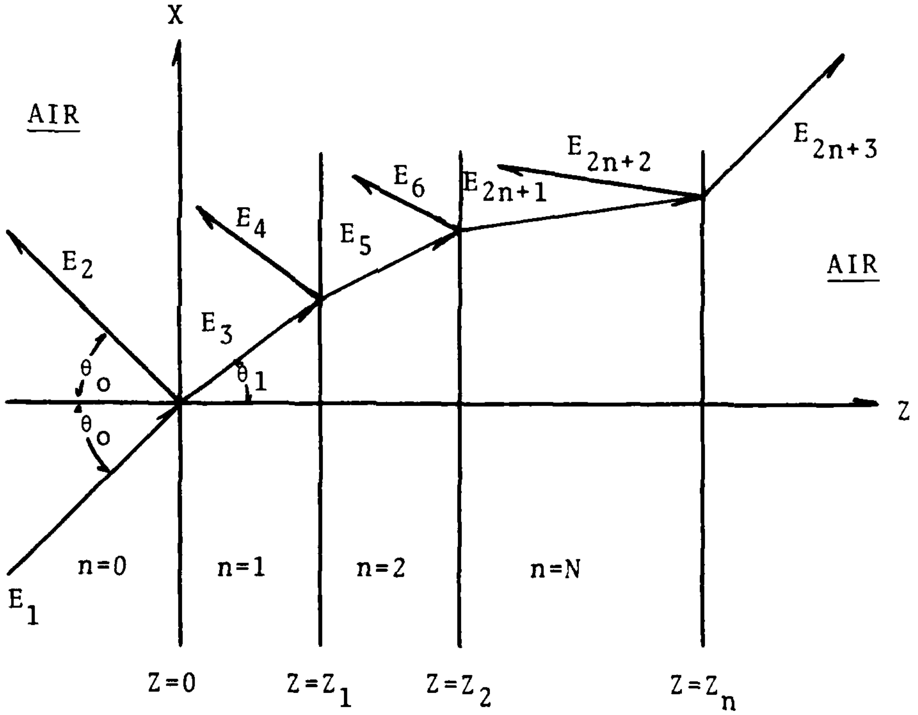
X
AIR
E_2
E_4
E_5
E_6
E_{2n+1}
E_{2n+2}
E_{2n+3}
AIR
E_3
θ_o
θ_1
θ_o
Z
E_1
n=0
n=1
n=2
n=N
Z=0
$Z=Z_1$
$Z=Z_2$
$Z=Z_n$

Figure 11: N-Layer Electromagnetic Interaction

Since we have N separate layers, E_{2n+1} defines the electric field of the wave traveling to the right in material n and E_{2n+2} defines the wave traveling to the left. As in the single boundary case, we may write the field components in each layer as follows:

E Parallel

$$\vec{E}_1 = E_1 e^{j\beta_o z \cos\theta_o} (\cos\theta_o \hat{x} - \sin\theta_o \hat{z}) \tag{73}$$

$$\vec{H}_1 = \frac{\beta_o}{\omega\mu} E_1 e^{j\beta_o z \cos\theta_o} \hat{y} \tag{74}$$

$$\vec{E}_2 = E_2 e^{-j\beta_o z \cos\theta_o} (\cos\theta_o \hat{x} + \sin\theta_o \hat{z}) \tag{75}$$

$$\vec{H}_2 = -\frac{\beta_o}{\omega\mu} E_2 e^{-j\beta_o z \cos\theta} \hat{y} \tag{76}$$

$$\vec{E}_3 = E_3 e^{j\beta_1 z \cos\theta_1} (\cos\theta_1 \hat{x} - \sin\theta_1 \hat{z}) \tag{77}$$

$$\vec{H}_3 = \frac{\beta_1}{\omega\mu_1} E_3 e^{j\beta_1 z \cos\theta_1} \hat{y} \tag{78}$$

$$\vec{E}_4 = E_4 e^{-j\beta_1 z \cos\theta_1} (\cos\theta_1 \hat{x} + \sin\theta_1 \hat{z}) \tag{79}$$

$$\vec{H}_4 = -\frac{\beta_1}{\omega\mu_1} E_4 e^{-j\beta_1 z \cos\theta_1} \hat{y} \tag{80}$$

$$\vdots \qquad\qquad \vdots$$

$$\vec{E}_{2n+1} = E_{2n+1} e^{j\beta_n z \cos\theta_n} (\cos\theta_n \hat{x} - \sin\theta_n \hat{z}) \tag{81}$$

$$\vec{H}_{2n+1} = \frac{\beta_n}{\omega\mu_n} E_{2n+1} e^{j\beta_n z \cos\theta_n} \hat{y} \tag{82}$$

$$\vec{E}_{2n+2} = E_{2n+2} e^{-j\beta_n z \cos\theta_n} (\cos\theta_n \hat{x} + \sin\theta_n \hat{z}) \tag{83}$$

$$\vec{H}_{2n+2} = -\frac{\beta_n}{\omega\mu_n} E_{2n+2} e^{-j\beta_n z \cos\theta_n} \hat{y} \tag{84}$$

$$\vec{E}_{2n+3} = E_{2n+3} e^{j\beta_o z \cos\theta_o} (\cos\theta_o \hat{x} - \sin\theta_o \hat{z}) \tag{85}$$

$$\vec{H}_{2n+3} = \frac{\beta_o}{\omega\mu} E_{2n+3} e^{j\beta_o z \cos\theta_o} \hat{y} \tag{86}$$

E Perpendicular

$$\vec{E}_1 = E_1 e^{j\beta_o z\cos\theta_o}\,\hat{y} \tag{87}$$

$$\vec{H}_1 = \frac{\beta_o}{\omega\mu} E_1 e^{j\beta_o z\cos\theta_o}\,(-\cos\theta_o\hat{x} + \sin\theta_o\hat{z}) \tag{88}$$

$$\vec{E}_2 = E_2 e^{-j\beta_o z\cos\theta_o}\,\hat{y} \tag{89}$$

$$\vec{H}_2 = \frac{\beta_o}{\omega\mu} E_2 e^{-j\beta_o z\cos\theta_o}\,(\cos\theta\,\hat{x} + \sin\theta\,\hat{z}) \tag{90}$$

$$\vec{E}_3 = E_3 e^{j\beta_1 z\cos\theta_1}\,\hat{y} \tag{91}$$

$$\vec{H}_3 = \frac{\beta_1}{\omega\mu_1} E_3 e^{j\beta_1 z\cos\theta_1}\,(-\cos\theta_1\,\hat{x} + \sin\theta_1\,\hat{z}) \tag{92}$$

$$\vec{E}_4 = E_4 e^{-j\beta_1 z\cos\theta_1}\,\hat{y} \tag{93}$$

$$\vec{H}_4 = \frac{\beta_1}{\omega\mu_1} E_4 e^{-j\beta_1 z\cos\theta_1}\,(\cos\theta_1\,\hat{x} + \sin\theta_1\,\hat{z}) \tag{94}$$

$$\vdots \qquad\qquad \vdots$$

$$\vec{E}_{2n+1} = E_{2n+1}\, e^{j\beta_n z\cos\theta_n}\,\hat{y} \tag{95}$$

$$\vec{H}_{2n+1} = \frac{\beta_n}{\omega\mu_n} E_{2n+1}\, e^{j\beta_n z\cos\theta_n}\,(-\cos\theta_n\,\hat{x} + \sin\theta_n\,\hat{z}) \tag{96}$$

$$\vec{E}_{2n+2} = E_{2n+2}\, e^{-j\beta_n z\cos\theta_n}\,\hat{y} \tag{97}$$

$$\vec{H}_{2n+2} = \frac{\beta_n}{\omega\mu_n} E_{2n+2}\, e^{-j\beta_n z\cos\theta_n}\,(\cos\theta_n\,\hat{x} + \sin\theta_n\,\hat{z}) \tag{98}$$

$$\vec{E}_{2n+3} = E_{2n+3}\, e^{j\beta_o z\cos\theta_o}\,\hat{y} \tag{99}$$

$$\vec{H}_{2n+3} = \frac{\beta_o}{\omega\mu} E_{2n+3}\, e^{j\beta_o z\cos\theta_o}\,(-\cos\theta_o\,\hat{x} + \sin\theta_o\,\hat{z}) \tag{100}$$

Application of the tangential boundary conditions at the interface yields the following:

E Parallel

$z = 0$:

$$E_1 \cos\theta_o + E_2 \cos\theta_o = E_3 \cos\theta_1 + E_4 \cos\theta_1 \tag{101}$$

$$E_1 \frac{\beta_o}{\mu} - E_2 \frac{\beta_o}{\mu} = E_3 \frac{\beta_1}{\mu_1} - E_4 \frac{\beta_1}{\mu_1} \tag{102}$$

$z = z_1$:

$$\begin{aligned} &E_3 \cos\theta_1 \, e^{j\beta_1 z_1 \cos\theta_1} + E_4 \cos\theta_1 \, e^{-j\beta_1 z_1 \cos\theta_1} = \\ &E_5 \cos\theta_2 \, e^{j\beta_2 z_1 \cos\theta_2} + E_6 \cos\theta_2 \, e^{-j\beta_2 z_1 \cos\theta_2} \end{aligned} \tag{103}$$

$$\begin{aligned} &E_3 \frac{\beta_1}{\mu_1} e^{j\beta_1 z_1 \cos\theta_1} - E_4 \frac{\beta_1}{\mu_1} e^{-j\beta_1 z_1 \cos\theta_1} = \\ &E_5 \frac{\beta_2}{\mu_2} e^{j\beta_2 z_1 \cos\theta_2} - E_6 \frac{\beta_2}{\mu_2} e^{-j\beta_2 z_1 \cos\theta_2} \end{aligned} \tag{104}$$

$$\vdots \qquad\qquad\qquad \vdots$$

$z = z_n$:

$$\begin{aligned} &E_{2n+1} \cos\theta_n \, e^{j\beta_n z_n \cos\theta_n} + E_{2n+2} \cos\theta_n \, e^{-j\beta_n z_n \cos\theta_n} = \\ &E_{2n+3} \cos\theta_o \, e^{j\beta_o z_n \cos\theta_o} \end{aligned} \tag{105}$$

$$\begin{aligned} &E_{2n+1} \frac{\beta_n}{\mu_n} e^{j\beta_n z_n \cos\theta_n} - E_{2n+2} \frac{\beta_n}{\mu_n} e^{-j\beta_n z_n \cos\theta_n} = \\ &E_{2n+3} \frac{\beta_o}{\mu} e^{j\beta_o z_n \cos\theta_n} \end{aligned} \tag{106}$$

E Perpendicular

$z = 0$:

$$E_1 + E_2 = E_3 + E_4 \tag{107}$$

$$-E_1 \frac{\beta_o\cos\theta_o}{\mu} + E_2 \frac{\beta_o\cos\theta_o}{\mu} = -E_3 \frac{\beta_1\cos\theta_1}{\mu_1} + E_4 \frac{\beta_1\cos\theta_1}{\mu_1} \tag{108}$$

$z = z_1$:

$$\begin{aligned} &E_3\ e^{j\beta_1 z_1\cos\theta_1} + E_4\ e^{-j\beta_1 z_1\cos\theta_1} = \\ &E_5\ e^{j\beta_2 z_1\cos\theta_2} + E_6\ e^{-j\beta_2 z_1\cos\theta_2} \end{aligned} \tag{109}$$

$$\begin{aligned} &-E_3 \frac{\beta_1}{\mu_1} \cos\theta_1\ e^{j\beta_1 z_1\cos\theta_1} + E_4 \frac{\beta_1\cos\theta_1}{\mu_1}\ e^{-j\beta_1 z_1\cos\theta_1} = \\ &-E_5 \frac{\beta_2\cos\theta_2}{\mu_2}\ e^{j\beta_2 z_1\cos\theta_2} + E_6 \frac{\beta_2\cos\theta_2}{\mu_2}\ e^{-j\beta_2 z_1\cos\theta_2} \end{aligned} \tag{110}$$

$z = z_n$:

$$E_{2n+1}\ e^{j\beta_n z_n\cos\theta_n} + E_{2n+2}\ e^{-j\beta_n z_n\cos\theta_n} = E_{2n+3}\ e^{j\beta_o z_n\cos\theta_o} \tag{111}$$

$$\begin{aligned} &-E_{2n+1} \frac{\beta_n\cos\theta_n}{\mu_n}\ e^{j\beta_n z_n\cos\theta_n} + E_{2n+2} \frac{\beta_n\cos}{\mu_n}\ n\ e^{-j\beta_n z_n\cos\theta_n} = \\ &-E_{2n+3} \frac{\beta_o\cos\theta_o}{\ }\ e^{j\beta_o z_n\cos\theta_o} \end{aligned} \tag{112}$$

Thus, we have generated N equations with N unknowns for both parallel and perpendicular incidence. These equations may easily be consolidated into matrix format; see Figures 12 and 13. Figure 14 is an example plot of a three layer system with layer conductivities of .5, 1, and

$$
\left[\begin{array}{ccccccccc:c}
\frac{k_o}{\beta_o} & -\frac{k_1}{\beta_1} & -\frac{k_1}{\beta_1} & 0 & 0 & \cdots & 0 & 0 & 0 & -E_1\frac{k_o}{\beta_o} \\
-\frac{\beta_o}{\mu} & -\frac{\beta_1}{\mu_1} & \frac{\beta_1}{\mu_1} & 0 & 0 & \cdots & & & 0 & -E_1\frac{\beta_o}{\mu} \\
0 & \frac{k_1}{\beta_1}e^{jz_1k_1} & \frac{k_1}{\beta_1}e^{-jz_1k_1} & -\frac{k_2}{\beta_2}e^{jz_1k_2} & -\frac{k_2}{\beta_2}e^{-jz_1k_2} & \cdots & & & 0 & 0 \\
0 & \frac{\beta_1}{\mu_1}e^{jz_1k_1} & -\frac{\beta_1}{\mu_1}e^{-jz_1k_1} & -\frac{\beta_2}{\mu_2}e^{jz_1k_2} & \frac{\beta_2}{\mu_2}e^{-jz_1k_2} & \cdots & \vdots & \vdots & 0 & 0 \\
0 & 0 & 0 & \frac{k_2}{\beta_2}e^{jz_2k_2} & \frac{k_2}{\beta_2}e^{-jz_2k_2} & \cdots & & & 0 & 0 \\
\vdots & \vdots & \vdots & \frac{\beta_2}{\mu_2}e^{jz_2k_2} & -\frac{\beta_2}{\mu_2}e^{-jz_2k_2} & \cdots & & & 0 & 0 \\
\vdots & \vdots & \vdots & \cdot & \cdot & \cdots & 0 & 0 & 0 & 0 \\
0 & 0 & 0 & 0 & 0 & \cdots & \frac{k_n}{\beta_n}e^{jz_nk_n} & \frac{k_n}{\beta_n}e^{-jz_nk_n} & -\frac{k_o}{\beta_o}e^{jz_nk_o} & 0 \\
0 & 0 & 0 & 0 & 0 & \cdots & \frac{\beta_n}{\mu_n}e^{jz_nk_n} & -\frac{\beta_n}{\mu_n}e^{-jz_nk_n} & -\frac{\beta_o}{\mu}e^{jz_nk_o} & 0
\end{array}\right]
$$

Figure 12: Auxiliary Matrix for Parallel Polarization ($k_n = \beta_n \mathrm{Cos}\theta_n$)

$$\left[\begin{array}{cccccccccc|c}
1 & -1 & -1 & 0 & 0 & \cdots & 0 & 0 & 0 & & -E_1 \\
-\frac{k_o}{\mu} & -\frac{k_1}{\mu_1} & \frac{k_1}{\mu_1} & 0 & 0 & \cdots & & & 0 & & -\frac{k_o}{\mu}E_1 \\
0 & e^{jz_1k_1} & e^{-jz_1k_1} & -e^{jz_1k_2} & -e^{-jz_1k_2} & \cdots & & & 0 & & 0 \\
0 & \frac{k_1}{\mu_1}e^{jz_1k_1} & -\frac{k_1}{\mu_1}e^{-jz_1k_1} & -\frac{k_2}{\mu_2}e^{jz_1k_2} & \frac{k_2}{\mu_2}e^{-jz_1k_2} & \cdots & \cdot & \cdot & \cdot & & \cdot \\
0 & 0 & 0 & e^{jz_2k_2} & e^{-jz_2k_2} & \cdots & \cdot & \cdot & \cdot & & \cdot \\
\vdots & \vdots & \vdots & \frac{k_2}{\mu_2}e^{jz_2k_2} & -\frac{k_2}{\mu_2}e^{-jz_2k_2} & \cdots & \cdot & \cdot & \cdot & & \cdot \\
\vdots & \vdots & \vdots & \vdots & \vdots & \cdots & 0 & 0 & 0 & & 0 \\
0 & 0 & 0 & 0 & 0 & \cdots & e^{jz_nk_n} & e^{-jz_nk_n} & -e^{jz_nk_o} & & 0 \\
0 & 0 & 0 & 0 & 0 & \cdots & \frac{k_n}{\mu_n}e^{jz_nk_n} & -\frac{k_n}{\mu_n}e^{-jz_nk_n} & -\frac{k_o}{\mu}e^{jz_nk_o} & & 0
\end{array}\right]$$

Figure 13: Auxiliary Matrix for Perpendicular Polarization ($k_n = \beta_n \text{Cos}\theta_n$)

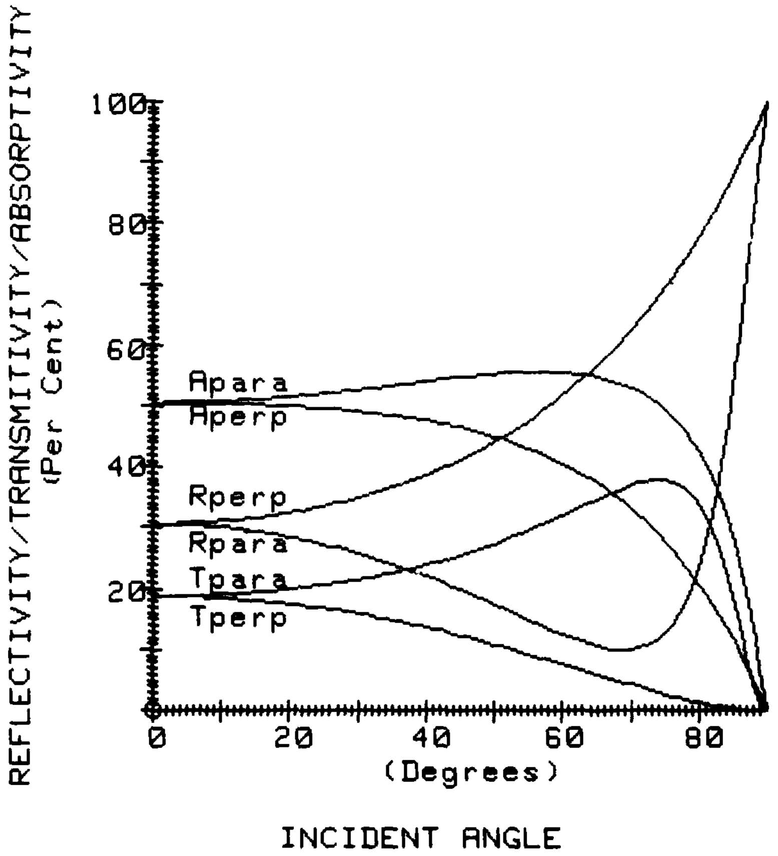

Figure 14: Three Layer Electromagnetic Response

1.5 mho/m respectively. See Appendix D for a listing of the computer program written for a Hewlett-Packard 9845B computer; it will handle up to 10 layers.

It should be pointed out that this is not the first time the electromagnetic N-layer problem has been solved. Hansen[16] develops a procedure in which explicit equations are derived for the mean-square electric fields induced by plane electromagnetic radiation in a single boundary, single layer, and N-layer system. His approach is to allow for a complex permittivity in the energy absorption process rather than using Ohm's law explicitly in the solution of Maxwell's equations. It is for this reason and as a result of the desire to present a more straight forward approach, that the preceding chapter was developed. Additionally, interested readers may also refer to Wait[17] for an in-depth discussion of electromagnetic absorption by stratified media. Most of Wait's discussion is directed at the electromagnetic interaction occurring at the surface of a stratified earth.

CHAPTER V

THERMAL ANALYSIS

The simplest analysis is one that assumes a steady state situation with no heat losses at the $z=z_n$ interface. In practice this is not a bad assumption since our Nth layer may be made of a low thermal conductivity material such as one of the many foams available. Also, it has been demonstrated that for relatively thin layers (thickness less than one millimeter) steady state is reached very quickly (in most cases less than five minutes for 10 mW/cm^2 incident power).

A rough estimate for the transient response of the system may be made as follows. Consider the semi-infinite slab insulated at z=L as shown in Figure 15 below.

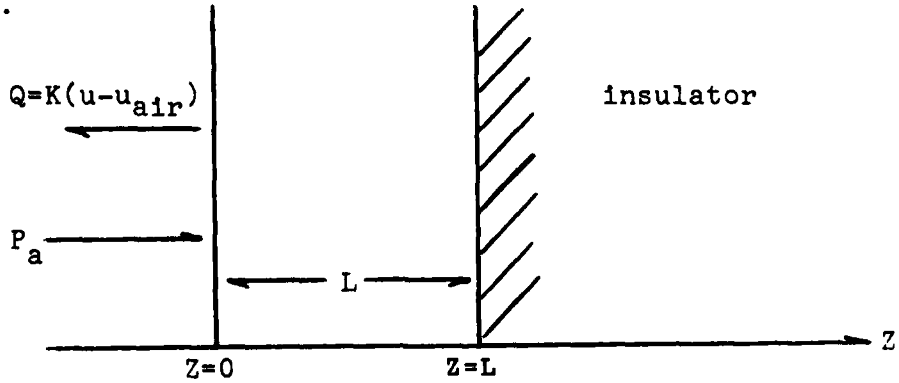

Figure 15: Three Layer Thermal Transient Response

P_a = total absorbed power (watt/m^2)

Q = total heat loss (Newton cooling)

u = temperature of the layer (K) which is assumed uniform throughout

If u is assumed constant throughout our thin layer (this assumes the thermal conductivity, κ, is large or the thickness, L, is small or both for the layer), we may write the energy equation for the system as follows:

$$P_a \Delta t = K(U-U_{air})\ \Delta t + \rho c\ \Delta u\ L \qquad (113)$$

where Δt = time (s)

K = constant ($J/s\text{-}m^2\text{-}K$)

ρ = mass density (Kg/m^3)

c = specific heat (J/Kg-K)

Solving for $\Delta u/\Delta t$, we have

$$\frac{\Delta u}{\Delta t} = \frac{1}{\rho c L}\ P_a - K(U - U_{air}) \qquad (114)$$

Taking the limit as $\Delta t \to 0$, we have

$$\frac{du}{dt} = \frac{1}{\rho c L}\ P_a - K(U - U_{air}) \qquad (115)$$

This is a linear homogenous differential equation which has a solution given by

$$U = U_{air} + \frac{P_a}{K}\left(1 - e^{-\frac{K}{\rho c L} t}\right) \qquad (116)$$

Thus, we may calculate a time constant τ given by

$$\tau = \frac{\rho c L}{K} \qquad (117)$$

For example, a thin layer of water 100 microns thick has a time constant of approximately 210 sec or about 3.5 minutes which is in agreement with our experimental observation. Finally, a thin system made up of N layers would yield a heat term given as $\Delta u \sum_{i=1}^{N} \rho_i c_i L_i$ if the layers are heated at a relatively constant rate (same u throughout); hence the time constant for the layered system may be approximated by

$$\tau \simeq \frac{1}{K} \sum_{i=1}^{N} \rho_i c_i L_i \qquad (118)$$

It is important to point out that the above development assumed a linear heat loss at the z=0 surface. In fact, this term consists of a convective term and a radiative (infrared) term which is in no way linear for large temperature increases (large P_a). However, the steady state surface temperature may still be calculated using numerical techniques for this non-linear case.

We begin the steady state solution as before by writing the energy equation for the system; thus, we have absorbed power, P_a, equal to convective losses, Q_{con}, plus infrared losses, Q_{ir}. For the two loss terms we have[18,19,20]

$$Q_{con} = h\ (U_o - U_{air})$$

and

$$Q_{ir} = F_e \gamma\ (U_o^4 - U_{air}^4)$$

where

h = convective heat transfer coefficient(watt/m^2-K)

U_o= steady state surface temperature (K)

U_{air}= ambient air temperature (K)

F_e= surface emissivity

γ = Stefan-Boltzman constant(5.67×10^{-8} watt/m^2-K^4)

It has been shown that h for a vertical flat plate may be approximated by [21]

$$h \simeq \frac{1.42\,(U_o - U_{air})^{\delta}}{H^{\delta}}$$

where H is the plate height and δ is a number that falls in the range $.1 < \delta < .6$. The number, δ, is a function of such things as atmospheric pressure, humidity, etc. Furthermore, P_a is simply the incident power minus the reflected and transmitted power; therefore, we may write,

$$\tfrac{1}{2}\sqrt{\frac{\varepsilon_o}{\mu_o}}\,({E_1}^2 - {E_2}^2 - {E_{2n+3}}^2) = \frac{1.42}{H^{\delta}}\,(U_o - U_{air})^{1+\delta} + F_e\gamma\,(U_o^4 - U_{air}^4) \quad (119)$$

It is important to note that it is necessary to consider both convection and infrared radiation in the temperature range near 20C as indicated in Figures 16 through 18. This figure illustrates the ratio of Q_{ir}/Q_{con} for a surface temperature increase of 10C with an ambient air temperature of 20C. This ratio is nominally between 1 and 2 over this range indicating that both processes are significant in the energy loss transport and therefore each must be considered.

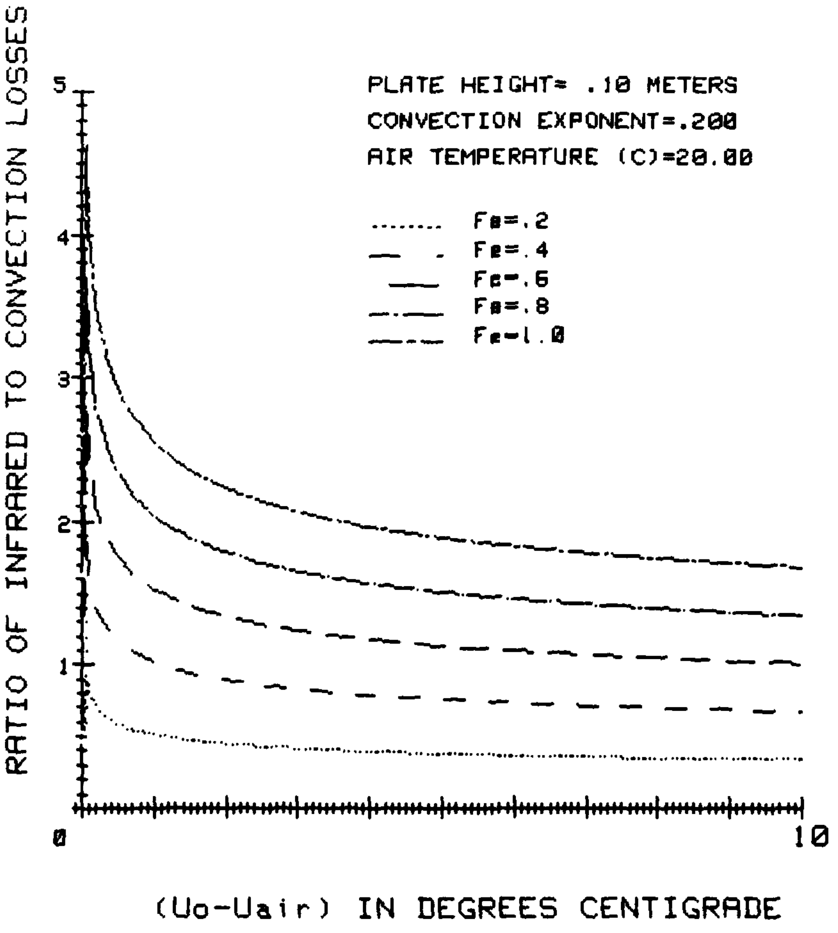

Figure 16: Infrared Versus Convection Comparison

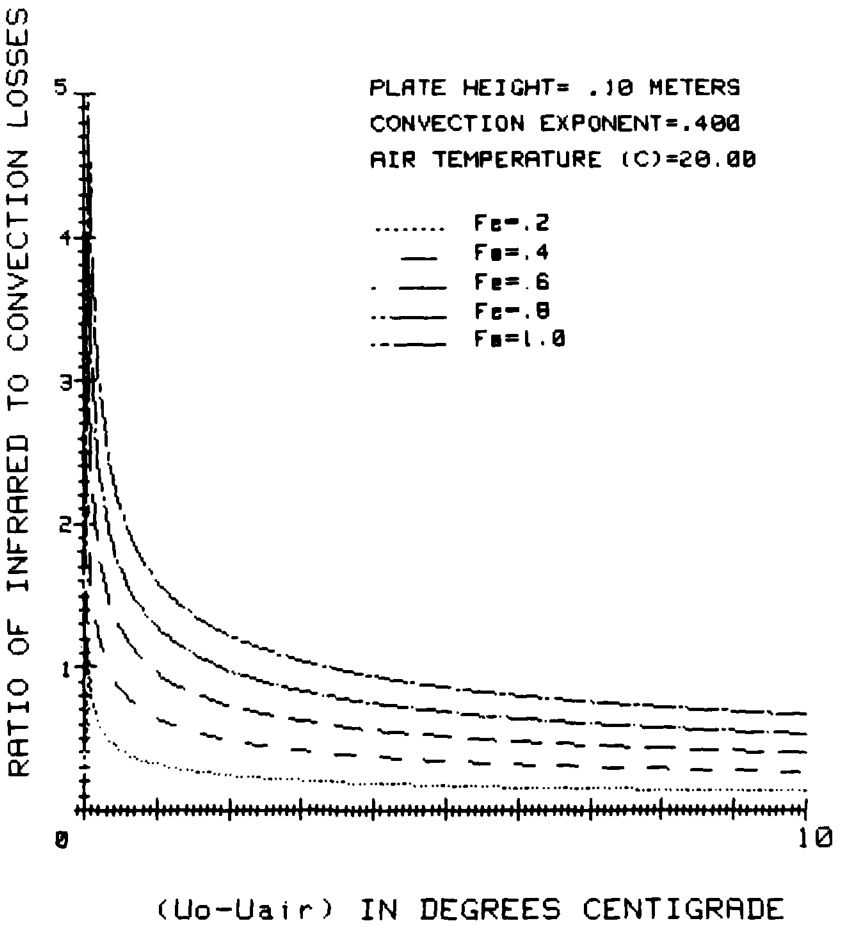

Figure 17: Infrared Versus Convection Comparison

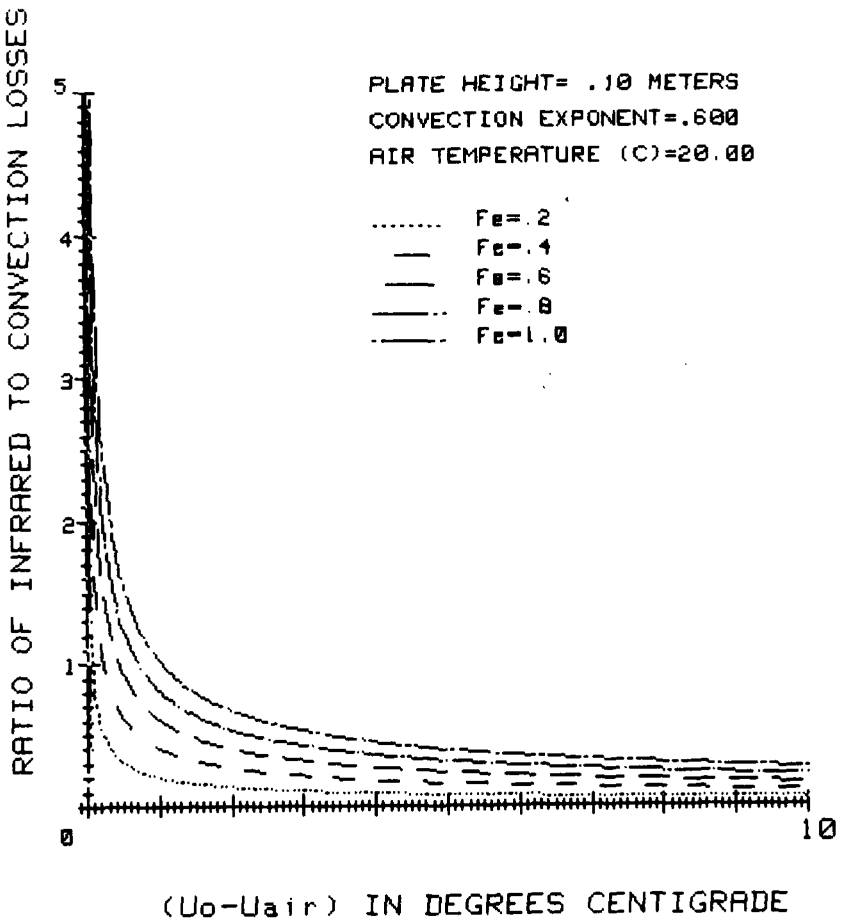

Figure 18: Infrared Versus Convection Comparison

Even though equation 119 is relatively simple in appearance, it is important to recognize that U_o is in fact a function of several variables. These variables include the layer thicknesses, relative permittivities, relative permeabilities, electrical conductivities, surface emissivity, convection exponent, convection coefficient, sample height, incident microwave power level, microwave frequency, and microwave incident angle. Thus, in general U_o is a function of 4N+7 variables where N is the number of layers considered. Even for the case of N=1, we see that U_o must be considered in 11 space in order to analyze all the variables and their interaction at once. Clearly, we can visually represent 3 space but not 11; therefore, in order to graphically display the interactions of the more dynamic variables--the ones over which we have direct control--we fix the values of such things as incident angle, power level, convection exponent, etc., and allow only coating thickness and coating electrical conductivity to vary which then yield our equilibrium surface temperature, U_o. Topologically then, by allowing only two of the variables to vary we are in effect looking only at a particular plane in 4N+7 space.[22] As was indicated earlier, this is sufficient for our analysis since we are observing the more easily manipulated variables in the actual design of a particular coating.

Equation 119 is readily solved numerically using a Newton algorithm. This equation is solved for the N-layer system and is represented on a three dimensional plot. The axis variables are layer number 1's electrical conductivity, layer number 1's thickness, and differential surface temperature increase. Figures 19 to 22 are representative plots of a typical 2 layer system at various incident angles and polarizations.

Later in the experimental verification in Chapter VI, it will be important to realize that a given coating will be considered as a function of incident power level only. The coating and all its particular characteristics are already fixed; they cannot be varied without constructing an entirely new coating configuration. Thus, we will calculate equilibrium temperature as a function of incident power level using equation 119 and then compare these values to the actual measured values. Topologically then, we will be considering single lines in 4N+7 space.

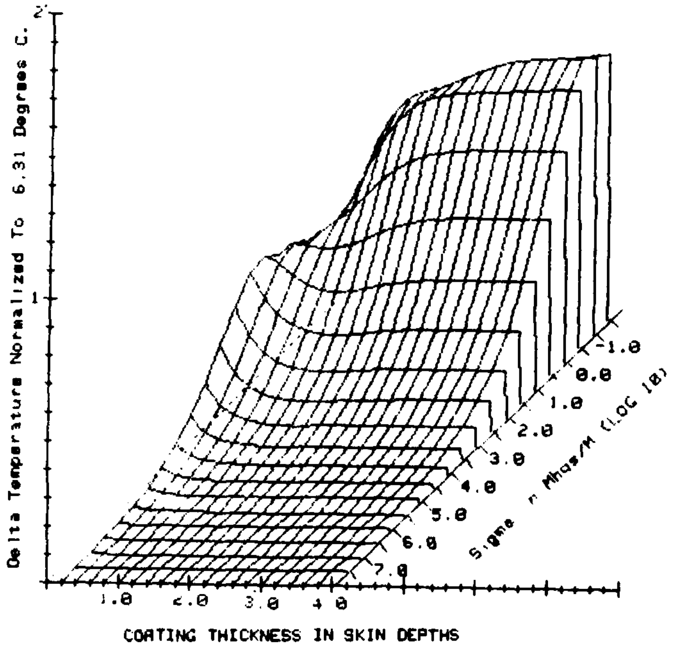

PARALLEL INCIDENCE: Theta= 0 Degrees

```
Number of Layers= 2        Power in W/Cm 2=10        Freq. in GHz=2.45
Air Temp (C)=19.7  Convective Exp= .48  Emissivity= .90  Plate Height (M)= .100

Sigma(1)=3.16E-02  Mu(1)= 1.0  Epsilon(1)=1.30  Thickness(1)=2.29E-01
Sigma(2)=0.00E+00  Mu(2)= 1.0  Epsilon(2)=2.40  Thickness(2)=1.25E-02
```

Figure 19: Two Layer Electromagnetic Heating Profiles

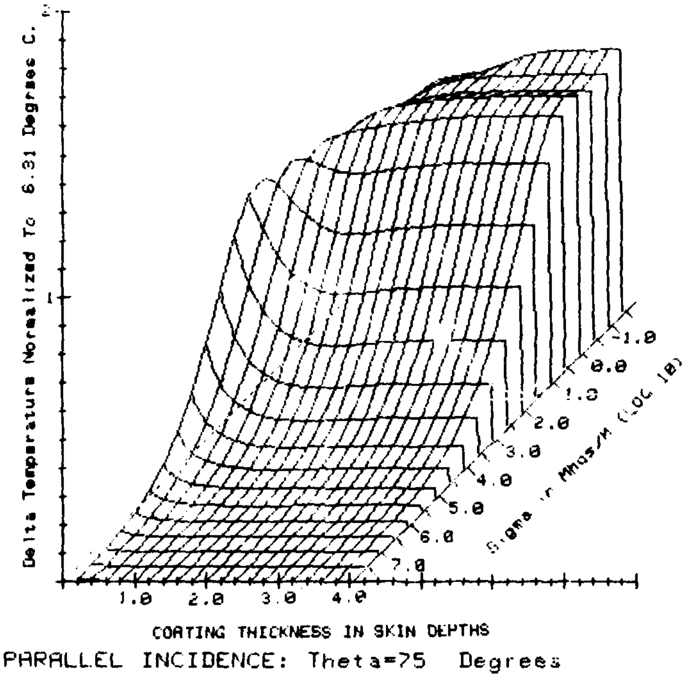

```
Number of Layers= 2        Power in W Cm^2=10        Freq. in GHz=2.45
Air Temp (C)=19.7  Convective Exp= .48  Emissivity= .90  Plate Height (M)= .100


Sigma(1)=3.16E-02  Mu(1)= 1.0  Epsilon(1)=1.30  Thickness(1)=2.29E-01
Sigma(2)=0.00E+00  Mu(2)= 1.0  Epsilon(2)=2.40  Thickness(2)=1.25E-02
```

Figure 20: Two Layer Electromagnetic Heating Profiles

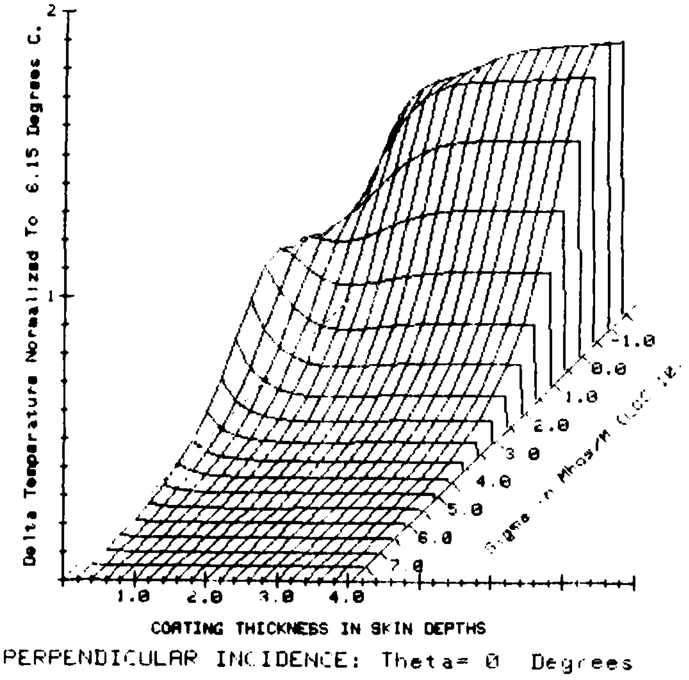

```
Number of Layers= 2        Power in W Cm 2=10        Freq. in GHz=2.45
Air Temp (C)=19.7  Convective Exp= .48  Emissivity= .90  Plate Height (M)= .100

Sigma(1)=3.16E-02  Mu(1)= 1.0  Epsilon(1)=1.30  Thickness(1)=2.29E-01
Sigma(2)=0.00E+00  Mu(2)= 1.0  Epsilon(2)=2.40  Thickness(2)=1.25E-02
```

Figure 21: Two Layer Electromagnetic Heating Profiles

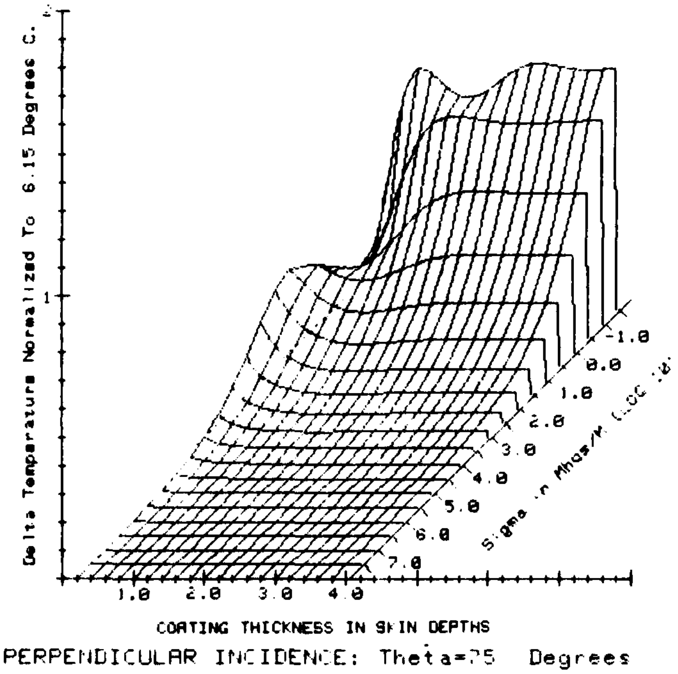

```
Number of Layers= 2        Power in W Cm 2=10        Freq. in GHz=2.45
Air Temp (C)=19.7  Convective E p= .48  Emissivity= .90  Plate Height (M)= .100

Sigma(1)=3.16E-02  Mu(1)= 1.0  Epsilon(1)=1.30  Thickness(1)=2.29E-01
Sigma(2)=0.00E+00  Mu(2)= 1.0  Epsilon(2)=2.40  Thickness(2)=1.25E-02
```

Figure 22: Two Layer Electromagnetic Heating Profiles

CHAPTER VI

EXPERIMENTAL VERIFICATION

The coupling of the electromagnetic solution with the thermodynamic solution for a system of N layers yields a theoretically valuable tool for predicting the surface temperatures of a layered system. However, before this development can be used with any certainty, we must experimentally verify the accuracy of the predicted results. The overall verification was a three step process. We first measured the convective heat transfer exponent, δ, and then examined five different conductive samples as they were exposed to various microwave power levels ranging from 10 to 40 mW/cm^2. Irradiation frequency was fixed at 2.54 GHz. An appropriate convective heat transfer coefficient was then chosen that would allow the best possible fit between experimental and theoretical data.

The convective heat transfer exponent was measured in the following manner. A constant power was generated within a thin conductive coating (aquadaq) by keeping a constant direct current voltage applied accross the sample. This sample was insulated with two inches of styrofoam insulation on the sides and back so that we could closely approximate our model which assumed no conductive heat losses. The sample was allowed to reach steady state conditions before the surface temperature was measured. Surface temperature measurements were made with an infrared camera capable of measuring temperature variations to within one tenth degree Centigrade. We then calculated an absorbed power density given by

$$P_a = VI/A \tag{123}$$

where

V = applied voltage across sample (volts)
I = current through the sample (amperes)
A = area of the sample (meters squared)

This absorbed power must be dissipated via surface convection and infrared radiation; therefore, as in the development in Chapter 5, we equated the power gains to the power losses which resulted in

$$VI/A = \frac{1.42}{H^{\delta}} (U_o - U_{air})^{1+\delta} + F_e \gamma (U_o^4 - U_{air}^4) \tag{124}$$

Surface emissivities have been measured by other researchers[23,24] and are thus known quantities. If we assume the convective coefficient (1.42) remains relatively constant, the only variable remaining is the convective exponent which may be calculated. Its value is given by

$$\delta = \frac{1}{\ln\left(\frac{U_o - U_{air}}{H}\right)} \ln \left[\frac{1}{1.42(U_o - U_{air})}\left(\frac{VI}{A} - F_e \gamma (U_o^4 - U_{air}^4)\right)\right] \tag{125}$$

Figure 23 illustrates the general layout of the experiment.

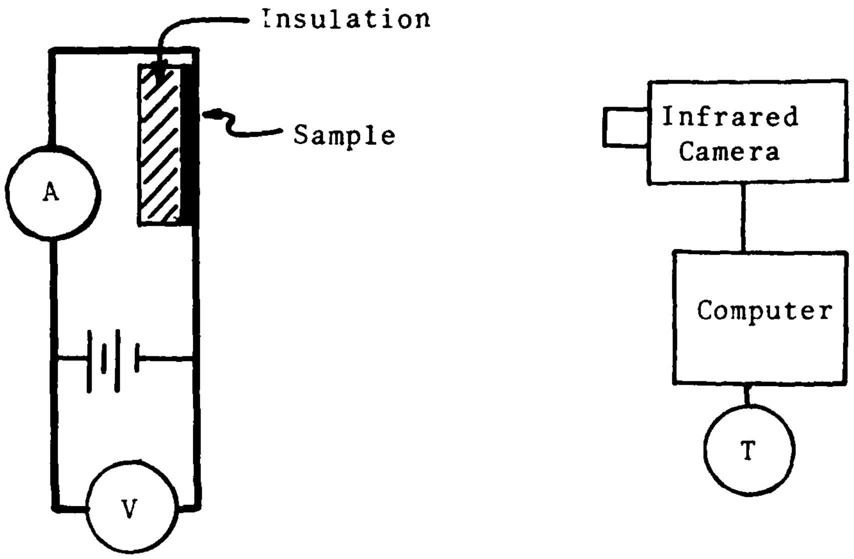
Insulation
Sample
A
V
Infrared Camera
Computer
T

Figure 23: Schematic of Convective Exponent Experiment

Test equipment used in the experiment consisted of the following:

Nomenclature	Identification
Power Supply	Regulated D.C. Power Supply 0-50 VDC, 0-1.5A Kepco Manufacturing Co. Flushing, New York
Ammeter	Digital Multimeter Model 3466A Hewlett-Packard Mfg. Co. Colorado Springs, CO

Voltmeter	Digital Multimeter Model 3466A Hewlett-Packard Mfg. Co. Colorado Springs, CO
Infrared Camera	Thermovision Model 680 AGA Manufacturing Co. Secaucus, New Jersey

The sample measured consisted of a 10 cm square of conductive coating 59 microns in thickness and mounted vertically. Room temperature was maintained at 20.5±.1 C throughout the experiment. Five different direct current power levels were observed to determine the linearity of the convection exponent with temperature. Figure 24 illustrates the experimental results in which the average value of the convective exponent was determined to be 0.53. Having a value for the convection exponent, we then verified the N-layer electromagnetic interaction.

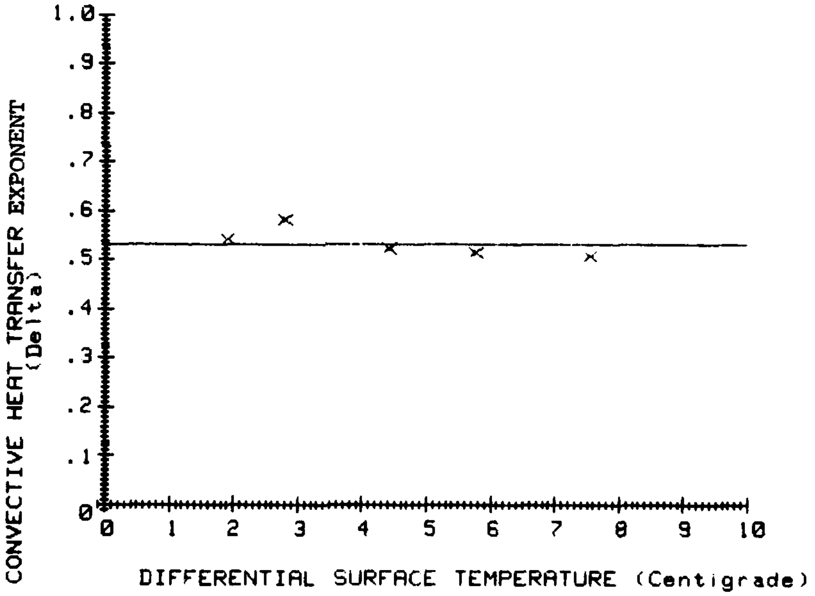

Figure 24: Results of Convective Exponent Measurements

There are two major shortfalls of the N-layer model which have a drastic impact on the verification. The first of these is the semi-infinite plane assumption. We obviously cannot construct a semi-infinite layered system in the laboratory and irradiate it uniformly with a plane electromagnetic wave; therefore, the approach is to use a very small (much less than a wavelength) multilayered sample. By avoiding resonant shapes and sizes the sample will experience a relatively uniform electric field across the surface and the observed surface temperature will approximate that observed on a semi-infinite sheet.

Secondly, from the thermodynamics point of view, we assumed the conductive coating would be placed on a perfect insulator and thus no thermal conduction would occur. Obviously, perfect thermal insulators do not exist either; hence, we have another source of error. To minimize the thermal conduction losses, samples were placed on styrofoam blocks with a minimum of two inches of insulation on all but the front surface. Styrofoam proved to be well suited for this purpose since it is an excellent insulator and has a measured electrical permittivity of approximately 1.1 (10 GHz). Electrically, therefore, the foam was virtually invisible while thermally it provided the desired insulation. The samples consisted of 1, 2, and 3 layer configurations all cut to be 1.5 cm square. In addition to the equipment already listed, the following instruments were also used:

Nomenclature	Identification
Microwave Generator	Microwave Generator 2.45 GHz, 0-200 Watt Kiva Instrument Co. Rockville, Maryland
Power Meter	Radiation Hazard Meter (RAHAM), Model 481 General Microwave Farmingdale, New York

Figure 25 illustrates the physical arrangement of the experiment.

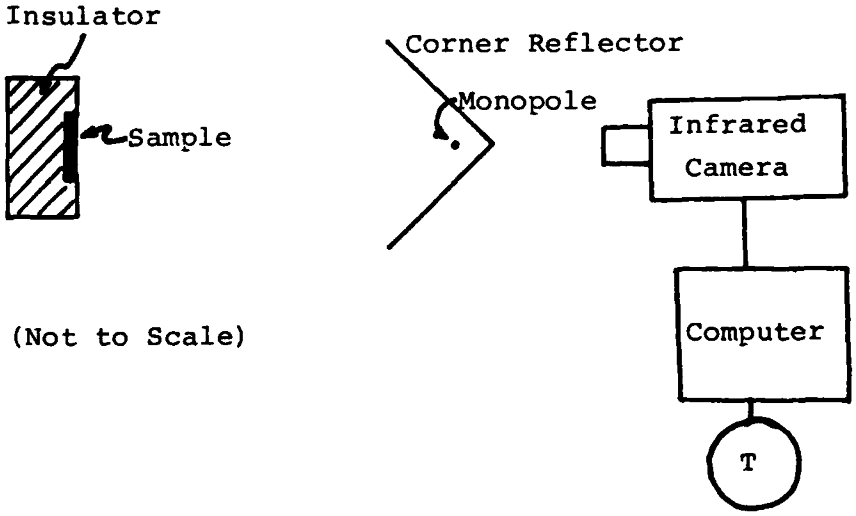
Insulator
Sample
Corner Reflector
Monopole
Infrared Camera
Computer
T
(Not to Scale)

Figure 25: Schematic of N-Layer Verification

The procedure itself was relatively straight forward. The microwave power meter was used to measure the free field power level of the 2.45 GHz radiation. After the power was adjusted to the proper value the layered sample was placed at the point where the power was measured. The samples were then allowed to reach thermal equilibrium prior to measuring their surface temperatures with the infrared camera. In most cases thermal equilibrium was reached in less than 10 minutes; however, the samples were irradiated at least 20 minutes each. Each sample was exposed to power levels of 10, 15, 20, 30, and 40 mW/cm^2. The measured temperature for each is plotted versus input power in figures 26 to 30. Calculated values are also plotted on the same graph for comparison purposes. The single greatest variation occurred for the two layer aquadaq/plexiglas combination. In this case the average deviation from theoretical values was about 33 percent. The other four samples yielded much better results of typically less than 20 percent variation. To obtain the theoretical values shown we had to use a convective coefficient of 15 rather than the 1.42 used in the theoretical discussion in Chapter V thus indicating that convection is much more significant than originally assumed.

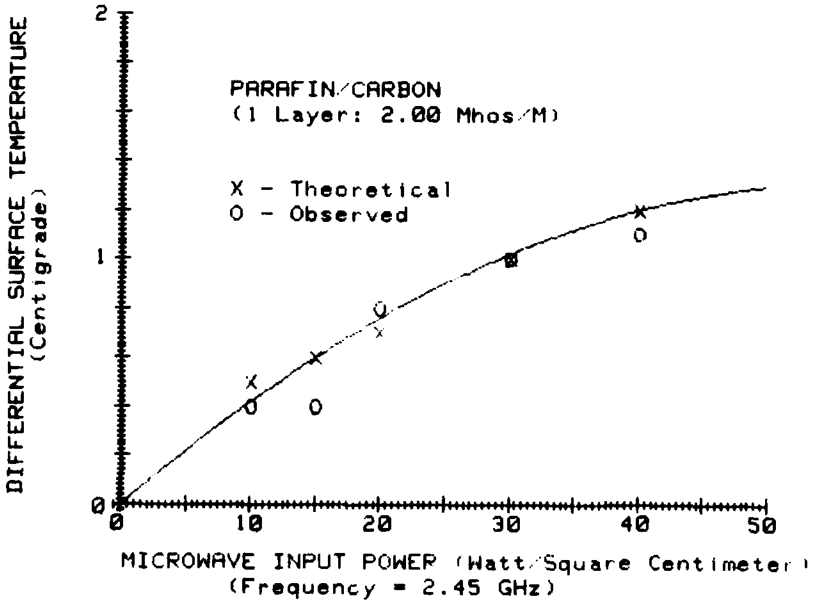

Figure 26: One Layer Electromagnetic Heating

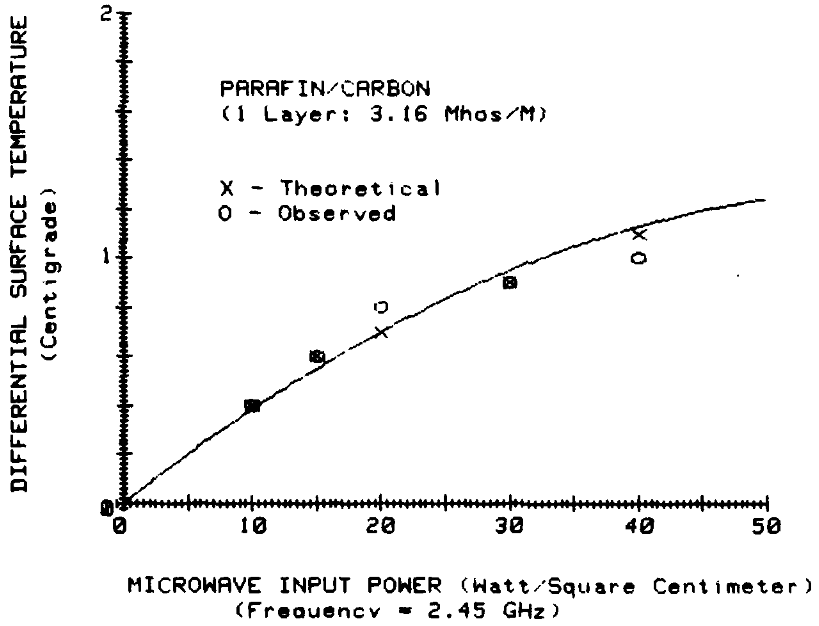

Figure 27: One Layer Electromagnetic Heating

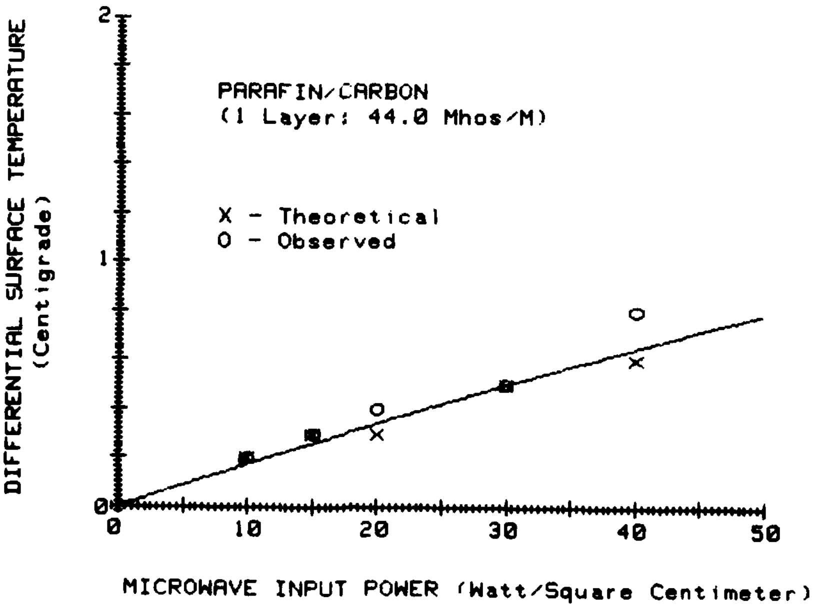

Figure 28: One Layer Electromagnetic Heating

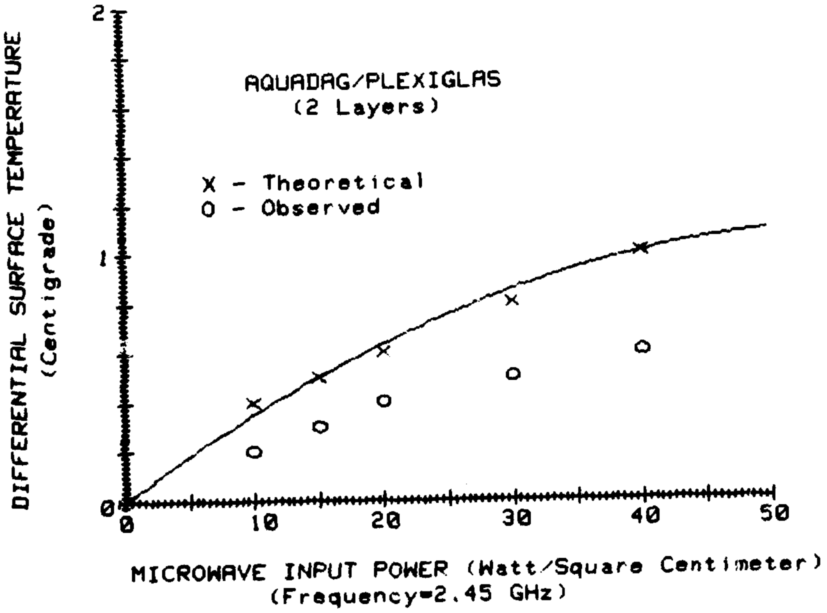

Figure 29: Two Layer Electromagnetic Heating

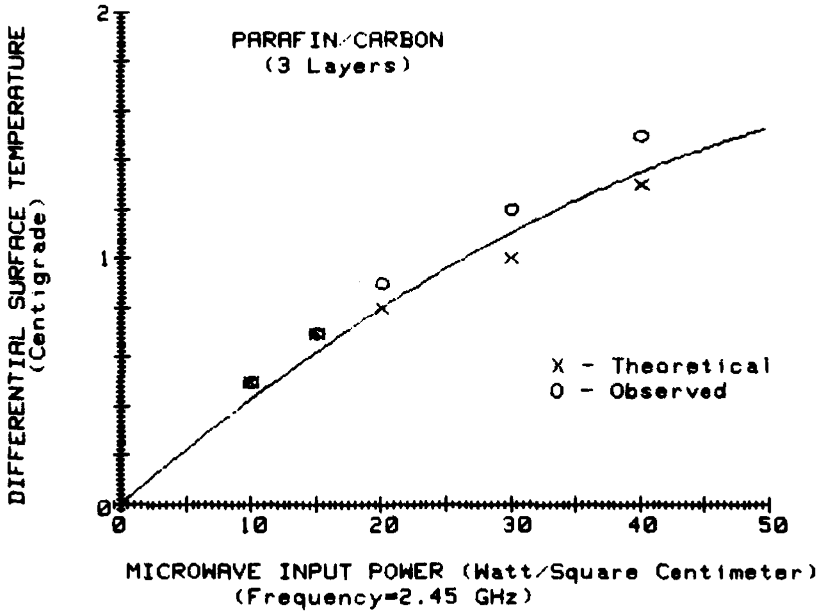

Figure 30: Three Layer Electromagnetic Heating

CHAPTER VII

APPLICATION OF MODEL TO TWO-DIMENSIONAL TARGETS

As was pointed out earlier in the initial development of our coating model, a possible limitation to its use results from the one-dimensional analysis itself. This chapter discusses the problem of applying the one-dimensionl coating model to the more "real world" two-dimensional problem. In particular, the experimental verification itself uses an electrically small two-dimensional square sample to approximate the current present in the semi-infinite one-dimesional case. Also, the question of "nearest neighbor" influence is important when considering electrically large samples. That is, when we observe a temperature at a point on the surface of a coated shape, how well does that relate to the currents present directly under it? Clearly, the currents in the neighborhood of this point must contribute something to the coating temperature but the question is, "how significant is their influence?" In order to qualitatively address each of these situations, we will first consider the electrically small sample as applied to the verification experiment and later discuss the "nearest neighbor" considerations in regards to electrically large models.

As was indicated earlier in Chapter VI, the verification process for the semi-infinite one-dimensional model is a difficult one. Physically, we were constrained in size by an anechoic chamber with a maximum usable width of approximately one meter. In the far field we had an area of approximately 20 x 15 cm in which the microwave power density was relatively uniform. Electrically we could achieve a power density of 20 $\mathrm{mW/cm^2}$ in the above area at a frequency of 2.45 GHz. The radiation pattern was formed by use of a quarter wave monopole in conjunction with a parabolic reflector over an aluminum ground plane. See figures 31, 32, and 33 below.

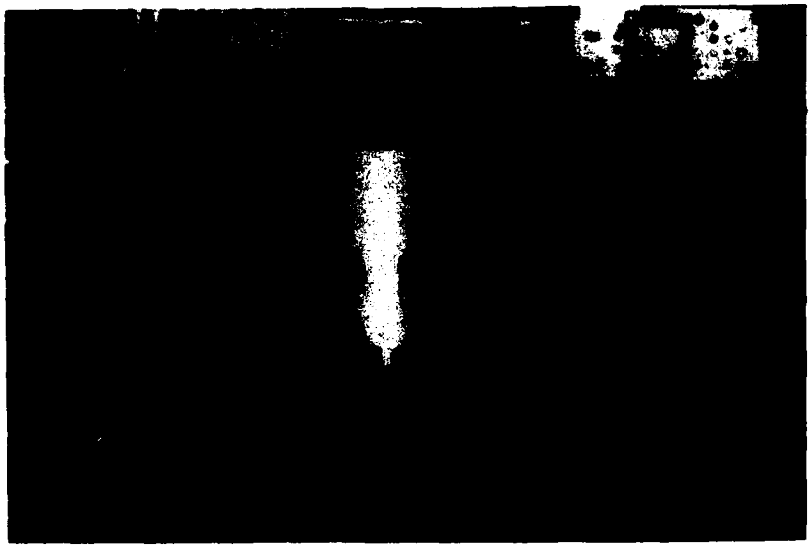

Figure 31: Photograph of Monopole and Parabolic Reflector

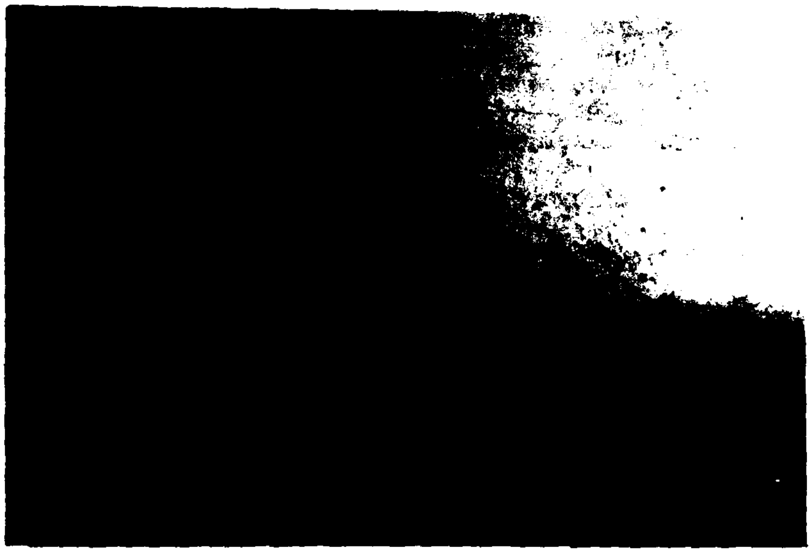

Figure 32: Actual Quarter Wave Monopole

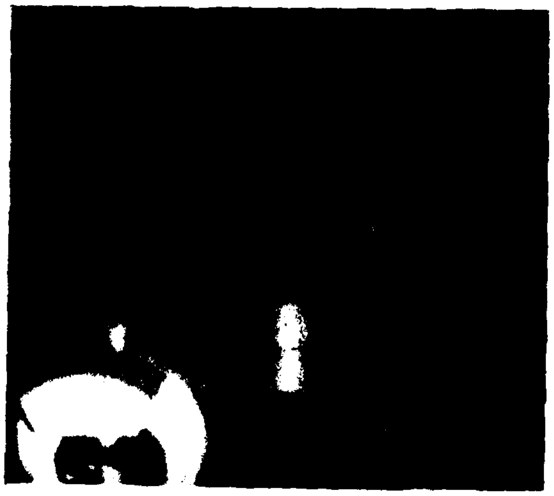

Figure 33: Anechoic Chamber With Electrically Small Target and Infrared Camera in Foreground

The verification problem is such that it could proceed in either of two ways. The first was to construct several electrically very large samples that by nature of their size would approximate the semi-infinite condition of our model. There are several problems associated with this approach. Large coated targets are considerably difficult to construct since they must have completely uniform conductive coatings over their surfaces. The problem is even more difficult with two or three composite layers. The largest problem, however, results from the nature of the anechoic chamber itself. That is, if we placed a large target completely across the chamber, nearly all of the incident microwave field would be back scattered into the parabolic emitter which in effect would turn our anechoic chamber into some type of tuned cavity. Thus, we would know nothing about the fields present at the coating. The back scatter problem could be reduced or eliminated by removing the parabolic reflector and substituting anechoic absorbers but then our incident field strength would have suffered drastically. Therefore, because of the mechanical and electrical difficulties inherent with the large model approximation, it appears more desirable to use an electrically small model to approximate the semi-infinite results.

The electrically small sample has several advantages. First, it is much easier to fabricate and characterize electrically. In fact we can measure the coating thickness directly using a good micrometer since the micrometer jaws nearly completely cover the sample's face. The back scatter problem is practically nonexistent. Similar to developments elsewhere, if we consider a sample which is electrically small and assume the incident field induces a relatively uniform surface current across the sample faces then we may treat it as a Huygen's source (We will discuss the uniformity assumption more later.)[25]. See figure 34 below.

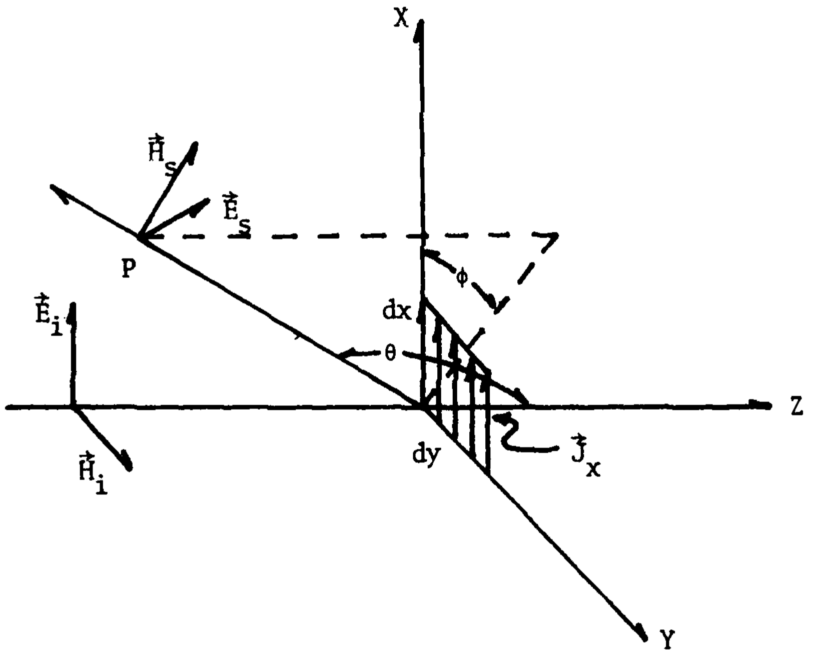

Figure 34: A Uniform Current Sheet Radiator

If we further assume the induced current is not only uniform but also the same as that induced on an infinite conductor and that contour charge is negligible, then we have $J_x = |\vec{H}_i|$. The radiation field is

$$\vec{E}_s = -j\omega\vec{A} \quad (126)$$

[25]

where

$$\vec{A} = A_x\,\hat{x} = \mu\,\frac{(J_x dy)\ d\,x\ e^{-j\beta r}}{4\pi\ r}\,\hat{x} \quad (127)$$

$$E_s^{\theta} = -\ j\omega\ A_x \cos\phi\ \cos\theta \quad (128)$$

$$E_s^{\phi} = j\ \omega\ A_x \sin\phi \quad (129)$$

Therefore, the approximate magnitude of the backscattered field on the z axis and polarized in the x direction ($\theta = 0$, $\phi = 0$) would be

$$|E_s|_0 = \omega\ \left(\frac{E_i\ dy\ dx}{4\pi c\ r}\right) \quad (130)$$

Assuming that this field is redirected by the parabolic reflector with some gain G, the redirected field strength at the target would be

$$|E_t| = \frac{\omega G E_i\ dy\ dx}{8\pi c\ r} \quad (131)$$

The percentage of re-reflected to incident power at the target face would be

$$\frac{|E_t|^2}{|E_i|^2} = \left[\frac{\omega\ G\ dy\ dx}{8\pi\ c\ r}\right]^2 \times 100 \quad (132)$$

For

$\omega = 2\pi \times 2.45 \times 10^9$ Hz

$dy = dx = .015$ m

$G \simeq 20$

$r = 1.3$ m

$c = 3 \times 10^8$ m/s

we have $\dfrac{|E_t|^2}{|E_i|^2} \doteq 5 \times 10^{-3}$ % (133)

In other words, our small sample size interferes with the incident field only a small amount. One obvious advantage of this is that we can measure and characterize the microwave fields within the anechoic chamber with no targets present and then be sure that this characterization changes very little with the addition of a small object.

Two other considerations that must be addressed before the small sample may be used with confidence concern the surface current uniformity and magnitude on such targets. Considerable insight is provided to both of these questions in an article by Wilton, et al, in which a method of moment solution is considered for various size flat conducting plates. See figures 35 and 36 below for a profile of surface currents on a 1.0λ and 0.15λ square plate[26].

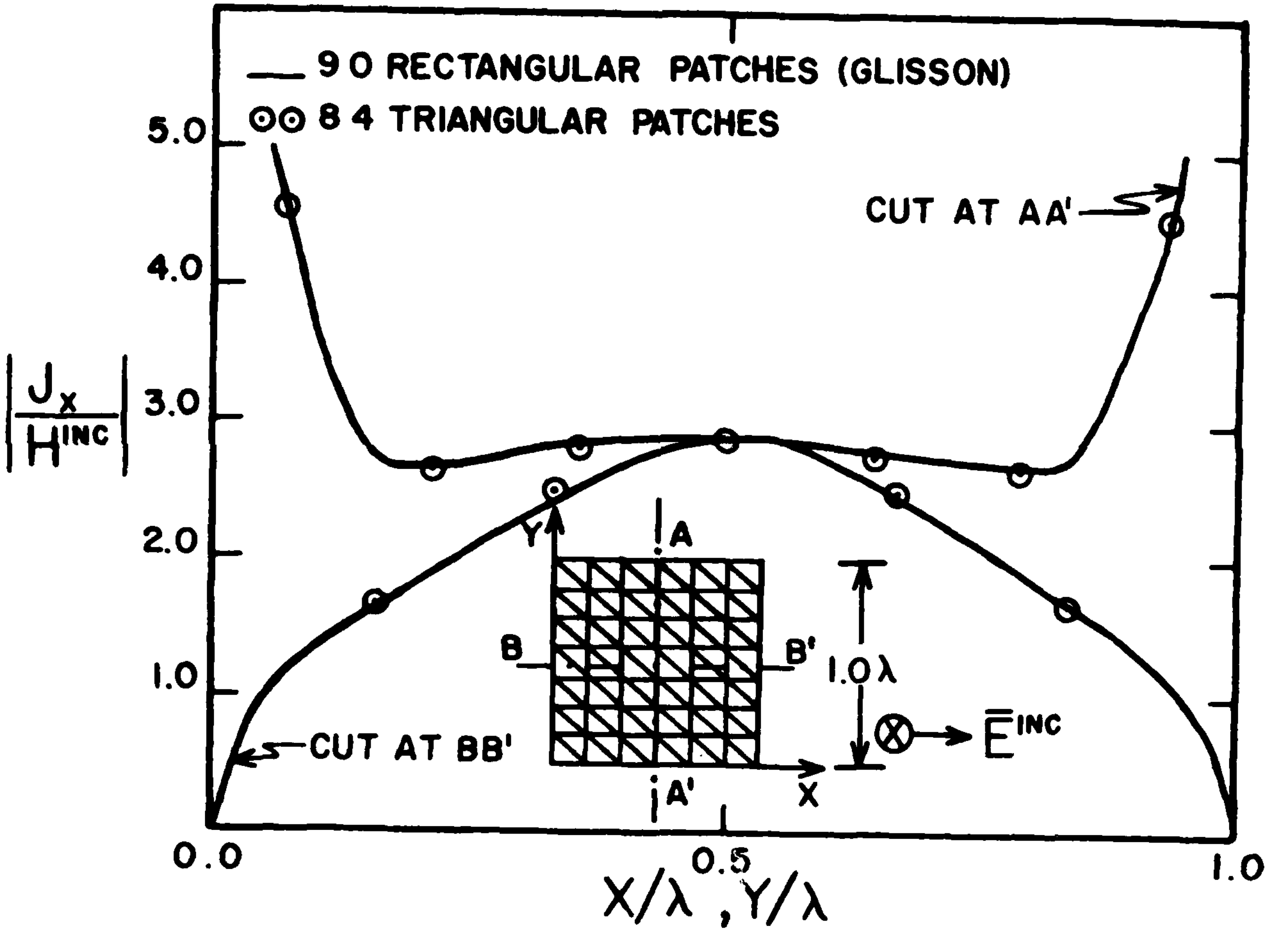

Figure 35: 1.0λ Square Plate Current Distribution

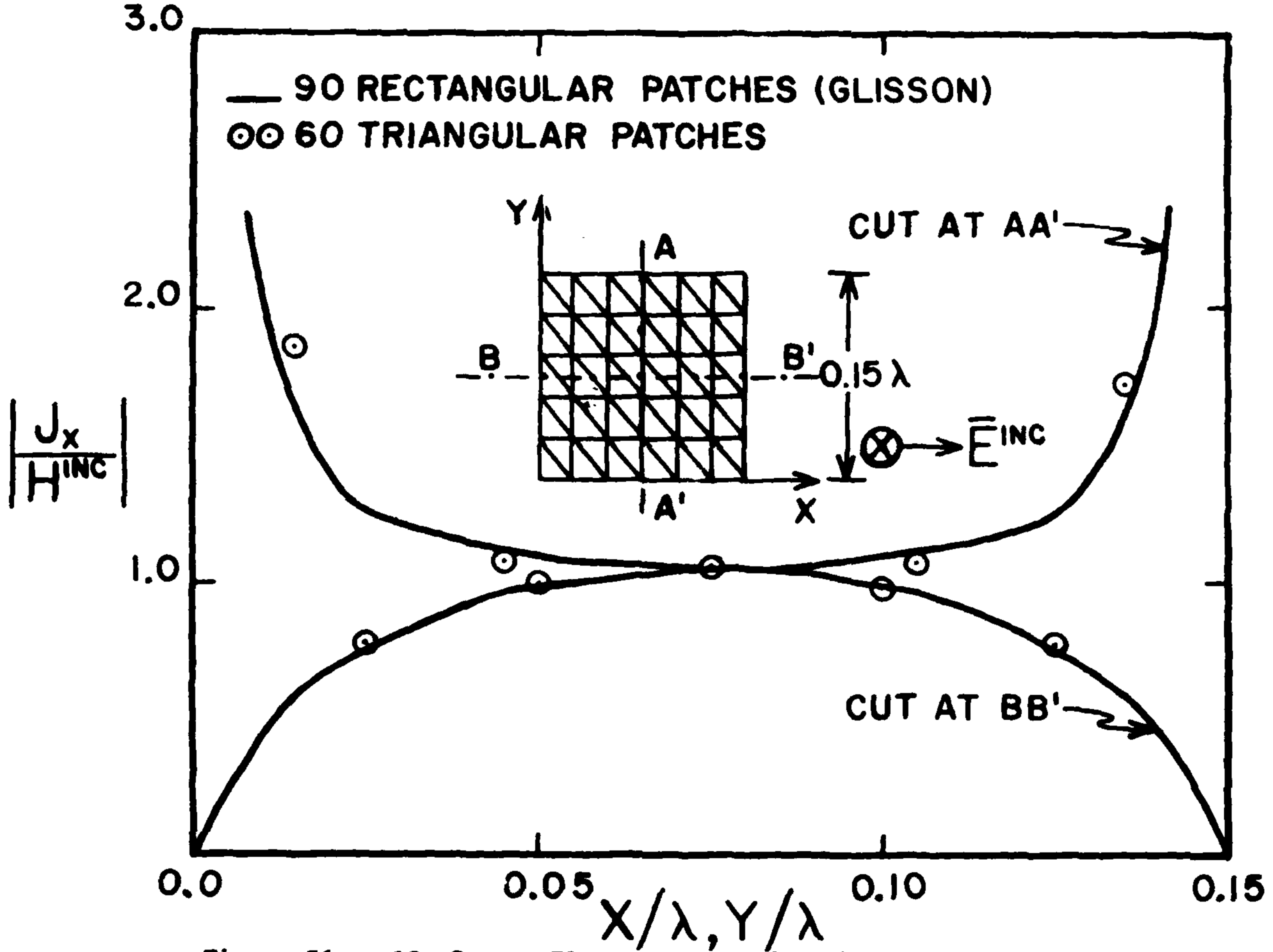

Figure 36: .15λ Square Plate Current Distribution

The important aspects to note are the magnitude of J as the plate size decreases and also the more uniform current distribution as the plate size reduces. In an experiment to observe these effects more graphically, 1.0λ, 0.5λ, and 0.25λ square plates were irradiated with normally incident microwaves at a power level of 20 mW/cm^2. See figures 37 to 45.

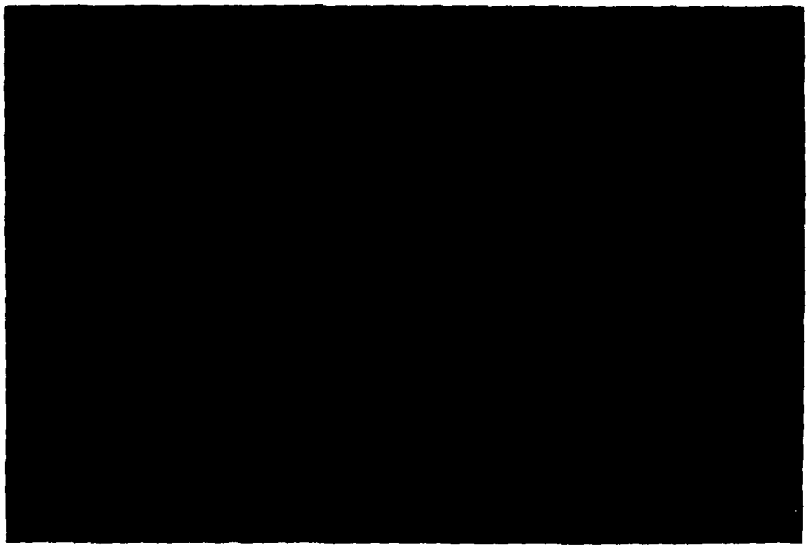

Figure 37: Photograph of 1.0λ Square Plate

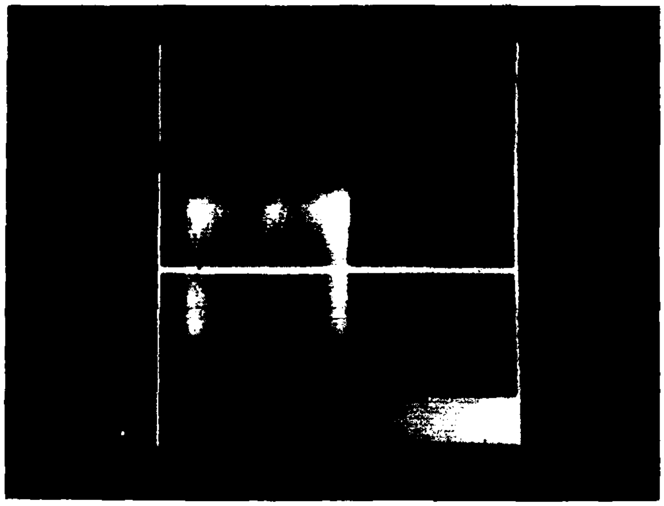

Figure 38: Infrared Photograph of a 1.0λ Square Plate

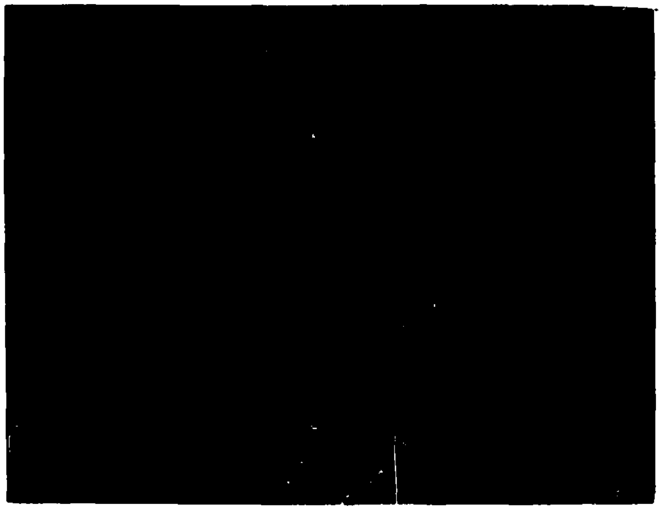

Figure 39: Thermal Profile Across the Center of a 1.0λ Square Plate

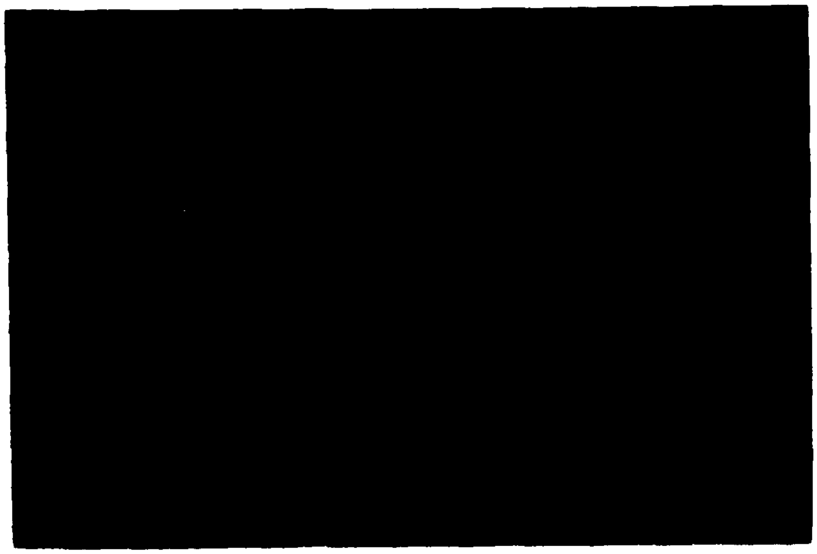

Figure 40: Actual Photograph of a 0.5λ Square Plate

Figure 41: Infrared Photograph of a 0.5λ Square Plate

Figure 42: Thermal Profile Across the Center of a 0.5λ Square Plate

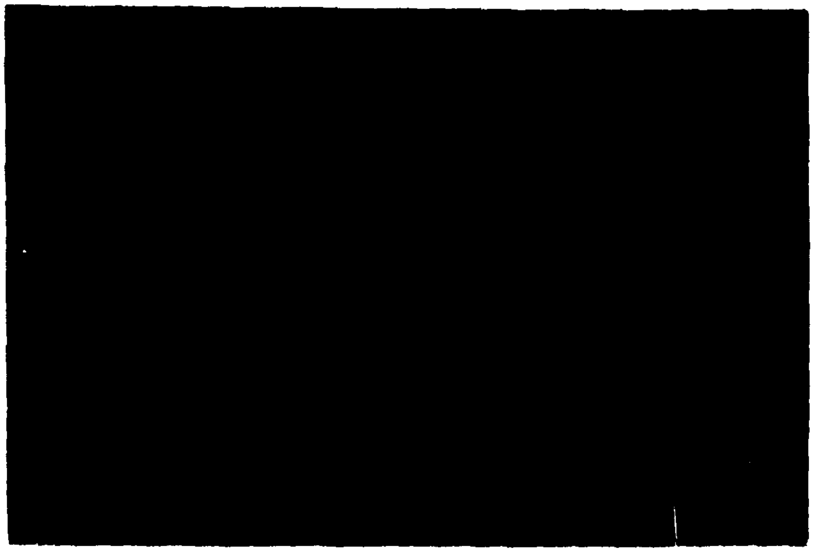

Figure 43: Actual Photograph of a 0.25λ Square Plate

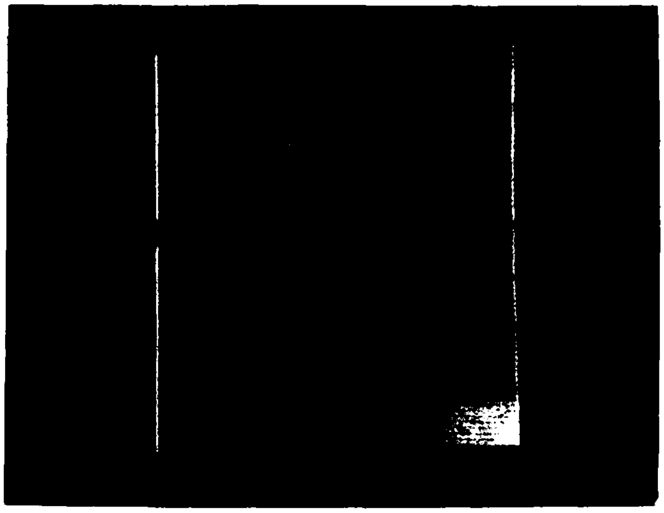

Figure 44: Infrared Photograph of a 0.25λ Square Plate

Figure 45: Thermal Profile Across the Center of a 0.25λ Square Plate

The lighter areas correspond to greater surface currents. A single temperature profile was taken across the middle of each target to allow comparison with the method of moments results by Wilton. Notice the great similarity between the 1.0λ experimental plate and theoretical results. To consider the question of uniformity more graphically, Figure 46 is a plot of a .15λ square plate in which the shading depicts those areas in which the surface current varied less than 20% from that which would be observed on an infinite conducting sheet. This information is graphically taken from the plot of Wilton, Figure 36.

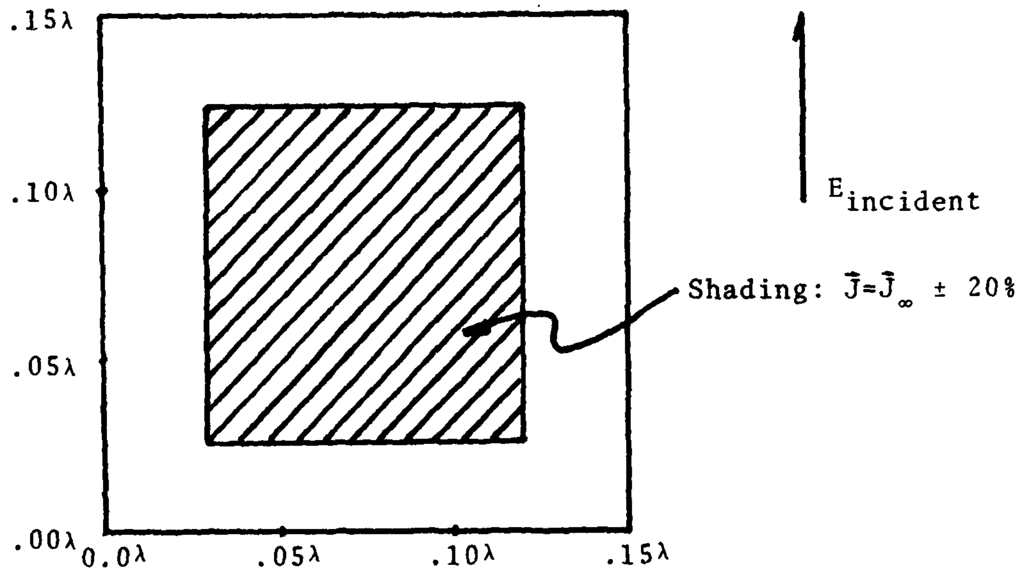

Figure 46: Current Uniformity on a .15λ Plate

Therefore, by observing the temperature at the center of our small sample, we are reasonably assured that our results are similar to what would be observed on a semi-infinite plate.

In the experimental verification small square samples were used which facilitated the above discussion; however, this is not an absolute requirement. Andrejewski[27] has computed the surface current at the center of a disc as a function of c where $c \equiv 2\pi(\frac{a}{\lambda})$ with "a" being the radius of a sample disc. See figure 47[28] for a plot of his results.

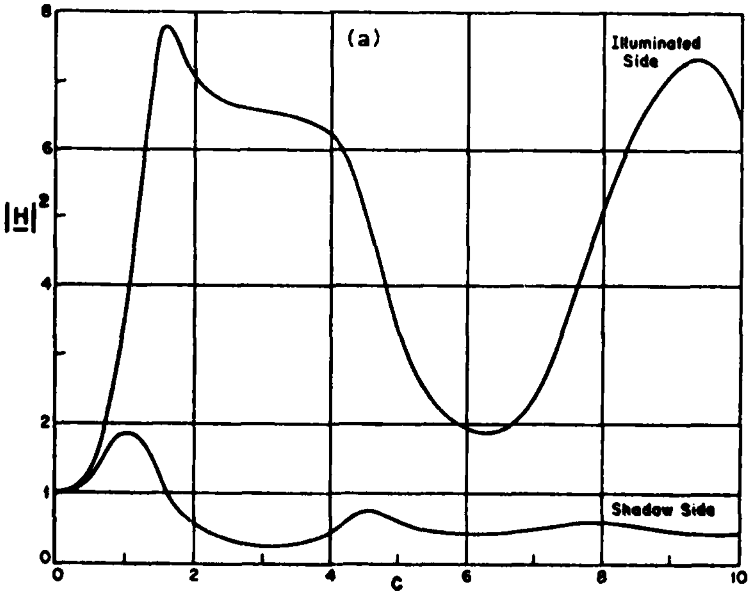

Figure 47: Current at the Center of a Disc as a Function of c

As in the case of the small square, notice that as c gets small the field at the center of the disc approaches the semi-infinite plane value ($|\vec{H}|=1$). In fact for a disc 1.5 cm in diameter the predicted surface current value at the center is within 10% of the value experienced by a semi-infinite conducting sheet. Therefore, it seems reasonable that we may use small discs as well as squares in the verification process with no loss in validity. For a more complete discussion of theoretical solutions of the disc one may refer to any of several good references.[28,29,30]

All the discussion to this point has been limited to the small samples used in the verification process. We have developed a model and have shown that it is valid in regards to whether or not a particular coating configuration will heat properly when exposed to microwave radiation. One final question which is relevant when considering electrically large samples is the question of "nearest neighbor" influence. That is, how well can our coating model predict surface currents below it?

Recall that in general our coating will be displaced from the surface of the object we are observing. Although, this displacement is necessary in order to observe heating, it is an overall detriment to the resolving power of the coating. We may begin to understand this problem more if we recognize that in order for a particular current element to interact with the coating, that current element must emit an electromagnetic wave which in turn must travel to the coating. See Figure 48.

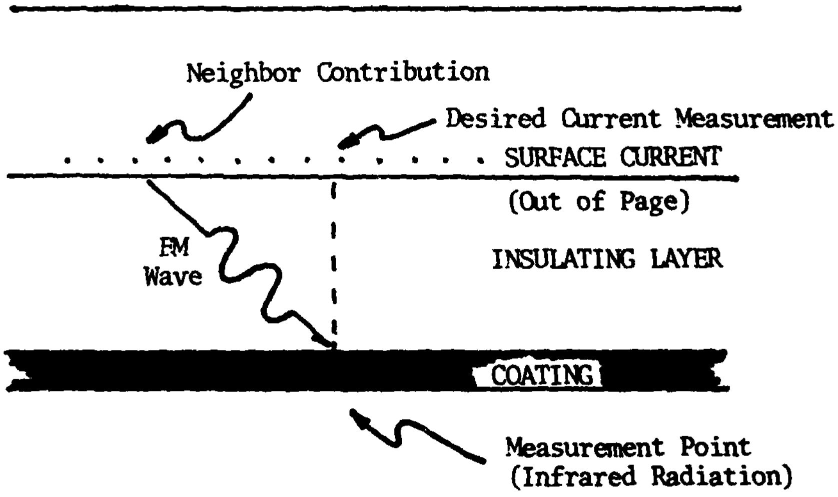
Neighbor Contribution
Desired Current Measurement
SURFACE CURRENT
(Out of Page)
EM
Wave
INSULATING LAYER
COATING
Measurement Point
(Infrared Radiation)

Figure 48: Cross Section of a Conductive Coating Displaced Away From Conductor Surface

The question then is how far away from the measurement point can this neighbor contribution be? We may receive some insight to the problem by considering the typical waveguide solution [31] to two semi-infinite planes separated by a distance "a". See figure 49 below.

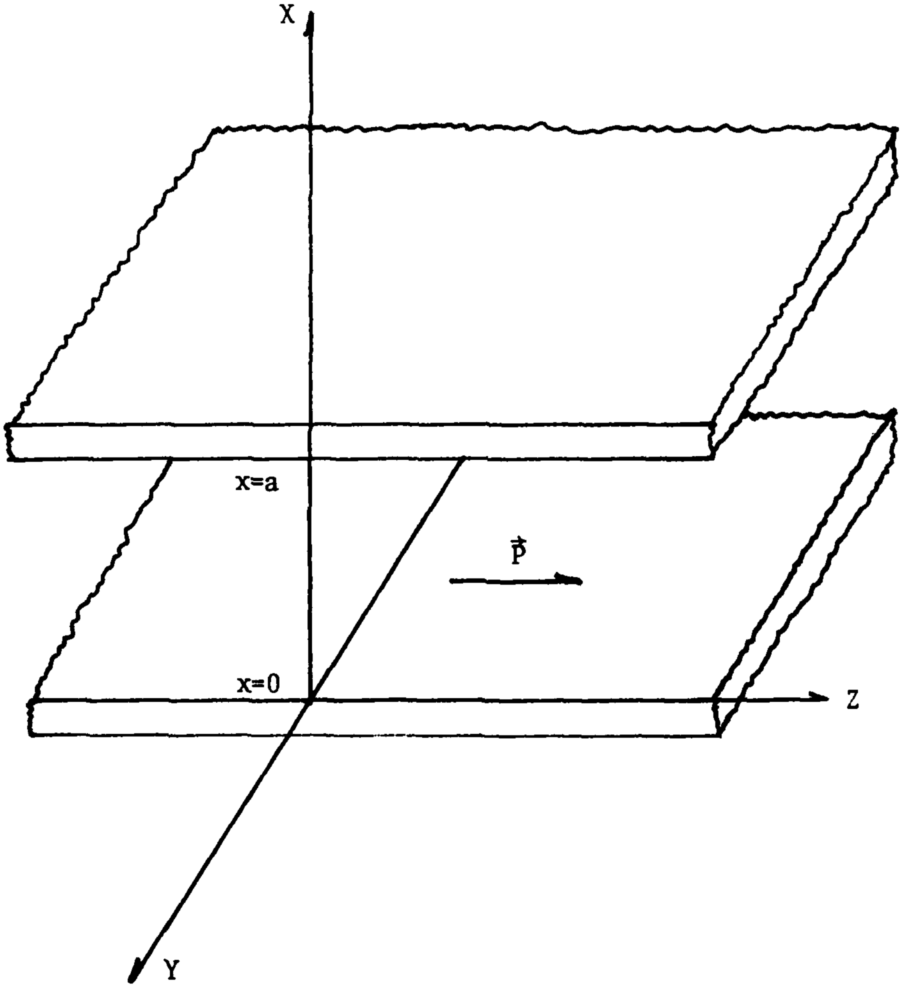
X
x=a
$\vec{P}$
x=0
Z
Y

Figure 49: Parallel Waveguide Sheets

Assuming wave propagation in the z direction and a TE mode, the solution is given as [11]

$$E_y = C_1 \sin\left(\frac{m\pi}{a} x\right) e^{-\overline{\gamma} z} \tag{134}$$

$$m = 1,2,3, \ldots \tag{135}$$

$$\overline{\gamma} = \sqrt{\left(\frac{m\pi}{a}\right)^2 - \omega^2 \mu\varepsilon} \tag{136}$$

We see that $\overline{\gamma}$ will either be pure imaginary or real depending on the argument under the radical. If $\overline{\gamma}$ is real, the wave will attenuate exponentially which is what we desire in order to reduce the nearest neighbor effect. We may solve for a minimum value of a in which this will occur. Forcing the argument to be greater than zero and solving for a, we find that attenuation will occur as long as

$$a < \frac{\lambda m}{2\sqrt{\varepsilon_r \mu_r}} \tag{137}$$

If we assume the simplest propagation mode (m = 1) and a foam insulating layer ($\varepsilon_r \approx \mu_r \approx 1$), then we have lateral attenuation as long as the insulator is less than $\frac{\lambda}{2}$ thick. Obviously the attenuation will be stronger as the layer gets thinner. The distance at which an attenuated wave has reduced to a value $\frac{1}{e}$ of its initial value is given by

$$z = \frac{1}{\sqrt{\left(\frac{m\pi}{a}\right)^2 - \omega^2 \mu\varepsilon}} \tag{138}$$

In the regime where we must operate in order to have significant lateral attenuation and thus little nearest neighbor influence, we have

$$\left(\frac{m\pi}{\lambda}\right)^2 \gg \omega^2 \mu\varepsilon \tag{139}$$

Therefore,

$$z \simeq \frac{a}{m\pi} \tag{140}$$

In other words, we would not expect to see significant nearest neighbor influence at distances much over a/π for the worse case of $m=1$.

An experiment was conducted in order to further understand the significance of the nearest neighbor problems. A large aluminum conductor was covered with a layer of foam 5.1 mm in thickness. The foam was subsequently coated with an aquadaq coating approximately 15 microns in thickness and electrical conductivity of approximately 315 mhos/m. As the large target was irradiated, 1.5 cm diameter holes were placed in the aluminum at closer and closer intervals. The holes behind the coating were observed as hot spots. A point was finally reached at which time the two spots had begun to merge. At this point the centers of the holes were 2.0 cm apart. See figures 50 to 61 for thermovision photographs and thermal profiles of the results.

AD-A131 091 MICROWAVE INTERACTION WITH THIN MULTIPLE CONDUCTIVE COATINGS(U) ROME AIR DEVELOPMENT CENTER GRIFFISS AFB NY V M MARTIN MAR 83 RADC-TR-83-62 2/3

UNCLASSIFIED F/G 11/3 NL

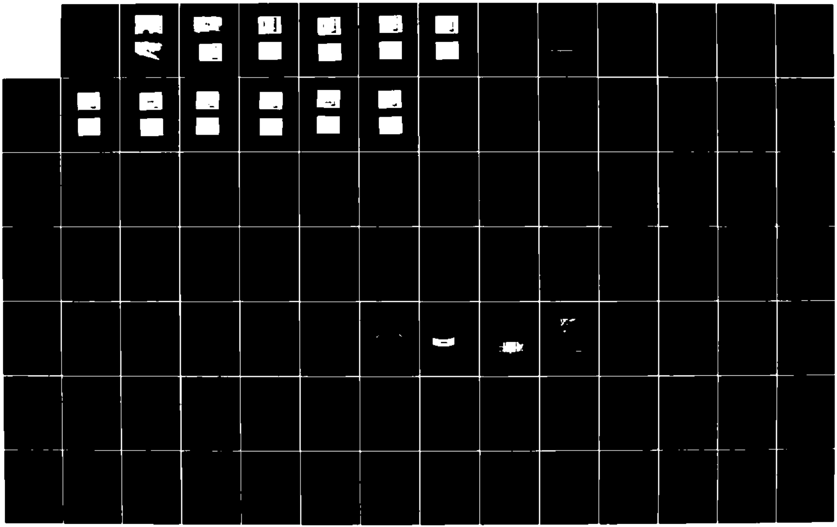

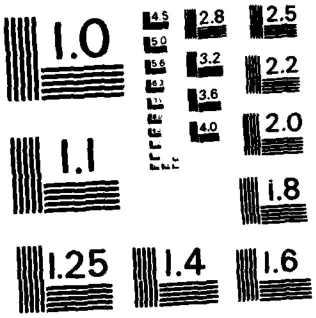
1.0
4.5
5.0
5.6
6.3
2.8
3.2
3.6
4.0
2.5
2.2
2.0
1.1
1.8
1.25
1.4
1.6

MICROCOPY RESOLUTION TEST CHART
NATIONAL BUREAU OF STANDARDS-1963-A

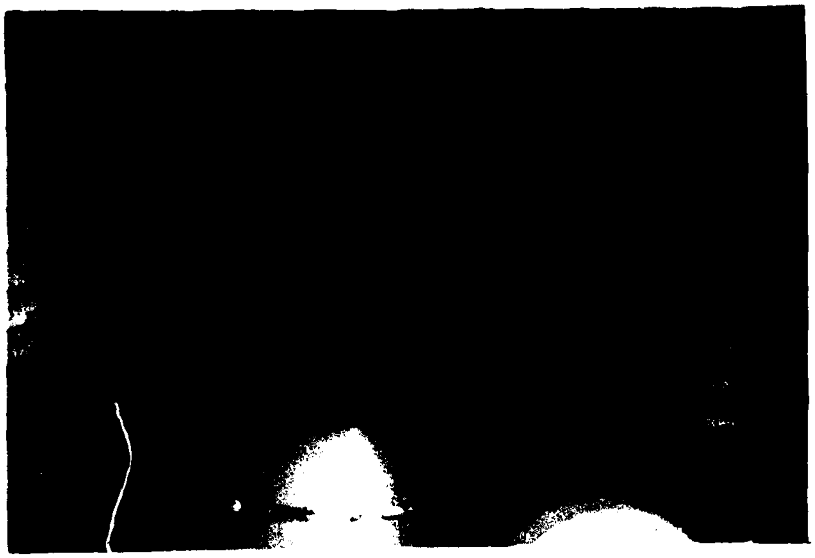

Figure 50: Photograph of Electrically Large Plate in Place in the Anechoic Chamber

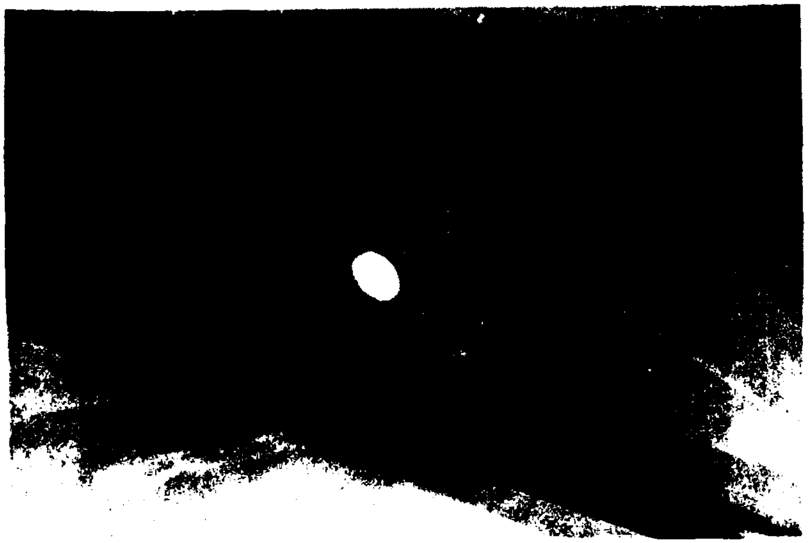

Figure 51: Photograph of the Single 1.5 cm Hole in the Aluminum Plate

Figure 52: Photograph of the Double Hole Configuration

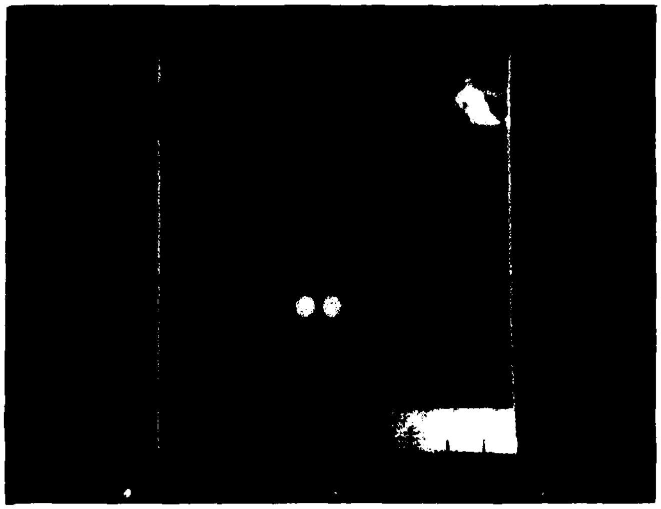

Figure 53: Infrared Photograph of Artificially Heated Double Hole Configuration for Size Comparison with Microwave Results

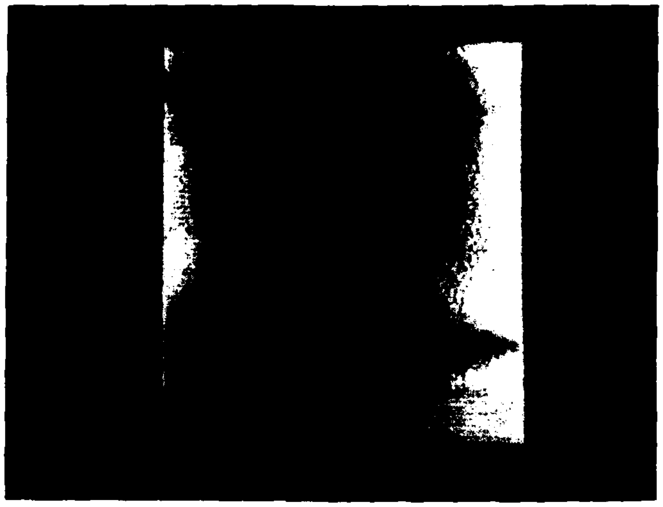

Figure 54: Infrared Photograph of Single Hole Heating Pattern Resulting from Microwave Radiation (1° C Scale)

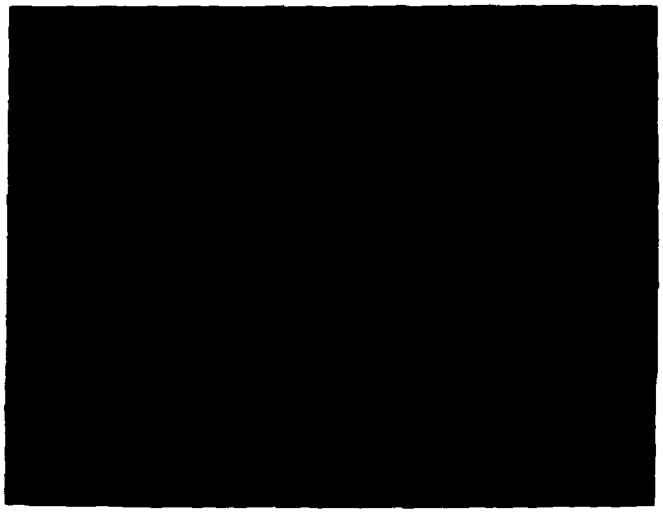

Figure 55: Horizontal Thermal Profile of Single Hole Heating Pattern (1° C Scale)

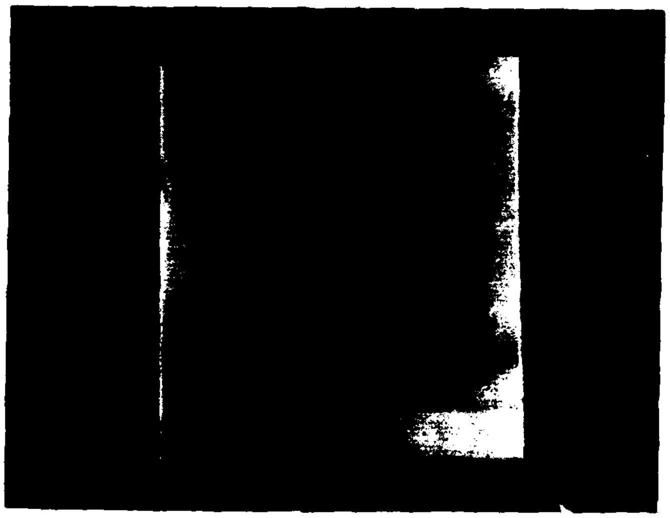

Figure 56: Same as Figure 54 Except 2° C Scale

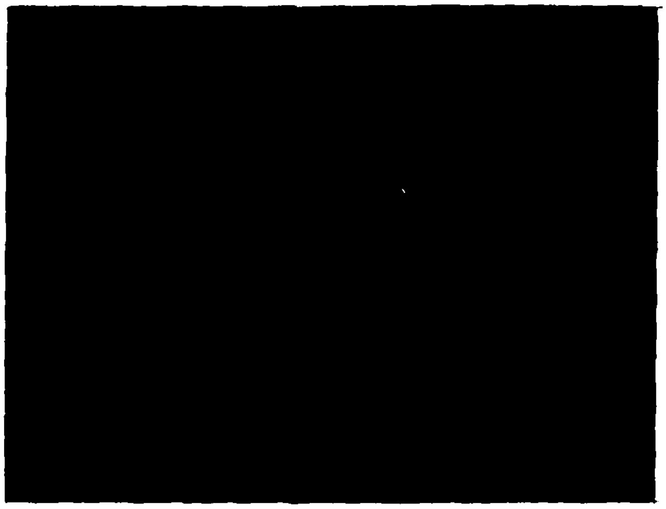

Figure 57: Same as Figure 55 Except 2° C Scale

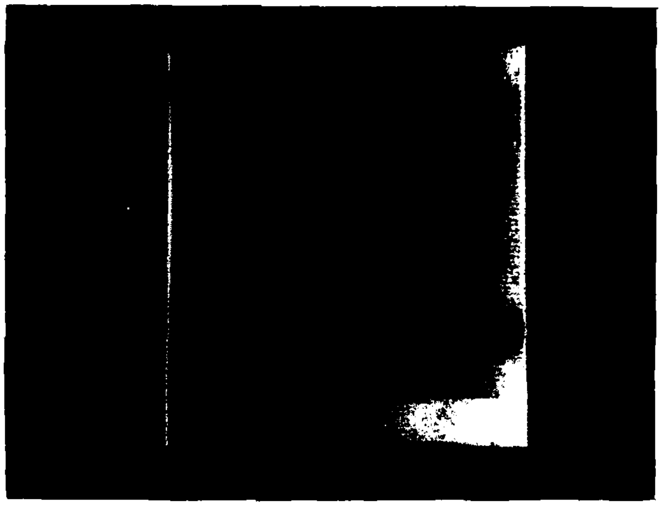

Figure 58: Infrared Results of Double Hole Microwave Heating Pattern (1^{o} C Scale)

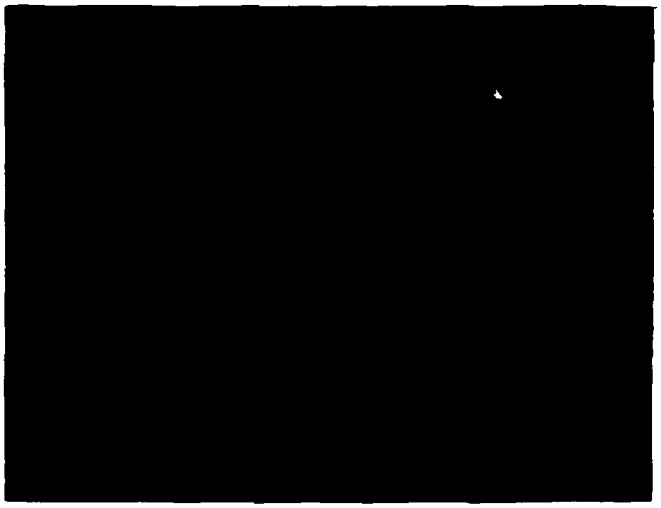

Figure 59: Horizontal Thermal Profile of Double Hole Heating (1^{o} C Scale)

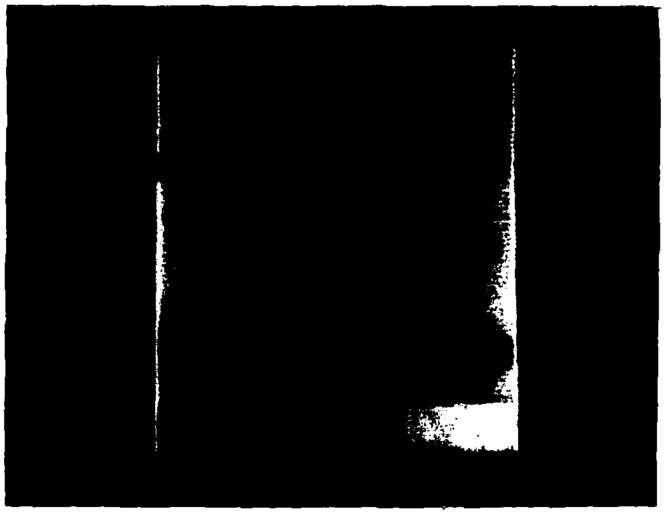

Figure 60: Same as Figure 58 Except 2° C Scale

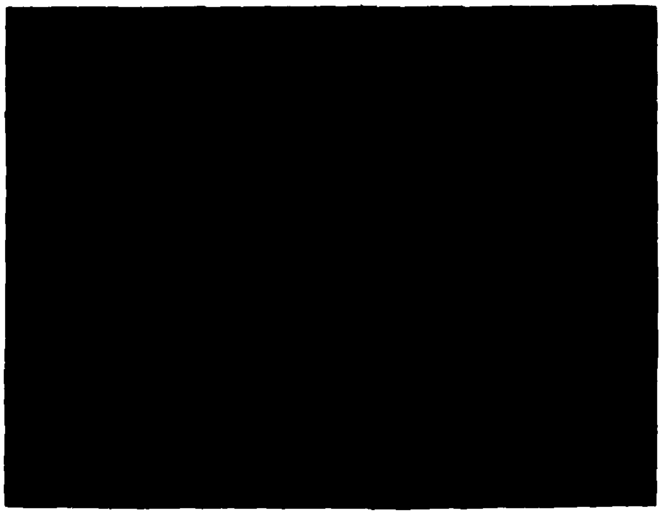

Figure 61: Same as Figure 59 Except 2° C Scale

A z calculated for the simplest (m=1) mode in this configuration is approximately .2 cm. Note that we may still observe separation of the two holes on the thermovision photographs and at that point the actual metal separating the holes was .5 cm. It is of note also, that the particular infrared camera/object separation distance for this experiment only provided a .17 cm camera resolution.

As a final note, it should be obvious that electrically large, finite dimensional, targets exhibit large variations in surface current density (See figures 35,38, and 39 for examples.). It is possible to gain some insight into how these variations relate to the one-dimensional model by considering the following. Suppose that we have a two-dimensional problem in which there are surface current variations in the x direction of a substrate as a result of its finite size. See Figure 62.

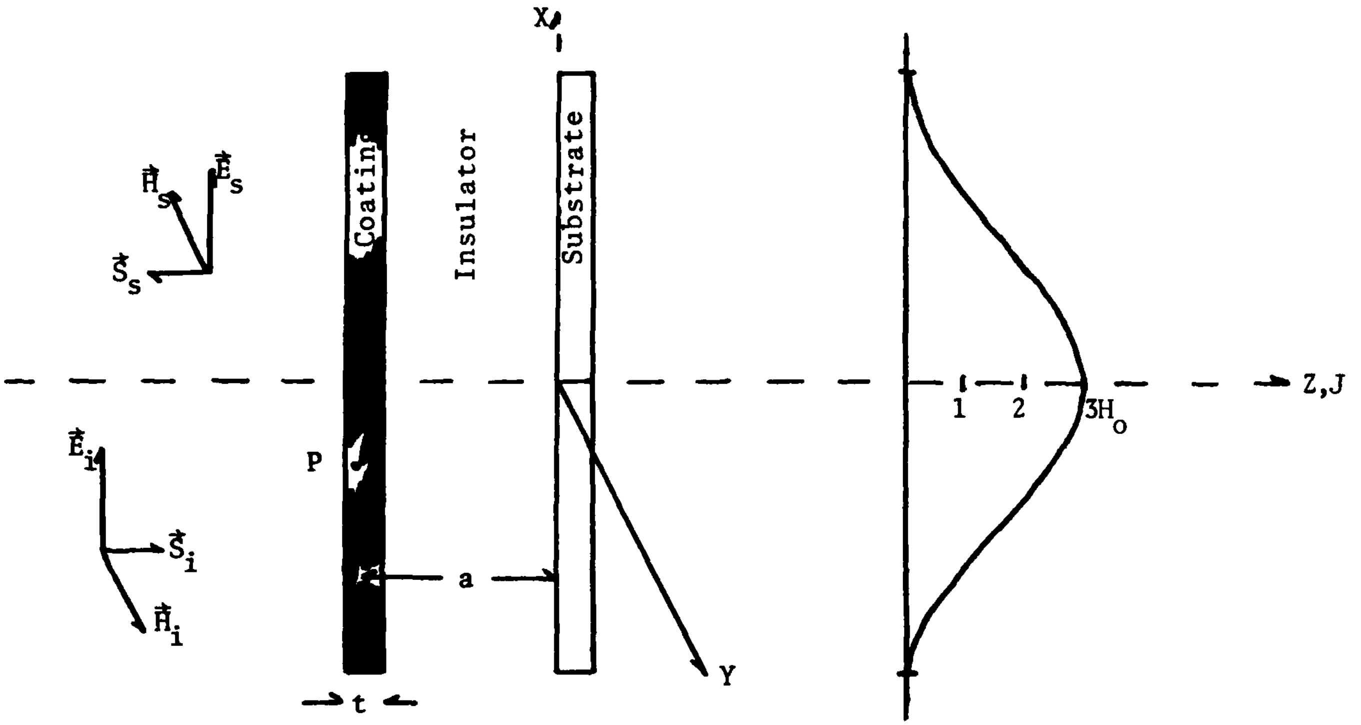
$\vec{H}_s$
$\vec{E}_s$
$\vec{S}_s$
$\vec{E}_i$
$\vec{S}_i$
$\vec{H}_i$
Coatin
P
t
Insulator
a
X
Substrate
Y
1
2
$3H_o$
Z,J

Figure 62: Irradiated, Finite Size, Conducting Substrate with Hypothetical Surface Current Distribution

Clearly, if the substrate were infinite in the x-y plane, the value of J would be a constant given by $|\vec{H}_i|$. However, as a result of its finite size in the x direction and the imposition of boundary conditions, we actually have a current distribution varying spatially in the x direction and supposed to be that illustrated in Figure 62. In this example only, the surface current is confined to the range $0<J<3H_i$.

We know that the total electric field in the coating will be the vector sum of the incident field plus the scattered field from the current element beneath the measurement point, P. The question of nearest neighbor contribution to the field at P has already been discussed. It was shown that most of the scattered field at P resulted from current distributions within a circular radius of approximately a/π. Therefore, if a is small, we may assume the radiating source to be located directly behind P. We have

$$\vec{E}_c = \vec{E}_i + \vec{E}_s \tag{141}$$

where $\vec{E}_c$ is the field in the coating, $\vec{E}_i$ is the incident field, and $\vec{E}_s$ is the scattered field. We may define a fourth field, $\vec{E}_\infty$, as the scattered field from an infinite substrate and $\vec{E}_p$ as a perturbing field that when combined with $\vec{E}_\infty$ would yield the actual scattered field from the finite size substrate. Thus,

$$\vec{E}_s = \vec{E}_\infty + \vec{E}_p \tag{142}$$

Substituting equation 142 into equation 141 we have,

$$\vec{E}_c = \vec{E}_i + \vec{E}_\infty + \vec{E}_p \tag{143}$$

Recalling the development in Chapter V, we may write an expression for the deposited power density in the coating, Q_c, as follows:

$$Q_c = \vec{J}_c \cdot \vec{E}_c = \sigma\vec{E}_c \cdot \vec{E}_c \tag{144}$$

Taking the dot product of $\vec{E}_c$ with itself, we have

$$Q_c = \sigma\{\, E_i^2 + E_\infty^2 + E_p^2 + 2(\,\vec{E}_i\cdot\vec{E}_\infty + \vec{E}_i\cdot\vec{E}_p + \vec{E}_\infty\cdot\vec{E}_p\,)\} \tag{145}$$

Rearranging, we have

$$Q_c = \sigma\{\, E_i^2 + E_\infty^2 + 2\vec{E}_i\cdot\vec{E}_\infty + (\,E_p^2 + 2(\vec{E}_i\cdot\vec{E}_p + \vec{E}_\infty\cdot\vec{E}_p))\} \tag{146}$$

Clearly, by considering temperature regimes in which no changes of state occur for our coating and by remembering the conservation of energy, we may infer that the temperature of the coating is a continuous, increasing function of Q_c; that is,

$$\Delta T = f(Q_c, H) \tag{147}$$

where H consists of several thermodynamic variables such as surface emissivity, sample height, orientation, roughness, etc.. The important point, however, is that for each increment we increase Q_c, ΔT will also increase. If we consider a simple case in which the power loss, Q_L, may be expressed in terms of Newton's law of cooling, we have

$$Q_L = g(H)\Delta T \tag{148}$$

where g(H) is some function of the thermodynamic variables listed above; for a given coating/substrate configuration it is assumed that g(H) will be relatively constant independent of temperature. For example, infrared emissivity is a function of coating electrical conductivity; electrical conductivity was measured versus absolute temperature for an aquadaq coating in Appendix A and found to vary less than 0.3% over the temperature ranges of interest. It can be shown that the emissivity would vary even less than the conductivity; thus, it is assumed to be constant. We may now write the conservation of energy equation for the coating/substrate system in dynamic equilibrium; we have

$$Q_L = Q_c(z=-a)t \tag{149}$$

where t is the coating thickness. In equation 149 we have assumed that the coating in this example is so thin that the power deposition is uniform throughout and is only a function of the coating separation from the substrate. Substituting equation 148 into equation 149, we find

$$\Delta T = \frac{t}{g(H)} Q_c(z=-a) \tag{150}$$

This is the sought after result; the differential surface temperature is directly proportional to the deposited power density. The importance of this arises from the composition of Q_c. The first part of equation 146, ($E_i^2 + E_\infty^2 + 2\vec{E}_i \cdot \vec{E}_\infty$), is what we might call the first order terms which result from a purely one-dimensional analysis of the problem (The coating/substrate combination is infinite in the x-y plane.). The remainder of equation 146, ($E_p^2 + 2\vec{E}_p \cdot (\vec{E}_i + \vec{E}_\infty)$), may be interpreted as the higher order contributions resulting from the imposed boundary conditions in a finite case. Thus, the differential temperatures we observe on our coating surface may be thought of as the sum of temperatures we would observe on an infinite configuration plus any changes that would occur as a result of observing a finite size; that is,

$$\Delta T = \Delta T_\infty + \Delta T_p \tag{151}$$

In equation 151 bear in mind that ΔT_p may have a negative value since only ΔT is required to be greater than zero by the law of conservation of energy. ΔT_p is the term that results from the interference of our perturbing field, E_p, with the total field that would be present in the case of an infinite coating/substrate configuration, ($\vec{E}_i+\vec{E}_\infty$). Also, ΔT typically is not directly proportional to the absorbed power density but rather approximates a square law to a large degree. This non-linearity is no problem since the infrared data is generally entered directly into a computer and may, therefore, be corrected for in a relatively straight forward manner.

The importance of all this is that in analyzing the current distribution on a finite plate via the coating temperature distribution we may wish to consider only the non-steady state term, ΔT_p. That is, in the process of completing an infrared measurement we may wish to scale the results by some additive constant in order to correlate the infrared results with a single probe measurement on a particular surface and thereby "calibrate" the infrared results for all other points on that surface.

Since we have shown earlier that small samples may be used to approximate the one dimensional infinite plane, it seems reasonable then to assume that we can use small samples to measure ΔT_∞ directly. A series of flat plate experiments were performed in which this was done. First, a small 1.5 cm square was irradiated with microwaves at a frequency of 2.45 GHz and a power of 25 mW/cm^2. This is the same sized sample used in the verification experiments. Therefore, by measuring the equilibrium temperatures on the surface of the small sample we have obtained ΔT_∞ for that particular coating configuration. Next, a 1.0λ square plate was irradiated in order to illustrate the process. An infrared photograph was made along with a single thermal profile. ΔT_p may be obtained by subtracting ΔT_∞ from the total temperature measured by the thermovision. ΔT_∞ was drawn on the profile photograph to illustrate the magnitude involved. Figures 63 to 68 were made from a coating of 15 microns of aquadaq (315 mhos/m) placed on 5.1 mm of foam insulator. Figures 69 through 74 were made using an aquadaq coating 15 microns thick and placed on 10.2 mm of foam insulation. Additionally, Figures 69 through 74 included a copper substrate whereas the earlier photographs contained no substrate.

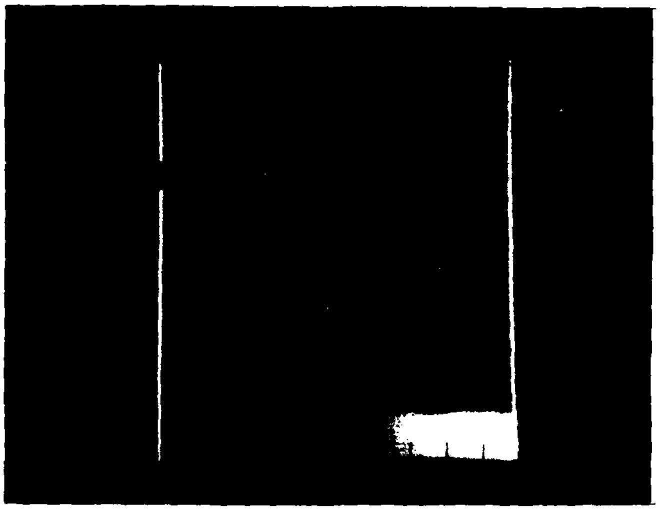

Figure 63: Thermovision Photograph of 1.5 cm Square Sample (No Substrate)

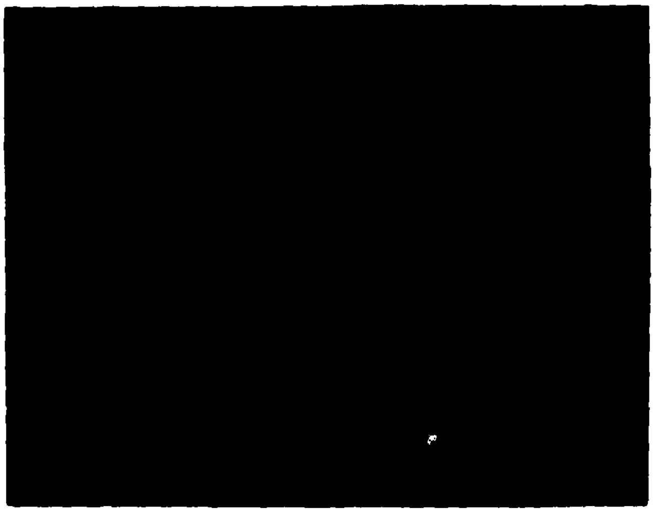

Figure 64: Thermal Profile (Horizontal) through the Center of the 1.5 cm Square Sample (2.45 GHz at 25 mw/cm^2)

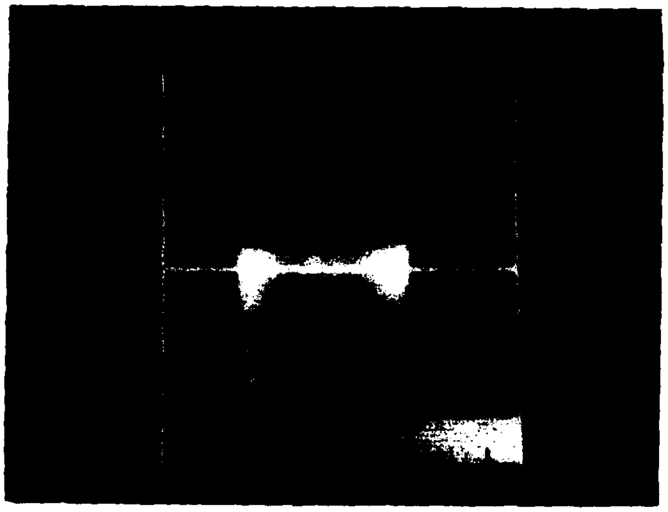

Figure 65: Thermovision Photograph of 1.0λ Square Plate (Horizontal white line indicates area where thermal profile was taken.)

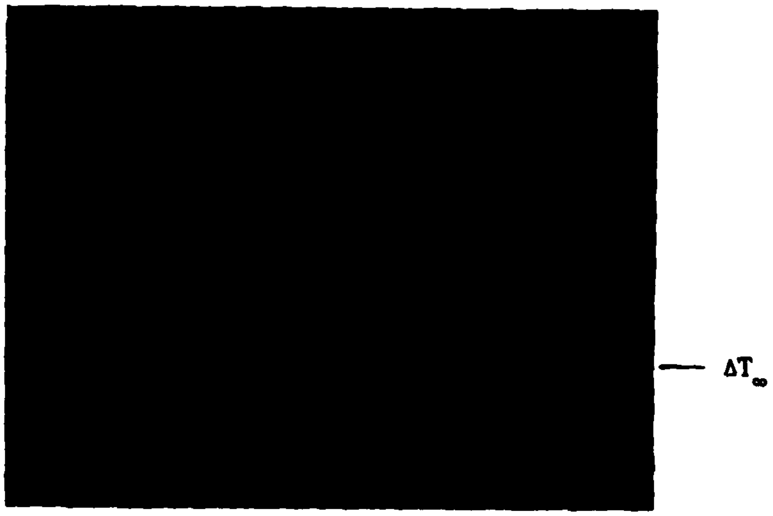

Figure 66: Thermal Profile from 1.0λ Square Plate with ΔT_∞ Plotted

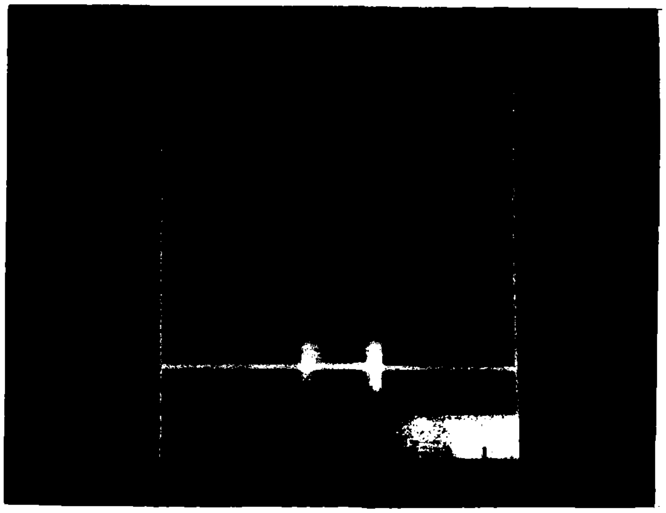

Figure 67: Thermovision Photograph of 0.5λ Square Plate (Horizontal white line indicates area where thermal profile was taken.)

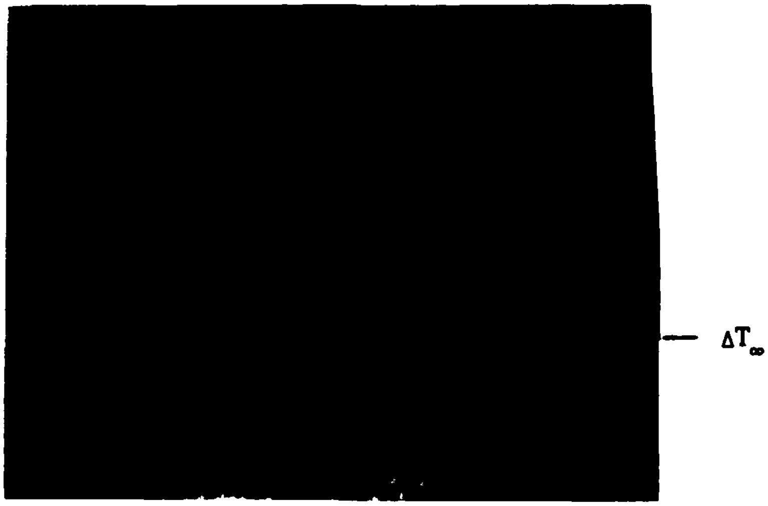

Figure 68: Thermal Profile from 0.5λ Square Plate with ΔT_∞ Plotted

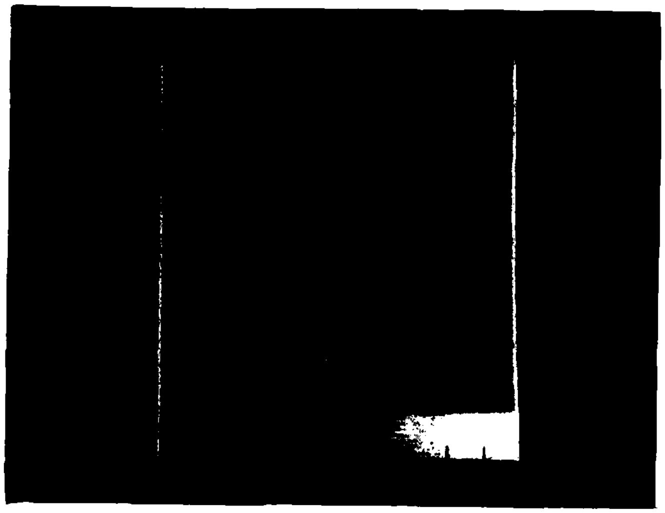

Figure 69: Thermovision Photograph of 1.5 cm Square Sample (Copper Substrate)

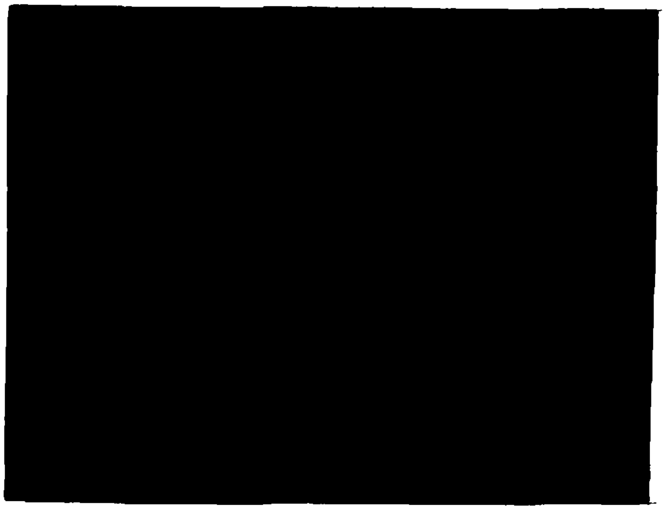

Figure 70: Thermal Profile (Horizontal) through the Center of the 1.5 cm Square Sample (2.45 GHz at 25 mw/cm^2)

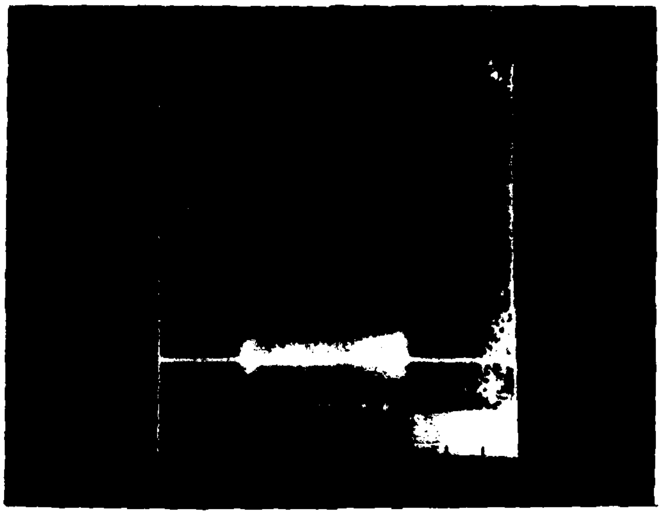

Figure 71: Thermovision Photograph of 1.0λ Square Plate with a Copper Substrate

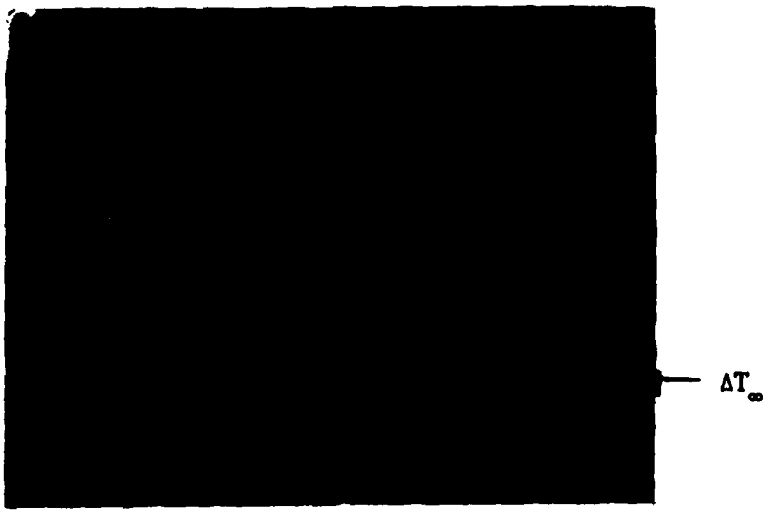

Figure 72: Thermal Profile Corresponding to White Line in Figure 71

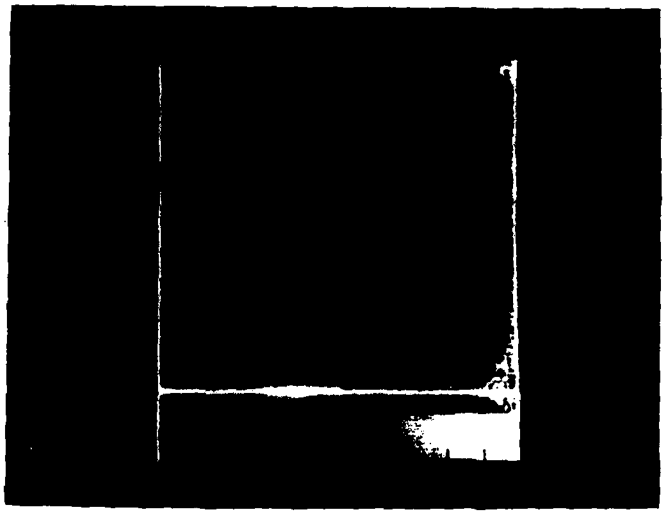

Figure 73: Thermovision Photograph of a 0.5λ Square Plate with a Copper Substrate

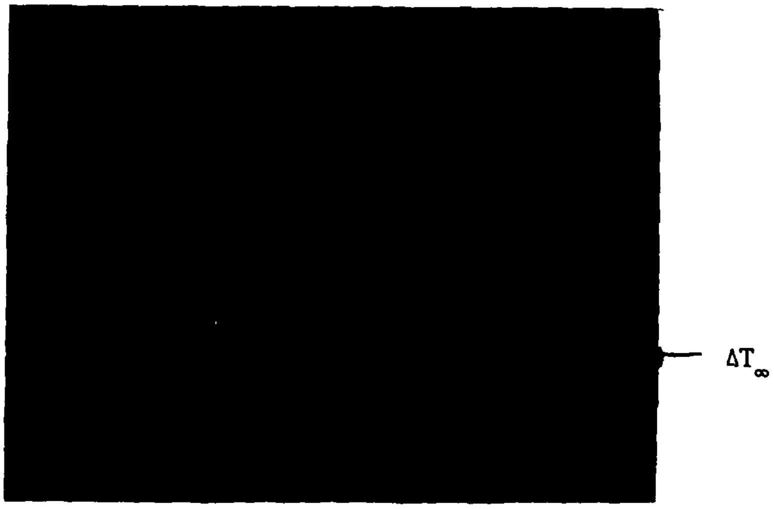

Figure 74: Thermal Profile Corresponding to White Line in Figure 73

In passing it should be pointed out that the preceding results are consistent with the theoretical analysis typically employed in the development of holography [36]. This is to be expected since the coating is simply recording the interference patterns resulting from the combined effects of the incident and scattered fields from the substrate surface. This would be the arrangement for a typical Gabor hologram [37]. As is the case of an optical hologram, we have both phase and amplitude information stored in the thermogram of the surface coating. Clearly, the points on a thermal profile lying below ΔT_∞ indicate that $\vec{E}_p$ must be out of phase with $(\vec{E}_i+\vec{E}_\infty)$ which would yield a negative value for the dot product in equation 146. It is not as easy to assess phase information for the ΔT's above ΔT_∞. These areas may correspond to $\vec{E}_p$'s out of phase with $(\vec{E}_i+\vec{E}_\infty)$ but much greater in magnitude such that $\vec{E}_p$ itself is the primary heating source. Continued research in this area may finally provide much needed information in regards to surface current phase. Fast Fourier Transform (FFT) techniques and optical reduction of the coating interference patterns into optical wavelengths for subsequent laser illumination are both techniques that may provide the desired phase information. [38]

This was not an attempt to quantitatively determine the resolving power of any particular coating. That effort is better left as a topic for further study on its own merit in another dissertation. However, it does illustrate that there are no far reaching "nearest neighbor" effects. We observed no shadows or false apertures as might be expected if there were some other propagation mode present. Thus, the end result of this series of experiments is a qualitative understanding of the nearest neighbor interaction in electrically large targets plus an assurance that the one dimensional model may be used with confidence in the design of a particular coating.

CHAPTER VIII

RECOMMENDATIONS AND CONCLUSIONS

This paper provides a method of selecting an optimum coating for use in the thermographic detection of microwave induced surface currents. Optimum in this sense implies two things. First, we needed a coating that would heat to at least 1 degree Centigrade above ambient temperature to achieve 10 levels of resolution on the infrared system. This is directed by the accuracy of the thermographic camera which can resolve temperatures to within 0.1° C. Secondly, we needed a coating that would heat to an acceptable level but minimally interfere with the fields present. This second requirement stems from the necessity of minimizing the effect any measurement device would have with the quantity being measured.

In attaining an optimum coating there were other constraints that we had to adhere to in order to have a realizable system. First, the coating should not contain ferrites, non-isotropic, or permeable materials. This requirement was established to ensure that the coating itself did not introduce possible intermodulation distortions resulting from non-linear materials.

Secondly, it was desired that the coating be easily fabricated for application to a variety of possible shapes. And thirdly, it had to be non-toxic to avoid possible health problems.

From an engineering point of view, there are only a finite number of variables that may be controlled to achieve the desired results. The material characteristics are limited to coating electrical conductivity and the insulating layer permittivity. Since we do not allow the use of ferrous materials in either, the relative permeability is approximately 1. The easiest factor to control, and the most effective, is the individual layer thickness.

Before explaining the coating development, it is appropriate to point out the two different uses of the coatings. The first involves a situation in which only the shape of a particular object is important in an electromagnetic interaction problem. To determine the current distribution in this problem, the simplest and most effective technique is to construct a model of the object from a foam material (low thermal mass) and then coat it with a thick (2-3 skin depths) coating of high electrical conductivity (300-500 mhos/m) material. Thus, we simulate a highly conductive object which may be made of something such as aluminum with one of lesser conductivity. Senior, et al [32] have demonstrated that the modeling would not be one-to-one for small conductivities but Sega has demonstrated that for reasonable conductivities (greater that 300 mhos/m) the comparison may be close[33]. A possible application of such a scheme might be to determine the current distributions on an aircraft, ship, or spacecraft to facilitate the proper placement of antennas or measure radar cross section. Additionally, this type information might be valuable when studying the vulnerability of an existing or future weapon system to the effects of an Electromagnetic Pulse.

The more difficult problem is one which cannot be modeled because the materials the object is made from are relevant factors in the particular microwave interaction. An example is a missile or satellite constructed from conductive composites, iron alloys, aluminum, etc. Here the object itself must be irradiated and the resulting surface currents measured. To measure these currents, a different type coating arrangement is required. Two requirements exist; the coating must be thermally isolated from the surface to allow heating, plus it should be sufficiently distant from the surface so that the total (reflected plus incident) electric field is reasonably large. That is, the electric field must be large enough so that the heating in the coating will result in a temperature increase greater than one degree Centigrade. Neoprene rubber fills several of the requirements for the insulating layer. It is a good thermal insulator; it is non-ferrous; it will easily conform to complex shapes with the aid of contact cement; and it has a high relative permittivity (measured to be 31 at 10 GHz). The high permittivity allows us to place the coating an electrically long distance from the surface even though the rubber may be physically thin. The advantage of this may be seen if one considers the infinite, perfectly conducting plane. At the surface we have a surface current magnitude given by $2H_0$, but the electric field is zero there; however, at a distance of one quarter wavelength from the plane the electric field magnitude is given by $2E_0$. Thus, if we placed a thin conductive layer at this distance from our infinite conducting plane, we would see maximum heating. A large permittivity material allows us to minimize the actual insulator thickness thus making it easier to apply. There is a disadvantage, however, in that the high permittivity insulator has a much higher reflection coefficient which has the effect of shielding the surface from the incident microwaves.

To optimize the above situation, that of placing our conductive coating on an insulating layer, we may use the following procedure. A computer program, Uthick, described in Appendix G , generates a square matrix in which the coating thickness and insulator thickness have been allowed to vary for the corresponding matrix elements. The coating thickness changes linearly along the rows and the insulator thickness changes linearly along the columns. After this matrix is generated for a particular conductivity and insulator configuration, the results are plotted on a contour plot. The contour program, Contor, is located in the appendix also. Each coating configuration is examined with and without a conductor behind the insulating layer, thus simulating the situation of having currents present and not present. Finally, for comparison purposes a different contour is presented which indicates the thermal differences between a coating scheme with and without the conductor behind the insulator. Therefore, we can determine at a glance what the optimum coating configuration would be for a given situation. For electrical conductivities ranging from 0.1 to 40 mhos/m the appendix on electrical conductivity describes in detail how a particular conductivity coating may be made using a carbon and paraffin mixture. Figures 75 to 95 illustrate the various contour plots for conductivities of 1, 5, and 10 mhos/m with insulators of styrofoam (permittivity = 1.1) and neoprene (permittivity = 31). Additionally, a plot of aquadaq (conductivity = 315 mhos/m) on 1/16 inch plexiglas is given. The incident microwave field was set at 10 mW/cm^2 and 2.45 GHz.

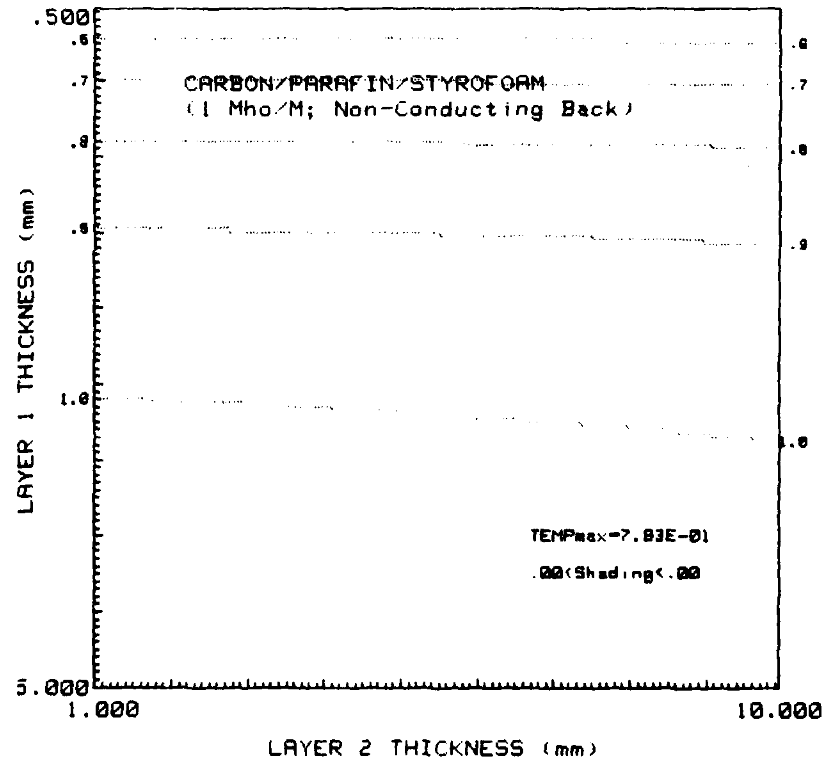

Figure 75: Carbon/Paraffin/Styrofoam Thermal Contours

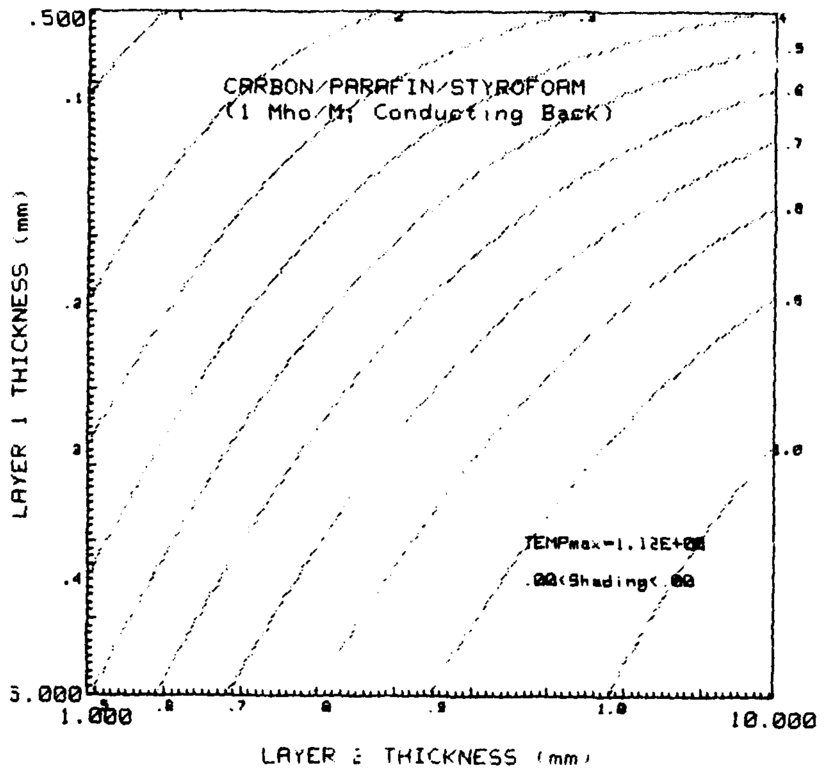

Figure 76: Carbon/Paraffin/Styrofoam/Copper Thermal Contours

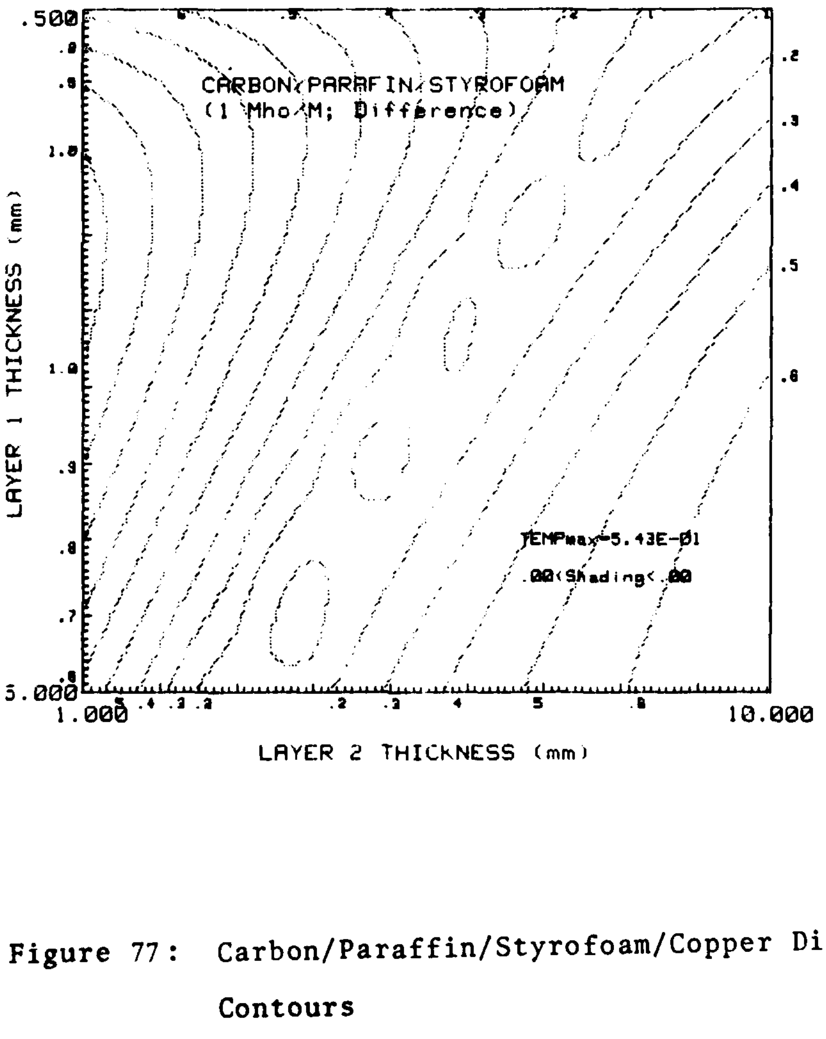

Figure 77: Carbon/Paraffin/Styrofoam/Copper Difference Contours

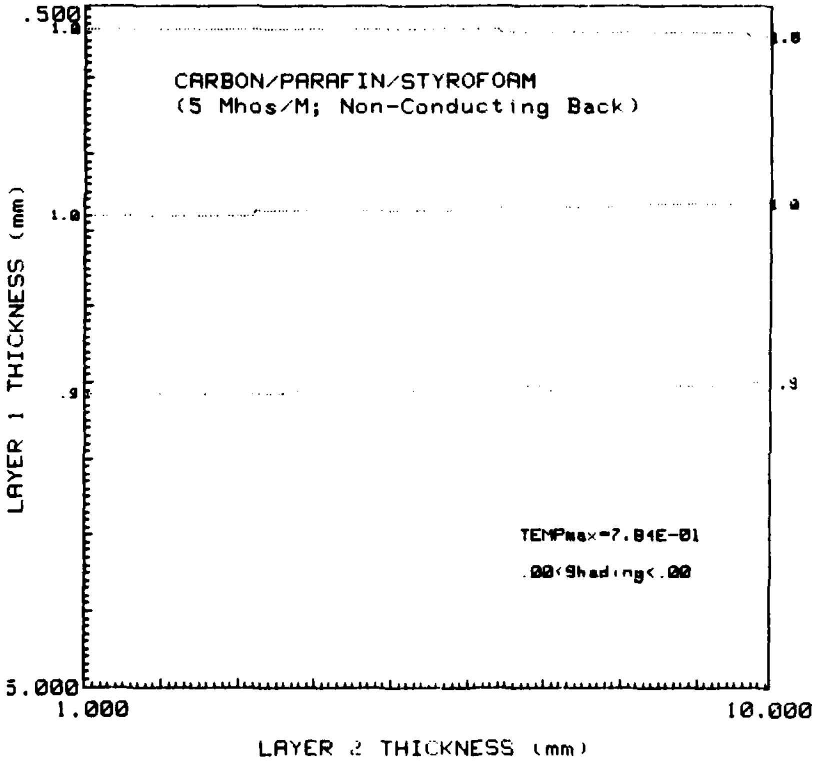

Figure 78: Carbon/Paraffin/Styrofoam/Thermal Contours

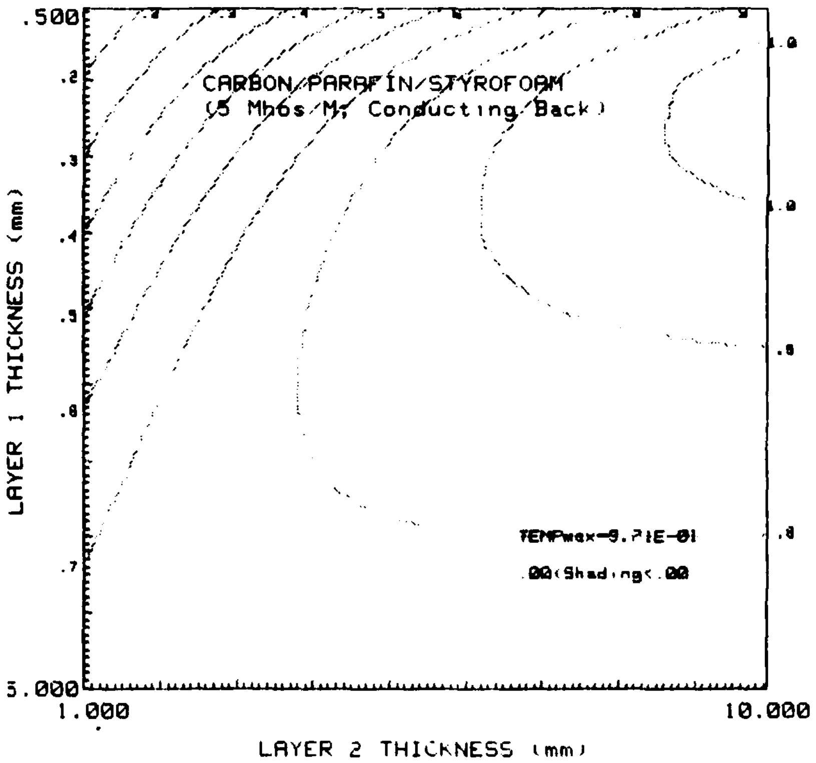

Figure 79: Carbon/Paraffin/Styrofoam/Copper Thermal Contours

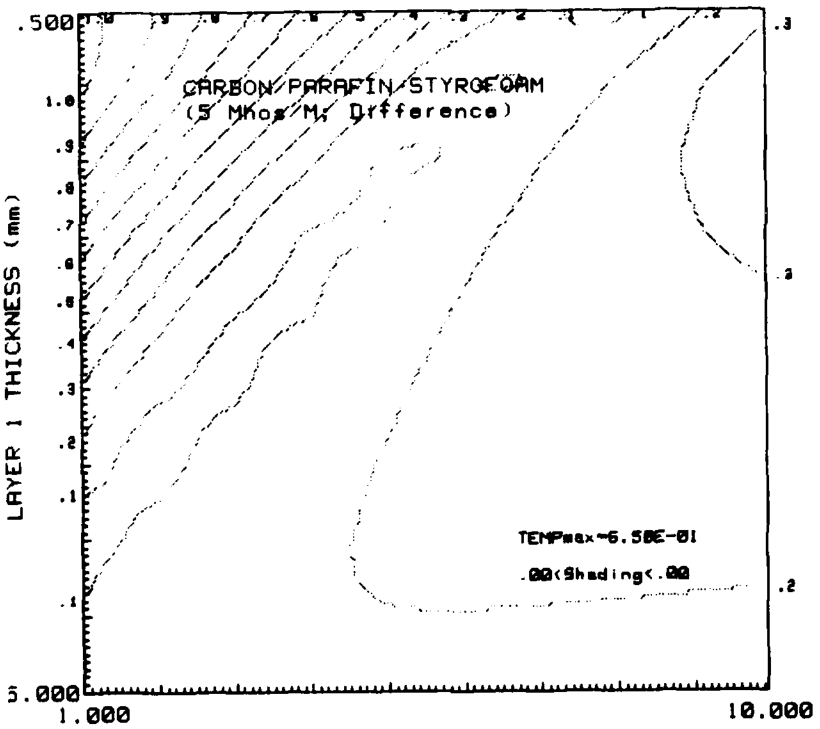

Figure 80: Carbon/Paraffin/Styrofoam/Copper Difference Contours

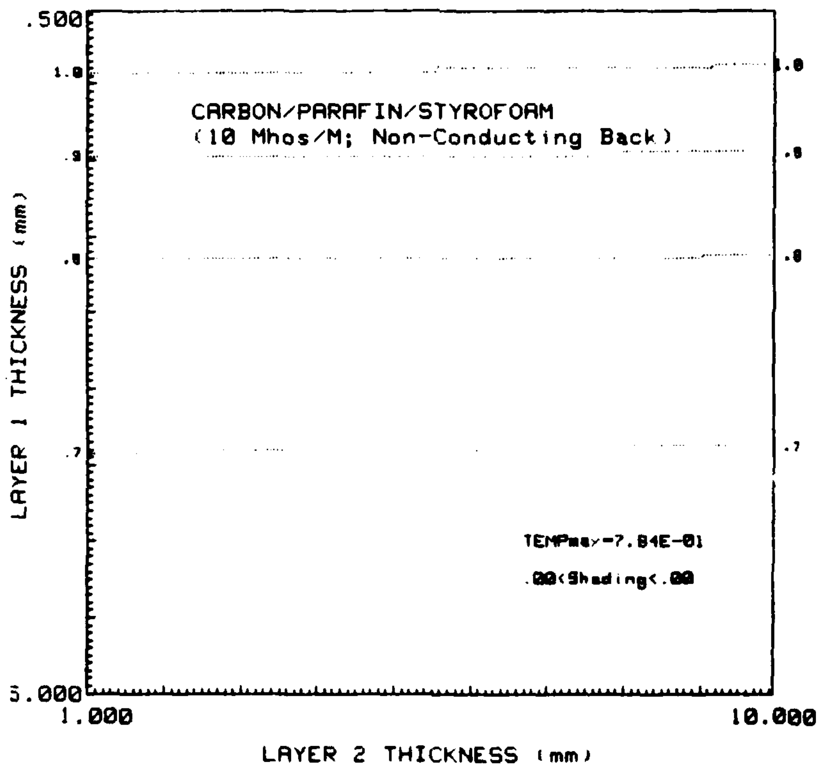

Figure 81: Carbon/Paraffin/Styrofoam/Thermal Contours

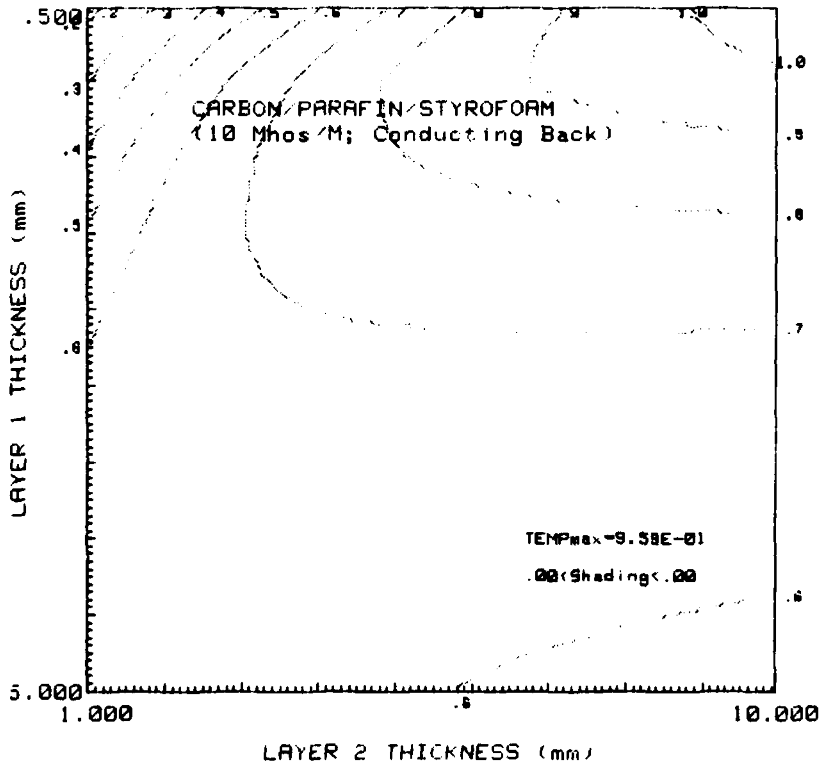

Figure 82: Carbon/Paraffin/Styrofoam/Copper Thermal Contours

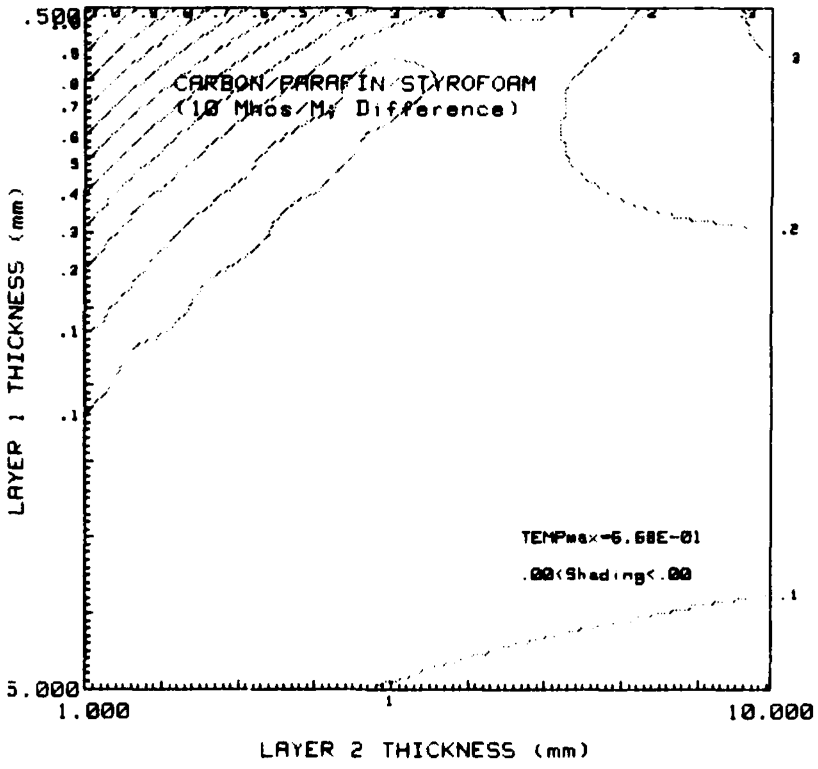

Figure 83: Carbon/Paraffin/Styrofoam/Copper Difference Contours

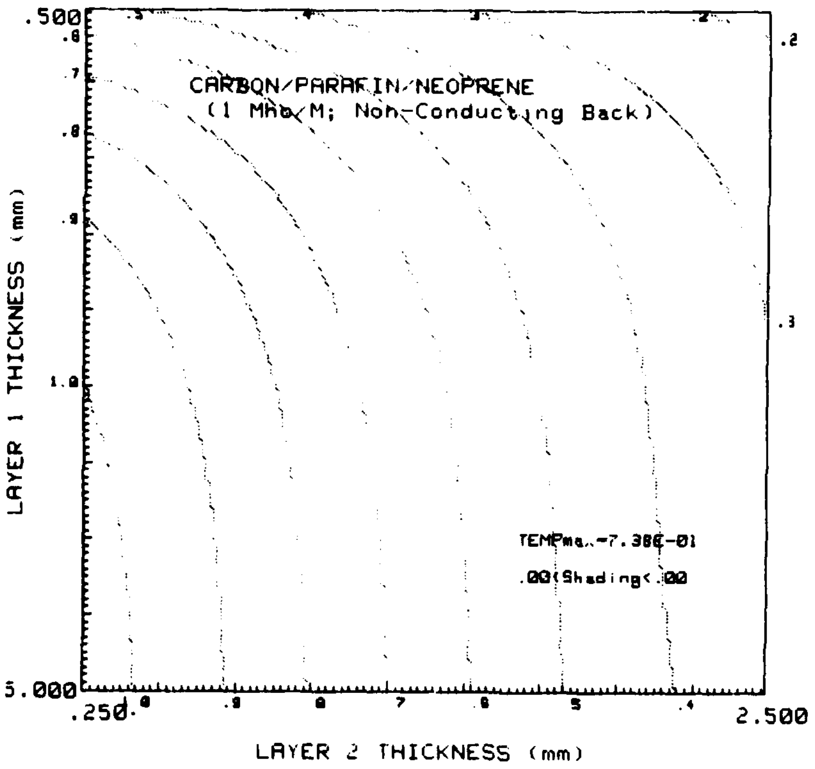

Figure 84: Carbon/Paraffin/Neoprene Thermal Profiles

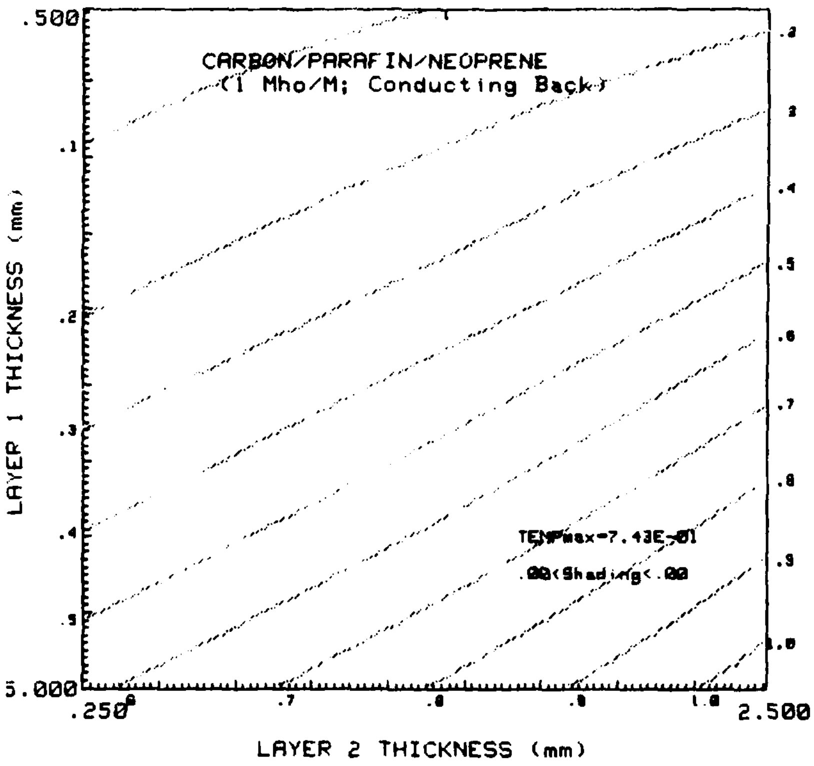

Figure 85: Carbon/Paraffin/Neoprene/Copper Thermal Profiles

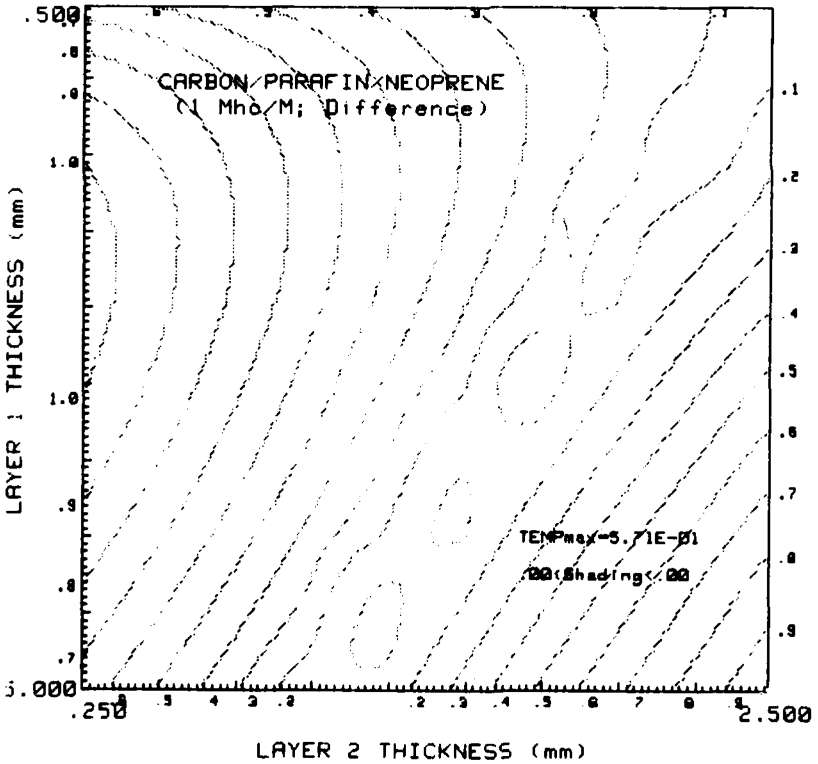

Figure 86: Carbon/Paraffin/Neoprene/Copper Difference Contours

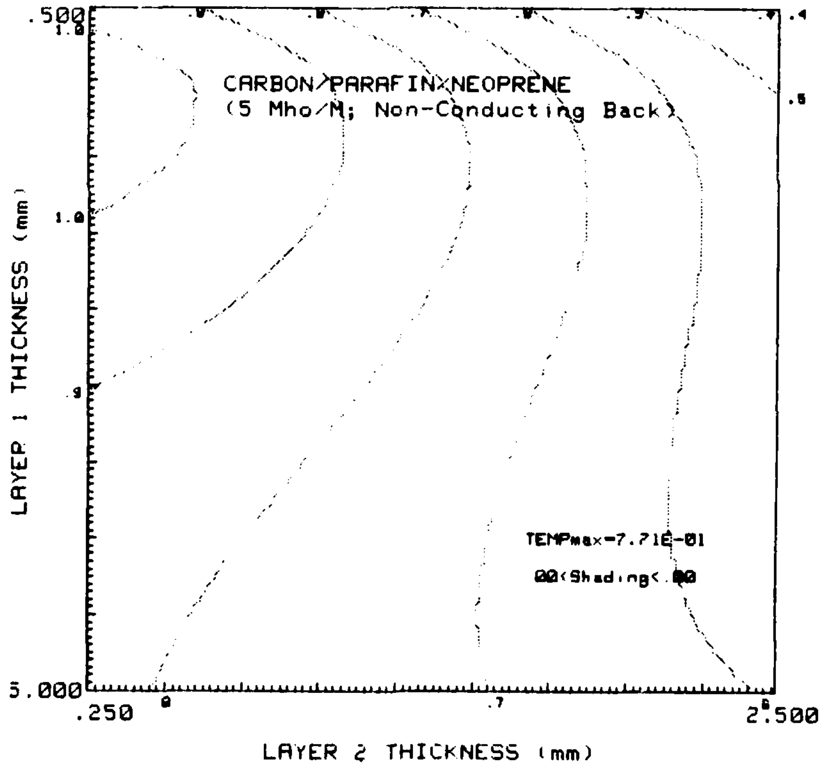

Figure 87: Carbon/Paraffin/Neoprene Thermal Contours

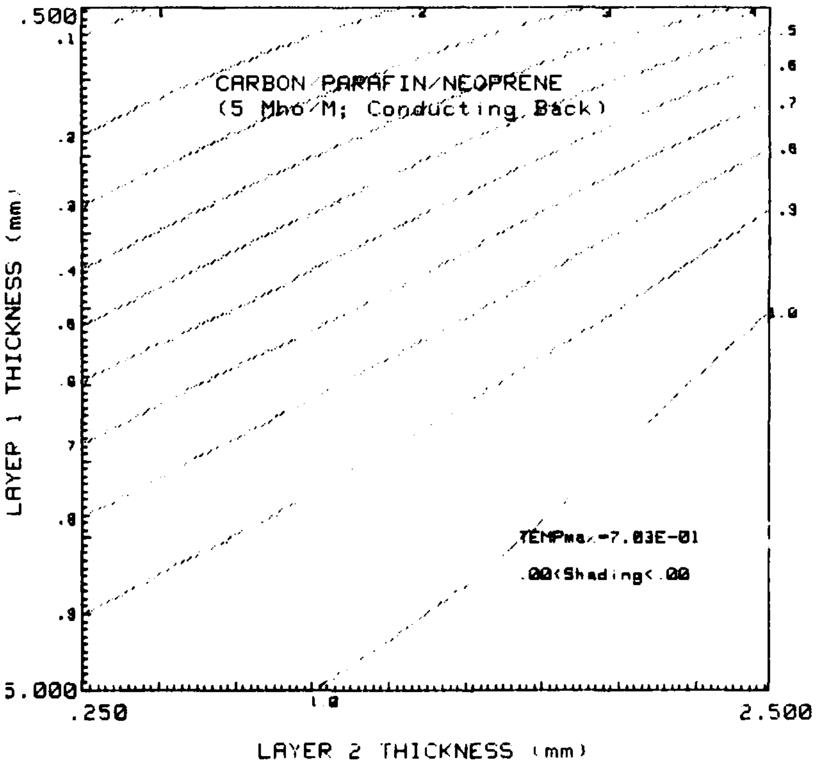

Figure 88 : Carbon/Paraffin/Neoprene/Copper Thermal Contours

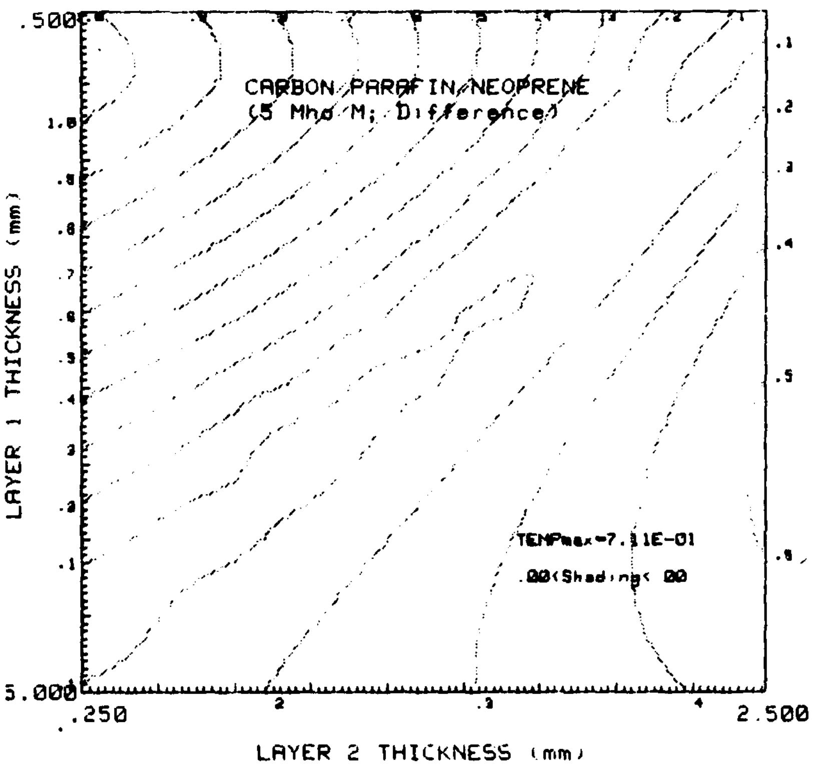

Figure 89: Carbon/Paraffin/Neoprene/Copper Difference Contours

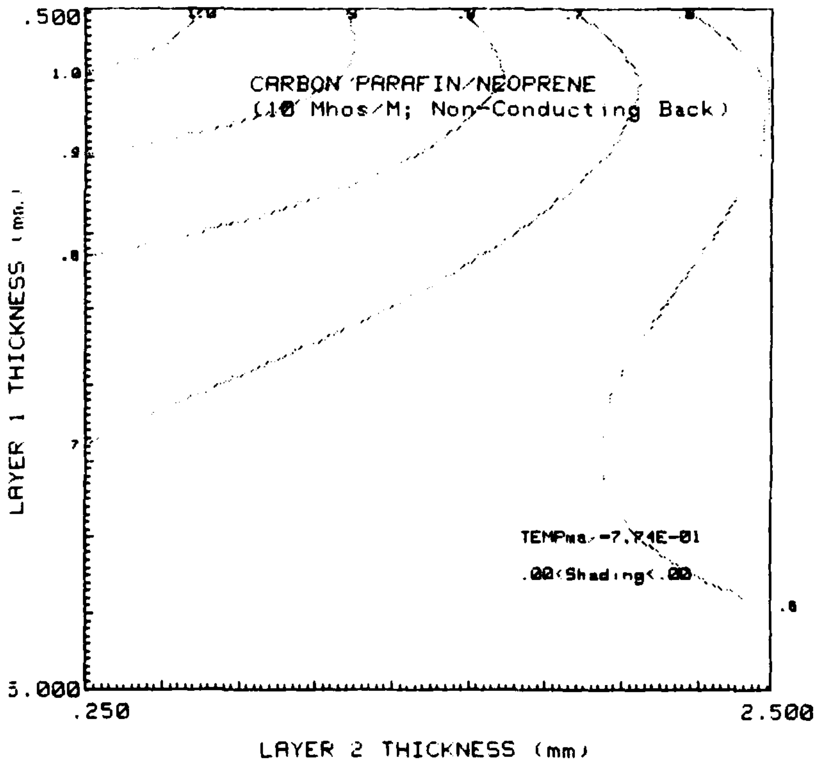

Figure 90: Carbon/Paraffin/Neoprene/Thermal Contours

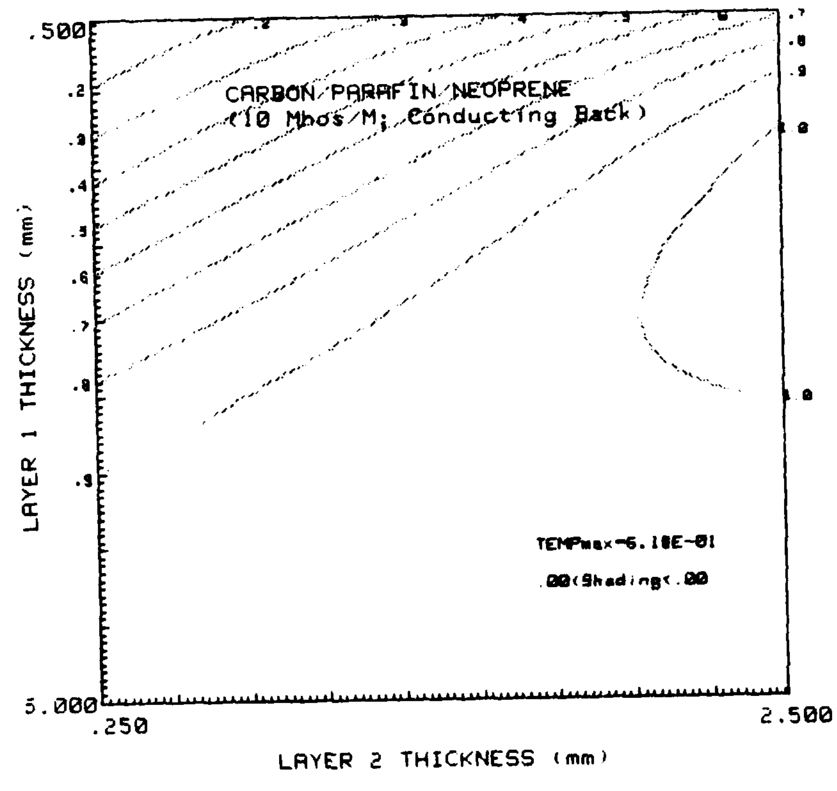

Figure 91: Carbon/Paraffin/Neoprene/Copper Thermal Contours

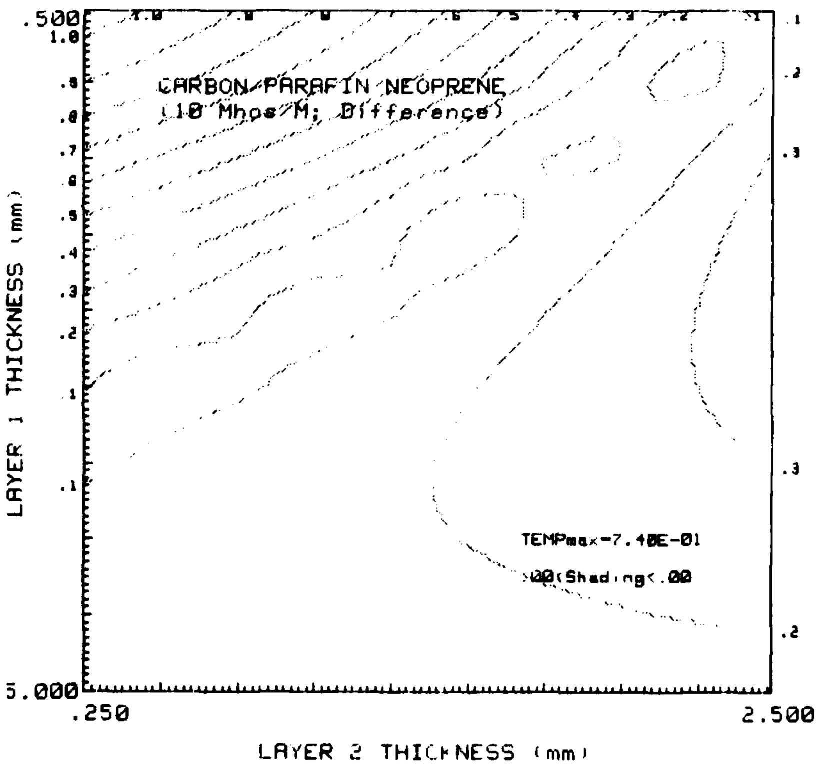

Figure 92: Carbon/Paraffin/Neoprene/Copper Difference Contours

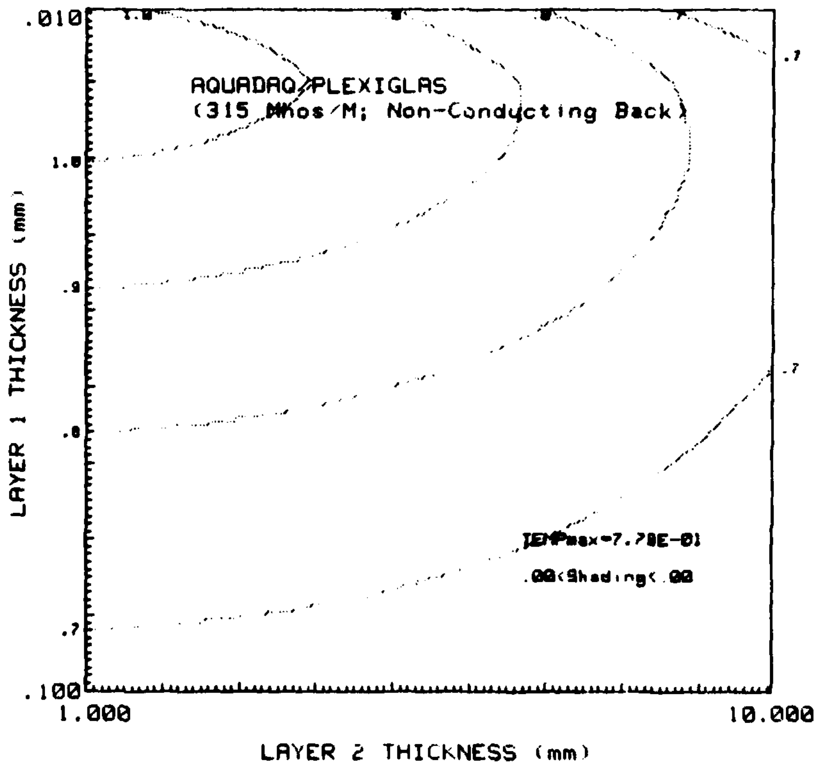

Figure 93: Aquadaq/Plexiglas Thermal Contours

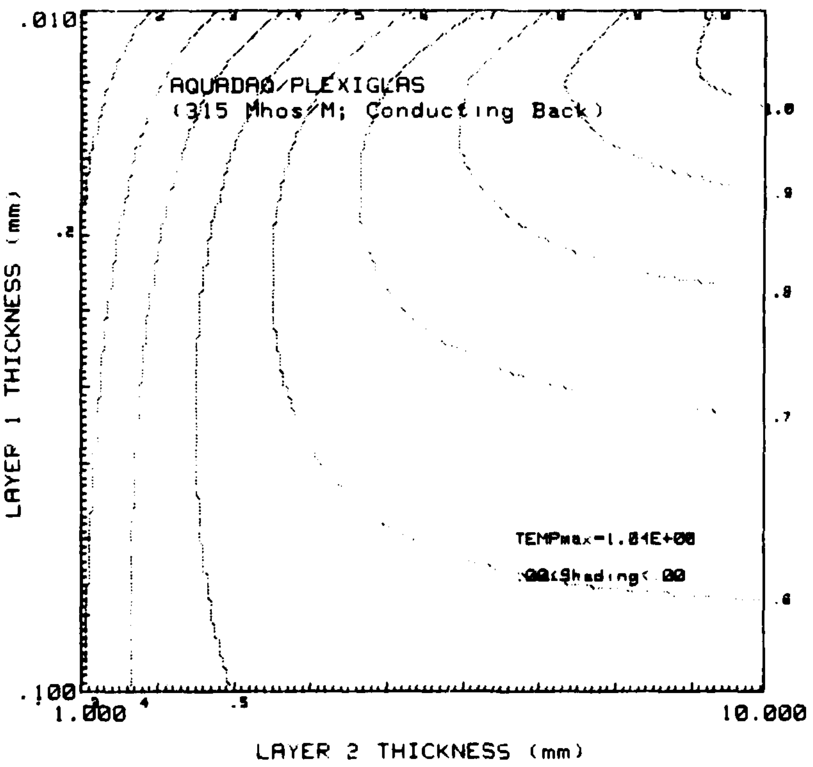

Figure 94: Aquadaq/Plexiglas/Copper Thermal Contours

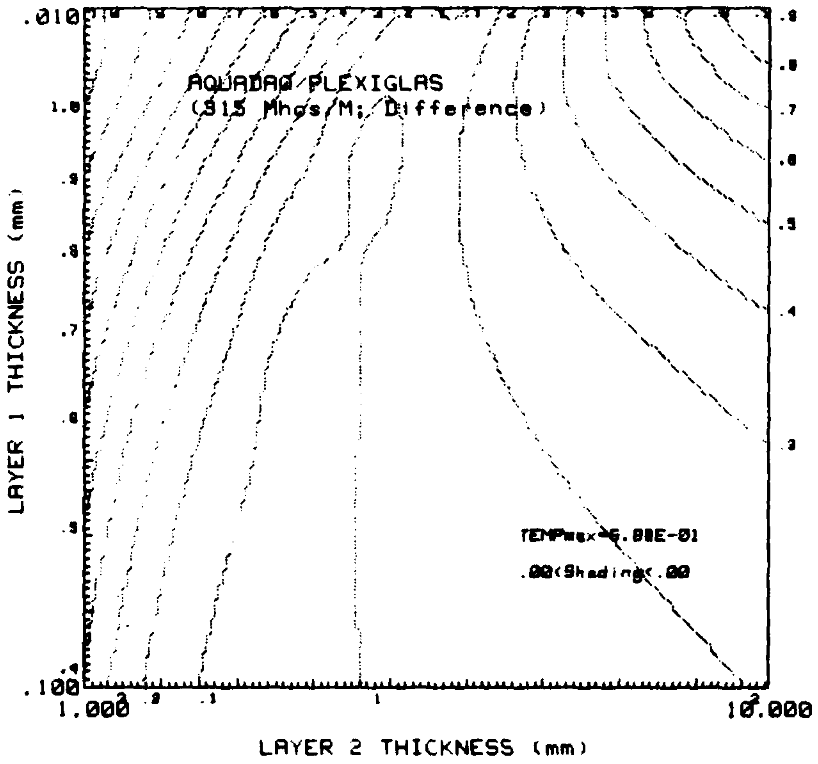

Figure 95: Aquadaq/Plexiglas/Copper Difference Contours

The preceding figures were included to primarily illustrate the effects of different coating/insulating layer combinations. Also, they are representative of the order in which one would use the algorithms included in the appendix in order to analyze a particular coating configuration. That is, assuming a certain material is available and has a measured electrical conductivity, how does one spatially arrange it for optimum effectiveness?

First of all, in addition to selecting a coating material, we must select a suitable thermal insulator. The four primary areas of concern in selecting an insulator are its electrical characteristics which include permittivity and electrical conductivity (or loss factor), its thermal conductivity, and its mechanical applicability. Extensive experimentation was conducted using Plexiglas, styrene plastic, styrofoam, urethane foam, neoprene rubber, glass, phenolic, paraffin wax, paper, etc.. It was found that the foams (styrofoam and urethane foam) exhibited superior electrical characteristics over the other materials. Their loss factors are very low and both have a relative permittivity very near 1; thus, the microwaves hardly know the insulators exist. In addition they are excellent thermal insulators. Therefore, where mechanical application is relatively straight forward, either of the foams will perform excellently. Urethane foam is impervious to nearly all chemicals and, therefore, nearly any coating may be used without reacting with it. Styrofoam, on the other hand, is a styrene and exhibits disastrous results when used with nearly any petroleum based coating. This is especially true with toluene which is the carrier for the aquadaq coating. It was found that styrofoam performed very well with paraffin/carbon coatings or by chemically shielding it from a petroleum based product. The shield may be a very thin layer of paraffin wax, stick-on Mylar, or stick-on paper. For flat surfaces, there is a ½ inch foam sheet available at most art supply stores with a paper coating on each side. It is extremely easy to work with, inexpensive, and comes in sheets up to 3x4 feet square. When working on complex surfaces, the neoprene rubber exhibited the most flexibility from an applications point of view; however, it has a very large relative permittivity. The permittivity problem may be partially overcome by using neoprene foam which is commercially available in thicknesses from 1/16 to 1/2 inch. Even though the permittivity for neoprene foam was not measured it should be significantly less than the value of 31 measured for solid neoprene. This is the same foam used in diver's wet suits and should also be relatively inexpensive. It is easily applied to almost any grease free surface using a typical rubber contact cement. It is also impervious to nearly all chemicals.

Having chosen a coating type and insulator, the final question that must be answered is related to the thickness of each. Using the algorithm included in the Appendix, we may generate a set of three contour plots similar to the ones presented earlier in this chapter. The first would be only with the coating and insulator and no substrate present. This will give us an idea of the differential temperatures that might be observed on the coating if there were zero surface currents located on the substrate. Next, we consider the coating/insulator/substrate combination. The temperatures illustrated would represent the ΔT_∞ that might be expected. This is the same ΔT_∞ discussed in the latter part of Chapter VII. In this case the surface currents on the substrate are not zero but something between zero and $|\vec{H}_i|$. The third step is to numerically subtract the above two results and display the difference as a contour. This is probably the most important step since it provides the insight required to choose the optimum thickness for both the coating and insulator. It allows us to choose thicknesses that will provide the greatest temperature difference between the case of no substrate ($\vec{J}=0$) and infinite substrate ($\vec{J}>0$).

Illustrative of the above process are two coating examples that have provided excellent results. The first is three layers of aquadaq (315 mhos/m), yielding a total thickness of approximately 15 μm, placed on a 5.1 mm thick sheet of paper covered foam. This was the scheme used in the resolution experiments in Chapter VII. The second was a paraffin/carbon conductive coating used by Sega[39] approximately 1.5 mm thick (≈2.0 mhos/m) and placed on a layer of styrofoam 12.5 mm in thickness. There were some difficulties with this scheme in that the coating thickness tended to vary greatly even after machining. This resulted primarily from foam/paraffin expansion problems; therefore, if the paraffin/carbon coating is to be used, it should be kept thin (preferably less than 1 mm).

In summary then, for the case of a coating/insulator/substrate experiment, attempt to use a foam as the insulator: preferably styrofoam, urethane, or last choice, neoprene foam. Use a coating that is easily applied to a uniform thickness. In this case differential surface temperature is almost directly proportional to coating thickness so uniformity is paramount. Typically, the electrical conductivity will be a fixed value; however, for a spray any value from 10 to 500 mhos/m will probably work well (A conductivity between 20 to 100 mhos/m would be optimum.). Execute the above mentioned computer program and determine the optimum thicknesses for the coating and insulator. Apply the coating/insulator to the substrate and after suitable curing the experiment should be ready for thermographic observation in the microwave field.

Most of the preceding discussion has centered predominantly on the coating/insulator/substrate problem; however, it should be pointed out again that this is not the only coating technique. If we are interested only in the geometrical shape of a particular object, the coating problem is much simplified. The idea, as was mentioned earlier, is to construct a model of foam and then coat it with 2 to 3 skin depths of conductive coating. In this case it can be shown that the surface temperature is independent of coating thickness and only a function of the surface currents present; thus, the coating application need not be critical. Clearly, if the coating has no conductivity (a dielectric) or infinite conductivity (perfect conductor), there will be no energy absorption and, thus, no surface temperature increase. The primary problem then is to determine the optimum conductivity. Chapter V provided the answer for us by referring to Figure 19. There it can be seen for an input power of 10 mW/cm^2 and at a frequency of 2.45 GHz that the maximum conductivity we may have, and still have a suitable temperature increase (1^o K), is 750 mhos/m. If we need to consider different microwave parameters, another three dimensional plot may be generated with the computer program included in the Appendix. In this coating scheme we must keep in mind that we want the electrical conductivity as large as possible so that it will more closely approximate a perfect conductor. If we absolutely need a conductivity greater than 750 mhos/m, we must increase our input power correspondingly in order to observe acceptable heating.

In conclusion we may reiterate some of the important aspects of this paper. Initially, a theoretical, one dimensional model is presented which couples the N-Layer electromagnetic problem with the thermodynamic problem; hence, we have a model which predicts equilibriur surface temperatures resulting from electromagnetic absorption in a system of N layers. This is provided as an analysis tool for the engineer interested in investigating different coating schemes. The computer program which solves this problem is included in the Appendix. This model is subsequently verified experimentally on particular multi-layered models. The applicability of the small sample verification process was discussed next. It was shown that a small sample may be a valid approximation for the one dimensional model. It was also shown that nearest neighbor considerations are minimized for coatings that are placed near the substrate surface. As a rough rule of thumb, it was shown that the coating resolution may be approximated by the value a/π, where "a" is the insulator thickness. It was also shown that the differential temperature observed on the coating of an electrically large object may be thought of as a steady state term resulting from the one dimensional solution plus a higher order term resulting from the finite boundary conditions present. As a result of this analysis, the experimental engineer may be allowed to scale his infrared results by an additive constant in order to "calibrate" the thermographic system. In addition to the above, two particular coating schemes are illustrated that provided reasonable results; these were the carbon/paraffin/ styrofoam and aquadaq/styrofoam coatings. Lastly, the Appendix includes information concerning techniques for measuring electrical permittivity and electrical conductivity as well as most of the major computer routines used.

Finally, it is important to reiterate that this entire development was classical in nature and thus only allowed for joule heating in the coating. Other absorption mechanisms, such as rotational coupling, may prove equally or more effective in coating design in the future. The thermographic detection of induced surface currents is only beginning to demonstrate its full capability. The benefits of such a scheme should prove invaluable to the systems design engineer working in the ever increasing electronic warfare environment.

BIBLIOGRAPHY

1. LaVarre, C.A. and Burton, R.W.; "Thermographic Imaging of Electromagnetic Fields," Thesis Report NPS-52ZN 75121; 1975; Monterey, CA; Naval Postgraduate School.

2. Martin, V.M., Sega, R.M., Stewart, C.V., and Burton, R.W.; "Applications of Infrared Thermography in the Analysis of Induced Surface Currents Due to Incident Electromagnetic (EM) Radiation on Complex Shapes," Proceedings of the Society of Photo-Optical Instrumentation Engineers/Infrared Systems; September 30-October 1, 1980, Volume 256; 16-26; Huntsville, AL.

3. Burton, R.W., Sega, R.M., and Martin, V.M.; "Experimental Determination of Electromagnetic Pulse (EMP) Absorption on Complex Shapes," NEM 1980 Record; August 5-7, 1980; 144; Anaheim, CA.

4. Burton, R.W. and Martin, V.M.; "Quantified Surface Current Detection Through the Use of Computer Enhanced Thermography," Prodeedings of the National Radio Science (URSI) Meeting; 12-16 January, 1981; 2; Boulder, CO.

5. Sega, R.M., Martin, V.M., and Burton, R.W.; "Experimental Determination of Electromagnetic Energy Absorption on Complex Shapes; A Progress Report," Proceedings of the National Radio Science (URSI) Meeting; June 16-19, 1981; 31; Los Angeles, CA.

6. Sega, R.M., Martin, V.M., Warmuth, D.B., and Burton R.W.; "Infrared Application to the Detection of Induced Surface Currents," Proceedings of the Society of Photo-Optical Instrumentation Engineers/Modern Utilization of Infrared Technology VII; August 27-28, 1981, Volume 304; 84-91; San Diego, CA.

7. Martin, V.M. and Burton, R.W.; "Thermal Response of Thin Conductive Coatings to Microwave Absorption," Proceedings of the National Radio Science (URSI) Meeting; 13-15 January, 1982; 43; Boulder, CO.

8. Martin, V.M., Stewart, C.V., and Burton, R.W.; "An Optimized Conductive Coating for Thermographic Measurement of Microwave Induced Surface Currents," Proceedings of Institute of Electrical and Electronic Engineers (IEEE) Region 5 Conference and Exposition; May 3-9, 1982; 182-185; Colorado Springs.

9. Sega, R.M., Martin, V.M., and Burton, R.W.; "Microwave Induced Surface Current Measurement via Infrared Detection," Antennas and Propagation Society (APS) Digest: May 24-28, 1982, Volume 1; 231; Albuquerque.

10. Jackson, J.D.; Classical Electrodynamics; 1975; New York; John Wiley and Sons, Inc.

11. Jordan, E.C., and Balmain, K.G.; Electromagnetic Waves and Radiating Systems: 1968; Englewood Cliffs, N.J.; Prentice-Hall, Inc.

12. Marion, Jerry B.; Classical Electromagnetic Radiation; 1972; New York; Academic Press Inc.

13. Churchill, Ruel V., Brown, James W., and Verhey, Roger F.; Complex Variables and Applications; 1974; New York; McGraw-Hill Book Company.

14. Nobel, Ben and Daniel, James W.; Applied Linear Algebra; 1977; Englewood Cliffs, New Jersey; Prentice-Hall, Inc.

15. Hohn, Franz E.; Elementary Matrix Algebra; 1965; New York; The Macmillan Company.

16. Hansen, Wilford N.; "Electric Fields Produced by the Propagation of Plane Coherent Electromagnetic Radiation in a Stratified Medium;" Journal of the Optical Society of America; March, 1968, Vol 58, No. 3; 380-390; Washington.

17. Wait, James R.; Electromagnetic Waves in Stratified Media; 1970; New York; Pergamon Press.

18. Holman, J.P.; Heat Transfer; 1968; New York; McGraw-Hill Book Company.

19. Kreith, Frank; Principles of Heat Transfer; 1973; New York; Intext Educational Publishers.

20. Siegel, Robert and Howell, John R; Thermal Radiation Heat Transfer; 1981; New York; McGraw-Hill Book Company.

21. McAdams, W.H.; Heat Transmission; 1954; New York: McGraw-Hill Book Company.

22. Giblm, P.J.; Graphs, Surfaces and Homology; 1977; New York; John Wiley and Sons.

23. Sega, R.M., Martin, V.M., Warmuth, D.B., and Burton R.S.; "Infrared Application to the Detection of Induced Surface Currents," Proceedings of the Society of Photo-Optical Instrumentation Engineers/Modern Utilization of Infrared Technology VII; August 27-28, 1981, Volume 304; 84-91; San Diego, CA.

24. Kreith, Frank; Principles of Heat Transfer; 1973; New York; Intext Educational Publishers.

25. Jordan, E.C., and Balmain, K.G.; Electromagnetic Waves and Radiating Systems; 1968; Englewood Cliffs, N.J.; Prentice-Hall, Inc.

26. Strait, Bradley J.; Application of the Method of Moments to Electromagnetic Fields; 1980; St Cloud, Florida; The Southeastern Center for Electrical Engineering Education (SCEEE).

27. Andrejewski, W., "Die Beugung Elektromagnetischer Wellen an der Leitenden Kreisscheibe und an der Kreisförmigen Offnung im *Leitenden Ebenen Schirm;" Z. Angew. Physics* 5, 178-186.

28. Bowman, J.J., Senior, T.B.A., and Uslenghi, P.L.E.; Electromagnetic and Acoustic Scattering by Simple Shapes; 1969; Amsterdam; North-Holland Publishing Company.

29. Mentzer, J.R.; Scattering and Diffraction of Radio Waves; 1955; New York; Pergamon Press.

30. Foch, V.A.; Electromagnetic Diffraction and Propagation Problems; 1965; New York; Pergamon Press Inc.

31. Skitch, G.G. and Marshall, S.V.; Electromagnetic Concepts and Application; 1982; Englewood Cliffs, N.J.; Prentice-Hall, Inc.

32. Naor, M. and Senior, T.B.A.; "Scattering by Resistive Plates," Technical Report, Contract F30602-78-C-0148; September 1981; Ann Arbor, MI; Southeastern Center for Electrical Engineering Education.

33. Sega, R.M., Martin, V.M., and Burton, R.W.; "Microwave Induced Surface Current Measurement via Infrared Detection," Antennas and Propagation Society (APS) Digest; May 24-28, 1982, Volume I; 231; Albuquerque.

34. Edwards, J.D.; Aluminum Paint and Powder; 1955; New York; Reinhold Publsihing Co.

35. Donnet, Jean-Baptiste; Carbon Black; 1976; New York; Moral Dekker Inc.

36. Erf, Robert K.; Holographic Nondestructive Testing; 1974; New York; The Academic Press.

37. Rogers, G.L.; "Gabor Diffraction Microscopy: The Hologram as a Generalized Zone Plate;" Nature (London); 1950, Vol 166; 237; London.

38. Iizuka, Keigo and Yen, Jui L.; Personal Conversation at the University of Toronto; June 25, 1982.

39. Sega, Ronald M.; "Infrared Detection of Microwave Induced Surface Currents on Flat Plates;" 1982; University of Colorado Dissertation for the Department of Electrical Engineering; Boulder, CO.

APPENDIX A

ELECTRICAL CONDUCTIVITY MEASUREMENTS

The purpose of the electrical conductivity measurements was to determine the value of the electrical conductivity of the various coatings used in the infrared current measurement schemes.

The most likely source of inconsistency in the measurement process resulted from the method used to attach or input the current to the test specimen. The two point measurement technique used in this testing is recognized by the American Society of Testing and Materials (ASTM) as the most precise method for determining conductivity. However, care must be exercised to assure that the electrical current passed through the specimen is uniformly distributed over the entire cross sectional area of the test specimen.

Tests were conducted using two possible specimen configurations. The first consisted of a 10cm x 10cm square of the material placed on a plexiglas substrate (Fig 96).

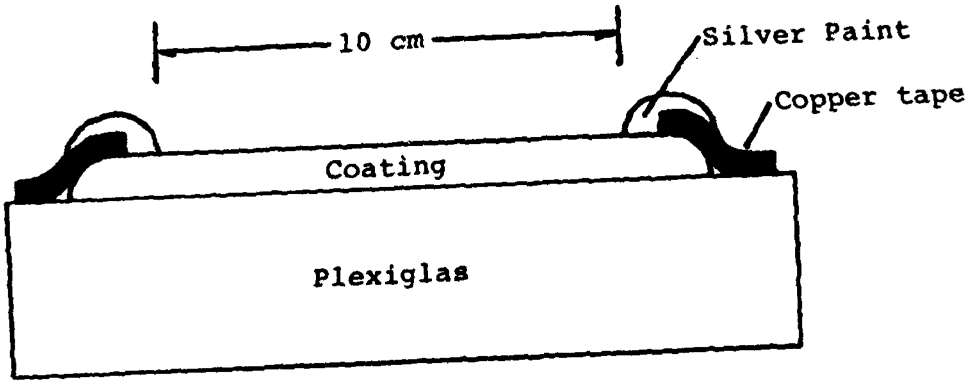
10 cm
Silver Paint
Copper tape
Coating
Plexiglas

Figure 96 : Coating Sample Cross Section

This arrangement was used predominately for thin coatings that were sprayed on the substrate from aerosol cans; thicknesses varied from 10-100 microns. The other configuration which was used with "moldable" materials such as carbon impregnated paraffin consisted of solid disks 2.54 cm in diameter and approximately 7mm thick (Fig 97).

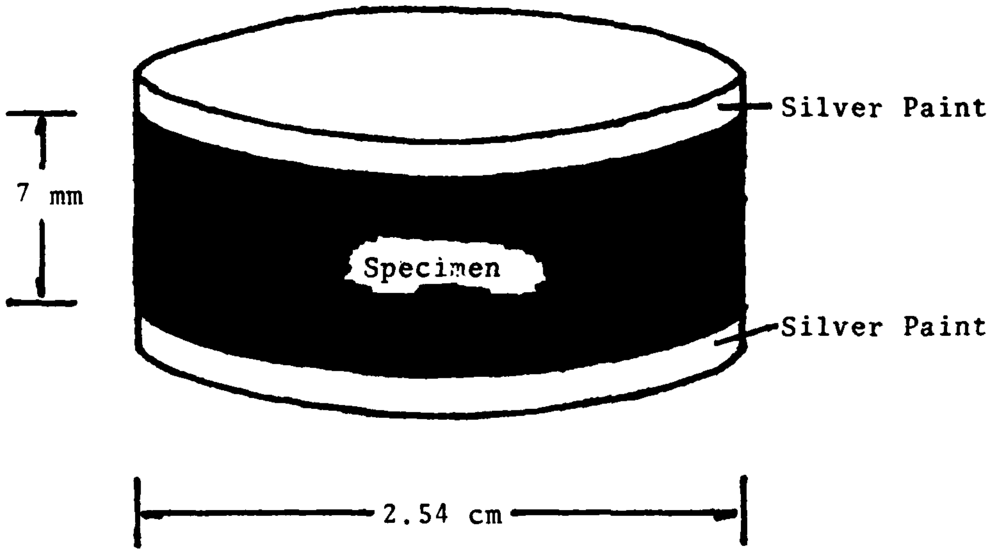

Figure 97 : Drawing of a Typical Disc Sample

In both cases a silver metal based lacquer was used to make final contact with the specimen thus helping insure a uniform electrical contact.

The current connections for the 10cm square were attached to each end of the specimen by means of a copper foil strip embedded in the silver lacquer. Connections for the disk were made by sandwiching it between copper plates which were subsequently clamped in three places with wave guide clamps. See Figures 98 and 99.

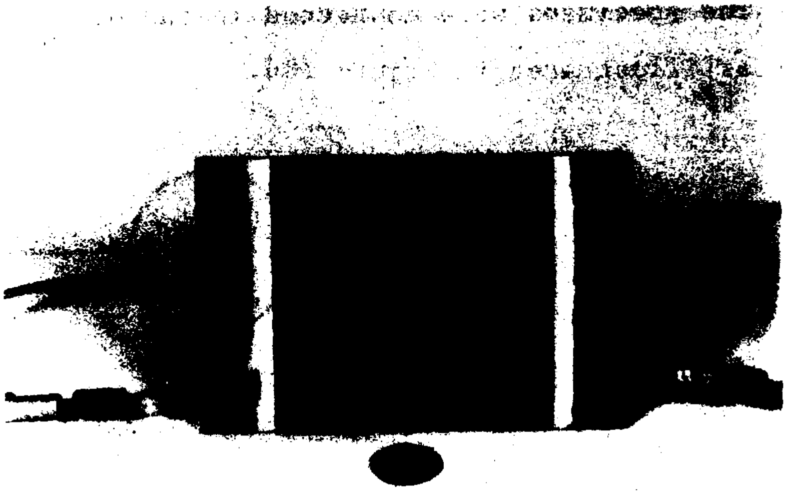

Figure 98: Square Sample Electrical Connections

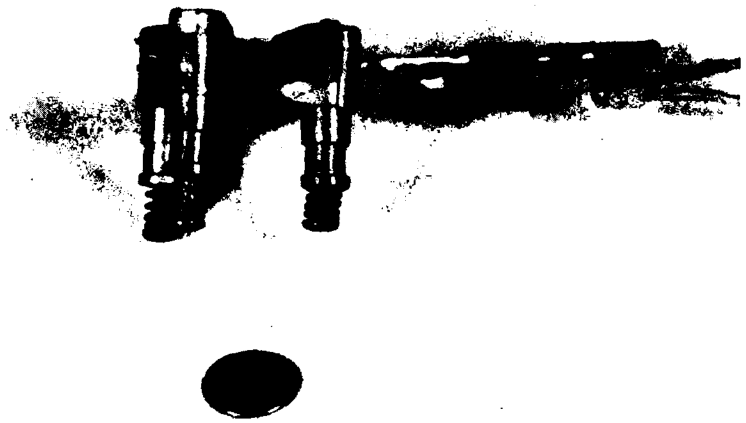

Figure 99: Disc Sample with Clamps Attached

The specimens were connected in the electrical circuit as illustrated in Figure 100.

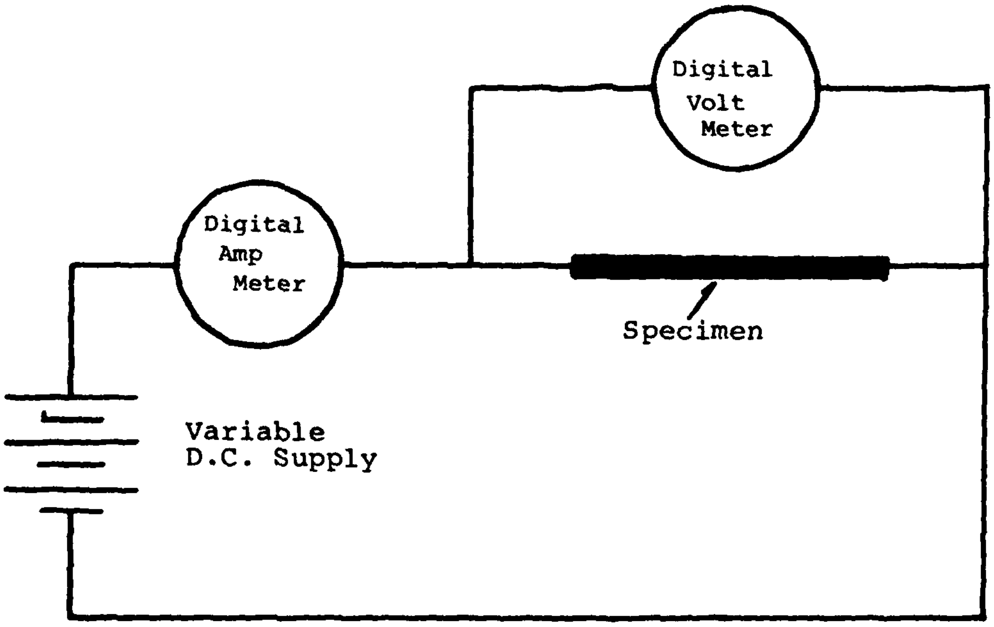
Digital
Volt
Meter
Digital
Amp
Meter
Specimen
Variable
D.C. Supply

Figure 100: Schematic of Conductivity Measurements

This test arrangement is the ASTM two-point method. The following test equipment was used in the test arrangement:

Nomenclature	Identification
Power Supply	Regulated D.C. Power Supply 0-50 VDC, 0-1.5A Kepco Mfg Co, Flushing, NY
Ammeter	Digital Multimeter Hewlett-Packard Model 3466A
Voltmeter	Digital Multimeter Hewlett-Packard Model 3466A
Micrometer	Metric Micrometer Central Scientific Co, Chicago, IL

The conductivity (σ) for each of the samples was calculated from the following equation:

$$\sigma = \frac{il}{VA}$$

where i = total current through specimens

l = length of current travel

V = voltage across sample

A = area through which current travels

Conductivity versus temperature was also investigated for the 10cm x 10cm samples with an aquadaq coating. An AGA Thermovision$_{(c)}$ 680 infrared camera was used to measure the steady state surface temperature of the sample for various current inputs. See Figure 101 for a plot of σ versus temperatures (u).

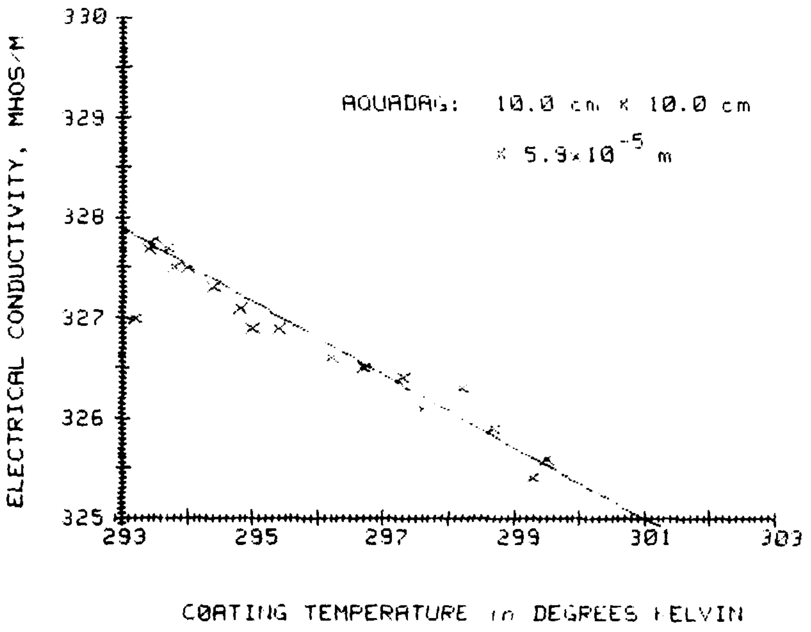

Figure 101: Electrical Conductivity Versus Absolute Temperature (Aquadaq Coating)

Using the technique outlined, the measured conductivity for a composite mixture of paraffin/carbon was measured for various mixing ratios. These plots simplify the process of designing a particular conductivity material since the particular mixing ratios are illustrated. See Figures 102 and 103 for a linear and log plot of sigma. The solid line is a plot of an empirical model of sigma as given in Figure 103.

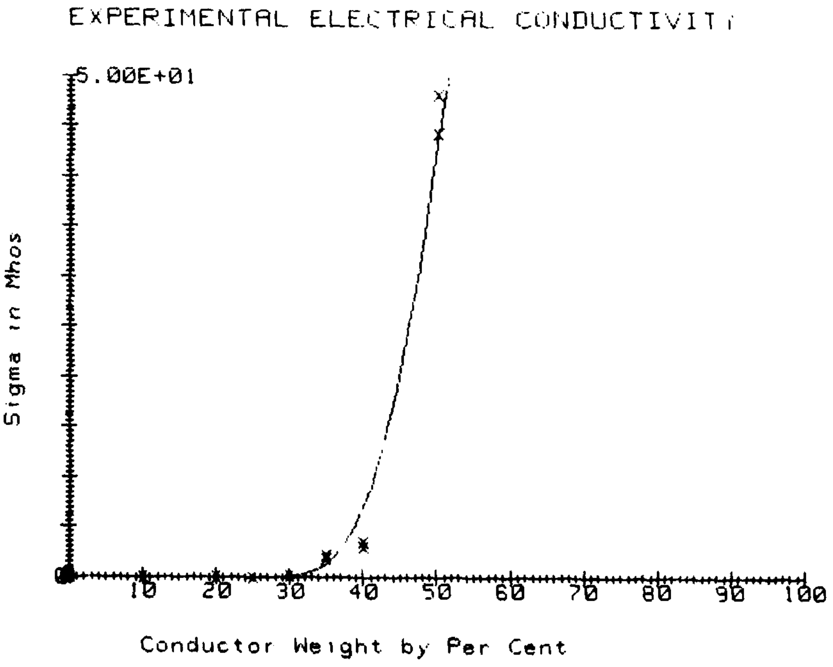

Figure 102: **Electrical Conductivity Versus Carbon/Paraffin Mixing Ratios**

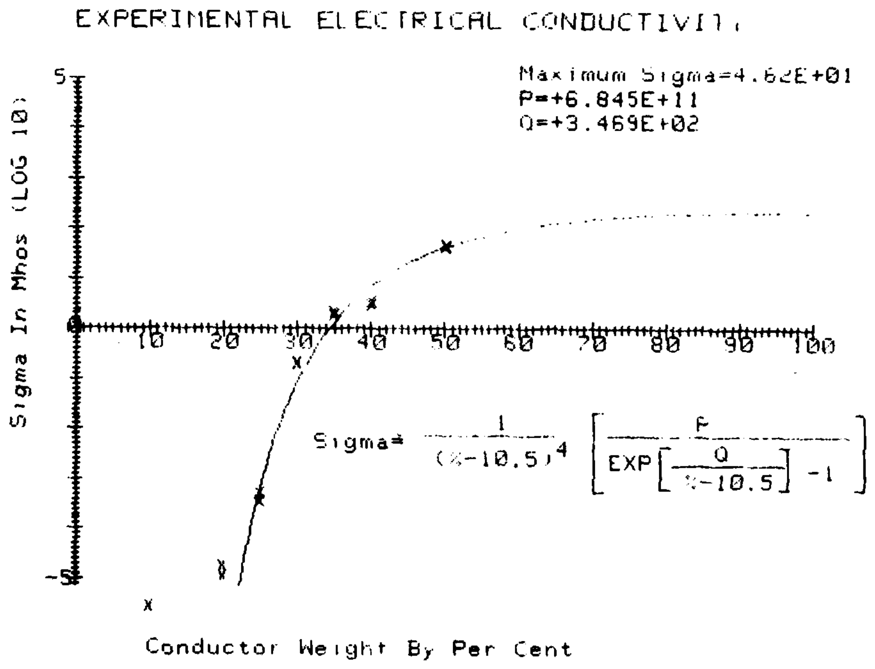

Figure 103: Electrical Conductivity Versus Carbon/Paraffin Mixing Ratios with Empirical Model

APPENDIX B

ELECTRICAL PERMITTIVITY

Electrical permittivity, ε, is an exceedingly important variable in the analysis of effects of microwave absorption in a multi-layered system. It is typically frequency dependent and therefore the value used must be measured for each different operating condition. Fortunately, it does not vary greatly; the table below lists values taken from the Chemical Rubber Company's Handbook of Chemistry and Physics, 60th Edition, for some common materials.

Table 1: Relative Permittivity for Various Dielectrics

	Sodium Light	1MHz	100 Mhz	Specific Heat
Paraffin	2.0	2-2.5	*	*
Glass	2.3-3.6	4.0	*	*
Rock Salt	2.3	*	*	*
Gelatin	2.3	*	*	*
Quartz	2.3	*	*	*
Nylon (66)	2.3	3.3	3.2	.4
Polyethylene	2.3	2.3	2.3	.55
Methylmethacrylate (Plexiglas)	2.2	2.8	*	.35
Polystyrene	2.6	2.5-2.7	2.6	.32
Silicon Rubber	*	3.1-3.2	*	*
Porcelain	*	6-8	*	*

*Value not available

Our permittivities were measured in the laboratory at a frequency of 10 GHz for styrofoam, window glass, paraffin, styrene, phenolic, plexiglas, and neoprene. Figure 104 illustrates the experimental arrangement. Test equipment used in this measurement scheme included the following:

Nomenclature	Identification
10 GHz Source	ED-SET MARK 2 Sargeant-Welch Scientific Co. Skokie, IL
10 GHz Detector	"
Microwave Bench	"

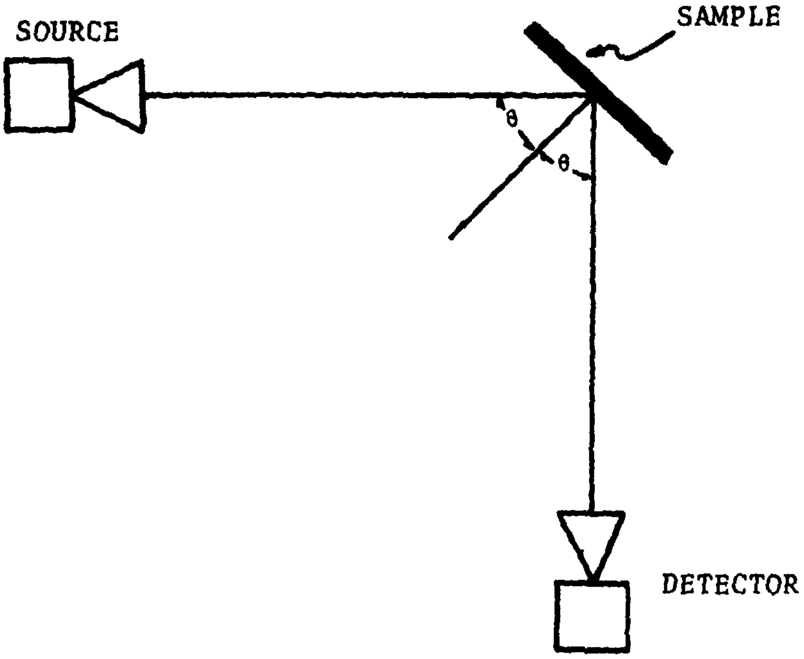

Figure 104 : Schematic Arrangement of Permittivity Measurements

The procedure was to measure the reflectance for a given sample at various angles of incidence. E was polarized perpendicular to the plane of incidence. Because of limited sample sizes, incident angles were limited to between 20 and 60 degrees with measurements taken in 5 degree increments. The measured value versus angle was then plotted on a graph on which theoretical curves of reflectivity versus permittivity had been drawn for a particular sample thickness and incident angle. The permittivity is where the measured reflectance value intersects the particular curve. Figures 105 to 111 illustrate the plots for styrofoam, glass, paraffin, styrene, phenolic, Plexiglas, and neoprene respectively. (Only 10 degree increments are plotted for illustration purposes.)

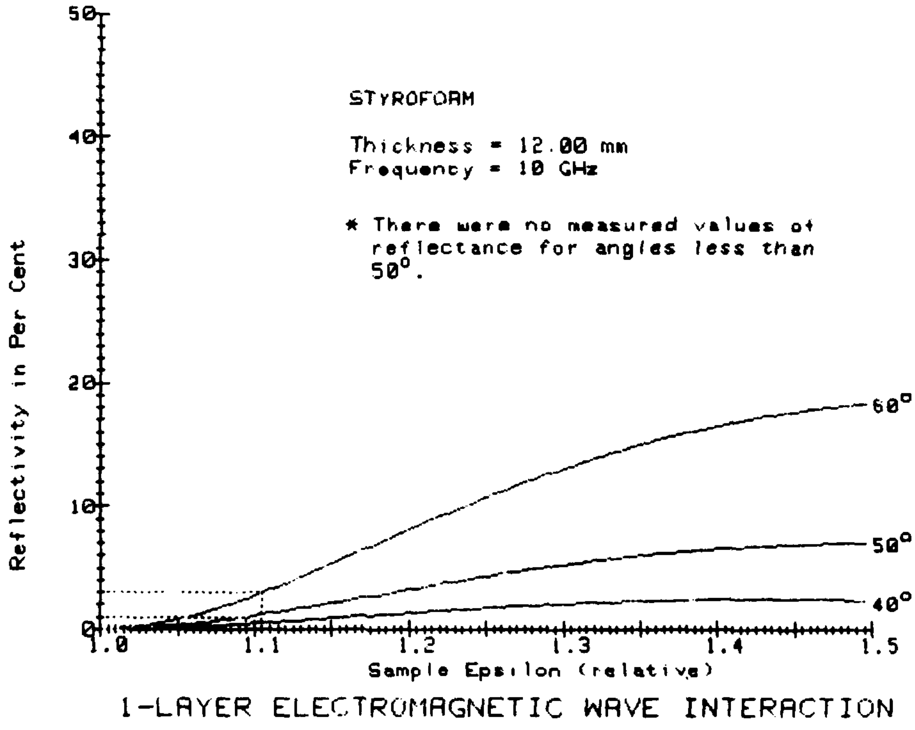

Figure 105: Permittivity Plot for Styrofoam at 10 GHz

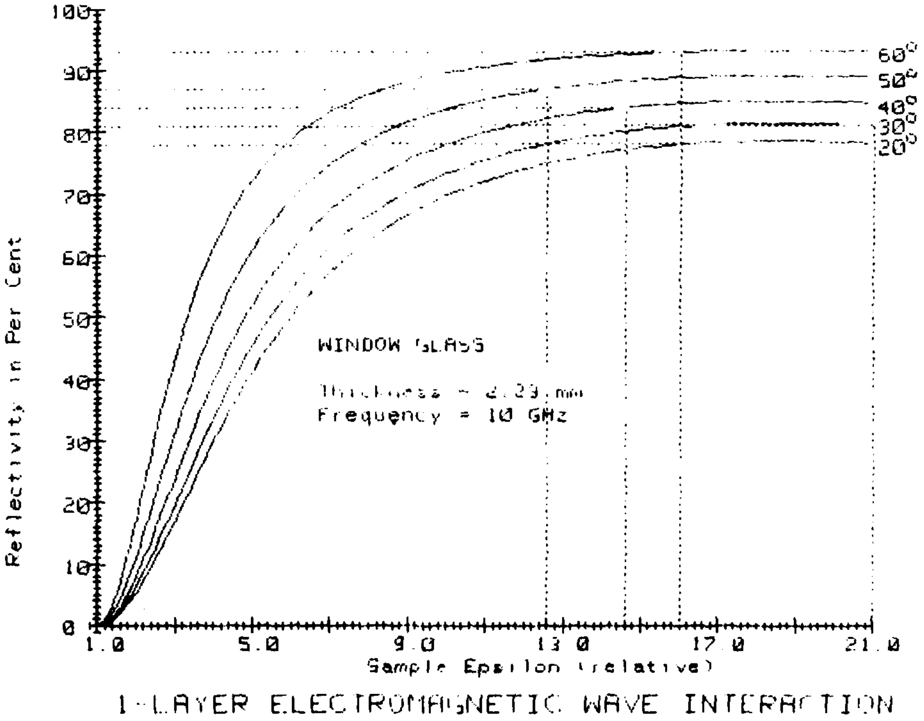

Figure 106: Permittivity Plot for Window Glass at 10 GHz

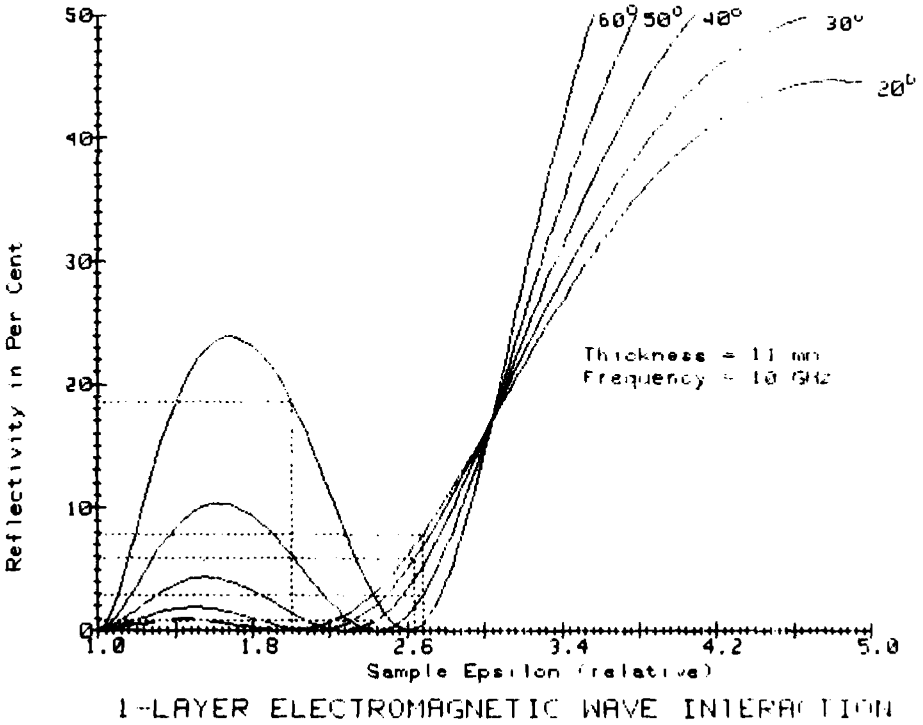

Figure 107 : Permittivity Plot for Paraffin at 10 GHz

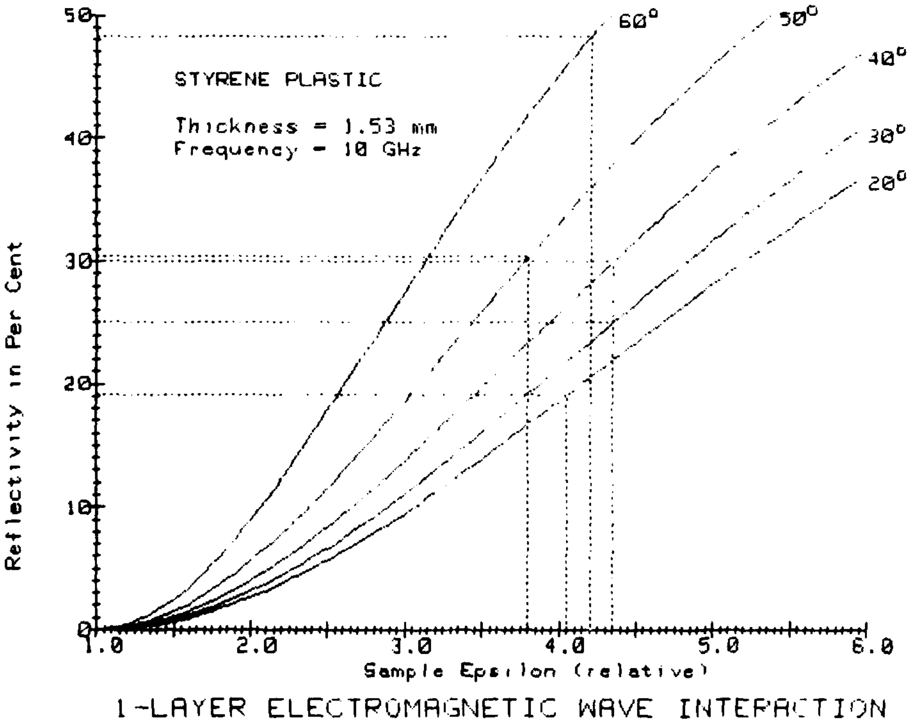

Figure 108: Permittivity Plot for Styrene at 10 GHz

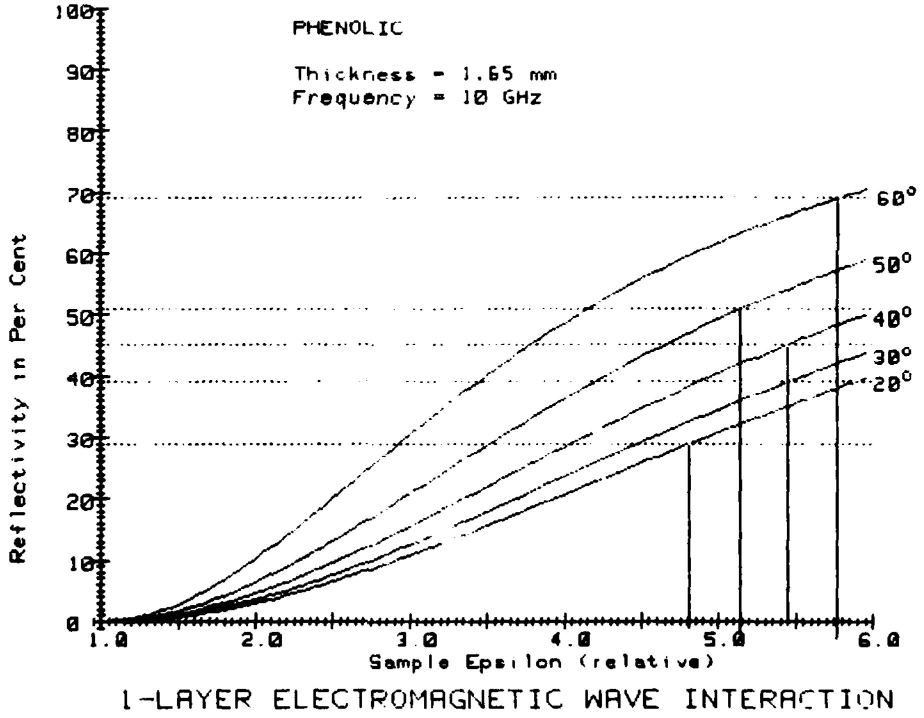

Figure 109 : Permittivity Plot for Phenolic at 10 GHz

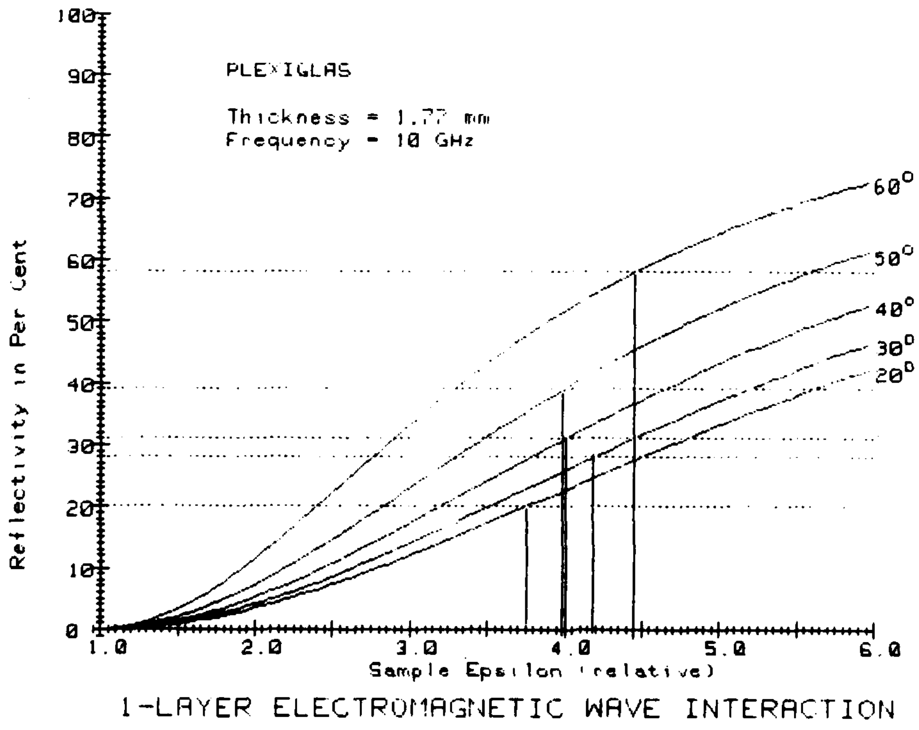

Figure 110 : **Permittivity Plot for Plexiglas at 10 GHz**

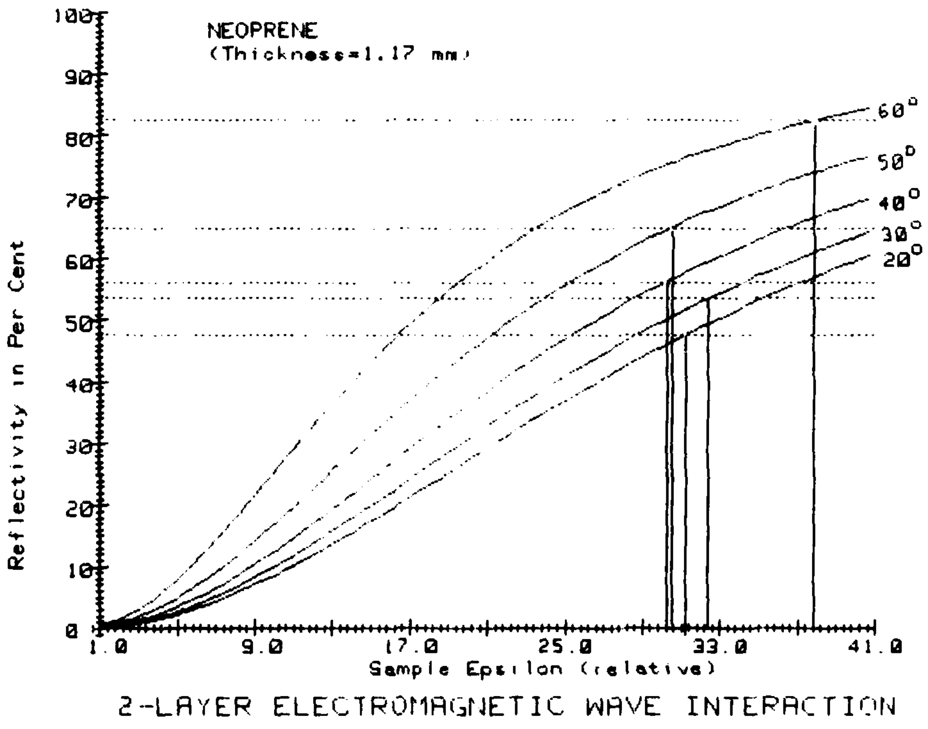

Figure 111 : **Permittivity Plot for Neoprene at 10 GHz**

No attempt was made to measure permittivities for any materials other than good dielectrics. Since Ohm's law was included explicitly in the solution of Maxwell's equations, it is not necessary to assume a complex permittivity for conductive materials; thus, the free space value is acceptable.

Table 2 lists the measured values of relative permittivity for the materials considered. The averaging procedure consisted of calculating an average value and a standard deviation for the nine incident angles. Then any measured permittivity outside the range ± one standard deviation from the average was rejected and a new average and standard deviation calculated. These are the values that appear in Table 2 below.

Table 2: Measured Relative Permittivity at 10 GHz

Material	Average Relative Permittivity (10 GHz)	
Styrofoam	1.11	(One data point)
Window Glass	14.2	(St. Dev. = 1.3)
Paraffin	2.55	(St. Dev. = .14)
Styrene	4.28	(St. Dev. = .08)
Phenolic	5.32	(St. Dev. = .33)
Plexiglas	4.07	(St. Dev. = .24)
Neoprene	31.1	(St. Dev. = .83)

APPENDIX C

COMPUTER PROGRAM

The name of this program is "One-B". It is written for use on a Hewlett-Packard 9845B minicomputer. It calculates reflectivity, transmissivity, and absorptivity for a single interface. It will also calculate infrared emissivity for 5.3 microns wavelength. Input variables are medium two electrical conductivity, index of refraction, and magnetic permeability (relative) as well as the incident frequency in gigahertz.

```
10    ! THE NAME OF THIS PROGRAM IS ONE-B!
20    INTEGER I,J,O,N,K,L,M
30    DIM Para(4,5),Perp(4,5),Theda(90),Refpar(90),Refper(90),Jeffpa(90)
40    DIM Jeffpe(90)
50    GCLEAR
60    EXIT GRAPHICS
70    INPUT "Enter Sigma of medium two.",Sigma
80    INPUT "Enter the relative permeability of medium two.",Mu2r
90    INPUT "Enter the index of refraction of medium two.",N2r
100   INPUT "Enter the incident frequency in Gigahertz.",F
110   INPUT "Enter the input power in MW/Square Centimeter.",P
120   INPUT "For IR emissivity enter a 1; otherwise 0.",Emiss
130   Mu=4*PI*1E-7                !ELEC. CONSTANTS ARE CALCULATED!
140   Eps=8.8542E-12
150   Eps2=N2r^2*Eps
160   Mu2=Mu2r*Mu
170   E1=(Mu/Eps)^.25*SQR(20*P)    !INCIDENT E IS CALCULATED FROM POWER!
180   IF Emiss=1 THEN F=1E5
190   Omega=2*PI*F*1E9
200   Lambda=2.998E8/(F*1E9)
210   Root=SQR(1+(Sigma/(Omega*Eps2))^2)
220   Coef=Omega*SQR(Mu2*Eps2/2)
230   Alpha=Coef*SQR(1+Root)       !REAL AND IMAG. PARTS OF WAVE VECTOR CALC.!
240   Gamma=Coef*SQR(-1+Root)
250   Mag=Alpha^2+Gamma^2
260   Mag2=Mag^2
270   Inc=PI/180
280   Bet0=2*PI/Lambda             !FREE SPACE WAVE VECTOR CALC.!
290   K2=Bet0^2
300   IF Sigma=0 THEN Sigma=1E-12
310   Delta=SQR(2/(Omega*Mu2*Sigma))     !SKIN  DEPTH IS CALC.!
320   Diff=Alpha^2-Gamma^2
330   FOR M=1 TO 90                !BEGIN ITERATION OF 1 TO 90 DEG. INCIDENCE!
340   IF M/10-M DIV 10=0 THEN PRINT USING 350;M
350   IMAGE "M=",DD
```

```
360   Cothed=COS(Theda)             !CALC. THE VALUE OF COS(THEDA)!
370   IF Cothed=0 THEN Cothed=1E-8
380   Sin2=SIN(Theda)^2
390   P=.5*(1-K2*Sin2*Diff/Mag2)    !THE REAL AND IMAG. PARTS OF COS(PHI) CALC.!
400   Q=K2*Sin2*Alpha*Gamma/Mag2
410   Cophir=SQR(P+SQR(P^2+Q^2))
420   Cophii=SQR(ABS(-P+SQR(P^2+Q^2)))
430   FOR I=1 TO 4                  !COEF. MATRICES ARE ZEROED!
440   FOR J=1 TO 5
450   Para(I,J)=0
460   Perp(I,J)=0
470   NEXT J
480   NEXT I
490   Para(1,1)=Cophir/Cothed       !DATA IS LOADED INTO THE COEF. MATRICES!
500   Para(2,1)=Cophii/Cothed
510   Para(3,1)=Alpha*Mu/(Bet0*Mu2)
520   Para(4,1)=Gamma*Mu/(Bet0*Mu2)
530   Para(1,2)=-Cophii/Cothed
540   Para(2,2)=Cophir/Cothed
550   Para(3,2)=-Gamma*Mu/(Bet0*Mu2)
560   Para(4,2)=Alpha*Mu/(Bet0*Mu2)
570   Para(1,3)=-1
580   Para(3,3)=1
590   Para(2,4)=-1
600   Para(4,4)=1
610   Perp(1,1)=1
620   Perp(3,1)=Mu*(Alpha*Cophir-Gamma*Cophii)/(Mu2*Bet0*Cothed)
630   Perp(4,1)=Mu*(Alpha*Cophii+Gamma*Cophir)/(Mu2*Bet0*Cothed)
640   Perp(2,2)=1
650   Perp(3,2)=-Mu*(Alpha*Cophii+Gamma*Cophir)/(Mu2*Bet0*Cothed)
660   Perp(4,2)=Mu*(Alpha*Cophir-Gamma*Cophii)/(Mu2*Bet0*Cothed)
670   Perp(1,3)=-1
680   Perp(3,3)=1
690   Perp(2,4)=-1
```

```
700   Perp(4,4)=1
710   Para(1,5)=E1
720   Para(3,5)=E1
730   Perp(1,5)=E1
740   Perp(3,5)=E1
750   FOR I=1 TO 4                  !Para MATRIX IS ROW REDUCED FOR SOLN!
760   IF Para(I,I)=0 THEN 780
770   GOTO 870
780   FOR N=I+1 TO 4
790   IF Para(N,I)=0 THEN 810
800   GOTO 810
810   NEXT N
820   FOR J=1 TO 5
830   V19=Para(I,J)
840   Para(I,J)=Para(N,J)
850   Para(N,J)=V19
860   NEXT J
870   FOR J=1 TO 5
880   IF I=J THEN 900
890   Para(I,J)=Para(I,J)/Para(I,I)
900   NEXT J
910   Para(I,I)=1
920   FOR O=I+1 TO 4
930   V20=Para(O,I)
940   FOR J=1 TO 5
950   Para(O,J)=Para(O,J)-V20*Para(I,J)
960   NEXT J
970   NEXT O
980   NEXT I
990   FOR I=0 TO 3
1000  FOR O=I+1 TO 3
1010  V20=Para(4-O,4-I)
1020  FOR J=4-I TO 5
1030  Para(4-O,J)=Para(4-O,J)-V20*Para(4-I,J)
1040  NEXT J
```

```
1050  NEXT O
1060  NEXT I
1070  FOR I=1 TO 4                 !Perp MATRIX IS ROW REDUCED FOR SOLN.!
1080  IF Perp(I,I)=0 THEN 1100
1090  GOTO 1190
1100  FOR N=I+1 TO 4
1110  IF Perp(N,I)=0 THEN 1130
1120  GOTO 1140
1130  NEXT N
1140  FOR J=1 TO 5
1150  V19=Perp(I,J)
1160  Perp(I,J)=Perp(N,J)
1170  Perp(N,J)=V19
1180  NEXT J
1190  FOR J=1 TO 5
1200  IF I=J THEN 1220
1210  Perp(I,J)=Perp(I,J)/Perp(I,I)
1220  NEXT J
1230  Perp(I,I)=1
1240  FOR O=I+1 TO 4
1250  V20=Perp(O,I)
1260  FOR J=1 TO 5
1270  Perp(O,J)=Perp(O,J)-V20*Perp(I,J)
1280  NEXT J
1290  NEXT O
1300  NEXT I
1310  FOR I=0 TO 3
1320  FOR O=I+1 TO 3
1330  V20=Perp(4-O,4-I)
1340  FOR J=4-I TO 5
1350  Perp(4-O,J)=Perp(4-O,J)-V20*Perp(4-I,J)
1360  NEXT J
1370  NEXT O
1380  NEXT I
1390  Theda(M)=Theda               !EFF. SURFACE CURRENTS ARE CALCULATED!
```

```
1400  Denom=Alpha*Cophii+Gamma*Cophir
1410  IF Denom=0 THEN Denom=1E-5
1420  Jeffpa(M)=Sigma*SQR(Para(1,5)^2+Para(2,5)^2)/(Delta*Denom)
1430  Jeffpe(M)=Sigma*SQR(Perp(1,5)^2+Perp(2,5)^2)/(Delta*Denom)
1440  Refpar(M)=(Para(3,5)^2+Para(4,5)^2)/E1^2
1450  Refper(M)=(Perp(3,5)^2+Perp(4,5)^2)/E1^2
1460  Theda=Theda+Inc
1470  NEXT M
1480  GCLEAR                         !REFLECTIVITY AND J ARE PLOTTED!
1490  GRAPHICS
1500  DEG
1510  CSIZE 3,9/15,15
1520  LINE TYPE 1
1530  LOCATE 20,115,15,80
1540  SCALE 0,PI/2,0,1
1550  LOCATE 19,115,14,80
1560  AXES PI/180,.01,0,0,10,10
1570  MOVE Theda(1),ABS(Emiss-Refpar(1))
1580  FOR M=2 TO 90
1590  DRAW Theda(M),ABS(Emiss-Refpar(M))
1600  NEXT M
1610  LINE TYPE 3
1620  MOVE Theda(1),ABS(Emiss-Refper(1))
1630  FOR M=2 TO 90
1640  DRAW Theda(M),ABS(Emiss-Refper(M))
1650  NEXT M
1660  IF Emiss=0 THEN GOTO 1720
1670  MOVE Theda(1),ABS(Emiss-Refper(1))
1680  LINE TYPE 4
1690  FOR M=2 TO 90
1700  DRAW Theda(M),1-(Refpar(M)+Refper(M))/2
1710  NEXT M
1720  IF Emiss=1 THEN 1830
1730  LINE TYPE 4
```

```
1740  MOVE Theda(1),LGT(Jeffpa(1))/10
1750  FOR M=2 TO 90
1760  DRAW Theda(M),LGT(Jeffpa(M))/10
1770  NEXT M
1780  LINE TYPE 5
1790  MOVE Theda(1),LGT(Jeffpe(1))/10
1800  FOR M=2 TO 90
1810  DRAW Theda(M),LGT(Jeffpe(M))/10
1820  NEXT M
1830  LINE TYPE 1
1840  Devx=PI/18
1850  Devy=.1
1860  MOVE -.3*Devx,-.5*Devy
1870  LABEL 0
1880  MOVE -.7*Devx,.8*Devy
1890  LABEL 10
1900  MOVE -.7*Devx,1.8*Devy
1910  LABEL 20
1920  MOVE -.7*Devx,2.8*Devy
1930  LABEL 30
1940  MOVE -.7*Devx,3.8*Devy
1950  LABEL 40
1960  MOVE -.7*Devx,4.8*Devy
1970  LABEL 50
1980  MOVE -.7*Devx,5.8*Devy
1990  LABEL 60
2000  MOVE -.7*Devx,6.8*Devy
2010  LABEL 70
2020  MOVE -.7*Devx,7.8*Devy
2030  LABEL 80
2040  MOVE -.7*Devx,8.8*Devy
2050  LABEL 90
2060  MOVE PI/2-.35*Devx,-.4*Devy
2070  LABEL 90
2080  MOVE -.7*Devx,-.2*Devy
```

```
2090  LABEL 0
2100  MOVE -.9*Devx,1-.2*Devy
2110  LABEL 100
2120  MOVE .65*Devx,-.4*Devy
2130  LABEL 10
2140  MOVE 1.65*Devx,-.4*Devy
2150  LABEL 20
2160  MOVE 2.65*Devx,-.4*Devy
2170  LABEL 30
2180  MOVE 3.65*Devx,-.4*Devy
2190  LABEL 40
2200  MOVE 2.5*Devx,-Devy
2210  LABEL "Incident Angle in Degrees"
2220  MOVE 4.65*Devx,-.4*Devy
2230  LABEL 50
2240  MOVE 5.65*Devx,-.4*Devy
2250  LABEL 60
2260  MOVE 6.65*Devx,-.4*Devy
2270  LABEL 70
2280  MOVE 7.65*Devx,-.4*Devy
2290  LABEL 80
2300  LDIR 90
2310  MOVE -1.2*Devx,Devy
2320  IF Emiss=1 THEN GOTO 2370
2330  LABEL "Reflectivity as a Per Cent"
2340  MOVE -.8*Devx,0
2350  LABEL "Effective Surface Current (LOG)x.1"
2360  GOTO 2390
2370  MOVE -Devx,Devy
2380  LABEL "Emissivity as a Per Cent"
2390  LDIR 0
2400  LOCATE 10,115,15,115
2410  MOVE -1.5*Devx,1.2
2420  DRAW 0,1.2
2430  MOVE .25*Devx,1.2
```

```
2440  IF Emiss=1 THEN GOTO 2470
2450  LABEL "Parallel Reflectivity"
2460  GOTO 2480
2470  LABEL "Parallel Emissivity"
2480  MOVE 4*Devx,1.2
2490  LINE TYPE 3
2500  DRAW 4.7*Devx,1.2
2510  MOVE 4.95*Devx,1.2
2520  LINE TYPE 1
2530  IF Emiss=1 THEN GOTO 2560
2540  LABEL "Perpendicular Reflectivity"
2550  GOTO 2570
2560  LABEL "Perpendicular Emissivity"
2570  IF Emiss=1 THEN GOTO 2690
2580  LINE TYPE 4
2590  MOVE -1.5*Devx,1.12
2600  DRAW 0,1.12
2610  LINE TYPE 5
2620  MOVE 4*Devx,1.12
2630  DRAW 5.5*Devx,1.12
2640  LINE TYPE 1
2650  MOVE .25*Devx,1.12
2660  LABEL "J Effective Parallel"
2670  MOVE 5.75*Devx,1.12
2680  LABEL "J Effective Perp."
2690  LOCATE 20,115,15,80
2700  LINE TYPE 1
2710  MOVE -Devx,-2*Devy
2720  CSIZE 4.2,9/15,0
2730  IF Emiss=1 THEN GOTO 2770
2740  LABEL "REFLECTIVITY FROM A SINGLE PLANE INTERFACE"
2750  CSIZE 3,9/15,15
2760  GOTO 2890
2770  LABEL "DIRECTIONAL SPECTRAL EMISSIVITY  AT 3 MICRONS"
2780  CSIZE 3,9/15,15
```

```
2790  IF Emiss=0 THEN GOTO 2890
2800  LOCATE 10,115,15,115
2810  MOVE -1.5*Devx,1.15
2820  LINE TYPE 4
2830  DRAW 0,1.15
2840  MOVE .25*Devx,1.15
2850  LINE TYPE 1
2860  LABEL "Total Emissivity (Parallel and Perpendicular Avg.)"
2870  LINE TYPE 1
2880  IF Emiss=1 THEN GOTO 2920
2890  MOVE 0,1.05
2900  LABEL USING 2910;F
2910  IMAGE "Freq. in GHz=",D.DD
2920  MOVE 3.3*Devx,1.05
2930  LABEL USING 2940;N2r
2940  IMAGE "N2="D.DD
2950  MOVE 5*Devx,1.05
2960  LABEL USING 2970;Sigma
2970  IMAGE "Sigma=",D.DDE
2980  MOVE 8*Devx,1.05
2990  LABEL USING 3000;Mu2r
3000  IMAGE "Mu=",DDD
3010  MOVE 5*Devx,1
3020  LABEL USING 3030;Delta
3030  IMAGE "Skin Depth=",D.DDE
3040  RAD
3050  STOP
```

APPENDIX D

COMPUTER PROGRAM

The name of this program is "Basic". It calculates the reflectivity, transmissivity, and absorptivity for an N-layer electromagnetic interaction problem. The input parameters are the number of layers (not to exceed 10), the incident frequency in gigahertz, the incident power in mW/cm^2, and the individual layer conductivities, permittivities, permeability, and thickness.

```
10    ! THE NAME OF THIS PROGRAM IS 'Basic'  !
20    ! IT CALCULATES THE REFLECTANCE, TRANSMITTANCE, AND ABSORBANCE FOR A N-LAY
ER SYSTEM!
30    INTEGER I,J,K,L,M,N,O,P,Q,R,Lp,Np
40    DIM Beta(11,2),Z(11),Cothed(12,2),Sigma(10),Mu(12),Epslon(12),Theda(91),Pa
ra(22,22,2),Perp(22,22,2),Paraex(44,45),Perpex(44,45)
50    DIM Reperp(91),Repara(91),Trperp(91),Trpara(91),Abpara(91),Abperp(91)
60    GCLEAR
70    EXIT GRAPHICS
80    INPUT "Enter the Number of Layers not to Exceed 10.",N
90    INPUT "Enter the Incident Power in MW/Cm^2",Power
100   INPUT "Enter the Incident Frequency in Gigahertz.",F
110   INPUT "Enter the 'STEP' increment for Theda.",Step
120   Np=N+1
130   L=4*Np                          !DIMENSION OF EXPANDED MATRICES!
140   Lp=L+1
150   Omega=2*PI*F*1E9                !ANGULAR FREQUENCY IS CALCULATED!
160   Beta0=Omega/2.998E8             !FREE SPACE WAVE VECTOR IS CALCULATED!
170   Beta02=Beta0^2                  !THE WAVE VECTOR IS SQUARED!
180   Power=10*Power                  !CONVERTS TO WATT/METER^2!
190   FOR I=1 TO N                    !ELEC. PROPERTIES OF LAYERS IS INSERTED!
200   DISP "Sigma(";I;")";            !ELECTRICAL CONDUCTIVITY IN MHOS!
210   INPUT Sigma(I)
220   DISP "Mu(";I;")";               !RELATIVE MAGNETIC PERMEABILITY!
230   INPUT Mu
240   Mu(I)=Mu*4*PI*1E-7
250   DISP "Epslon(";I;")";           !RELATIVE ELECTRIC PERMITTIVITY!
260   INPUT Epslon
270   Epslon(I)=Epslon*8.8542E-12
280   DISP "Thickness(";I;")";        !EACH LAYER THICKNESS IN METERS!
290   INPUT Thick
300   Z(I)=Z(I-1)+Thick               !Z(n) IS CALCULATED FROM THICKNESSES!
310   Coef=Omega*SQR(Mu(I)*Epslon(I)/2)
320   Sqroot=SQR(1+(Sigma(I)/(Omega*Epslon(I)))^2)
```

```
330    Beta(I,1)=Coef*SQR(1+Sqroot)      !REAL WAVE VECTOR (Alpha) IS CALC.!
340    Beta(I,2)=Coef*SQR(Sqroot-1)      !IMAG WAVE VECTOR (Gamma) IS CALC.!
350    NEXT I
360    Mu(0)=4*PI*1E-7                   !ELEC. CHARAC. EA. SIDE OF LAYERS!
370    Epslon(0)=8.8542E-12
380    Mu(Np)=4*PI*1E-7
390    Epslon(Np)=8.8542E-12
400    Z(0)=0
410    Beta(0,1)=Beta0
420    Beta(0,2)=0
430    Beta(Np,1)=Beta0
440    Beta(Np,2)=0
450    E1=(Mu(0)/Epslon(0))^.25*SQR(2*Power)
460    E12=E1^2
470    Deg=PI/180
480    ! !
490    ! WE BEGIN ITERATING FROM 0 TO 90 DEGREES ANGLE OF INCIDENCE!
500    ! !
510    FOR Theda=0 TO 90 STEP Step
520    IF Theda/10-Theda DIV 10=0 THEN PRINT USING 530;Theda
530    IMAGE "Theda=",DD
540    X=COS(Theda*Deg)
550    IF X=0 THEN X=1E-8
560    Cothed(Np,1)=X
570    Cothed(Np,2)=0
580    Cothed(0,1)=X
590    Cothed(0,2)=0
600    ! !
610    ! WE CALCULATE REAL AND IMAGINARY COS(Theda).!
620    ! !
630    FOR I=1 TO N
640    Sin2=SIN(Theda*Deg)^2                     !WE CALC. SIN(Theda) SQUARED!
650    Denom=(Beta(I,1)^2+Beta(I,2)^2)^2
660    Pee=.5*(1-Beta02*Sin2*(Beta(I,1)^2-Beta(I,2)^2)/Denom)
670    Que=Beta02*Sin2*Beta(I,1)*Beta(I,2)/Denom
```

```
680   X=SQR(Pee^2+Que^2)
690   Cothed(I,1)=SQR(Pee+X)          !REAL COS(Theda N) IS CALCULATED!
700   Cothed(I,2)=SQR(ABS(X-Pee))      !IMAG COS(Theda N) IS CALCULATED!
710   A(I)=Beta(I,1)*Cothed(I,1)-Beta(I,2)*Cothed(I,2)
720   B(I)=Beta(I,1)*Cothed(I,2)+Beta(I,1)*Cothed(I,1)
730   NEXT I
740   ! !
750   ! WE BEGIN TO CALCULATE THE COMPLEX MATRIX!
760   ! !
770   FOR I=1 TO 2*N+1 STEP 2
780   K=(I-1)/2
790   M=I-1
800   R=I+1
810   O=I+2
820   X=-Z(K)*(Beta(K,1)*Cothed(K,2)+Beta(K,2)*Cothed(K,1))
830   Y=Z(K)*(Beta(K,1)*Cothed(K,1)-Beta(K,2)*Cothed(K,2))
840   P=K+1
850   Xx=-Z(K)*(Beta(P,1)*Cothed(P,2)+Beta(P,2)*Cothed(P,1))
860   Yy=Z(K)*(Beta(P,1)*Cothed(P,1)-Beta(P,2)*Cothed(P,2))
870   IF X>200 THEN X=200      !X>200 IMPLIES A LAYER THICKNESS >200 SKIN DEPTHS!
880   IF Xx>200 THEN Xx=200  !Xx>200 IMPLIES A LAYER THICKNESS >200 SKIN DEPTHS!
890   Expx=EXP(X)
900   Expmx=EXP(-X)
910   Expxx=EXP(Xx)
920   Expmxx=EXP(-Xx)
930   Cosy=COS(Y)
940   Siny=SIN(Y)
950   Cosyy=COS(Yy)
960   Sinyy=SIN(Yy)
970   Expr=Expx*Cosy          !Bcr IMPLIES THE REAL PART OF Beta*COS(Theda)!
980   Expi=Expx*Siny          !Bci IMPLIES THE IMAG PART OF Beta*COS(Theda)!
990   Bcr=Beta(K,1)*Cothed(K,1)-Beta(K,2)*Cothed(K,2)
1000  Bci=Beta(K,1)*Cothed(K,2)+Beta(K,2)*Cothed(K,1)
1010  ! !
1020  ! WE CALCULATE THE (I,I-1) AND (I+1,I-1) COMPLEX MATRIX ELEMENTS!
```

```
1030  ! !
1040  IF I=1 THEN 1140
1050  Para(I,M,1)=Cothed(K,1)*Expr-Cothed(K,2)*Expi
1060  Para(I,M,2)=Cothed(K,1)*Expi+Cothed(K,2)*Expr
1070  Perp(I,M,1)=Expr
1080  Perp(I,M,2)=Expi
1090  Para(R,M,1)=(Beta(K,1)*Expr-Beta(K,2)*Expi)/Mu(K)
1100  Para(R,M,2)=(Beta(K,1)*Expi+Beta(K,2)*Expr)/Mu(K)
1110  Perp(R,M,1)=(Bcr*Expr-Bci*Expi)/Mu(K)
1120  Perp(R,M,2)=(Bcr*Expi+Bci*Expr)/Mu(K)
1130  ! !
1140  ! WE  CALCULATE THE (I,I) AND (I+1,I) COMPLEX MATRIX ELEMENTS!
1150  ! !
1160  Expr=Expmx*Cosy
1170  Expi=-Expmx*Siny
1180  Para(I,I,1)=Cothed(K,1)*Expr-Cothed(K,2)*Expi
1190  Para(I,I,2)=Cothed(K,1)*Expi+Cothed(K,2)*Expr
1200  Perp(I,I,1)=Expr
1210  Perp(I,I,2)=Expi
1220  Para(R,I,1)=-(Beta(K,1)*Expr-Beta(K,2)*Expi)/Mu(K)
1230  Para(R,I,2)=-(Beta(K,1)*Expi+Beta(K,2)*Expr)/Mu(K)
1240  Perp(R,I,1)=-(Bcr*Expr-Bci*Expi)/Mu(K)
1250  Perp(R,I,2)=-(Bcr*Expi+Bci*Expr)/Mu(K)
1260  ! !
1270  ! WE CALCULATE THE (I,I+1) AND (I+1,I+1) COMPLEX MATRIX ELEMENTS!
1280  ! !
1290  Expr=Expxx*Cosyy
1300  Expi=Expxx*Sinyy
1310  Bcr=Beta(P,1)*Cothed(P,1)-Beta(P,2)*Cothed(P,2)
1320  Bci=Beta(P,1)*Cothed(P,2)+Beta(P,2)*Cothed(P,1)
1330  Para(I,R,1)=-(Cothed(P,1)*Expr-Cothed(P,2)*Expi)
1340  Para(I,R,2)=-(Cothed(P,1)*Expi+Cothed(P,2)*Expr)
1350  Perp(I,R,1)=-Expr
1360  Perp(I,R,2)=-Expi
```

```
1370  Para(R,R,1)=-(Beta(P,1)*Expr-Beta(P,2)*Expi)/Mu(P)
1380  Para(R,R,2)=-(Beta(P,1)*Expi+Beta(P,2)*Expr)/Mu(P)
1390  Perp(R,R,1)=-(Bcr*Expr-Bci*Expi)/Mu(P)
1400  Perp(R,R,2)=-(Bcr*Expi+Bci*Expr)/Mu(P)
1410  ! !
1420  ! WE CALCULATE THE (I,I+2) AND (I+1,I+2) COMPLEX MATRIX ELEMENTS!
1430  ! !
1440  Expr=Expmxx*Cosyy
1450  Expi=-Expmxx*Sinyy
1460  IF I=2*N+1 THEN 1550
1470  Para(I,O,1)=-(Cothed(P,1)*Expr-Cothed(P,2)*Expi)
1480  Para(I,O,2)=-(Cothed(P,1)*Expi+Cothed(P,2)*Expr)
1490  Perp(I,O,1)=-Expr
1500  Perp(I,O,2)=-Expi
1510  Para(R,O,1)=(Beta(P,1)*Expr-Beta(P,2)*Expi)/Mu(P)
1520  Para(R,O,2)=(Beta(P,1)*Expi+Beta(P,2)*Expr)/Mu(P)
1530  Perp(R,O,1)=(Bcr*Expr-Bci*Expi)/Mu(P)
1540  Perp(R,O,2)=(Bcr*Expi+Bci*Expr)/Mu(P)
1550  NEXT I
1560  ! !
1570  ! COMPLEX MATRICES ARE EXPANDED INTO REAL MATRICES!
1580  ! !
1590  MAT Paraex=ZER                 !ZEROES PREVIOUS ROW REDUCTION DATA!
1600  MAT Perpex=ZER
1610  FOR I=1 TO L/2
1620  FOR J=I-2 TO I+2               !AVOIDS CYCLING THRU THE WHOLE MATRIX!
1630  IF J<1 THEN 1770
1640  IF J>L/2 THEN 1770
1650  M=2*I
1660  R=2*J
1670  O=M-1
1680  P=R-1
1690  Paraex(O,P)=Para(I,J,1)
1700  Paraex(M,R)=Para(I,J,1)
1710  Paraex(M,P)=Para(I,J,2)
```

AD-A131 091 MICROWAVE INTERACTION WITH THIN MULTIPLE CONDUCTIVE 3/3
COATINGS(U) ROME AIR DEVELOPMENT CENTER GRIFFISS AFB NY
V M MARTIN MAR 83 RADC-TR-83-62
UNCLASSIFIED F/G 11/3 NL

END
DATE
FILMED
8 83
DTIC

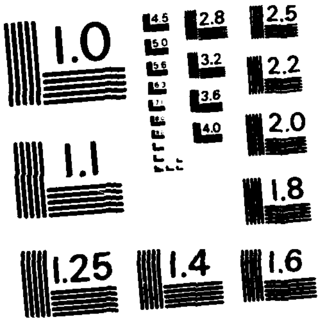
1.0
4.5
5.0
5.6
6.3
7.1
8.0
2.8
3.2
3.6
4.0
2.5
2.2
2.0
1.1
1.8
1.25
1.4
1.6

MICROCOPY RESOLUTION TEST CHART
NATIONAL BUREAU OF STANDARDS-1963-A

```
1720  Paraex(0,R)=-Para(I,J,2)
1730  Perpex(0,P)=Perp(I,J,1)
1740  Perpex(M,R)=Perp(I,J,1)
1750  Perpex(M,P)=Perp(I,J,2)
1760  Perpex(0,R)=-Perp(I,J,2)
1770  NEXT J
1780  NEXT I
1790  Paraex(1,Lp)=-E1*Cothed(Np,1)
1800  Paraex(3,Lp)=-E1*(Beta0/Mu(0))
1810  Perpex(1,Lp)=-E1
1820  Perpex(3,Lp)=-E1*Cothed(Np,1)*(Beta0/Mu(0))
1830  ! !
1840  ! AT THIS POINT WE ARE READY FOR THE MATRIX SOLUTION!
1850  ! !
1860  FOR I=1 TO L            !L IS THE DIMENSION OF THE EXPANDED MATRICES!
1870  FOR J=I-5 TO I+5        !1810-1870 DIVIDES THE Ith ROW BY DIAGONAL ELE.!
1880  IF J>L THEN 1930
1890  IF J<1 THEN 1930
1900  IF I=J THEN 1930
1910  Paraex(I,J)=Paraex(I,J)/Paraex(I,I)
1920  Perpex(I,J)=Perpex(I,J)/Perpex(I,I)
1930  NEXT J
1940  Paraex(I,Lp)=Paraex(I,Lp)/Paraex(I,I)
1950  Perpex(I,Lp)=Perpex(I,Lp)/Perpex(I,I)
1960  Paraex(I,I)=1
1970  Perpex(I,I)=1
1980  FOR K=I+1 TO I+5        !WE ZERO THE COLUMN BELOW THE Ith DIAGONAL!
1990  IF K>L THEN 2090
2000  X=Paraex(K,I)
2010  Y=Perpex(K,I)
2020  FOR J=I TO I+5
2030  IF J>L THEN 2060
2040  Paraex(K,J)=Paraex(K,J)-X*Paraex(I,J)
2050  Perpex(K,J)=Perpex(K,J)-Y*Perpex(I,J)
2060  NEXT J
```

```
2070  Paraex(K,Lp)=Paraex(K,Lp)-X*Paraex(I,Lp)
2080  Perpex(K,Lp)=Perpex(K,Lp)-Y*Perpex(I,Lp)
2090  NEXT K
2100  NEXT I
2110  ! !
2120  ! Paraex AND Perpex ARE NOW IN UPPER TRIANGULAR FORM!
2130  ! !
2140  FOR I=0 TO L-1
2150  FOR K=I+1 TO I+5
2160  IF K>L-1 THEN 2280
2170  O=L-K
2180  P=L-I
2190  X=Paraex(O,P)
2200  Y=Perpex(O,P)
2210  FOR J=P TO P+4
2220  IF J>L THEN 2250
2230  Paraex(O,J)=Paraex(O,J)-X*Paraex(P,J)
2240  Perpex(O,J)=Perpex(O,J)-Y*Perpex(P,J)
2250  NEXT J
2260  Paraex(O,Lp)=Paraex(O,Lp)-X*Paraex(P,Lp)
2270  Perpex(O,Lp)=Perpex(O,Lp)-Y*Perpex(P,Lp)
2280  NEXT K
2290  NEXT I
2300  ! !
2310  ! THE MAG. OF THE ELECTRIC FIELDS ARE NOW CALCULATED IN THE L+1 COLUMN!
2320  ! !
2330  Repara(Theda)=(Paraex(1,Lp)^2+Paraex(2,Lp)^2)/E12
2340  Reperp(Theda)=(Perpex(1,Lp)^2+Perpex(2,Lp)^2)/E12
2350  Trpara(Theda)=(Paraex(L-1,Lp)^2+Paraex(L,Lp)^2)/E12
2360  Trperp(Theda)=(Perpex(L-1,Lp)^2+Perpex(L,Lp)^2)/E12
2370  Abpara(Theda)=1-Repara(Theda)-Trpara(Theda)
2380  Abperp(Theda)=1-Reperp(Theda)-Trperp(Theda)
2390  Theda(Theda)=Theda
2400  NEXT Theda
2410  ! !
```

```
2420  ! WE BEGIN THE GRAPHICS PORTION HERE !
2430  ! !
2440  GCLEAR
2450  GRAPHICS
2460  CSIZE 3.3,9/15,0
2470  LINE TYPE 1
2480  LOCATE 20,80,20,80
2490  SCALE 0,90,0,1
2500  LOCATE 19,80,19,80
2510  AXES 1,.01,0,0,10,10
2520  MOVE Theda(0),Repara(0)
2530  FOR J=Step TO 90 STEP Step
2540  DRAW Theda(J),Repara(J)
2550  NEXT J
2560  LETTER
2570  MOVE Theda(0),Reperp(0)
2580  FOR J=Step TO 90 STEP Step
2590  DRAW Theda(J),Reperp(J)
2600  NEXT J
2610  LETTER
2620  MOVE Theda(0),Trpara(0)
2630  FOR J=Step TO 90 STEP Step
2640  DRAW Theda(J),Trpara(J)
2650  NEXT J
2660  LETTER
2670  MOVE Theda(0),Trperp(0)
2680  FOR J=Step TO 90 STEP Step
2690  DRAW Theda(J),Trperp(J)
2700  NEXT J
2710  LETTER
2720  MOVE Theda(0),Abpara(0)
2730  FOR J=Step TO 90 STEP Step
2740  DRAW Theda(J),Abpara(J)
2750  NEXT J
2760  LETTER
```

```
2770  MOVE Theda(0),Abperp(0)
2780  FOR J=Step TO 90 STEP Step
2790  DRAW Theda(J),Abperp(J)
2800  NEXT J
2810  LETTER
2820  ! !
2830  ! PLOTS ARE DRAWN NOW LABELING IS INSERTED !
2840  ! !
2850  PAUSE
2860  PEN 1
2870  GOTO 2810
2880  INPUT "For Data Printout Enter 1; 0 otherwise.",Data
2890  GOTO 2810
2900  IF Data=1 THEN PRINTER IS 0
2910  CSIZE 3.3,9/15,0
2920  PRINT
2930  PRINT
2940  PRINT
2950  PRINT
2960  PRINT
2970  PRINT
2980  PRINT
2990  PRINT USING 3000;N;Power/10;F
3000  IMAGE "Number of Layers=",DD,"        Power in W/Cm^2=",DD,"        Freq. in
 GHz=",D.DD
3010  PRINT USING 3020;Uair-273.16;Del;Fe;H
3020  IMAGE "Air Temp (C)=",DD.D,"  Convective Exp=",D.DD,"  Emissivity=",D.DD,"
  Plate Height (M)=",D.DDD
3030  PRINT
3040  PRINT
3050  FOR I=1 TO N
3060  X=4*PI*1E-7
3070  Y=8.8542E-12
3080  PRINT USING 3090;I,Sigma(I),I,Mu(I)/X,I,Epslon(I)/Y,I,Z(I)-Z(I-1)
```

```
3090  IMAGE "Sigma(",D,")=",D.DDE,"  Mu(",D,")=",DD.D,"  Epsilon(",D,")=",D.DD,"
  Thickness(",D,")=",D.DDE
3100  NEXT I
3110  PRINTER IS 16
3120  STOP
```

APPENDIX E

COMPUTER PROGRAM

The name of this program is "SIGNIF". It calculates the ratio of heat lost through infrared radiation to that lost by way of heat convection on a vertical flat surface. The input variables are air temperature (C), the convection exponent, and plate height (m).

```
10    ! THEN NAME OF THIS PROGRAM IS 'SIGNIF'. IT CALCULATES THE MAX. SURFACE
 TEMP SUCH THAT IR LOSSES ARE INSIGNIFICANT REL. TO CONVECTION!
20    ! !
30    INPUT "ENTER Uair.",Uair
40    INPUT "ENTER Delta, THE CONVECTION EXP.",Del
50    INPUT "ENTER THE PLATE HEIGHT.",H
60    DIM U(200),Ratio(200,10)
70    INTEGER I,J
80    Uair=Uair+273.16
90    Uo=Uair
100   Gamma=5.67E-8
110   Inc=.05
120   FOR I=1 TO 200
130   Uo=Uo+Inc
140   FOR J=2 TO 10 STEP 2
150   Fe=.1*J
160   Qir=Gamma*Fe*(Uo^4-Uair^4)
170   Qcon=1.42/H^Del*(Uo-Uair)^(Del+1)
180   Ratio(I,J)=Qir/Qcon
190   U(I)=Uo-Uair
200   NEXT J
210   NEXT I
220   BEEP
230   PAUSE
240   GRAPHICS
250   GCLEAR
260   CSIZE 3.3,9/15,0
270   LINE TYPE 1
280   LOCATE 15,85,15,85
290   SCALE 0,10,0,5
300   LOCATE 14,85,14,85
310   AXES .1,.1,0,0,10,10
320   FOR J=2 TO 10 STEP 2
330   Fe=.1*J
```

```
340   LINE TYPE J/2+2
350   MOVE 0,4*Gamma*Fe*Uair^3/(1.42*(1+Del)/H^Del)
360   FOR I=1 TO 200
370   DRAW U(I),Ratio(I,J)
380   NEXT I
390   MOVE 4,4.25-.1*J
400   DRAW 5,4.25-.1*J
410   NEXT J
420   LINE TYPE 1
430   MOVE 1,-.75
440   LABEL "(Uo-Uair) IN DEGREES CENTIGRADE"
450   MOVE -.8,.25
460   LDIR PI/2
470   LABEL "RATIO OF INFRARED TO CONVECTION LOSSES"
480   LDIR 0
490   MOVE 9.6,-.25
500   LABEL 10
510   CSIZE 2.5,9/15,0
520   MOVE 4,5
530   LABEL USING 540;H
```

```
540   IMAGE "PLATE HEIGHT=",D.DD," METERS"
550   MOVE 4,4.75
560   LABEL USING 570;Del
570   IMAGE "CONVECTION EXPONENT=",.DDD
580   MOVE 4,4.5
590   LABEL USING 600;Uair-273.16
600   IMAGE "AIR TEMPERATURE (C)=",DD.DD
610   MOVE -.6,5
620   LABEL 5
630   MOVE -.6,-.25
640   LABEL 0
650   LETTER
660   CSIZE 3.3,9/15,0
670   GOTO 230
680   GCLEAR
690   EXIT GRAPHICS
700   STOP
```

APPENDIX F

COMPUTER PROGRAM

The name of this program is "Uo-3D". It calculates the equilibrium surface temperature for a system of N layers in the presence of electromagnetic radiation. It plots the temperature as a function of the first layer thickness and conductivity on a three dimensional plot. The input variables are the number of layers, the incident power, the incident frequency, the ambient air temperature, the convection exponent, the surface emissivity, the vertical flat plate height, the incident angle, and the smallest electrical conductivity for the first layer. Additionally, the inputs for the various other layers are the permittivity, conductivity, permeability, and thickness.

```
10     ! THE NAME OF THIS PROGRAM IS 'Uo-3D'  !
20     ! IT CALCULATES THE SURFACE TEMPERATURE (Uo) ON THE Z=0 INTERFACE IF THERE
 ARE  NO HEAT LOSSES FROM THE Z=Zn INTERFACE !
30     ! IT CALCULATES Uo AS A FUNCTION OF SIGMA AND THICKNESS IN SKIN DEPTHS AND
THEN PLOTS THE RESULTS ON A THREE DIMENSIONAL DISPLAY!
40     ASSIGN #1 TO "UoVBL:T14"
50     ASSIGN #2 TO "UoSML:T14"
60     ASSIGN #3 TO "UoBIG:T14"
70     INTEGER I,J,K,L,M,N,O,P,Q,R,Lp,Np,Aye,Jay,Thed
80     SHORT Beta(11,2),Z(11),Cothed(12,2),Sigma(10),Mu(12),Epslon(12),Para(22,22
,2),Perp(22,22,2),Paraex(44,45),Perpex(44,45),A(10),B(10)
90     SHORT Uoperp(20,22,10),Uopara(20,22,10),Thick(10),Max(60,10),Last(60,10),P
amax(10),Pemax(10),Delta(20)
100    INPUT "For data calculation enter 1; for replot a 2.",Plot
110    GCLEAR
120    EXIT GRAPHICS
130    IF Plot=2 THEN 3020
140    INPUT "Enter the Number of Layers not to Exceed 10.",N
150    INPUT "Enter the Incident Power in MW/Cm^2",Power
160    INPUT "Enter the Incident Frequency in Gigahertz.",F
170    INPUT "Enter the ambient air temperature in Centigrade.",Uair
180    INPUT "Enter the convection exponent, Delta.",Del
190    INPUT "Enter the surface emissivity.",Fe
200    INPUT "Enter the plate height in meters.",H
210    INPUT "Enter the Theda Step>=10 degrees.",Step
220    INPUT "Enter the Sigma Step>=1.",Stepp
230    Np=N+1
240    L=4*Np                              !DIMENSION OF EXPANDED MATRICES!
250    Lp=L+1
260    Gamma=5.67E-8
270    Uair=Uair+273.16                    !CONVERTS Uair TO KELVIN!
280    Omega=2*PI*F*1E9                    !ANGULAR FREQUENCY IS CALCULATED!
290    Beta0=Omega/2.998E8                 !FREE SPACE WAVE VECTOR IS CALCULATED!
```

```
300   Beta02=Beta0^2                    !THE WAVE VECTOR IS SQUARED!
310   Power=10*Power                    !CONVERTS TO WATT/METER^2!
320   FOR I=1 TO N                      !ELEC. PROPERTIES OF LAYERS IS INSERTED!
330   IF I=1 THEN 360
340   DISP "Sigma(";I;")";              !ELECTRICAL CONDUCTIVITY IN MHOS!
350   INPUT Sigma(I)
360   DISP "Mu(";I;")";                 !RELATIVE MAGNETIC PERMEABILITY!
370   INPUT Mu
380   Mu(I)=Mu*4*PI*1E-7
390   DISP "Epslon(";I;")";             !RELATIVE ELECTRIC PERMITTIVITY!
400   INPUT Epslon
410   Epslon(I)=Epslon*8.8542E-12
420   IF I=1 THEN 450
430   DISP "Thickness(";I;")";          !EACH LAYER THICKNESS IN METERS!
440   INPUT Thick(I)
450   Coef=Omega*SQR(Mu(I)*Epslon(I)/2)
460   Sqroot=SQR(1+(Sigma(I)/(Omega*Epslon(I)))^2)
470   Beta(I,1)=Coef*SQR(1+Sqroot)      !REAL WAVE VECTOR (Alpha) IS CALC.!
480   Beta(I,2)=Coef*SQR(Sqroot-1)      !IMAG WAVE VECTOR (Gamma) IS CALC.!
490   NEXT I
500   Mu(0)=4*PI*1E-7                   !ELEC. CHARAC. EA. SIDE OF LAYERS!
510   Epslon(0)=8.8542E-12
520   Mu(Np)=4*PI*1E-7
530   Epslon(Np)=8.8542E-12
540   Z(0)=0
550   Beta(0,1)=Beta0
560   Beta(0,2)=0
570   Beta(Np,1)=Beta0
580   Beta(Np,2)=0
590   E1=(Mu(0)/Epslon(0))^.25*SQR(2*Power)
600   E12=E1^2
610   Deg=PI/180
620   ! !
630   ! WE BEGIN ITERATING FROM 0 TO 90 DEGREES ANGLE OF INCIDENCE!
640   ! !
```

```
650   FOR Theda=0 TO 90 STEP Step
660   IF Theda/10-Theda DIV 10=0 THEN PRINT USING 670;Theda
670   IMAGE "Theda=",DD
680   FOR Aye=1 TO 20 STEP Stepp                !WE BEGIN ITERATING OVER SIGMA!
690   Sigma(1)=10^(8-.5*(Aye-1))                !SIGMA IS INCREMENTED BY 10^.5!
700   PRINT USING 710;Aye
710   IMAGE "WE ARE ON SIGMA ROW NUMBER ",DD
720   Delta(Aye)=SQR(2/(Omega*Mu(1)*Sigma(1)))
730   Thick(1)=0
740   MAT Z=ZER
750   Coef=Omega*SQR(Mu(1)*Epslon(1)/2)
760   Sqroot=SQR(1+(Sigma(1)/(Omega*Epslon(1)))^2)
770   Beta(1,1)=Coef*SQR(1+Sqroot)
780   Beta(1,2)=Coef*SQR(Sqroot-1)
790   FOR Jay=2 TO 21                           !WE ITERATE OVER THICKNESS HERE!
800   Thick(1)=Thick(1)+Delta(Aye)/5
810   FOR I=1 TO N
820   Z(I)=Z(I-1)+Thick(I)
830   NEXT I
840   X=COS(Theda*Deg)
850   IF X=0 THEN X=.01
860   Cothed(Np,1)=X
870   Cothed(Np,2)=0
880   Cothed(0,1)=X
890   Cothed(0,2)=0
900   ! !
910   ! WE CALCULATE REAL AND IMAGINARY COS(Theda).!
920   ! !
930   FOR I=1 TO N
940   Sin2=SIN(Theda*Deg)^2                 !WE CALC. SIN(Theda) SQUARED!
950   IF Sin2=1 THEN Sin2=.99
960   Denom=(Beta(I,1)^2+Beta(I,2)^2)^2
970   Pee=.5*(1-Beta02*Sin2*(Beta(I,1)^2-Beta(I,2)^2)/Denom)
980   Que=Beta02*Sin2*Beta(I,1)*Beta(I,2)/Denom
990   X=SQR(Pee^2+Que^2)
```

```
1000  Cothed(I,1)=SQR(Pee+X)         !REAL COS(Theda N) IS CALCULATED!
1010  Cothed(I,2)=SQR(ABS(X-Pee))     !IMAG COS(Theda N) IS CALCULATED!
1020  A(I)=Beta(I,1)*Cothed(I,1)-Beta(I,2)*Cothed(I,2)
1030  B(I)=Beta(I,1)*Cothed(I,2)+Beta(I,1)*Cothed(I,1)
1040  NEXT I
1050  ! !
1060  ! WE BEGIN TO CALCULATE THE COMPLEX MATRIX!
1070  ! !
1080  FOR I=1 TO 2*N+1 STEP 2
1090  K=(I-1)/2
1100  M=I-1
1110  R=I+1
1120  O=I+2
1130  X=-Z(K)*(Beta(K,1)*Cothed(K,2)+Beta(K,2)*Cothed(K,1))
1140  Y=Z(K)*(Beta(K,1)*Cothed(K,1)-Beta(K,2)*Cothed(K,2))
1150  P=K+1
1160  Xx=-Z(K)*(Beta(P,1)*Cothed(P,2)+Beta(P,2)*Cothed(P,1))
1170  Yy=Z(K)*(Beta(P,1)*Cothed(P,1)-Beta(P,2)*Cothed(P,2))
1180  IF X>75 THEN X=75     !X>75 IMPLIES A LAYER THICKNESS >75 SKIN DEPTHS!
1190  IF Xx>75 THEN Xx=75  !Xx>75 IMPLIES A LAYER THICKNESS >75 SKIN DEPTHS!
1200  Expx=EXP(X)
1210  Expxx=EXP(Xx)
1220  IF X<-75 THEN X=-75
1230  IF Xx<-75 THEN Xx=-75
1240  Expmx=EXP(-X)
1250  Expmxx=EXP(-Xx)
1260  Cosy=COS(Y)
1270  Siny=SIN(Y)
1280  Cosyy=COS(Yy)
1290  Sinyy=SIN(Yy)
1300  Expr=Expx*Cosy         !Bcr IMPLIES THE REAL PART OF Beta*COS(Theda)!
1310  Expi=Expx*Siny         !Bci IMPLIES THE IMAG PART OF Beta*COS(Theda)!
1320  Bcr=Beta(K,1)*Cothed(K,1)-Beta(K,2)*Cothed(K,2)
1330  Bci=Beta(K,1)*Cothed(K,2)+Beta(K,2)*Cothed(K,1)
1340  ! !
```

```
1350  ! WE CALCULATE THE (I,I-1) AND (I+1,I-1) COMPLEX MATRIX ELEMENTS!
1360  ! !
1370  IF I=1 THEN 1470
1380  Para(I,M,1)=Cothed(K,1)*Expr-Cothed(K,2)*Expi
1390  Para(I,M,2)=Cothed(K,1)*Expi+Cothed(K,2)*Expr
1400  Perp(I,M,1)=Expr
1410  Perp(I,M,2)=Expi
1420  Para(R,M,1)=(Beta(K,1)*Expr-Beta(K,2)*Expi)/Mu(K)
1430  Para(R,M,2)=(Beta(K,1)*Expi+Beta(K,2)*Expr)/Mu(K)
1440  Perp(R,M,1)=(Bcr*Expr-Bci*Expi)/Mu(K)
1450  Perp(R,M,2)=(Bcr*Expi+Bci*Expr)/Mu(K)
1460  ! !
1470  ! WE  CALCULATE THE (I,I) AND (I+1,I) COMPLEX MATRIX ELEMENTS!
1480  ! !
1490  Expr=Expmx*Cosy
1500  Expi=-Expmx*Siny
1510  Para(I,I,1)=Cothed(K,1)*Expr-Cothed(K,2)*Expi
1520  Para(I,I,2)=Cothed(K,1)*Expi+Cothed(K,2)*Expr
1530  Perp(I,I,1)=Expr
1540  Perp(I,I,2)=Expi
1550  Para(R,I,1)=-(Beta(K,1)*Expr-Beta(K,2)*Expi)/Mu(K)
1560  Para(R,I,2)=-(Beta(K,1)*Expi+Beta(K,2)*Expr)/Mu(K)
1570  Perp(R,I,1)=-(Bcr*Expr-Bci*Expi)/Mu(K)
1580  Perp(R,I,2)=-(Bcr*Expi+Bci*Expr)/Mu(K)
1590  ! !
1600  ! WE CALCULATE THE (I,I+1) AND (I+1,I+1) COMPLEX MATRIX ELEMENTS!
1610  ! !
1620  Expr=Expxx*Cosyy
1630  Expi=Expxx*Sinyy
1640  Bcr=Beta(P,1)*Cothed(P,1)-Beta(P,2)*Cothed(P,2)
1650  Bci=Beta(P,1)*Cothed(P,2)+Beta(P,2)*Cothed(P,1)
1660  Para(I,R,1)=-(Cothed(P,1)*Expr-Cothed(P,2)*Expi)
1670  Para(I,R,2)=-(Cothed(P,1)*Expi+Cothed(P,2)*Expr)
1680  Perp(I,R,1)=-Expr
1690  Perp(I,R,2)=-Expi
```

```
1700  Para(R,R,1)=-(Beta(P,1)*Expr-Beta(P,2)*Expi)/Mu(P)
1710  Para(R,R,2)=-(Beta(P,1)*Expi+Beta(P,2)*Expr)/Mu(P)
1720  Perp(R,R,1)=-(Bcr*Expr-Bci*Expi)/Mu(P)
1730  Perp(R,R,2)=-(Bcr*Expi+Bci*Expr)/Mu(P)
1740  ! !
1750  ! WE CALCULATE THE (I,I+2) AND (I+1,I+2) COMPLEX MATRIX ELEMENTS!
1760  ! !
1770  Expr=Expmxx*Cosyy
1780  Expi=-Expmxx*Sinyy
1790  IF I=2*N+1 THEN 1880
1800  Para(I,O,1)=-(Cothed(P,1)*Expr-Cothed(P,2)*Expi)
1810  Para(I,O,2)=-(Cothed(P,1)*Expi+Cothed(P,2)*Expr)
1820  Perp(I,O,1)=-Expr
1830  Perp(I,O,2)=-Expi
1840  Para(R,O,1)=(Beta(P,1)*Expr-Beta(P,2)*Expi)/Mu(P)
1850  Para(R,O,2)=(Beta(P,1)*Expi+Beta(P,2)*Expr)/Mu(P)
1860  Perp(R,O,1)=(Bcr*Expr-Bci*Expi)/Mu(P)
1870  Perp(R,O,2)=(Bcr*Expi+Bci*Expr)/Mu(P)
1880  NEXT I
1890  ! !
1900  ! COMPLEX MATRICES ARE EXPANDED INTO REAL MATRICES!
1910  ! !
1920  MAT Paraex=ZER                 !ZEROES PREVIOUS ROW REDUCTION DATA!
1930  MAT Perpex=ZER
1940  FOR I=1 TO L/2
1950  FOR J=I-2 TO I+2               !AVOIDS CYCLING THRU THE WHOLE MATRIX!
1960  IF J<1 THEN 2100
1970  IF J>L/2 THEN 2100
1980  M=2*I
1990  R=2*J
2000  O=M-1
2010  P=R-1
2020  Paraex(O,P)=Para(I,J,1)
2030  Paraex(M,R)=Para(I,J,1)
2040  Paraex(M,P)=Para(I,J,2)
```

```
2050  Paraex(O,R)=-Para(I,J,2)
2060  Perpex(O,P)=Perp(I,J,1)
2070  Perpex(M,R)=Perp(I,J,1)
2080  Perpex(M,P)=Perp(I,J,2)
2090  Perpex(O,R)=-Perp(I,J,2)
2100  NEXT J
2110  NEXT I
2120  Paraex(1,Lp)=-E1*Cothed(Np,1)
2130  Paraex(3,Lp)=-E1*(Beta0/Mu(0))
2140  Perpex(1,Lp)=-E1
2150  Perpex(3,Lp)=-E1*Cothed(Np,1)*(Beta0/Mu(0))
2160  ! !
2170  ! AT THIS POINT WE ARE READY FOR THE MATRIX SOLUTION!
2180  ! !
2190  FOR I=1 TO L            !L IS THE DIMENSION OF THE EXPANDED MATRICES!
2200  FOR J=I-5 TO I+5        !1810-1870 DIVIDES THE Ith ROW BY DIAGONAL ELE.!
2210  IF J>L THEN 2280
2220  IF J<1 THEN 2280
2230  IF I=J THEN 2280
2240  IF Paraex(I,I)=0 THEN Paraex(I,I)=1E-12
2250  IF Perpex(I,I)=0 THEN Perpex(I,I)=1E-12
2260  Paraex(I,J)=Paraex(I,J)/Paraex(I,I)
2270  Perpex(I,J)=Perpex(I,J)/Perpex(I,I)
2280  NEXT J
2290  Paraex(I,Lp)=Paraex(I,Lp)/Paraex(I,I)
2300  Perpex(I,Lp)=Perpex(I,Lp)/Perpex(I,I)
2310  Paraex(I,I)=1
2320  Perpex(I,I)=1
2330  FOR K=I+1 TO I+5        !WE ZERO THE COLUMN BELOW THE Ith DIAGONAL!
2340  IF K>L THEN 2440
2350  X=Paraex(K,I)
2360  Y=Perpex(K,I)
2370  FOR J=I TO I+5
2380  IF J>L THEN 2410
2390  Paraex(K,J)=Paraex(K,J)-X*Paraex(I,J)
```

```
2400  Perpex(K,J)=Perpex(K,J)-Y*Perpex(I,J)
2410  NEXT J
2420  Paraex(K,Lp)=Paraex(K,Lp)-X*Paraex(I,Lp)
2430  Perpex(K,Lp)=Perpex(K,Lp)-Y*Perpex(I,Lp)
2440  NEXT K
2450  NEXT I
2460  ! !
2470  ! Paraex AND Perpex ARE NOW IN UPPER TRIANGULAR FORM!
2480  ! !
2490  FOR I=0 TO L-1
2500  FOR K=I+1 TO I+5
2510  IF K>L-1 THEN 2630
2520  O=L-K
2530  P=L-I
2540  X=Paraex(O,P)
2550  Y=Perpex(O,P)
2560  FOR J=P TO P+4
2570  IF J>L THEN 2600
2580  Paraex(O,J)=Paraex(O,J)-X*Paraex(P,J)
2590  Perpex(O,J)=Perpex(O,J)-Y*Perpex(P,J)
2600  NEXT J
2610  Paraex(O,Lp)=Paraex(O,Lp)-X*Paraex(P,Lp)
2620  Perpex(O,Lp)=Perpex(O,Lp)-Y*Perpex(P,Lp)
2630  NEXT K
2640  NEXT I
2650  ! !
2660  ! THE MAG. OF THE ELECTRIC FIELDS ARE NOW CALCULATED IN THE L+1 COLUMN!
2670  ! !
2680  ! WE NOW FIND THE SURF. TEMP. Uo FOR NO LOSSES ON Zn BOUNDRY!
2690  ! !
2700  Papara=Power-.5*SQR(Epslon(0)/Mu(0))*(Paraex(1,Lp)^2+Paraex(2,Lp)^2+Paraex
(L-1,Lp)^2+Paraex(L,Lp)^2)
2710  Paperp=Power-.5*SQR(Epslon(0)/Mu(0))*(Perpex(1,Lp)^2+Perpex(2,Lp)^2+Perpex
(L-1,Lp)^2+Perpex(L,L+1)^2)
2720  ! WE NOW DO A NEWTON ALGORITHM TO FIND THE SURFACE TEMP., Uo!
```

```
2730  Uopa=Uair
2740  Uope=Uair
2750  J=0
2760  Fupara=1.42/H^Del*ABS(Uopa-Uair)^(Del+1)+Fe*Gamma*(Uopa^4-Uair^4)-Papara
2770  Fuperp=1.42/H^Del*ABS(Uope-Uair)^(Del+1)+Fe*Gamma*(Uope^4-Uair^4)-Paperp
2780  Fupap=(Del+1)*(1.42/H^Del)*ABS(Uopa-Uair)^Del+4*Fe*Gamma*Uopa^3
2790  Fupep=(Del+1)*(1.42/H^Del)*ABS(Uope-Uair)^Del+4*Fe*Gamma*Uope^3
2800  Uopa1=Uopa-Fupara/Fupap
2810  Uope1=Uope-Fuperp/Fupep
2820  IF (ABS(Uopa-Uopa1)<1E-8) AND (ABS(Uope-Uope1)<1E-8) THEN 2880
2830  Uopa=Uopa1
2840  Uope=Uope1
2850  J=J+1
2860  IF J=100 THEN 2880
2870  GOTO 2760
2880  IF J>=100 THEN BEEP
2890  Thed=(Theda+Step)/Step       !Thed IS THE MAT STORAGE ELE FOR Theda STEPS!
2900  Uopara(Aye,Jay,Thed)=Uopa
2910  Uoperp(Aye,Jay,Thed)=Uope
2920  IF Uopa>Pamax(Thed) THEN Pamax(Thed)=Uopa
2930  IF Uope>Pemax(Thed) THEN Pemax(Thed)=Uope
2940  PRINT "Uopa=",Uopa-Uair,"  Papara=",Papara
2950  NEXT Jay
2960  NEXT Aye
2970  NEXT Theda
2980  PRINT #1;Step,Stepp,Uair,N,Power,F,Del,Fe,H
2990  MAT PRINT #2;Sigma,Mu,Epslon,Z,Pamax,Pemax
3000  MAT PRINT #3;Uopara,Uoperp
3010  IF Plot=1 THEN 3050
3020  READ #1;Step,Stepp,Uair,N,Power,F,Del,Fe,H
3030  MAT READ #2;Sigma,Mu,Epslon,Z,Pamax,Pemax
3040  MAT READ #3;Uopara,Uoperp
3050  ! WE BEGIN THE GRAPHICS PORTION HERE !
3060  ! !
3070  INPUT "ENTER: 1-Uopara; 2-Uoperp",Mat
```

```
3080  IF Mat=0 THEN GOTO 4370
3090  PRINT "THE Theda STEP VALUE=",Step
3100  INPUT "ENTER: Incident Angle (multiple of step).",Theda
3110  Thed=(Theda+Step)/Step
3120  FOR I=1 TO 20
3130  Uopara(I,22,Thed)=Uopara(I,21,Thed)
3140  Uoperp(I,22,Thed)=Uoperp(I,21,Thed)
3150  NEXT I
3160  GRAPHICS
3170  GCLEAR
3180  MAT Max=ZER
3190  MAT Last=ZER
3200  CSIZE 2.3,9/15,0
3210  LINE TYPE 1
3220  LDIR 0
3230  LOCATE 15,90,15,90
3240  SCALE 0,40,0,40
3250  LOCATE 14,90,14,90
3260  AXES 1,2,0,0,5,10
3270  Tmax=0
3280  FOR I=1 TO 10
3290  IF (Pamax(I)>Tmax) AND (Mat=1) THEN Tmax=Pamax(I)
3300  IF (Pemax(I)>Tmax) AND (Mat=2) THEN Tmax=Pemax(I)
3310  NEXT I
3320  Tmax=Tmax-Uair
3330  FOR I=1 TO 20 STEP Stepp                !WE DRAW THE X CONTOURS!
3340  MOVE 19+I,I-1
3350  FOR J=21 TO 1 STEP -1
3360  Jj=J-2+I
3370  IF Mat<>1 THEN 3410
3380  Var=I-1+20*(Uopara(I,J,Thed)-Uair)/Tmax
3390  Varp=I-1+20*(Uopara(I,J+1,Thed)-Uair)/Tmax
3400  Varm=I-1+20*(Uopara(I,J-1,Thed)-Uair)/Tmax
3410  IF Mat<>2 THEN 3450
3420  Var=I-1+20*(Uoperp(I,J,Thed)-Uair)/Tmax
```

```
3430  Varp=I-1+20*(Uoperp(I,J+1,Thed)-Uair)/Tmax
3440  Varm=I-1+20*(Uoperp(I,J-1,Thed)-Uair)/Tmax
3450  X1=Jj-1+1E-8
3460  X2=Jj+1E-9
3470  X3=Jj+1+1E-10
3480  Y1=Varm
3490  Y2=Var
3500  Y3=Varp
3510  Det=X1^2*X2+X1*X3^2+X3*X2^2-X2*X3^2-X3*X1^2-X1*X2^2
3520  A=(X2*Y1+X1*Y3+Y2*X3-X2*Y3-Y1*X3-X1*Y2)/Det
3530  B=(X1^2*Y2+Y1*X3^2+Y3*X2^2-Y2*X3^2-Y3*X1^2-Y1*X2^2)/Det
3540  C=(X2*Y3*X1^2+X1*Y2*X3^2+Y1*X3*X2^2-Y1*X2*X3^2-X3*Y2*X1^2-X1*Y3*X2^2)/Det
3550  FOR K=1 TO 10
3560  X=Jj-.1*K
3570  Y=A*X^2+B*X+C
3580  IF (J=21) AND (K=1) THEN DRAW X,Y
3590  IF I=1 THEN 3610
3600  Last(Jj+1-Stepp,K)=Max(Jj+1-Stepp,K)
3610  IF Y>Max(Jj,K) THEN 3640
3620  MOVE X,Y
3630  GOTO 3660
3640  Max(Jj,K)=Y
3650  DRAW X,Y
3660  NEXT K
3670  NEXT J
3680  ! !
3690  ! HERE IS THE PLACE TO DRAW Y CONTOURS!
3700  ! !
3710  FOR J=21 TO 2 STEP -1
3720  Jj=J-2+I
3730  MOVE Jj-Stepp,Last(Jj+1-Stepp,10)       !(Jj+1,10) YIELDS THE Jj COORD.!
3740  IF I=1 THEN 3760
3750  IF Max(Jj+1,10)>Last(Jj+1,10) THEN DRAW Jj,Max(Jj+1,10)
3760  NEXT J
```

```
3770  NEXT I
3780  MOVE 9,-2
3790  LABEL "COATING THICKNESS IN SKIN DEPTHS"
3800  CSIZE 3.3,9/15,0
3810  MOVE -4,-6
3820  IF Mat=1 THEN LABEL USING 3830;Theda
3830  IMAGE "PARALLEL INCIDENCE: Theta=",DD,"  Degrees"
3840  IF Mat=2 THEN LABEL USING 3850;Theda
3850  IMAGE "PERPENDICULAR INCIDENCE: Theta=",DD,"  Degrees"
3860  CSIZE 2.5,9/15,0
3870  LDIR PI/2
3880  MOVE -2,1
3890  LABEL USING 3900;Tmax
3900  IMAGE "Delta Temperature Normalized To ",DD.DD," Degrees C."
3910  LDIR 0
3920  LINE TYPE 3
3930  MOVE 0,0
3940  DRAW 20,20
3950  LINE TYPE 1
3960  MOVE 20.25,0
3970  DRAW 40,19.75
3980  FOR I=1 TO 19
3990  MOVE I+20.25,I
4000  DRAW I+20.75,I-.5
4010  MOVE I+20.25,I-1.2
4020  J=I/2
4030  IF ABS(I/2-J)>0 THEN 4060
4040  LABEL USING 4050;7.5-.5*(I-1)
4050  IMAGE DD.D
4060  NEXT I
4070  LDIR PI/4
4080  MOVE 30,2
4090  LABEL "Sigma in Mhos/M (LOG 10)"
4100  LDIR 0
4110  PAUSE
```

```
4120  INPUT "For a paper copy enter a 1; otherwise 0.",Copy
4130  IF Copy=1 THEN DUMP GRAPHICS
4140  EXIT GRAPHICS
4150  IF Copy=1 THEN PRINTER IS 0
4160  PRINT
4170  PRINT
4180  PRINT
4190  PRINT
4200  PRINT
4210  PRINT
4220  PRINT
4230  PRINT USING 4240;N;Power/10;F
4240  IMAGE "Number of Layers=",DD,"       Power in W/Cm^2=",DD,"       Freq. in
 GHz=",D.DD
4250  PRINT USING 4260;Uair-273.16;Del;Fe;H
4260  IMAGE "Air Temp (C)=",DD.D,"  Convective Exp=",D.DD,"  Emissivity=",D.DD,"
  Plate Height (M)=",D.DDD
4270  PRINT
4280  PRINT
4290  FOR I=1 TO N
4300  X=4*PI*1E-7
4310  Y=8.8542E-12
4320  PRINT USING 4330;I,Sigma(I),I,Mu(I)/X,I,Epslon(I)/Y,I,Z(I)-Z(I-1)
4330  IMAGE "Sigma(",D,")=",D.DDE,"  Mu(",D,")=",DD.D,"  Epsilon(",D,")=",D.DD,"
  Thickness(",D,")=",D.DDE
4340  NEXT I
4350  PRINTER IS 16
4360  GOTO 3070
4370  STOP
```

APPENDIX G

COMPUTER PROGRAM

The name of this program is "Uthick". It calculates the surface temperature of a system of N layers as a function of the thickness of any two of the layers. The result is plotted on contour plot of constant temperatures. The input variables are the number of layers, which layers to vary the thickness of, the incident power, the incident frequency, the incident angle, the ambient air temperature, the plate height, surface emissivity, the convective exponent, and the layer characteristics of conductivity, permittivity, permeability, and thickness.

```
10    ! THE NAME OF THIS PROGRAM IS 'UThick'  !
20    ! IT CALCULATES THE SURFACE TEMPERATURE OF A SYSTEM OF N LAYERS AS A FUNCT
ION OF COATING THICKNESS AND LAYER THICKNESS!
30    INTEGER I,J,K,L,M,N,O,P,Q,R,Lp,Np,Aye,Jay,L1,L2
40    SHORT Beta(11,2),Z(11),Cothed(12,2),Sigma(10),Mu(12),Epslon(12),Para(22,22
,2),Perp(22,22,2),Paraex(44,44),Perpex(44,44),Sithed(12,2),Betcos(10,2)
50    SHORT Parabx(44),Perpbx(44),Epara(44),Eperp(44),Dum(44,44),Thick(11),X(10,
10),Y(10,10)
60    SHORT Jpara(10,50),Jperp(10,50),Ppara(10,50),Pperp(10,50),Jparat(10),Jperp
t(10),Uopara(10,10),Uoperp(10,10),Jpapct(10,10),Jpepct(10,10)
70    PRINTER IS 16
80    PRINT PAGE
90    GCLEAR
100   EXIT GRAPHICS
110   PRINT "THE FIRST RUN SHOULD BE WITHOUT A PERFECT LAST CONDUCTOR."
120   Second=0
130   INPUT "For Second Run Enter 2.",Second
140   INPUT "Enter the Number of Layers not to Exceed 10.",N
150   INPUT "Enter Which Layer Thickness to Vary (Two).",L1,L2
160   INPUT "Enter the Step Increment for Each Layer (Two).",Inc1,Inc2
170   INPUT "Enter the Incident Power in MW/Cm^2",Power
180   INPUT "Enter the Incident Frequency in Gigahertz.",F
190   INPUT "Enter the Ambient Air Temperature in Centigrade.",Uair
200   INPUT "Enter the Plate Height in Meters.",H
210   INPUT "Enter  Theda.",Theda
220   INPUT "Enter the Surface Emissivity.",Fe
230   INPUT "Enter the Convective Heat Transfer Coefficient.",Del
240   ASSIGN #1 TO "UoBIG"
250   IF Second<>2 THEN 330
260   MAT READ #1;Uopara,Uoperp,Jpapct,Jpepct
270   MAT X=Uopara
280   MAT Y=Jpapct
290   PURGE "UoBIG"
300   CREATE "UoBIG",4,1E3
```

```
310   ASSIGN #1 TO "UoBIG"
320   GOTO 360
330   PURGE "UoBIG"
340   CREATE "UoBIG",4,1E3
350   ASSIGN #1 TO "UoBIG"
360   Gamma=5.67E-8                     !STEFAN-BOLTZMAN CONSTANT!
370   Uair=Uair+273.16                  !AIR TEMPERATURE IN KELVIN!
380   Omega=2*PI*F*1E9                  !ANGULAR FREQUENCY IS CALCULATED!
390   Beta0=Omega/2.998E8               !FREE SPACE WAVE VECTOR IS CALCULATED!
400   Beta02=Beta0^2                    !THE WAVE VECTOR IS SQUARED!
410   Power=10*Power                    !CONVERTS TO WATT/METER^2!
420   FOR I=1 TO N                      !ELEC. PROPERTIES OF LAYERS IS INSERTED!
430   DISP "Sigma(";I;")";              !ELECTRICAL CONDUCTIVITY IN MHOS!
440   INPUT Sigma(I)
450   IF Sigma(I)=0 THEN Sigma(I)=1E-12
460   DISP "Mu(";I;")";                 !RELATIVE MAGNETIC PERMEABILITY!
470   INPUT Mu
480   Mu(I)=Mu*4*PI*1E-7
490   DISP "Epslon(";I;")";             !RELATIVE ELECTRIC PERMITTIVITY!
500   INPUT Epslon
510   Epslon(I)=Epslon*8.8542E-12
520   DISP "Initial Thickness(";I;")";          !EACH LAYER THICKNESS IN METERS!
530   INPUT Thick(I)
540   Delta=SQR(2/(Omega*Mu(I)*Sigma(I)))
550   IF Thick(I)<23*Delta THEN 620
560   Thick(I)=23*Delta
570   N=I
580   Key=1
590   PRINT USING 600;I,I,I,Thick(I)
600   IMAGE "LAYER ",DD," WAS THICKER THAN 23 SKIN DEPTHS. THE PROBLEM IS TRUNCA
TED AT ",DD," LAYERS, WITH LAYER ",DD,", ",D.DDE," METERS THICK."
610   PRINT
620   Coef=Omega*SQR(Mu(I)*Epslon(I)/2)
630   Sqroot=SQR(1+(Sigma(I)/(Omega*Epslon(I)))^2)
640   Beta(I,1)=Coef*SQR(1+Sqroot)      !REAL WAVE VECTOR (Alpha) IS CALC.!
```

```
650     Beta(I,2)=Coef*SQR(Sqroot-1)       !IMAG WAVE VECTOR (Gamma) IS CALC.!
660     NEXT I
670     Np=N+1
680     L=4*Np
690     Lp=L+1
700     Mu(0)=4*PI*1E-7                    !ELEC. CHARAC. EA. SIDE OF LAYERS!
710     Epslon(0)=8.8542E-12
720     Mu(Np)=4*PI*1E-7
730     Epslon(Np)=8.8542E-12
740     Beta(0,1)=Beta0                    !REAL Beta 0!
750     Beta(0,2)=0                        !IMAGINARY Beta 0!
760     Beta(Np,1)=Beta0
770     Beta(Np,2)=0
780     E1=(Mu(0)/Epslon(0))^.25*SQR(2*Power)
790     E12=E1^2
800     Deg=PI/180
810     Tck1=Thick(L1)
820     Tck2=Thick(L2)
830     Aye=1
840     ! !
850               ! !!!  NOW WE START !!!!!
860     ! !
870     FOR Thick1=Tck1 TO 9*Inc1+Tck1 STEP Inc1
880     Jay=1
890     Thick(L1)=Thick1
900     FOR Thick2=Tck2 TO 9*Inc2+Tck2 STEP Inc2
910     Thick(L2)=Thick2
920     FOR I=1 TO N                           !CALCULATES Z's FOR THICKNESSES!
930     Z(I)=Z(I-1)+Thick(I)
940     NEXT I
950     IF Key<>1 THEN 1000                    !SHIFTS AXIS IN CASE OF TRUNCATION!
960     Shift=Z(N-1)
970     FOR I=0 TO N
980     Z(I)=Z(I)-Shift
990     NEXT I
```

```
1000  X=COS(Theda*Deg)
1010  Y=SIN(Theda*Deg)
1020  IF X=0 THEN X=1E-5
1030  IF Y=1 THEN Y=.999999999999
1040  Sin2=Y^2
1050  H1para=2*E1*SQR(Epslon(0)/Mu(0))
1060  H1perp=H1para*X
1070  Cothed(Np,1)=X
1080  Cothed(Np,2)=0
1090  Cothed(0,1)=X
1100  Cothed(0,2)=0
1110  Sithed(Np,1)=Y
1120  Sithed(Np,2)=0
1130  Sithed(0,1)=Y
1140  Sithed(0,2)=0
1150  ! !
1160  ! WE CALCULATE REAL AND IMAGINARY COS(Theda) AND SIN(Theda) !
1170  ! !
1180  FOR I=1 TO N
1190  Denom=(Beta(I,1)^2+Beta(I,2)^2)^2
1200  Pee=.5*(1-Beta02*Sin2*(Beta(I,1)^2-Beta(I,2)^2)/Denom)
1210  Que=Beta02*Sin2*Beta(I,1)*Beta(I,2)/Denom
1220  X=SQR(Pee^2+Que^2)
1230  Cothed(I,1)=SQR(Pee+X)                      !REAL COS(Theda N) IS CALCULATED!
1240  Cothed(I,2)=SQR(ABS(X-Pee))                 !IMAG COS(Theda N) IS CALCULATED!
1250  Sithed(I,1)=Beta(0,1)*Y*Beta(I,1)/(Beta(I,1)^2+Beta(I,2)^2)
1260  Sithed(I,2)=-Beta(0,1)*Y*Beta(I,2)/(Beta(I,1)^2+Beta(I,2)^2)
1270  Betcos(I,1)=Beta(I,1)*Cothed(I,1)-Beta(I,2)*Cothed(I,2)  !REAL Beta x Cos(
Theda)!
1280  Betcos(I,2)=Beta(I,1)*Cothed(I,2)+Beta(I,1)*Cothed(I,1)  !IMAG Beta x Cos(
Theda)!
1290  IF Betcos(I,1)*Z(I)>75 THEN Betcos(I,1)=75/Z(I)
1300  IF Betcos(I,2)*Z(I)>75 THEN Betcos(I,2)=75/Z(I)
1310  NEXT I
```

```
1320  ! !
1330  ! WE BEGIN TO CALCULATE THE COMPLEX MATRIX!
1340  ! !
1350  FOR I=1 TO 2*(N-Key)+1 STEP 2        ! WE ENTER ROWS BY BOUNDRY, 2 PER BOU
NDRY !
1360  K=(I-1)/2
1370  M=I-1
1380  R=I+1
1390  O=I+2
1400  X=-Z(K)*(Beta(K,1)*Cothed(K,2)+Beta(K,2)*Cothed(K,1))
1410  Y=Z(K)*(Beta(K,1)*Cothed(K,1)-Beta(K,2)*Cothed(K,2))
1420  P=K+1
1430  Xx=-Z(K)*(Beta(P,1)*Cothed(P,2)+Beta(P,2)*Cothed(P,1))
1440  Yy=Z(K)*(Beta(P,1)*Cothed(P,1)-Beta(P,2)*Cothed(P,2))
1450  IF X>170 THEN X=170    !X>170 IMPLIES A LAYER THICKNESS >170 SKIN DEPTHS!
1460  IF Xx>170 THEN Xx=170  !Xx>170 IMPLIES A LAYER THICKNESS >170 SKIN DEPTHS!
1470  Expx=EXP(X)
1480  Expxx=EXP(Xx)
1490  IF X<-170 THEN X=-170
1500  IF Xx<-170 THEN Xx=-170
1510  Expmx=EXP(-X)
1520  Expmxx=EXP(-Xx)
1530  Cosy=COS(Y)
1540  Siny=SIN(Y)
1550  Cosyy=COS(Yy)
1560  Sinyy=SIN(Yy)
1570  Expr=Expx*Cosy          !Bcr IMPLIES THE REAL PART OF Beta*COS(Theda)!
1580  Expi=Expx*Siny          !Bci IMPLIES THE IMAG PART OF Beta*COS(Theda)!
1590  Bcr=Beta(K,1)*Cothed(K,1)-Beta(K,2)*Cothed(K,2)
1600  Bci=Beta(K,1)*Cothed(K,2)+Beta(K,2)*Cothed(K,1)
1610  ! !
1620  ! WE CALCULATE THE (I,I-1) AND (I+1,I-1) COMPLEX MATRIX ELEMENTS!
1630  ! !
1640  IF I=1 THEN 1740
```

```
1650  Para(I,M,1)=Cothed(K,1)*Expr-Cothed(K,2)*Expi
1660  Para(I,M,2)=Cothed(K,1)*Expi+Cothed(K,2)*Expr
1670  Perp(I,M,1)=Expr
1680  Perp(I,M,2)=Expi
1690  Para(R,M,1)=(Beta(K,1)*Expr-Beta(K,2)*Expi)/Mu(K)
1700  Para(R,M,2)=(Beta(K,1)*Expi+Beta(K,2)*Expr)/Mu(K)
1710  Perp(R,M,1)=(Bcr*Expr-Bci*Expi)/Mu(K)
1720  Perp(R,M,2)=(Bcr*Expi+Bci*Expr)/Mu(K)
1730  ! !
1740  ! WE  CALCULATE THE (I,I) AND (I+1,I) COMPLEX MATRIX ELEMENTS!
1750  ! !
1760  Expr=Expmx*Cosy
1770  Expi=-Expmx*Siny
1780  Para(I,I,1)=Cothed(K,1)*Expr-Cothed(K,2)*Expi
1790  Para(I,I,2)=Cothed(K,1)*Expi+Cothed(K,2)*Expr
1800  Perp(I,I,1)=Expr
1810  Perp(I,I,2)=Expi
1820  Para(R,I,1)=-(Beta(K,1)*Expr-Beta(K,2)*Expi)/Mu(K)
1830  Para(R,I,2)=-(Beta(K,1)*Expi+Beta(K,2)*Expr)/Mu(K)
1840  Perp(R,I,1)=-(Bcr*Expr-Bci*Expi)/Mu(K)
1850  Perp(R,I,2)=-(Bcr*Expi+Bci*Expr)/Mu(K)
1860  ! !
1870  ! WE CALCULATE THE (I,I+1) AND (I+1,I+1) COMPLEX MATRIX ELEMENTS!
1880  ! !
1890  Expr=Expxx*Cosyy
1900  Expi=Expxx*Sinyy
1910  Bcr=Beta(P,1)*Cothed(P,1)-Beta(P,2)*Cothed(P,2)
1920  Bci=Beta(P,1)*Cothed(P,2)+Beta(P,2)*Cothed(P,1)
1930  Para(I,R,1)=-(Cothed(P,1)*Expr-Cothed(P,2)*Expi)
1940  Para(I,R,2)=-(Cothed(P,1)*Expi+Cothed(P,2)*Expr)
1950  Perp(1,R,1)=-Expr
1960  Perp(I,R,2)=-Expi
1970  Para(R,R,1)=-(Beta(P,1)*Expr-Beta(P,2)*Expi)/Mu(P)
1980  Para(R,R,2)=-(Beta(P,1)*Expi+Beta(P,2)*Expr)/Mu(P)
1990  Perp(R,R,1)=-(Bcr*Expr-Bci*Expi)/Mu(P)
```

```
2000  Perp(R,R,2)=-(Bcr*Expi+Bci*Expr)/Mu(P)
2010  ! !
2020  ! WE CALCULATE THE (I,I+2) AND (I+1,I+2) COMPLEX MATRIX ELEMENTS!
2030  ! !
2040  Expr=Expmxx*Cosyy
2050  Expi=-Expmxx*Sinyy
2060  IF I=2*N+1 THEN 2150
2070  Para(I,O,1)=-(Cothed(P,1)*Expr-Cothed(P,2)*Expi)
2080  Para(I,O,2)=-(Cothed(P,1)*Expi+Cothed(P,2)*Expr)
2090  Perp(I,O,1)=-Expr
2100  Perp(I,O,2)=-Expi
2110  Para(R,O,1)=(Beta(P,1)*Expr-Beta(P,2)*Expi)/Mu(P)
2120  Para(R,O,2)=(Beta(P,1)*Expi+Beta(P,2)*Expr)/Mu(P)
2130  Perp(R,O,1)=(Bcr*Expr-Bci*Expi)/Mu(P)
2140  Perp(R,O,2)=(Bcr*Expi+Bci*Expr)/Mu(P)
2150  NEXT I
2160  ! !
2170  ! COMPLEX MATRICES ARE EXPANDED INTO REAL MATRICES!
2180  ! !
2190  MAT Paraex=IDN(L,L)             ! FORMS AN IDENTITY MATRIX !
2200  MAT Perpex=IDN(L,L)
2210  MAT Dum=IDN(L,L)
2220  FOR I=1 TO L/2-2*Key            ! LOADS 4 ELEMENTS FOR EACH COMPLEX ONE !
2230  FOR J=I-2 TO I+2                !AVOIDS CYCLING THRU THE WHOLE MATRIX!
2240  IF J<1 THEN 2380
2250  IF J>L/2-2*Key THEN 2380
2260  M=2*I
2270  R=2*J
2280  O=M-1
2290  P=R-1
2300  Paraex(O,P)=Para(I,J,1)
2310  Paraex(M,R)=Para(I,J,1)
2320  Paraex(M,P)=Para(I,J,2)
2330  Paraex(O,R)=-Para(I,J,2)
2340  Perpex(O,P)=Perp(I,J,1)
```

```
2350  Perpex(M,R)=Perp(I,J,1)
2360  Perpex(M,P)=Perp(I,J,2)
2370  Perpex(O,R)=-Perp(I,J,2)
2380  NEXT J
2390  NEXT I
2400  Parabx(1)=-E1*Cothed(0,1)
2410  Parabx(3)=-E1*(Beta0/Mu(0))
2420  Perpbx(1)=-E1
2430  Perpbx(3)=-E1*Cothed(0,1)*(Beta0/Mu(0))
2440  ! !
2450  ! AT THIS POINT WE ARE READY FOR THE MATRIX SOLUTION!
2460  ! !
2470  MAT Dum=INV(Paraex)
2480  FOR I=1 TO L
2490  Epara(I)=Dum(I,1)*Parabx(1)+Dum(I,3)*Parabx(3)
2500  NEXT I
2510  MAT Dum=INV(Perpex)
2520  FOR I=1 TO L
2530  Eperp(I)=Dum(I,1)*Perpbx(1)+Dum(I,3)*Perpbx(3)
2540  NEXT I
2550  ! !
2560  ! THE MAG. OF THE ELECTRIC FIELDS ARE NOW CALCULATED IN Epara AND Eperp !
2570  ! !
2580  ! WE NOW CALCULATE THE VALUE OF J THROUGHOUT THE N LAYERS!
2590  ! !
2600  J=3
2610  FOR I=1 TO N                       ! WE STEP THROUGH EACH LAYER !
2620  Z=Z(I-1)
2630  FOR K=1 TO 50
2640  Zinc=(Z(I)-Z(I-1))/49
2650  U=EXP(-Betcos(I,2)*Z)
2660  Rv=COS(Betcos(I,1)*Z)
2670  Iv=SIN(Betcos(I,1)*Z)
2680  X=EXP(Betcos(I,2)*Z)
2690  Ry=Rv
```

```
2700  Iy=-Iv
2710  Rt=U*(Epara(J)*Rv-Epara(J+1)*Iv)
2720  It=U*(Epara(J)*Iv+Epara(J+1)*Rv)
2730  Rw=X*(Epara(J+2)*Ry-Epara(J+3)*Iy)
2740  Iw=X*(Epara(J+2)*Iy+Epara(J+3)*Ry)
2750  Rf=Rt+Rw
2760  If=It+Iw
2770  Rg=Rt-Rw
2780  Ig=It-Iw
2790  Ppara(I,K)=Sigma(I)*((Rf^2+If^2)*(Cothed(I,1)^2+Cothed(I,2)^2)+(Rg^2+Ig^2)
*(Sithed(I,1)^2+Sithed(I,2)^2))
2800  Jpara(I,K)=Sigma(I)*SQR((Rf^2+If^2)*(Cothed(I,1)^2+Cothed(I,2)^2)+(Rg^2+Ig
^2)*(Sithed(I,1)^2+Sithed(I,2)^2))
2810  IF K=1 THEN 2860
2820  Alpha=-LOG(Jpara(I,K)/Jpara(I,K-1))/Zinc
2830  IF Alpha=0 THEN Alpha=1E-10
2840  Coef=Jpara(I,K-1)*EXP(Alpha*(Z-Zinc))
2850  Jparat(I)=Jparat(I)-Coef/Alpha*EXP(-Alpha*Z)*(EXP(-Alpha*Zinc)-1)
2860  Rt=U*(Eperp(J)*Rv-Eperp(J+1)*Iv)
2870  It=U*(Eperp(J)*Iv+Eperp(J+1)*Rv)
2880  Rw=X*(Eperp(J+2)*Ry-Eperp(J+3)*Iy)
2890  Iw=X*(Eperp(J+2)*Iy+Eperp(J+3)*Ry)
2900  Pperp(I,K)=Sigma(I)*((Rt+Rw)^2+(It+Iw)^2)
2910  Jperp(I,K)=Sigma(I)*SQR((Rt+Rw)^2+(It+Iw)^2)
2920  IF K=1 THEN 2970
2930  Alpha=-LOG(Jperp(I,K)/Jperp(I,K-1))/Zinc
2940  IF Alpha=0 THEN Alpha=1E-10
2950  Coef=Jperp(I,K-1)*EXP(Alpha*(Z-Zinc))
2960  Jperpt(I)=Jperpt(I)-Coef/Alpha*EXP(-Alpha*Z)*(EXP(-Alpha*Zinc)-1)
2970  Z=Z+Zinc
2980  NEXT K
2990  J=J+4
3000  NEXT I
3010  FOR I=1 TO N
```

```
3020  Jao=Jao+Jparat(I)
3030  Jeo=Jeo+Jperpt(I)
3040  NEXT I
3050  ! !
3060  ! THE PARALLEL AND PERPENDICULAR CURRENT DENSITIES ARE NOW CALCULATED!
3070  ! !
3080  Jpapct(Aye,Jay)=(Jao-Jparat(N))/Jao*100
3090  Jpepct(Aye,Jay)=(Jeo-Jperpt(N))/Jeo*100
3100  !
3110  ! WE NOW FIND THE SURF. TEMP. Uo FOR NO LOSSES ON Zn BOUNDARY!
3120  !
3130  Papara=Power-.5*SQR(Epslon(0)/Mu(0))*(Epara(1)^2+Epara(2)^2+Epara(L-1)^2+E
para(L)^2)
3140  Paperp=Power-.5*SQR(Epslon(0)/Mu(0))*(Eperp(1)^2+Eperp(2)^2+Eperp(L-1)^2+E
perp(L)^2)
3150  ! WE NOW DO A NEWTON ALGORITHM TO FIND THE SURFACE TEMP., Uo!
3160  Uopa=Uair
3170  Uope=Uair
3180  J=0
3190  Fupara=15/H^Del*ABS(Uopa-Uair)^(Del+1)+Fe*Gamma*(Uopa^4-Uair^4)-Papara
3200  Fuperp=15/H^Del*ABS(Uope-Uair)^(Del+1)+Fe*Gamma*(Uope^4-Uair^4)-Paperp
3210  Fupap=(Del+1)*(15/H^Del)*ABS(Uopa-Uair)^Del+4*Fe*Gamma*Uopa^3
3220  Fupep=(Del+1)*(15/H^Del)*ABS(Uope-Uair)^Del+4*Fe*Gamma*Uope^3
3230  Uopa1=Uopa-Fupara/Fupap
3240  Uope1=Uope-Fuperp/Fupep
3250  IF (ABS(Uopa-Uopa1)<1E-8) AND (ABS(Uope-Uope1)<1E-8) THEN 3310
3260  Uopa=Uopa1
3270  Uope=Uope1
3280  J=J+1
3290  IF J=100 THEN 3310
3300  GOTO 3190
3310  IF J>100 THEN PRINT "SURFACE TEMP. WOULD NOT CONVERGE."
3320  Uopara(Aye,Jay)=Uopa-Uair
3330  Uoperp(Aye,Jay)=Uope-Uair
```

```
3340  PRINT "Aye=",Aye,"  Jay=",Jay
3350  PRINT "Uopa=",Uopa-Uair,"   Papct=",Jpapct(Aye,Jay)
3360  Jay=Jay+1
3370  NEXT Thick2
3380  Aye=Aye+1
3390  NEXT Thick1
3400  IF Second<>2 THEN 3430
3410  MAT Uoperp=X
3420  MAT Jpepct=Y
3430  MAT PRINT #1;Uopara,Uoperp,Jpapct,Jpepct
3440  ! CONDUCTING LAST LAYER IS IN Uopara AND Jpapct !
3450  STOP
```

APPENDIX H

COMPUTER PROGRAM

The name of this program is "CONTOR". It will plot and smooth contour lines for an arbitrary matrix of values. It will do linear smoothing, circular or parabolic smoothing. The matrix data is read from a data file named "X-Data". Plot labeling is accomplished manually when the flashing cursor appears on the 9845 CRT. The only inputs are the number of rows and columns of the input matrix.

```
10     ! THE NAME OF THIS PROGRAM IS CONTOR !
20     ! IT WILL PLOT AND SMOOTH CONTOURS FOR AN ARBITRARY MATRIX !
30     ! IT DOES A SECOND ORDER CURVE FIT BETWEEN POINTS !
40     ! THE DATA MATRIX MUST BE INPUTED INTO THE X MATRIX !
50     ! THE DATA IS TO BE READ FROM THE 'X-Data' FILE IN LOCATION T14!
60     GCLEAR
70     EXIT GRAPHICS
80     OPTION BASE 1
90     INPUT "ENTER THE HEIGHT/WIDTH RATIO OF PRINTOUT.",Ratio
100    INTEGER I,J,K,L,L1,L2,M,N,Center,Up,Down,Left,Right
110    SHORT X(64,64),Fit(180,180),Coef(3,3),Inv(3,3),B(3),Abc(3),Ctest(180)
120    ASSIGN #1 TO "X-Data:T14"
130    INPUT "ENTER NUMBER OF ROWS OF INPUT MATRIX.",M
140    INPUT "ENTER NUMBER OF COLUMNS OF INPUT MATRIX.",N
150    REDIM X(M,N)
160    MAT READ #1;X
170    Devx=18
180    Devy=18
190    INPUT "ENTER 1 FOR PARABOLIC FIT, 2 CIRCLE FIT, 3 LINEAR.",Type
200    FOR I=1 TO M
210    X=1
220    K=1
230    L=(I-1)*179/(M-1)+1
240    PRINT USING 250;I
250    IMAGE "I=",DD
260    FOR J=1 TO N-2
270    X1=(J-1)*179/(N-1)+1
280    X2=J*179/(N-1)+1
290    X3=(J+1)*179/(N-1)+1
300    Y1=X(I,J)
310    Y2=X(I,J+1)
320    Y3=X(I,J+2)
330    IF Type<>1 THEN 540                    ! PARABOLIC SMOOTHING!
340    Coef(1,1)=X1^2
```

```
350    Coef(1,2)=X1
360    Coef(1,3)=1
370    Coef(2,1)=X2^2
380    Coef(2,2)=X2
390    Coef(2,3)=1
400    Coef(3,1)=X3^2
410    Coef(3,2)=X3
420    Coef(3,3)=1
430    B(1)=Y1
440    B(2)=Y2
450    B(3)=Y3
460    MAT Inv=INV(Coef)
470    MAT Abc=Inv*B
480    Fit(L,K)=Abc(1)*X^2+Abc(2)*X+Abc(3)
490    IF Fit(L,K)>Max THEN Max=Fit(L,K)
500    X=X+1
510    K=K+1
520    IF X<X2 THEN 480
530    GOTO 860
540    IF Type<>2 THEN 770                    ! CIRCULAR SMOOTHING!
550    MAT Coef=IDN
560    Coef(1,1)=2*(X2-X1)
570    Coef(1,2)=2*(Y2-Y1)
580    Coef(2,1)=2*(X2-X3)
590    Coef(2,2)=2*(Y2-Y3)
600    B(1)=X2^2+Y2^2-X1^2-Y1^2
610    B(2)=X2^2+Y2^2-X3^2-Y3^2
620    B(3)=0
630    MAT Inv=INV(Coef)
640    MAT Abc=Inv*B
650    C2=(X1-Abc(1))^2+(Y1-Abc(2))^2
660    Sign=1
670    Slop12=(Y1-Y2)/(X1-X2)
680    Cons12=(X1*Y2-X2*Y1)/(X1-X2)
690    Y3prim=Slop12*X3+Cons12
```

```
700   IF Y3-Y3prim>0 THEN Sign=-1
710   Fit(L,K)=Abc(2)+Sign*SQR(C2-(X-Abc(1))^2)
720   IF Fit(L,K)>Max THEN Max=Fit(L,K)
730   X=X+1
740   K=K+1
750   IF X<X2 THEN 710
760   GOTO 860
770   IF Type<>3 THEN 860                       ! LINEAR SMOOTHING !
780   Slope=(Y1-Y2)/(X1-X2)
790   Const=(X1*Y2-X2*Y1)/(X1-X2)
800   Fit(L,K)=Slope*X+Const
810   IF Fit(L,K)>Max THEN Max=Fit(L,K)
820   X=X+1
830   K=K+1
840   IF X<X2 THEN 800
850   GOTO 860
860   NEXT J
870   IF Type<>1 THEN 930
880   Fit(L,K)=Abc(1)*X^2+Abc(2)*X+Abc(3)
890   IF Fit(L,K)>Max THEN Max=Fit(L,K)
900   X=X+1
910   K=K+1
920   IF K<=180 THEN 880
930   IF Type<>2 THEN 990
940   Fit(L,K)=Abc(2)+Sign*SQR(C2-(X-Abc(1))^2)
950   IF Fit(L,K)>Max THEN Max=Fit(L,K)
960   X=X+1
970   K=K+1
980   IF K<=180 THEN 940
990   IF Type<>3 THEN 1050
1000  Fit(L,K)=Slope*X+Const
1010  IF Fit(L,K)>Max THEN Max=Fit(L,K)
1020  X=X+1
1030  K=K+1
```

```
1040  IF K<=180 THEN 1000
1050  NEXT I
1060  ! !
1070  ! THE COLUMNS ARE EXPANDED INTO 180 COLUMNS; NOW WE EXPAND THE ROWS !
1080  !
1090  FOR J=1 TO 180
1100  PRINT USING 1110;J
1110  IMAGE "WE ARE ON COLUMN ",DDD
1120  X=180
1130  K=1
1140  FOR I=1 TO M-2
1150  L=(I-1)*179/(M-1)+1
1160  L1=I*179/(M-1)+1
1170  L2=(I+1)*179/(M-1)+1
1180  X1=181-L
1190  X2=181-L1
1200  X3=181-L2
1210  Y1=Fit(L,J)
1220  Y2=Fit(L1,J)
1230  Y3=Fit(L2,J)
1240  IF Type<>1 THEN 1450                 !  PARABOLIC SMOOTHING !
1250  Coef(1,1)=X1^2
1260  Coef(1,2)=X1
1270  Coef(1,3)=1
1280  Coef(2,1)=X2^2
1290  Coef(2,2)=X2
1300  Coef(2,3)=1
1310  Coef(3,1)=X3^2
1320  Coef(3,2)=X3
1330  Coef(3,3)=1
1340  B(1)=Y1
1350  B(2)=Y2
1360  B(3)=Y3
1370  MAT Inv=INV(Coef)
1380  MAT Abc=Inv*B
```

```
1390  Fit(K,J)=Abc(1)*X^2+Abc(2)*X+Abc(3)
1400  IF Fit(K,J)>Max THEN Max=Fit(K,J)
1410  X=X-1
1420  K=K+1
1430  IF X2<X THEN 1390
1440  GOTO 1770
1450  IF Type<>2 THEN 1680                  ! CIRCULAR SMOOTHING !
1460  MAT Coef=IDN
1470  Coef(1,1)=2*(X2-X1)
1480  Coef(1,2)=2*(Y2-Y1)
1490  Coef(2,1)=2*(X2-X3)
1500  Coef(2,2)=2*(Y2-Y3)
1510  B(1)=X2^2+Y2^2-X1^2-Y1^2
1520  B(2)=X2^2+Y2^2-X3^2-Y3^2
1530  B(3)=0
1540  MAT Inv=INV(Coef)
1550  MAT Abc=Inv*B
1560  C2=(X1-Abc(1))^2+(Y1-Abc(2))^2
1570  Sign=1
1580  Slop12=(Y1-Y2)/(X1-X2)
1590  Cons12=(X1*Y2-X2*Y1)/(X1-X2)
1600  Y3prin=Slop12*X3+Cons12
1610  IF Y3-Y3prin>0 THEN Sign=-1
1620  Fit(K,J)=Abc(2)+Sign*SQR(C2-(X-Abc(1))^2)
1630  IF Fit(K,J)>Max THEN Max=Fit(K,J)
1640  X=X-1
1650  K=K+1
1660  IF X2<X THEN 1620
1670  GOTO 1770
1680  IF Type<>3 THEN 1770                      ! LINEAR SMOOTHING !
1690  Slope=(Y1-Y2)/(X1-X2)
1700  Const=(X1*Y2-X2*Y1)/(X1-X2)
1710  Fit(K,J)=Slope*X+Const
1720  IF Fit(K,J)>Max THEN Max=Fit(K,J)
```

```
1730  X=X-1
1740  K=K+1
1750  IF X2<X THEN 1710
1760  GOTO 1770
1770  NEXT I
1780  IF Type<>1 THEN 1840
1790  Fit(K,J)=Abc(1)*X^2+Abc(2)*X+Abc(3)
1800  IF Fit(K,J)>Max THEN Max=Fit(K,J)
1810  X=X-1
1820  K=K+1
1830  IF K<=100 THEN 1790
1840  IF Type<>2 THEN 1900
1850  Fit(K,J)=Abc(2)+Sign*SQR(C2-(X-Abc(1))^2)
1860  IF Fit(K,J)>Max THEN Max=Fit(K,J)
1870  X=X-1
1880  K=K+1
1890  IF K<=100 THEN 1850
1900  IF Type<>3 THEN 1950
1910  Fit(K,J)=Slope*X+Const
1920  X=X-1
1930  K=K+1
1940  IF K<=100 THEN 1910
1950  NEXT J
1960  GCLEAR
1970  GRAPHICS
1980  LINE TYPE 1
1990  K=10+Ratio*90
2000  IF Ratio>=1 THEN 2030
2010  LOCATE 10,100,10,K
2020  GOTO 2040
2030  LOCATE 10,K,10,100
2040  SCALE 1,100,1,100
2050  FRAME
2060  LINE TYPE 2
```

```
2070  FOR I=2 TO 179
2080  FOR J=2 TO 179
2090  Center=10*Fit(I,J)/Max
2100  Up=10*Fit(I-1,J)/Max
2110  Down=10*Fit(I+1,J)/Max
2120  Left=10*Fit(I,J-1)/Max
2130  Right=10*Fit(I,J+1)/Max
2140  IF Center<>Left THEN DRAW J-1,181.5-I
2150  IF Center<>Up THEN DRAW J-.5,182-I
2160  IF Center<>Right THEN DRAW J,181.5-I
2170  IF Center<>Down THEN DRAW J-.5,181-I
2180  NEXT J
2190  NEXT I
2200  BEEP
2210  LINE TYPE 1
2220  LETTER
2230  PAUSE
2240  GOTO 190
2250  STOP
```

APPENDIX I

COMPUTER PROGRAM

The name of this program is "EPSLON". It calculates the per cent of reflected to incident power and plots it versus relative permittivity for the layer. The input variables are the number of layers, the maximum permittivity to be considered, the incident frequency, the incident angle, and the measured reflectivity.

```
10     ! THE NAME OF THIS PROGRAM IS 'EPSLON'  !
20     ! IT CALCULATES THE PER CENT OF REFLECTED POWER TO INCIDENT POWER AND
PLOTS IT VERSUS RELATIVE EPSILON!
30     INTEGER I,J,K,L,M,N,O,P,Q,R,Lp,Np
40     DIM Beta(11,2),Z(11),Cothed(12,2),Sigma(10),Mu(12),Epslon(12),Para(22,22,2
),Perp(22,22,2),Paraex(44,44),Perpex(44,44),Sithed(12,2),Betcos(10,2)
50     DIM Parabx(44),Perpbx(44),Epara(44),Eperp(44),Dum(44,44),Epsiln(102),Percn
t(102)
60     INPUT "Enter the Number of Layers not to Exceed 10.",N
70     INPUT "Enter Relative Epsilon Max.",Epsmax
80     INPUT "Enter the Incident Frequency in Gigahertz.",F
90     INPUT "Enter  Theda.",Theda
100    INPUT "Enter the Measured Reflectivity (%).",Pin
110    Power=10
120    Omega=2*PI*F*1E9                    !ANGULAR FREQUENCY IS CALCULATED!
130    Beta0=Omega/2.998E8                 !FREE SPACE WAVE VECTOR IS CALCULATED!
140    Beta02=Beta0^2                      !THE WAVE VECTOR IS SQUARED!
150    Power=10*Power                      !CONVERTS TO WATT/METER^2!
160    FOR I=1 TO N                        !ELEC. PROPERTIES OF LAYERS IS INSERTED!
170    DISP "Sigma(";I;")";                !ELECTRICAL CONDUCTIVITY IN MHOS!
180    INPUT Sigma(I)
190    IF Sigma(I)=0 THEN Sigma(I)=1E-12
200    DISP "Mu(";I;")";                   !RELATIVE MAGNETIC PERMEABILITY!
210    INPUT Mu
220    Mu(I)=Mu*4*PI*1E-7
230    IF I=1 THEN 270
240    DISP "Epslon(";I;")";               !RELATIVE ELECTRIC PERMITTIVITY!
250    INPUT Epslon
260    Epslon(I)=Epslon*8.8542E-12
270    DISP "Thickness(";I;")";            !EACH LAYER THICKNESS IN METERS!
280    INPUT Thick
290    Delta=SQR(2/(Omega*Mu(I)*Sigma(I)))
300    IF Thick<23*Delta THEN 370
310    Thick=23*Delta
320    N=I
```

```
330   Key=1
340   PRINT USING 350;I,I,I,Thick
350   IMAGE "LAYER ",DD," WAS THICKER THAN 23 SKIN DEPTHS. THE PROBLEM IS TRUNCA
TED AT ",DD," LAYERS, WITH LAYER ",DD,", ",D.DDE," METERS THICK."
360   PRINT
370   Z(I)=Z(I-1)+Thick                 !Z(n) IS CALCULATED FROM THICKNESSES!
380   IF I=1 THEN 430
390   Coef=Omega*SQR(Mu(I)*Epslon(I)/2)
400   Sqroot=SQR(1+(Sigma(I)/(Omega*Epslon(I)))^2)
410   Beta(I,1)=Coef*SQR(1+Sqroot)      !REAL WAVE VECTOR (Alpha) IS CALC.!
420   Beta(I,2)=Coef*SQR(Sqroot-1)      !IMAG WAVE VECTOR (Gamma) IS CALC.!
430   NEXT I
440   IF Key<>1 THEN 490
450   Shift=Z(N-1)
460   FOR I=0 TO N
470   Z(I)=Z(I)-Shift
480   NEXT I
490   Count=1
500   FOR Eps=1 TO Epsmax STEP (Epsmax-1)/100
510   PRINT Eps
520   Epslon(1)=Eps*8.8542E-12
530   Coef=Omega*SQR(Mu(1)*Epslon(1)/2)
540   Sqroot=SQR(1+(Sigma(1)/(Omega*Epslon(1)))^2)
550   Beta(1,1)=Coef*SQR(1+Sqroot)      !REAL WAVE VECTOR (Alpha) IS CALC.!
560   Beta(1,2)=Coef*SQR(Sqroot-1)      !IMAG WAVE VECTOR (Gamma) IS CALC.!
570   Np=N+1
580   L=4*Np
590   Lp=L+1
600   Mu(0)=4*PI*1E-7                   !ELEC. CHARAC. EA. SIDE OF LAYERS!
610   Epslon(0)=8.8542E-12
620   Mu(Np)=4*PI*1E-7
630   Epslon(Np)=8.8542E-12
640   Beta(0,1)=Beta0                   !REAL Beta 0!
650   Beta(0,2)=0                       !IMAGINARY Beta 0!
660   Beta(Np,1)=Beta0
```

```
670   Beta(Np,2)=0
680   E1=(Mu(0)/Epslon(0))^.25*SQR(2*Power)
690   E12=E1^2
700   Deg=PI/180
710   ! !
720             ! !!!  NOW WE START !!!!!
730   ! !
740   X=COS(Theda*Deg)
750   Y=SIN(Theda*Deg)
760   IF X=0 THEN X=1E-5
770   IF Y=1 THEN Y=.999999999999
780   Sin2=Y^2
790   H1perp=H1para*X
800   Cothed(Np,1)=X
810   Cothed(Np,2)=0
820   Cothed(0,1)=X
830   Cothed(0,2)=0
840   Sithed(Np,1)=Y
850   Sithed(Np,2)=0
860   Sithed(0,1)=Y
870   Sithed(0,2)=0
880   ! !
890   ! WE CALCULATE REAL AND IMAGINARY COS(Theda) AND SIN(Theda) !
900   ! !
910   FOR I=1 TO N
920   Denom=(Beta(I,1)^2+Beta(I,2)^2)^2
930   Pee=.5*(1-Beta02*Sin2*(Beta(I,1)^2-Beta(I,2)^2)/Denom)
940   Que=Beta02*Sin2*Beta(I,1)*Beta(I,2)/Denom
950   X=SQR(Pee^2+Que^2)
960   Cothed(I,1)=SQR(Pee+X)                    !REAL COS(Theda N) IS CALCULATED!
970   Cothed(I,2)=SQR(ABS(X-Pee))               !IMAG COS(Theda N) IS CALCULATED!
980   Sithed(I,1)=Beta(0,1)*Y*Beta(I,1)/(Beta(I,1)^2+Beta(I,2)^2)
990   Sithed(I,2)=-Beta(0,1)*Y*Beta(I,2)/(Beta(I,1)^2+Beta(I,2)^2)
1000  Betcos(I,1)=Beta(I,1)*Cothed(I,1)-Beta(I,2)*Cothed(I,2)  !REAL Beta x Cos(
Theda)!
```

```
1010  Betcos(I,2)=Beta(I,1)*Cothed(I,2)+Beta(I,1)*Cothed(I,1)  !IMAG Beta x Cos(
Theda)!
1020  IF Betcos(I,1)*Z(I)>75 THEN Betcos(I,1)=75/Z(I)
1030  IF Betcos(I,2)*Z(I)>75 THEN Betcos(I,2)=75/Z(I)
1040  NEXT I
1050  ! !
1060  ! WE BEGIN TO CALCULATE THE COMPLEX MATRIX!
1070  ! !
1080  FOR I=1 TO 2*(N-Key)+1 STEP 2        ! WE ENTER ROWS BY BOUNDRY, 2 PER
 BOUNDARY !
1090  K=(I-1)/2
1100  M=I-1
1110  R=I+1
1120  O=I+2
1130  X=-Z(K)*(Beta(K,1)*Cothed(K,2)+Beta(K,2)*Cothed(K,1))
1140  Y=Z(K)*(Beta(K,1)*Cothed(K,1)-Beta(K,2)*Cothed(K,2))
1150  P=K+1
1160  Xx=-Z(K)*(Beta(P,1)*Cothed(P,2)+Beta(P,2)*Cothed(P,1))
1170  Yy=Z(K)*(Beta(P,1)*Cothed(P,1)-Beta(P,2)*Cothed(P,2))
1180  IF X>170 THEN X=170    !X>170 IMPLIES A LAYER THICKNESS >170 SKIN DEPTHS!
1190  IF Xx>170 THEN Xx=170  !Xx>170 IMPLIES A LAYER THICKNESS >170 SKIN DEPTHS!
1200  Expx=EXP(X)
1210  Expxx=EXP(Xx)
1220  IF X<-170 THEN X=-170
1230  IF Xx<-170 THEN Xx=-170
1240  Expmx=EXP(-X)
1250  Expmxx=EXP(-Xx)
1260  Cosy=COS(Y)
1270  Siny=SIN(Y)
1280  Cosyy=COS(Yy)
1290  Sinyy=SIN(Yy)
1300  Expr=Expx*Cosy          !Bcr IMPLIES THE REAL PART OF Beta*COS(Theda)!
1310  Expi=Expx*Siny          !Bci IMPLIES THE IMAG PART OF Beta*COS(Theda)!
1320  Bcr=Beta(K,1)*Cothed(K,1)-Beta(K,2)*Cothed(K,2)
1330  Bci=Beta(K,1)*Cothed(K,2)+Beta(K,2)*Cothed(K,1)
```

```
1340  ! !
1350  ! WE CALCULATE THE (I,I-1) AND (I+1,I-1) COMPLEX MATRIX ELEMENTS!
1360  ! !
1370  IF I=1 THEN 1430
1380  Perp(I,M,1)=Expr
1390  Perp(I,M,2)=Expi
1400  Perp(R,M,1)=(Bcr*Expr-Bci*Expi)/Mu(K)
1410  Perp(R,M,2)=(Bcr*Expi+Bci*Expr)/Mu(K)
1420  ! !
1430  ! WE  CALCULATE THE (I,I) AND (I+1,I) COMPLEX MATRIX ELEMENTS!
1440  ! !
1450  Expr=Expmx*Cosy
1460  Expi=-Expmx*Siny
1470  Perp(I,I,1)=Expr
1480  Perp(I,I,2)=Expi
1490  Perp(R,I,1)=-(Bcr*Expr-Bci*Expi)/Mu(K)
1500  Perp(R,I,2)=-(Bcr*Expi+Bci*Expr)/Mu(K)
1510  ! !
1520  ! WE CALCULATE THE (I,I+1) AND (I+1,I+1) COMPLEX MATRIX ELEMENTS!
1530  ! !
1540  Expr=Expxx*Cosyy
1550  Expi=Expxx*Sinyy
1560  Bcr=Beta(P,1)*Cothed(P,1)-Beta(P,2)*Cothed(P,2)
1570  Bci=Beta(P,1)*Cothed(P,2)+Beta(P,2)*Cothed(P,1)
1580  Perp(I,R,1)=-Expr
1590  Perp(I,R,2)=-Expi
1600  Perp(R,R,1)=-(Bcr*Expr-Bci*Expi)/Mu(P)
1610  Perp(R,R,2)=-(Bcr*Expi+Bci*Expr)/Mu(P)
1620  ! !
1630  ! WE CALCULATE THE (I,I+2) AND (I+1,I+2) COMPLEX MATRIX ELEMENTS!
1640  ! !
1650  Expr=Expmxx*Cosyy
1660  Expi=-Expmxx*Sinyy
1670  IF I=2*N+1 THEN 1720
1680  Perp(I,O,1)=-Expr
1690  Perp(I,O,2)=-Expi
1700  Perp(R,O,1)=(Bcr*Expr-Bci*Expi)/Mu(P)
```

```
1710  Perp(R,O,2)=(Bcr*Expi+Bci*Expr)/Mu(P)
1720  NEXT I
1730  ! !
1740  ! COMPLEX MATRICES ARE EXPANDED INTO REAL MATRICES!
1750  ! !
1760  MAT Perpex=IDN(L,L)
1770  FOR I=1 TO L/2-2*Key              ! LOADS 4 ELEMENTS FOR EACH COMPLEX ONE !
1780  FOR J=I-2 TO I+2                  !AVOIDS CYCLING THRU THE WHOLE MATRIX!
1790  IF J<1 THEN 1890
1800  IF J>L/2-2*Key THEN 1890
1810  M=2*I
1820  R=2*J
1830  O=M-1
1840  P=R-1
1850  Perpex(O,P)=Perp(I,J,1)
1860  Perpex(M,R)=Perp(I,J,1)
1870  Perpex(M,P)=Perp(I,J,2)
1880  Perpex(O,R)=-Perp(I,J,2)
1890  NEXT J
1900  NEXT I
1910  Perpbx(1)=-E1
1920  Perpbx(3)=-E1*Cothed(0,1)*(Beta0/Mu(0))
1930  ! !
1940  ! AT THIS POINT WE ARE READY FOR THE MATRIX SOLUTION!
1950  ! !
1960  MAT Dum=INV(Perpex)
1970  FOR I=1 TO L
1980  Eperp(I)=Dum(I,1)*Perpbx(1)+Dum(I,3)*Perpbx(3)
1990  NEXT I
2000  ! !
2010  ! THE MAG. OF THE ELECTRIC FIELDS ARE NOW CALCULATED IN Epara AND Eperp !
2020  ! !
2030  Epsiln(Count)=Eps
2040  Percnt(Count)=(Eperp(1)^2+Eperp(2)^2)/E1^2*100
```

```
2050  IF (Percnt(Count)>Pin-.5) AND (Percnt(Count)<Pin+.5) THEN Xxx=Eps
2060  IF (Percnt(Count)>Pin-.5) AND (Percnt(Count)<Pin+.5) THEN Yyy=Percnt(Count
)
2070  Count=Count+1
2080  NEXT Eps
2090  ! !
2100  ! WE BEGIN THE GRAPHICS PORTION HERE !
2110  ! !
2120  GRAPHICS
2130  CSIZE 2.5,9/15,0
2140  LINE TYPE 1
2150  LOCATE 15,115,15,95
2160  SCALE 1,Epsmax,0,100
2170  LOCATE 14,115,14,95
2180  Xtick=(Epsmax-1)/100
2190  AXES Xtick,1,1,0,10,10
2200  MOVE Epsiln(1),Percnt(1)
2210  FOR I=1 TO 100
2220  DRAW Epsiln(I),Percnt(I)
2230  NEXT I
2240  LINE TYPE 3
2250  MOVE 1,Pin
2260  DRAW Epsmax,Pin
2270  LINE TYPE 1
2280  ! !
2290  ! PLOTS ARE DRAWN NOW LABELING IS INSERTED !
2300  ! !
2310  MOVE .35*(Epsmax-1)+1,-7.5
2320  CSIZE 3,9/15,0
2330  LABEL "Sample Epsilon (relative)"
2340  MOVE 1-.1*(Epsmax-1),10
2350  LDIR PI/2
2360  LABEL "Reflectivity in Per Cent"
2370  LDIR 0
2380  MOVE 1-.06*(Epsmax-1),-1.5
```

```
2390  LABEL 0
2400  FOR I=0 TO 100 STEP 10
2410  IF I=100 THEN 2470
2420  MOVE 1-.06*(Epsmax-1),8.5+I                               !LABEL Y AXIS!
2430  LABEL USING 2440;10+I
2440  IMAGE DDD
2450  J=I/20-.1
2460  IF I/20-J>0 THEN 2520
2470  MOVE 1+I/100*(Epsmax-1),-2                              !LABEL X AXIS!
2480  LORG 6
2490  LABEL USING 2500;I/100*(Epsmax-1)+1
2500  IMAGE DD.D
2510  LORG 1
2520  NEXT I
2530  CSIZE 4.2,9/15,0
2540  MOVE 1,-14
2550  LABEL USING 2560;N
2560  IMAGE DD,"-LAYER ELECTROMAGNETIC WAVE INTERACTION "
2570  CSIZE 3,9/15,0
2580  LETTER
2590  EXIT GRAPHICS
2600  STOP
```

END

DATE
FILMED

8-83

DTIC